# "The Neural Core of Fear and Anxiety – Commonalities and Differences of Fear and Anxiety Circuits"

**UR**

Dissertation

zur Erlangung des Doktorgrades

der Humanwissenschaften

(Dr. sc. hum.)


der

Fakultät für Medizin

der Universität Regensburg


vorgelegt von

Viola Wagner

aus

Frankfurt am Main


im Jahr

2020

# "The Neural Core of Fear and Anxiety – Commonalities and Differences of Fear and Anxiety Circuits"

Dissertation
zur Erlangung des Doktorgrades
der Humanwissenschaften
(Dr. sc. hum.)

der
Fakultät für Medizin
der Universität Regensburg

vorgelegt von
Viola Wagner
aus
Frankfurt am Main

im Jahr
2020

Dekan:                   Prof. Dr. Dirk Hellwig
Betreuer:           Prof. Dr. Jens V. Schwarzbach

# CONTENT

# LIST OF FIGURES

7

# LIST OF TABLES

12

# ZUSAMMENFASSUNG

Das Ziel dieses Promotionsvorhabens war es, die neuronalen Gemeinsamkeiten und Unterschiede von Furcht- und Angstreaktionen im menschlichen Gehirn zu untersuchen. Angststörungen stellen eine Gruppe von mentalen Erkrankungen dar, die durch übermäßige Angst (Besorgnis über zukünftige Ereignisse) und Furcht (eine Reaktion auf gegenwärtige Ereignisse) gekennzeichnet sind. Die neuronalen Muster und zugrundeliegenden Mechanismen von phasischen (Furcht) und anhaltenden (Angst) Reaktionen konnten bisher noch nicht vollständig erklärt werden. Die Identifikation einer neuronalen Biosignatur für Furcht und Angst, insbesondere die Identifikation von Unterschieden und Gemeinsamkeiten unabhängig von der Modalität der aversiven Ereignisse (z.B. aversive somatosensorische im Vergleich zu aversiven Bildern), ist ein wichtiges Ziel von bildgebenden Verfahren in der Psychiatrie, welche zukünftig im Rahmen der „precision psychiatry" große Auswirkungen hinsichtlich einer Verbesserung von Diagnose und Vorhersage von Behandlungsergebnissen haben kann. Als wesentliche Voraussetzung für die Untersuchung dieser neuralen Repräsentationen habe ich eine standardisierte und effiziente Methode entwickelt, um die individuelle Stimulusintensität an der Schmerzschwelle zu bestimmen, und konnte in einem Verhaltensexperiment ($N$ = 40) zeigen, dass diese neue Methode verlässliche, und zeitlich stabile Messungen erlaubt. In der nachfolgenden fMRT-Studie, dem Hauptexperiment dieser Arbeit, durchliefen 35 gesunde Teilnehmer ein experimentelles Paradigma, welches unterschiedliche Versuchsbedingungen zur Auslösung von Furcht- und Angstreaktionen beinhaltete. Dabei wurden verhaltensbezogene, psychologische (Persönlichkeitsmerkmale und Zustandsgrößen), physiologische (Herz- und Atemfrequenz) Parameter sowie Hirnaktivität erhoben. Furcht- und angstbezogene Reaktionen wurden mit Hilfe eines Zwischensubjektdesigns mittels vorhersagbaren und nicht vorhersagbaren Stimuli mit negativer oder neutraler Valenz auf zwei sensorischen Ebenen (visuell, somatosensorisch) erzeugt. Während einige Gehirnregionen modalitätsspezifische Verarbeitung zeigten, offenbarten andere modalitätsunabhängige Aktivierungsmuster für Furcht (Stammhirn und medialer prefrontalen Cortex) und Angst (frontaler mittlerer und superiorer Gyrus), welche auf eine multisensorische oder abstrakte Verarbeitung von Bedrohungen hinweisen.

# ABSTRACT

The main goal of the present PhD project was to investigate the neural commonalities and differences of fear and anxiety responses in the human brain. Anxiety disorders are a group of mental disorders characterized by excessive anxiety (a worry about future events) and fear (a reaction to current events). The neural patterns and underlying mechanisms of transient (fear) and sustained (anxiety) responses are not yet fully understood. Identifying a neural biosignature of fear and anxiety, i.e. identifying their differences and commonalities irrespective of modality of aversive events is an important goal in psychiatric neuroimaging and may have major future implications in precision psychiatry in terms of better diagnostics and predicting treatment outcome. As a prerequisite for investigating these neural representations with neuroimaging, I developed a standardized and fast method for assessing individual stimulus intensity at pain threshold and demonstrated in a behavioral experiment ($N = 40$) that the new method produced reliable intensity estimates that were stable over time. In a subsequent fMRI study, the main experiment of this thesis, 35 healthy participants underwent an experimental paradigm that consisted of different conditions for evoking fear and anxiety responses. During the experiment, behavioral, psychological (trait and state variables), physiological (heart and respiratory rate) variables as well as brain activity were acquired. Fear- and anxiety related responses were evoked within a fully factorial within-subjects design with predictable and unpredictable stimuli from two sensory modalities (visual, somatosensory), which had negative or neutral valence. While some brain areas showed modality-specific processing, neuroimaging results revealed modality-general activation patterns coding for fear (in brain stem and paracingulate cortex) and anxiety (in middle and superior frontal gyri) hinting at multisensory or abstract processing of threat.

# ABBREVIATIONS

| | |
|---|---|
| ACC | Anterior cingulate cortex |
| AIC | Anterior insula cortex |
| ALD | Arm left dorsal |
| ALV | Arm left ventral |
| AMY | Amygdala |
| ANOVA | Analysis of variance |
| ARD | Arm right dorsal |
| AROMA | Automatic Removal Of Motion Artifacts |
| ARD | Arm right ventral |
| AS | Anxiety sensitivity |
| ASI | Anxiety Sensitivity Index |
| AUC | Area under the curve |
| BOLD | Blood oxygenation level-dependent |
| BL | Basolateral |
| BLA | Basolateral amygdaloid nucleus |
| BM | Basomedial |
| BNST | Bed nucleus of the stria terminalis |
| BST | Bed nucleus of the stria terminalis |
| CB | Cerebellum |
| CC | Cingulate cortex |
| Ce | Central |
| CeA | Central amygdaloid nucleus |
| CI | Confidence interval |
| CS | Conditioned stimulus |
| dACC | Dorsal anterior cingulate cortex |
| dlPFC | Dorsolateral prefrontal cortex |
| dmPFC | Dorsomedial prefrontal cortex |
| DRN | Dorsal raphe nucleus |
| DSM | Diagnostic and Statistical Manual of Mental Disorders |
| ESTIMATE | Estimating STIMulus pAin ThrEshold |
| EPI | Echo-planar imaging |

| | |
|---|---|
| EU | European Union |
| EV | Explanatory variable |
| FA | Flip angle |
| FEAT | FMRI Expert Analysis Tool |
| FFA | Fusiform face area |
| FG | Fusiform gyrus |
| FIR | Finite impulse response |
| fMRI | Functional magnetic resonance imaging |
| FOP | Fear of pain |
| FLIRT | FMRIB's Linear Image Registration Tool |
| FSL | FMRIB Software Library |
| FUS | Fusiform |
| FEW | Family wise error |
| FWHM | Full width at half maximum |
| GABA | Gamma-amino-butyric-acid |
| GAD | Generalized anxiety disorder |
| GLM | General linear model |
| HR | Heart rate |
| HRF | Hemodynamic response function |
| HY | Hypothalamus |
| IAPS | International Affective Picture System |
| ICA | Independent component analysis |
| ICC | Intraclass correlation coefficient |
| ICD | International Statistical Classification of Diseases and Related Health |
| IE | Interaction effect |
| INS | Insula |
| IFJ | Inferior frontal junction |
| IL | Infralimbic cortex |
| ITC | Intercalated cell masses |
| ITI | Intertrial interval |
| IU | Intolerance to Uncertainty |
| IUS | Intolerance to Uncertainty Scale |

| | |
|---|---|
| La | Lateral |
| LA | Lateral amygdala |
| LG | Lingual gyrus |
| LOTC | Lateral occipital temporal cortex |
| LL | Leg left |
| LR | Leg right |
| mA | Milliampere |
| MB | Multiband |
| MCC | Middle cingulate cortex |
| Me | Medial |
| ME | Main effect |
| MNSD | Mental, neurological and substance use disorders |
| mPFC | Medial prefrontal cortex |
| MPRAGE | Magnetization-prepared rapid gradient-echo |
| MOD | Modality |
| MRI | Magnetic resonance imaging |
| MRM | Multivariate and Repeated Measures toolbox |
| ms | milliseconds |
| MSE | Mean squared error |
| MTG | Middle temporal gyrus |
| MVP | Multivariate pattern |
| MVPA | Multivariate pattern analysis |
| NA | Negative affect |
| NAcc | Nucleus accumbens |
| NAPS | Nencki Affective Picture System |
| Neg | Negative condition |
| Neu | Neutral condition |
| NPU | No (N), predictable (P) and unpredictable (U) threat task |
| NRS | Numeric Rating Scales |
| OFC | Orbitofrontal cortex |
| OG | Occipital gyrus |
| PA | Positive affect |
| PAG | Periaqueductal gray |

| | |
|---|---|
| PANAS | Positive and Negative Affect Schedule |
| PCC | Posterior Cingulate Cortex |
| PE | Parameter estimate |
| PFC | Prefrontal cortex |
| PFCs | Prefrontal cortices |
| pFMC | Posterior frontomedian cortex |
| PH | Parahippocampus |
| PicNegPred | Picture negative predictable condition |
| PicNegUnpr | Picture negative unpredictable condition |
| PicNeuPred | Picture neutral predictable condition |
| PicNeuUnpr | Picture neutral unpredictable condition |
| Pics | Pictures |
| PL | Prelimbic cortex |
| PMC | Primary motor cortex |
| PreC | Precuneus |
| PreCG | Precentral gyrus |
| Pred | Predictable condition |
| PRED | Predictability |
| QST | Quantitative sensory testing |
| RDM | Representational dissimilarity matrix |
| rmANOVA | Repeated measures analysis of variance |
| rIFG | Right inferior frontal gyrus |
| ROI | Region of interest |
| rmANOVA | Repeated measures analysis of variance |
| RT | Reaction time |
| RSA | Representational similarity analysis |
| S2 | Secondary somatosensory cortex |
| SD | Standard deviation |
| sec | Seconds |
| SEM | Standard error of the mean |
| sgACC | Sagittal anterior cingulate cortex |
| Skew | Skewness |
| SMA | Supplementary motor area |

| | |
|---|---|
| SMG | Supramarginal gyrus |
| SMG | Superior parietal lobule |
| SPM | Statistical parameter estimates |
| SS | Sum of squares |
| STAI | State-Trait Anxiety Inventory |
| STAI-S | State-Trait Anxiety Inventory – trait scale |
| STAI-T | State-Trait Anxiety Inventory – state scale |
| STG | Superior Temporal Gyrus |
| TE | Echo time |
| TFCE | Threshold free cluster enhancement |
| TG | Temporal gyrus |
| Th | Thalamus |
| THAL | Thalamus |
| TR | Repetition time |
| Unpr | Unpredictable condition |
| US | Unconditioned stimulus |
| VAL | Valence |
| VAS | Visual Analogue Scale |
| VAS-A | Visual Analogue Scale – Anxiety |
| Var | Variance |
| VBF | Ventral basal forebrain |
| vlPFC | Ventrolateral prefrontal cortex |
| vmPFC | Ventromedial prefrontal cortex |
| VR | Voxel resolution |
| Zap | Electrical stimulus |
| ZapNegPred | Electrical stimulus negative predictable condition |
| ZapNegUnpr | Electrical stimulus negative unpredictable condition |
| ZapNeuPred | Electrical stimulus neutral predictable condition |
| ZapNeuUnpr | Electrical stimulus neutral unpredictable condition |
| zSkew | z-score of the skew |

# 1 THEORETICAL BACKGROUND

## 1.1 Anxiety Disorder– Status Quo

Mental, neurological and substance use disorders (MNSD) currently rank among the upper third of global disease burden with an increasing trend over the past decades (Murray et al., 2015); (Collins et al., 2011). The relevance of mental disorders in particular is not only shown by their high prevalence, which reaches up to 38.2 % for the EU (Wittchen et al., 2011), but also by an early age onset and estimated economic consequences of € 798 billion for the EU in 2010 ((Pātil, Chisholm, Dua, Laxminarayan, & Medina Mora, 2015); (Gustavsson et al., 2011). The subgroup of anxiety disorders which include panic disorders, agoraphobia, social and generalized anxiety disorders (GAD), form a substantial part of global prevalence rate within the MNSD with a lifetime prevalence of around 4 % (Global Burden of Disease Collaborative Network, 2018). In Europe, the lifetime prevalence of anxiety disorders is reported to be 14 %, which corresponds to 61.5 million affected persons (Wittchen et al., 2011). The impact of anxiety disorder's becomes further obvious considering the fact that it is approximately twice as common as unipolar depression (Wittchen et al., 2011).

Nevertheless, these estimates might represent only the tip of the iceberg with respect to the costs and number of people living with anxiety disorders, as there are high rates of under- and miss-diagnosed cases (Kasper, 2006). Merely 36.9 % of people suffering from anxiety disorders are searching for professional help and treatment (Wang et al., 2005). Overcoming this so-called "treatment gap", which refers to the absolute difference of people receiving treatment and the people not receiving mental health care (Kohn, Saxena, Levav, & Saraceno, 2004), represents a further challenge that needs to be addressed and might even be underestimated, considering that most surveys include inpatient treated cases only (Bandelow & Michaelis, 2015). From the patients view, reasons for unrecorded cases include treatment avoidance due to a limited understanding of symptoms and their relevance (Henderson, Evans-Lacko, & Thornicroft, 2013); (Henderson et al., 2013). For healthcare professionals characterizing and classifying symptoms as clinically relevant can be challenging considering the broad spectrum and high dimensionality of symptoms. Internationally acknowledged diagnostic schemes such as the "International Statistical Classification

of Diseases and Related Health "(ICD-10; (World Health Organization, 1993) and the "Diagnostic and Statistical Manual of Mental Disorders" (DSM-5; American Psychiatric Association, 2013) are try to describe and classify symptoms based on operational criteria. In the ICD-10, anxiety disorders are specified with "F40 – Phobic anxiety disorders" and "F41 Other anxiety disorders". GAD (F41.1) is characterized as a period of "tension, worry and feelings of apprehension, about every-day events and problems" for at least six months. Further, at least four out of 22 defined symptoms must be present, which comprise at least one item of the autonomic arousal symptom criteria (such as palpitations or accelerated heart rate, sweating, trembling or shaking or dry mouth (World Health Organization, 1993). According to the DSM-5, GAD is characterized with "excessive anxiety and worry" – defined as at least three out of six symptoms (restlessness, feeling keyed up or on edge, being easily fatigued, difficulty concentrating or mind going blank, irritability, muscle tension or sleep disturbance) for at least six months.

Nevertheless, the validity and reliability of mental disorder diagnosis is still in the focus of scientific debates and needs to be improved (Tyrer, 2014). High variability in symptom characteristics, constellation and comorbidities complicate diagnosis labelling. As an example, two patients diagnosed with major depression disorder according to the DSM criteria might share solely one common symptom (Biomarkers for Mental Disorders, 2017) representing the heterogeneity of the symptoms under one diagnosis. Further, validity and reliability of diagnosis are influenced by additional aspects, including patient´s factors (e.g. psychological state), clinician´s factors (e.g. experience) and variance in diagnosis methods (e.g. interviews vs. self-report instruments). Improving reliability via uncovering of suitable biomarkers is the desired goal to improve symptom description and diagnosis category validation (Aboraya, Rankin, France, El-Missiry, & John, 2006).

The need for additional data becomes even more important when choosing appropriate treatment strategy, monitoring therapy progress and predicting the treatment outcome. The rate of diagnosed patients receiving adequate therapy after contact to professionalized medicine lies between 12.7-48.3% for any mental disorder (Wang et al., 2005). The current treatment for anxiety disorder is a combination of pharmacotherapy and psychotherapy. Thereby pharmacotherapy is often described as "a trial and error" approach with several antidepressant and anxiolytic medications in

line if the initial medication remains without response (a symptom reduction of 25 % over a period of six weeks (Farach et al., 2012)). Meta-analyses report mixed effects regarding the method of choice. Some studies have found that both treatment strategies, pharmacotherapy and psychotherapy, are equally effective (Cuijpers et al., 2013) while others revealed a clear benefit of combining both approaches (Bandelow, Seidler-Brandler, Becker, Wedekind, & Rüther, 2007). This lack of consensus has several reasons: First, psychotherapy contains several different therapy schemes which have to be compared to a variety of pharmacological agents on the other side giving rise to a huge number of necessary comparisons. Second, therapy sessions are adjusted to individual needs and therefore hard to compare interindividually and with pharmacotherapy. Further, treatment outcome is dependent on anxiety (sub-)type and comorbidities (often with depression) that is moderating the patient's treatment response (Cuijpers et al., 2013). Additionally, other factors like personality traits, genetic variants and functional activation patterns have been named to predict treatment outcome (Ferreira-Garcia, Mochcovitch, Costa do Cabo, Nardi, & Christophe Freire, 2017). In conclusion, there is no guideline for choosing the most suitable treatment strategy for any given individual, yet. Pharmacotherapy over a long period, often years, increases the probability of adverse events in person's life, reduced patient's compliance and negative treatment outcome. The present lack of consensus in effective treatment schemes and high variability in treatment outcome clearly indicate the need for a new approach. This approach needs to control for inappropriate treatment strategies while including further objective (data driven) parameters for predicting therapy outcome at an individual level.


## 1.2  Precision Psychiatry Approach

Great advances have been made over the last 50 years in the evaluation of risk factors of mental disorder development, maintenance and treatment responsiveness. Nevertheless, research in this period focused mainly on retrospective-descriptive (patient´s case descriptions) and insight-directed (group difference) methods (Hahn, Nierenberg, & Whitfield-Gabrieli, 2017), while translation into clinical practice and treatment planning was limited (Figure 1.1). Replacing "reactive" with "proactive" approach, that claims to be "predictive, personalized, preventive and participatory"

(Hood & Friend, 2011) represents a so-called "paradigm shift" (Kuhn & Hacking, 2012) in the whole medical domain. This shift represents the next revolutionary step towards answering individually directed medical questions and is discussed to be especially beneficial for psychiatry for enhancing clinical utility (Hahn et al., 2017). A personalized approach is already grounded in the field of "personalized medicine". Later renamed into "precision medicine" and adapted within the field of psychiatry ("precision psychiatry"), it is described as choosing the "right treatment for the right person at the right time" (Wium-Andersen, Vinberg, Kessing, & McIntyre, 2017). More precisely, it refers to adjusting medical decisions while considering multiple characteristics based on individual dispositional, environmental and lifestyle factors (National Research Council, 2011).

**Figure 1.1**

*Paradigm Shift Towards Precision Medicine*
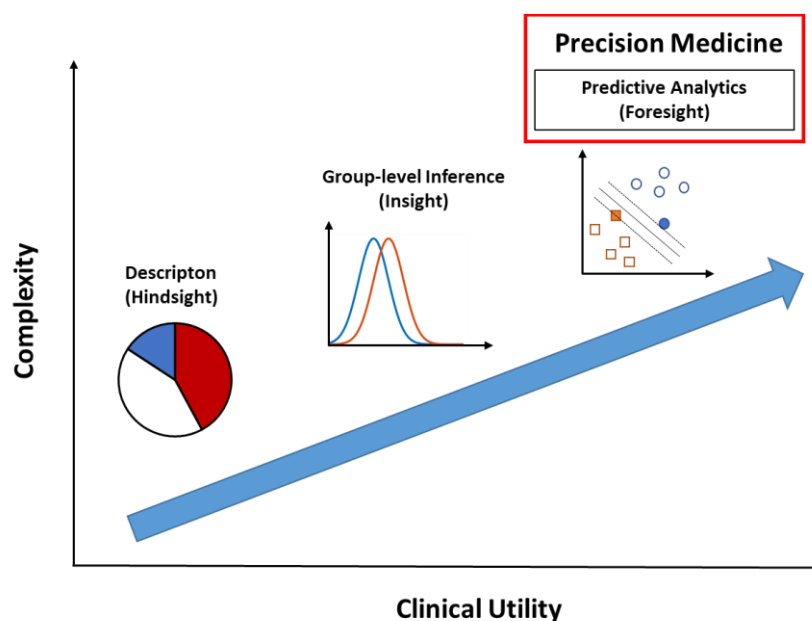


Prior mental health research has mainly focused on case descriptions (hindsight) and group-level analysis (insight). Forthcoming predictive approach (foresight), is fundamental in precision medicine and promising to enhance the clinical utility of research findings while including and combining factors at an individual level. Thus, such an individual approach comes along with extensive data analysis and complex predictive models. Figure adapted from "Predictive analytics in mental health: applications, guidelines, challenges and perspectives" by T. Hahn, A. A. Nierenberg, and S. Whitfield-Gabrieli, 2017, Molecular Psychiatry,22, p. 38.

But what is meant with "multiple characteristics" that are promising in driving personalized decisions and predicting the individual clinical outcome? Traditionally labelled as "independent variables", they are representing risk factors that contribute

to the development of mental disorders, their maintenance and prognosis. Reaching from psychosocial to biological research domains (Fernandes et al., 2017a), these risk-factors seem to be present in a wide range of clinical subgroups (Manchia, Pisanu, Squassina, & Carpiniello, 2020).

Psychological and social risk factors are classified as individual (e.g. sadness, loneliness feelings), family-related (e.g. low emotional support of parents), drug-related (e.g. tobacco, alcohol and other drugs consumption), school-related (e.g. low school performance and school drop-out), social (e.g. experienced aggression and physical violence) as well as sexually-transmitted disease and AIDS-related (e.g. HIV risk behavior) factors (Pinto et al., 2014). These psychosocial conditions could occur during any period of person's life span and are thus known to be crucial in mental disease prevention and development.

Further promising with regard to mental health diagnostics, predictions and treatment response monitoring, are so-called "biomarkers". They are defined as "objectively measured and evaluated as an indicator of normal biological processes, pathogenic processes, or pharmacologic responses to a therapeutic intervention" (Biomarkers and surrogate endpoints, 2001). These markers are mainly beneficial as so-called "surrogate endpoints", e.g. while investigating efficacy in pharmacological interventions in clinical trials (Biomarkers and surrogate endpoints, 2001). Biomarkers are commonly divided into subgroups of genetic, molecular, and neuroimaging markers (Wium-Andersen et al., 2017) which together result in a biosignature (Fernandes et al., 2017a). A schematic overview of biomarker concept in precision psychiatry is depicted in Figure 1.2.

**Figure 1.2**

*Factors Contributing to the Biosignature Identification in Precision Psychiatry*
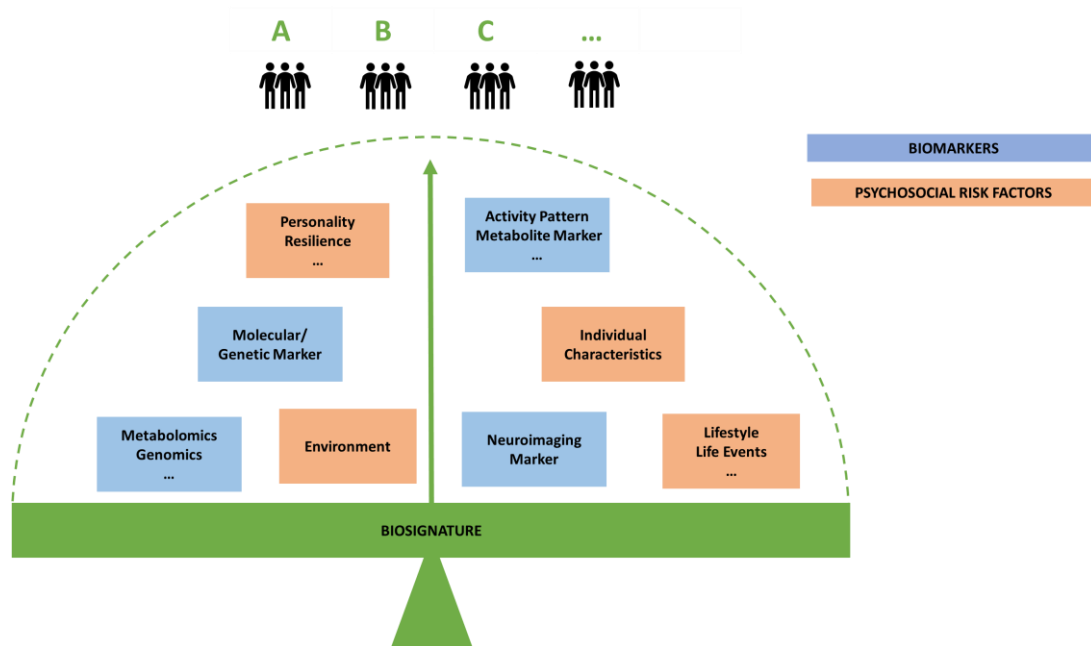


The key point of precision psychiatry is based on combining markers yielded by biological (blue) and psychosocial (orange) domains. Weighting and classification of these factors lead to more precise characterization of different patient subgroups concerning their shared objective, biosignature (green).

Molecular markers could be measured for instance from peripheral blood and contribute to biological read-out. Protein markers, like cytokines that indicate inflammation, are known to be involved in major mental disorder modulation (Miłkowska, Popko, Demkow, & Wolańczyk, 2017). Although there is no single molecular marker that could classify different mental disorders (Wium-Andersen et al., 2017), peripheral blood could still serve as a suitable tool for further assessment of e.g. genetic markers. Heritability of mental disorders has interested many since the early beginning of mental health research and is still in the focus of genome-wide association studies. Genome variants (such as polymorphisms) are fundamental in pharmacogenetics approach since the individual differences in pharmacodynamics and -kinetics can have an impact on psychopharmacological treatment outcome (Baune, 2020). Importantly, neuroimaging methods are providing us a "brain read-out" and serve as a suitable tool for targeting biomarkers non-invasively. Early neuroimaging studies have revealed abnormalities when examining group differences in morphometric, functional (e.g. differences in blood oxygenation level-dependent signal (BOLD)) and metabolite markers between patient and healthy control groups.

These markers appear to be promising treatment monitoring tools in enhance to e.g. gray matter volume (McDonald, 2015) and functional connectivity changes (Scult et al., 2019), as they could detect a neural activation pattern which might be able to specify diagnosis and complement diagnosis criteria (Sprooten et al., 2017).

Nevertheless, biomarkers are still rarely considered in clinical practice as well as hard criteria in existing diagnosis schemes (Insel et al., 2010). One major reason might be that single biomarker still need further validation and certainty. Additional evidence for developing e.g. diagnostic assays is needed for identifying "breakthrough" biomarkers with high sensitivity and specificity (Bahn et al., 2013). Until now, it is not fully understood to what extent a single biomarker is related to specific questions regarding a mental disorder. Still, the multitude of potential risk factors from different domains support the evidence for an interplay and multiple-causes concept and highlight the need for patient sub-categorization with regard to the underlying pathomechanism. Dividing patients into subgroups while clustering symptoms from multidimensional space could help to overcome the rigid classification of traditional symptom schemes (Boksa, 2013). Further, focusing on individual symptom-patterns while considering genetic and psychosocial markers (rather than simply diagnostic labelling) represents a further shift in perspective. Therefore, it is more promising to know what kind of person is suffering from symptoms rather than labelling the symptom complex. Nevertheless, one major challenge in precision psychiatry approach is the successful validation and replication of potential biomarkers that may improve clinical decisions. The lack of reproducibility has been identified to be related to differences at sample level, study design and analysis strategy, which contribute to a lack of biomarker standardization (Bahn et al., 2013). Hence, a single "breakthrough" biomarker has not been found yet which can be attributed to a high variety of symptom patterns in mental disorders. Additionally, the extent of contribution of one biomarker to a cluster of biomarkers is another rather extensive scientific goal. Therefore, a cascade of steps has been proposed to overcome the irreproducibility problem. A single biomarker should be considered and validated with respect to an additional dependent biomarker for building up the biomarker panel (Teixeira, Salem, Frey, Barbosa, & Machado-Vieira, 2016). Validation of the whole panels, instead of single criteria, and identifying them in clinical subjects would further contribute to their clinical utility. In conclusion, the paradigm shift towards precision psychiatry represents a necessary step for

towards personalized health care while considering the complex nature of mental disorders.

## 1.3  Fear vs. Anxiety

### 1.3.1  Conceptualization

The literature reports several ways of how to conceptualize fear and anxiety derived from a multitude of research domains. Major progress has been made over the past decades in disentangling fear from characteristics of anxiety considering psychological, behavioral and physiological findings (Steimer, 2002). Nevertheless, an overarching concept is still lacking and this might be the reason why both terms are often used interchangeably (Sylvers, Lilienfeld, & LaPrairie, 2011). Different perspectives on fear and anxiety conceptualization will be discussed in the following section.

Among other aspects, the psychological view focusses on individual differences in anxiety proneness and conceptualizes anxiety based on a state-trait distinction. Spielberger (1966) proposed a unidimensional framework in which trait-anxiety refers to individual differences in evaluating an uncertain situation as potentially threatening and the individual degree in responding to these situations. In contrast, state anxiety represents a transitory emotional condition, that modulates psychological and physiological responses (Spielberger, 1966). In line with this conceptualization, Endler and colleagues (1983) assumed a multidimensional concept of state and trait anxiety resulting from four different factors: social evaluation, physical danger, ambiguous, and daily routines, whereas state-anxiety loads on two distinct dimensions: cognitive worry and autonomic-emotional (Endler, 1983). Considering recent definitions, trait-anxiety represents a stable individual disposition that regulates the extent of negative emotion experiences (i.e. fears, worries) and continuous threat monitoring while state-anxiety represents the expression at the perceptual level (Yori, 2013). This combination of trait anxiety with continuously experienced state anxiety biases cognitive-perceptual experiences (Yori, 2013), leads to maladaptive thoughts and behavior that is fundamental in developing an anxiety disorder symptomatic. Distinction at threat level and response level is compatible with the basic emotion theory approach (Ekman, 1992). In this view, negative feelings are generally labelled as "fear" which describes the response to potential physical, emotional and psychological harm (Ekman, 1992;

Ekman & Cordaro, 2011). Fearful experiences are modulated by further decisive factors, such as timing of harm and the ability to cope with danger. In addition, the intensity of threat represents a third factor that varies along a continuum from least intense (e.g. trepidation) to most intense (e.g. terror). In this continuum, anxiety represents a facet of fear experience and is characterized with middle-scaled threat intensity, response to an anticipated threat and coping with uncertainty (The Ekmans' Atlas of Emotion, 2020).

Originating from an evolutionary perspective, fear allows us to promptly react (fight vs. flight vs. freeze) to aversive events and initiates adequately adaptive responding, that is fundamental to survival (LeDoux & Pine, 2016). This assumption is supported by the preference for fear-relevant vs. fear-irrelevant stimuli that are modulated by certainty of the threat (Hayes, 2000) and further supports the hypothesis of biological preparedness (Seligman, 1970). In this context, the term "state" is used for fear and anxiety conceptualization while both terms represent distinct response states towards potential threat, resulting from selective association processes (Mineka & Öhman, 2002). Here, fear represents adaptive, phasic response state that occurs following the threat onset while anxiety is characterized by a tonic state that reflects preparedness (Adolphs, 2013). Neuroimaging evidence contributes to revive perspective of distinct affective states while integrating evolutionary aspects and focusing on their neural underlying mechanisms. From the neuroscientific point of view, fear and anxiety represent distinct mental brain states, evoked from external and internal cues, that cause specific autonomic, behavioral and physiological responses (Tovote, Fadok, & Lüthi, 2015) while contributing to different neural structures and operating circuits (Steimer, 2002). Aversive state of fear is associated with negatively valanced thoughts and nervousness whereas distinct, survival-relevant fear state feelings come along with autonomic and behavioral consequences (Panksepp, Fuchs, & Iacobucci, 2011). Nevertheless, there is an ongoing debate, whether anxiety is representing a conscious negative feeling that could be disentangled from evolutionary-based fear processes, or if it represents a facet of fear-related defensive response behavior. Reviewing different scientific perspectives yielded several distinctions at the threat and response level that are displayed in Figure 1.1.

**Table 1.1**

*Overview of Threat and Response Related Characteristics of Fear and Anxiety Concepts*

|  | Dimension | Fear | Anxiety |
|---|---|---|---|
| Threat | Predictability | Predictable | Unpredictable |
|  | Certainty | Certain | Uncertain |
|  | Specificity | Specific | Unspecific |
|  | Temporal direction | Threat present (Identification) | Future-directed threat (Anticipatory) |
|  | Attentional direction | Focalized | Hypervigilance |
| Response | Temporal aspect | Immediate (Identification) | Persisting (Anticipation) |
|  | Magnitude | Acute | Attenuated |
|  | Specificity | Specific | Unspecific |
|  | Defensive direction | Avoidance | Approach |
|  | Duration | Phasic | Sustained |

*Note.* This table was adapted from "Differences between trait fear and trait anxiety: Implications for psychopathology" by P. Sylvers, S. O. Lilienfield and J. L. LaPraire, 2011, Clinical Psychology Review, 31, p.126 and supplemented with further literature (Davis, Walker, Miles, & Grillon, 2010; Grillon, Baas, Lissek, Smith, & Milstein, 2004; Grupe & Nitschke, 2013; LeDoux, 1998; Naaz, Knight, & Depue, 2019; Somerville et al., 2013).

A variety of research approaches have revealed several commonalities and differences of fear and anxiety underlying each's characteristics. Nevertheless, a commonly accepted conceptualization is still missing. Both terms are often used interchangeably which is also reflected by unprecise terminology usage in common diagnosis manuals. When describing and classifying anxiety disorders a common conceptual distinction states that fear, in contrast to anxiety, is associated with a specific object like in specific phobia (Perusini & Fanselow, 2015).

In the past, the examination of neurobiological mechanisms is evolving and seems promising to support previous conceptualization, although an ongoing discussion between neuroscience research experts still continues (see chapter 1.3.4). However, this persistent debate further highlights the need for additional evidence yielded from underlying neural mechanisms. Shedding further light into the neural representation and core mechanisms could replace the preliminary psychological definitions that are assumed to represent "place-markers" (Panksepp et al., 2011) for concepts that we do not fully understanding yet. Note, that within this thesis the term "fear" will be used to

describe an acute transient reaction to an immediate, upcoming and external threat (LeDoux, 1998). In contrast, the term of "anxiety" is representing the persisting state of an internal conflict as a response to an unpredictable or diffuse threat that might occur distal in space and time (Davis et al., 2010; Steimer, 2002).

### 1.3.2 How to Evoke Fear and Anxiety Responses?

Fear conditioning paradigms are the most common ways to examine the mechanisms of fear acquisition, maintenance and extinction learning related to anxiety disorder pathology (Lonsdorf et al., 2017). Classical conditioning represents an example of threat learning that describes the mechanism of acquiring knowledge about a stimulus-to-threat association and the use of this in predicting future harmful events (Plamper & Lazier, 2012). During the fear conditioning phase, a previously neutral stimulus, e.g. a geometric shape, will be presented and paired with a negatively valent stimulus (unconditioned stimulus; US), e.g. an electrical stimulus. As a consequence of repeated presentation and pairing, the previously neutral stimulus becomes a "conditioned stimulus" (CS) that triggers a measurable conditioned fear response on its own (Lonsdorf et al., 2017). However, such fear responses could also be evoked exclusively by the US, without requiring pairing, because of its universally threatening nature depending on its intensity (Lonsdorf et al., 2017) and often used in so-called „threat of shock" paradigms, e.g. for assessing the neural mechanisms of fear and anxiety (Balderston, Liu, Roberson-Nay, Ernst, & Grillon, 2017; Grillon et al., 2004). Common threat stimuli consist of visual (e.g. pictures), auditory (e.g. tones) and olfactory (e.g. odors) modalities while tactile stimuli (e.g. electrical shocks) are mostly used (Sehlmeyer et al., 2009).

With focus on visual modality, threat-related negatively valent images have been found to be most appropriate in evoking threat responses, mainly as they elicit faster reaction times (RT), smaller error rates (Schacht & Sommer, 2009) and higher percentage signal change (e.g. in the prefrontal cortex (PFC)), e.g. in comparison to threat-related words (Kensinger & Schacter, 2006). Although, while they are used repeatedly in number of studies, it is known that encoding threat from emotional pictures is not universal - rather often highly individual and controlling for these differences is nearly impossible (Lonsdorf et al., 2017). However, most of the pictures originate from the

International Affective Picture System (IAPS; (Lang, 2005)) which is a large picture database. IAPS is widely used for investigating emotional responses in respect to arousal, dominance and valence dimensions (Mikels et al., 2005). IAPS pictures have been successfully used in fear conditioning experiments (Levine et al., 2018a) and in evoking fear and anxiety responses (Somerville et al., 2013) in the human brain. Nevertheless, the use of IAPS has been discussed for its constrained image number which leads to picture repetitions in demanding experimental designs (e.g. in fMRI study designs; (Marchewka, Zurawski, Jednoróg, & Grabowska, 2014). Further, IAPS images suffer from poor quality (low resolution) which might affect the visual stimulus processing and therefore needs to be controlled (Marchewka et al., 2014).

To overcome these limitations of IAPS, the "Nencki Affective Picture System" (NAPS; (Marchewka et al., 2014) was created and validated in 2014. This dataset contains high-quality photographs (1356 images), divided into five categories (people, faces, animals, objects, and landscapes) and which are rated with regard to arousal (relaxed vs. aroused), motivational direction (approach vs. avoidance) and valence (positive vs. negative; (Marchewka et al., 2014). Further, NAPS pictures have been evaluated with respect to basic emotions and discrete emotional categories, which provide several advantages for addressing a broad range of research questions (Riegel et al., 2016). Nevertheless, until now, NAPS pictures are mostly used in experimental studies to supplement the limited number of pictures that are provided by the IAPS. This combined stimulus set has been successfully used to investigate the neural mechanisms of fear and anxiety underlying while providing appropriate negative (and neutral) image categories that were able to evoke threat-related neural responses (Pedersen, Muftuler, & Larson, 2019; Quiñones-Camacho, Wu, & Davis, 2018). However, NAPS images still need further validation in evoking reliable fear and anxiety responses, considering the database's categories and the images' effect of social and non-social cues.

Somatosensory, e.g. electro-tactile stimulation has been frequently used as threatening sensory US in animal (e.g. electric foot shock for rodents; (Zoicas, Slattery, & Neumann, 2014) as well as in human studies (Schmitz & Grillon, 2012). Electro-tactile stimulation is commonly used because of its noxious nature, that is universally perceived as aversive and unpleasant (Elman & Borsook, 2018; Sehlmeyer et al., 2009). Aversive electric pulses are produced with a constant current stimulator while

the current intensity is adapted to an individual strength, based on given instructions prior to the start of the main experiment. In threat evoking experiments, individual intensity usually refers to a threshold at which the electrical stimulus is perceived and reported as unpleasant but bearable by the participant (Levine, Kumpf, Rupprecht, & Schwarzbach, 2020). Electric shock lasting 100 ms with an intensity range of 1-5 mA have been reported to be most effective in evoking desired fear responses (Schmitz & Grillon, 2012). Nevertheless, standardized shock strength calibration procedures are still missing for now and conducted procedures are often described insufficiently (Ferry & Nelson, 2020; Glenn, Lieberman, & Hajcak, 2012; Grillon et al., 2004). However, the publication of (Onat & Büchel, 2015) is often cited for its modification originating from a Bayesian adaptive psychometric method (Watson & Pelli, 1983). The procedure starts with a presentation of an electrical stimulus with an initial strength that will be increased step-by-step until participants report the intensity level painful but bearable (Onat & Büchel, 2015). Another research area that is using such quantitative sensory testing (QST) procedures focusses on quantifying sensory function in patients suffering from neurologic conditions (e.g. fibromyalgia). These sensory testing procedures are psychophysical in their nature as well, meaning that an objective physical stimulus (electrical stimulus or thermal stimulus) will be rated in order to assess sensory dysfunction (Shy et al., 2003). Using the so-called "method of limits" for such estimating sensory thresholds, stimulus intensity will be increased continuously while participants need to respond with respect to a specific prior set criterion (Shy et al., 2003). Such methods commonly used for detecting neuropathological dysfunction are often better standardized and psychometric characteristics could be easily extracted from psychometric function. Still, such detailed descriptions of the aversive stimulus calibration are lacking in threat of shock paradigms. However, electrode location is typically poorly standardized and described such as, at the non-dominant hand (Ferry & Nelson, 2020), the right wrist (Grillon et al., 2004), the left shin (Tabbert, Stark, Kirsch, & Vaitl, 2005) or at the right foot top without any further specification with respect to exact position. In contrast, in pain research these locations are more precise, i.e. "tibial bone, 100 mm distal from the caudal end of the patella." (Hay, Okkerse, van Amerongen, & Groeneveld, 2016) or "right forearm 7cm distal to the cubital fossa." (Xia, Mørch, & Andersen, 2016). In summary, picture stimuli are often used because of their high practicability while being appropriate for subjects in a wide range of

population (e.g. children). Fear and anxiety responses could be evoked successfully, but the impact of individual factors that contribute to image evaluation and responding cannot be controlled. Electrical stimulus properties could be controlled better, but a separate calibration procedure is needed for each participant. These procedures often contain a large number of shocks until a suitable intensity is found. Additionally, such procedures are biased by experimenter-participant interaction that could have effects on threshold intensity while calibration procedure. An efficient and standardized procedure, that causes minimal discomfort to the participant while they still could stop the procedure at any time, is yet missing.

### 1.3.3  How to Measure Fear and Anxiety Responses?

Overall, emotional responses can be derived from behavioral (e.g. RT), neurobiological (e.g. functional neuroimaging), physiological (e.g. heart rate (HR)) or subjective (e.g. self-report) parameters (for an overview see: (Lonsdorf et al., 2017)). The assessment of emotional discrete as well as dimensional response patterns, while in consideration of their convergence (e.g. correlation; (Mauss & Robinson, 2009), remains to be one of the main challenges in emotion research. Response pattern extraction from various data sources could lead to better symptom descriptions and patient´s classification with a promise to enhance the accuracy of clinical decisions. The methods used in this thesis regarding psychological variables and functional neuroimaging methods to assess and validate fear and anxiety responses will be the focus of the following section.

The psychological perspective of fear and anxiety comprises several self-report measures for state and trait variables. These methods have been successfully used over the past decades for sample description and group differentiation, for instance in high vs. low anxious subjects with respect to their individual state and trait.

The State-Trait Anxiety Inventory (STAI; (Spielberger, 1983), which is a self-report instrument for measuring both trait (STAI-T) and state anxiety (STAI-S) by assessing two subscales of 20 items each, is used in clinical practice and research (Gustafson et al., 2020). STAI-S has been widely used for assessing fluctuations of anxiety levels, for example in pre-post measuring of the effect of task-evoked anxiety as an outcome variable in experimental paradigms (Rossi & Pourtois, 2012). Further, both scales are

often successfully discriminating high anxious and low anxious participants by using a median split method in a healthy subject sample. Given an example from conditioning research, it was found that low and high anxious trait participants did not differ in evaluating predictable threat, but high anxious individuals showed hypersensitivity to the unpredictable threat highlighting a biased threat evaluation (e.g. overestimating occurrence and extend of aversiveness) in comparison to the ambiguous threat (Stegmann, Reicherts, Andreatta, Pauli, & Wieser, 2019). Moreover, higher STAI-S anxiety was found to be able to predict increased left amygdala and superior temporal sulcus activity as a response to negatively valanced face stimuli in high perceptual load conditions, thus pointing to a disruptive effect on perceptual processing and top-down control during transient anxiety (Bishop, Jenkins, & Lawrence, 2007). Evidence suggests that the STAI represents a suitable tool for categorizing subjects into subclasses and point to investigating trait and state anxiety as a potential risk factor in threat processing.

Anxiety Sensitivity (AS) represents another stable psychological trait which describes a fear of anxiety-related symptoms (e.g. heart palpitations) that could potentially have harmful (e.g. somatic, social) consequences and suggest a risk factor in developing an anxiety disorder symptomatic (Hovenkamp-Hermelink et al., 2019; Rodriguez, Bruce, Pagano, Spencer, & Keller, 2004). An Unidimensional level of AS is commonly assessed by the Anxiety Sensitivity Index (ASI; (Reiss, 1987; Reiss, Peterson, Gursky, & McNally, 1986). Evidence suggests that higher AS individuals show threat attentional bias (Hunt, Keogh, & French, 2007), higher startle potentiation in unpredictable threat anticipation and reported higher anxiety levels in general with respect to both predictable and unpredictable threat condition (Nelson, Hodges, Hajcak, & Shankman, 2015). Level of AS, representing the general trait anxiety level towards physical concerns, has been termed out to be a crucial determinant in threat possessing and is directly related to the maintenance of symptomatic anxiety and depression disorder (Nelson et al., 2015). Functional connectivity studies suggested that higher scores in the cognitive subscale of the ASI was associated with increased amygdala-vmPFC coupling (Porta-Casteràs et al., 2020) as well as heightened amygdala activity during processing of fear-symptom words when presented following unexpected timings (Yang et al., 2016).

Intolerance to Uncertainty (IU) signifies a further cognitive vulnerable risk-factor in anxiety disorder symptomatic. IU is especially related to the thoughts of worry and tendency to interpret ambiguous situations as potentially threatening and negative cognitions about uncertainty (Birrell, Meares, Wilkinson, & Freeston, 2011; Koerner & Dugas, 2008). More, IU was assumed to be directly involved in modulating anxiety-related cognition and behavior (e.g. worry, hypervigilance; (Holaway, Heimberg, & Coles, 2006; Krohne, 1993) and is a fundamental feature for assessing GAD treatment course and outcome (Dugas et al., 2005). However, for measuring the impact of intolerance to uncertainty trait, the Intolerance to Uncertainty Scale has been developed (IUS; (Michel Dugas, Mark Freeston, & Robert Ladouceur, 1997). Further, it causes increased skin conductance response as well as amygdala and ventromedial prefrontal cortex (vmPFC) activity for both learned threat and safety cues. This finding was supposed to result in poor fear extinction learning, indicating biased threat discrimination (Morriss, Christakou, & van Reekum, 2016). Moreover, amygdala hyperactivity was found in correlation with weakened posterior frontomedian cortex (pFMC), dorsolateral prefrontal cortex (dlPFC) and anterior cingulate cortex (ACC) activity during threat uncertainty, which indicated higher engagement during threat encoding, but weaker emotion regulation in high-IU individuals (Schienle, Köchel, Ebner, Reishofer, & Schäfer, 2010). In sum, previous findings point out that IU reflects the fear of the unknown and is a crucial risk factor in uncertain threat evaluation contributing to the complex of anxiety disorder symptoms.

Affect represents a further psychological construct of mood states and plays a crucial role in evaluating fearful feelings. Positive affect (PA) includes positively valanced feelings (e.g. interest, joy; (Miller, 2011) and will be often contrasted to negative affect (NA), which is characterized by negatively-valanced emotions (e.g. fear, shame; (Stringer, 2013). Individual differences in current PA and NA could be measured independently by the 20-item self-report inventory, called "The Positive And Negative Affect Schedule" (PANAS; (Watson, Clark, & Tellegen, 1988). The PANAS is often used in experimental studies in assessment of actual affect or fluctuations in affect and can be assessed repeatedly (Rossi & Pourtois, 2012). Given the so-called "risk-as-feelings hypothesis", that refers to the key role of affect during present threat and decision-making process (Loewenstein, Weber, Hsee, & Welch, 2001), higher risk perception was found to be associated with higher negative affect and stress level,

indicating the crucial role of feelings besides rational cognitive evaluation (Sobkow, Traczyk, & Zaleskiewicz, 2016). Another study evaluated the relation of affect dimensions on anxiety and depression in a clinical sample and found that NA was highly correlated with depression and anxiety symptoms, while PA is inversely correlated with anxiety and depression (Díaz-García et al., 2020). Further, a subpattern in social anxiety disorder was discovered to be related to low PA levels while NA levels were high (Cohen et al., 2017). With regard to threat processing, NA, considered as a trait, could successfully be decoded from threat-related brain patterns (e.g. dmPFC, vmPFC and Insula), while no reliable pattern was found for PA trait. Therefore the involvement of specific brain regions in NA-modulated threat processing can be discussed (Fernandes et al., 2017b). Furthermore, results from similar studies indicate that amygdala-related threat encoding of unpleasant pictures is diminished in high PA trait individuals, suggesting threat attention modulation by PA (Sanchez et al., 2015).

Visual analogue scales (VAS), as well as related numeric rating scales (NRS), are commonly used for measuring pain- and anxiety-related individual responses via self-report with respect to, e.g. a threat condition or the efficacy of treatment at a conscious subjective level. The VAS consists of a straight continuous horizontal scale while a vertical mark at the beginning and end represents a scale limit (Phan et al., 2012). In contrast, the NRS represents a discontinuous measure that is displayed in a numerical sequence ranging from 0 to 10 in single steps (Phan et al., 2012). Given a specific question, participants are rating, e.g. their actual feeling or perception along this scale. For the retrospective study of anxiety responses and fluctuations, the VAS-Anxiety (VAS-A) scale estimates the actual perceived anxiety level (e.g. "How anxious do you feel at the moment?") with two extreme anchors at both ends, for example "not anxious at all" to "highly anxious" (Rossi & Pourtois, 2012). In pain perception experiments such an item would be used to measure pain perception in respect to stimulus intensity (e.g. "slight pain" to "maximum pain"; (Carlsson, 1983). Both methods have been found to be suitable, although they represent a one-item tool. Nevertheless, asking explicitly for "anxiety" could bias responding (Rossi & Pourtois, 2012) and might be the reason why some studies implicitly ask for specific anxiety dimension facets (e.g. "nervousness"; (Somerville et al., 2013) to assess anxiety experiences indirectly. Higher task-evoked anxiety was reported during unpredictable threat conditions in comparison to predictable and neutral threat conditions (Schroijen et al., 2016; Somerville, Whalen,

& Kelley, 2010), which suggests that such measures are able to illustrate and capture conscious individual responses with regard to threat properties.

Taken together, a lot of evidence points to the conclusion that anxiety-related state and trait risk factors play a crucial role in threat encoding, processing and coping. Thereby psychological measures like self-reported questionnaires and rating scales are valid markers of fear- and anxiety states and inter-individual disposition.

During the past decades, functional neuroimaging has emerged as a suitable tool for indirectly encoding brain states and identifying corresponding brain regions. Dynamic changes in brain activity can be measured with functional magnetic resonance imaging (fMRI) techniques and evaluated via mass-univariate and further multivariate pattern analyses. fMRI detects dynamic changes in blood flow, which can be linked to local neuronal activation. Deoxygenated and oxygenated hemoglobin have different magnetic properties that are disturbing the surrounding magnetic field of the MRI scanner. Thus, the blood BOLD signal refers to the ratio of oxygenated and deoxygenated blood (assumed to depict differences in neural activation level) and the global MRI signal change (field changes; (Jenkinson & Chappell, 2018). Neural activity, elicited from a stimulus, can be estimated by a hemodynamic response function (HRF) that represents the idealized BOLD signal following stimulus onset over time. The peak of the canonical HRF function lies in a range of 6-20 seconds (Jenkinson & Chappell, 2018) and therefore time-to-time recording of brain activity needs to be acquired quickly. Echo-planar imaging (EPI) allows fast, straightforward acquisition of 2-dimensional individual images (so-called slices) in sequential order, often complemented with simultaneous acquisition of multiple slices (e.g. parallel or multiband sequences (Jenkinson & Chappell, 2018). One single MR-slice contains a matrix of voxels and time series of acquired brain activation can be extracted from each single voxel across slices in order to analyze differences in BOLD response (Jenkinson & Chappell, 2018). After the preprocessing of such volumes, encoding models are using neural activity patterns as an input for predicting, e.g. different stimulus types of an experimental condition for further analysis (Kriegeskorte & Kievit, 2013). Commonly the ratio of measured and predicted responses is estimated via general linear model (GLM) in respect to a prior set model of task-based fMRI (Jenkinson & Chappell, 2018). Model-based experimental conditions, formulated as contrasts, are used for statistical hypotheses testing (i.e. analysis of variance; ANOVA) at first- and group-level analysis.

The mass-univariate approach is the most commonly used technique for investigating location-based information processing in the brain (Popov, Ostarek, & Tenison, 2018). Its underlying analysis is based on averaged activation comparisons at single voxel-level, in a specific pre-defined region, with respect to experimental conditions (e.g. condition A vs. condition B). Even if relational information at the individual voxel level (e.g. location A > location B) helps to understand engagement of specific locations in different (task) conditions, such univariate subtraction analyses do not help us to understand inter-voxel representations, so-called neural activity patterns(Davis & Poldrack, 2013). Further, upcoming evidence from resting-state fMRI, for instance, has indicated that brain regions communicate with each other and are functionally linked, rather than work in isolation (van den Heuvel & Hulshoff Pol, 2010) which raises the need for further sophisticated encoding models such as multivariate pattern analyses (MVPA; (Haxby, Connolly, & Guntupalli, 2014; Popov et al., 2018). MVPA has been often used for detecting spatial patterns of neural representations, although it may provide considerable further benefit for assessing representational dynamics (King & Dehaene, 2014).

### 1.3.4  Neural Representational Models

Since the early beginning of emotion research, the amygdala has been named as a crucial structure involved in threat detection, fear expression and caring for defensive response behavior. Initial evidence for its fundamental role in threat detection was drawn from lesion studies which found that amygdala damage was related to deficits in recognizing fearful face expression (Adolphs et al., 1999; Adolphs, Tranel, & Damasio, 1998). Further, neurofunctional studies found amygdala hyperactivity (Morris et al., 1998) during a presentation of survival-relevant aversive stimuli of spiders and snakes, which are known to be universally threatening and usually provoking selective attention bias in most of the participants (Ohman & Mineka, 2001).

A simplified overview of its anatomical structure and its respective functional projections is provided in Figure 1.3 (Shackman & Fox, 2016). Evidence suggests, that glutamatergic neurons within the basolateral amygdaloid nucleus (BLA) receive and integrate sensory input from primary sensory areas, while this information is passed through higher cortical areas such as prefrontal cortices (PFCs) and hippocampus (Di Marino, Etienne, & Niddam, 2016; Janak & Tye, 2015). BLA mainly forwards the signal

to the central amygdaloid nucleus (CeA), nucleus accumbens (NAcc) and the bed nucleus of the stria terminalis (BNST) to initiate defensive responses and control for response expression (Janak & Tye, 2015; LeDoux, 2000).

**Figure 1.3**

*Overview of Information Flow within Amygdaloid Nuclei*
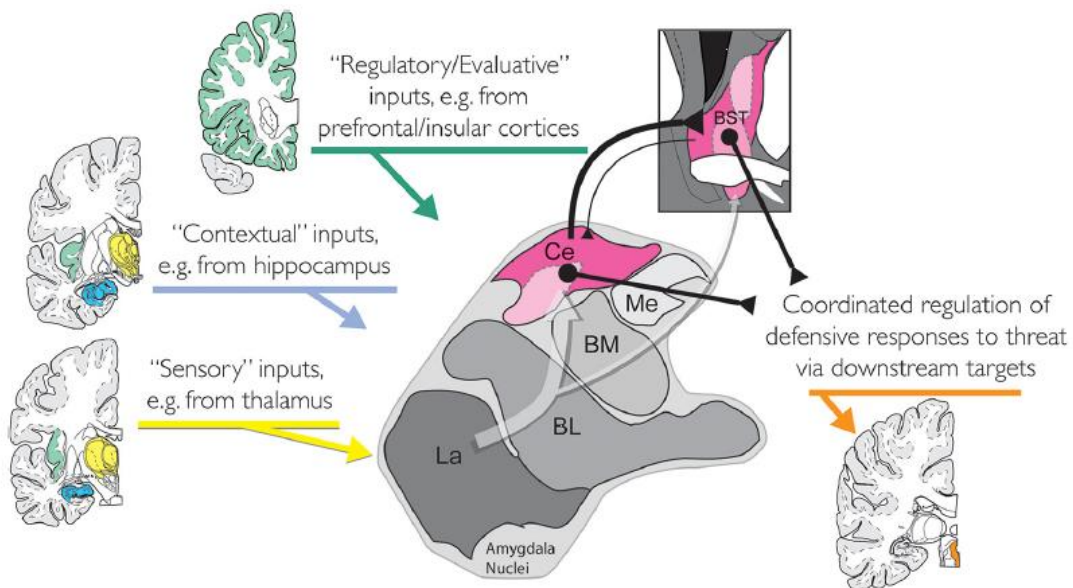


Indirect input signal (translucent white arrow) coming from sensory (yellow), contextual (blue), and regulatory (green) input areas pass through the different lower-level amygdala subnuclei and is subsequently forwarded to central amygdala complex (Ce) and bed nucleus of the stria terminals (BST), or directly to BST. Ce and BST (pink) are interconnected and project (efferent connection) to further downstream regions (orange) for initiating and modulating fear and anxiety states. (BL, Basolateral; BM, basomedial; Ce, central; La, lateral; Me, medial subnuclei of the amygdala). Figure was reprinted from "Contributions of the Central Extended Amygdala to Fear and Anxiety" by A. J. Shackman and A. S. Fox, 2016, *The Journal of Neuroscience*,36(31), p. 8051.

Over the past decades, great progress in investigating the neural mechanisms underlying fear and anxiety mental states ("fearful feelings") has been made, while studies directly focused on threat properties of both concepts. Investigating threat processing mechanisms within the amygdala subregions yielded further evidence for the involvement of extended amygdala regions caring for uncertain threat processing. With respect to anxiety state, the BNST, an extended amygdala region, is a key structure and therefore needs to be considered in neural models with respect to an uncertain threat. The crucial role of BNST, especially for anxiety, originates from research of anxiety threat properties. The initial neural model from Davis (1998) for presenting structures underlying fear and anxiety, suggested that conditioned explicit

cues evoke short term activation within the CeA, while BNST was identified to be involved in unconditioned diffuse cues that cause long term activation (Davis, 1998). However, given a large amount of evidence coming from animal and human research, an entire model of threat underlying mechanisms, that consider a cortical network, is still missing. Advanced fear- and anxiety neural processing models originating from several perspectives have been postulated, although they are still under revision and in the focus of current scientific debates. Current models will be presented and discussed in the following section.

Evidence for detecting fearful events, as well as expressing and initiating related responses, does not necessarily imply that the amygdala is also responsible for fear and anxiety experiences and feelings. Fearful feelings are fundamental in models that consider an emotional consciousness view; this view proposes existing divergent neural mechanisms dependent on the threat differences and consciousness. In the year 1996, LeDoux already assumed the existence of two separate operating pathways: the so-called "low" and "high" road signaling cascades (LeDoux, 1996). Affective stimulus information is recognized at the sensory thalamus level that forwards fear information either directly (low road; quick detection) or while bypassing it to the sensory and frontal cortex (high road; slower detection) to the amygdala (Acevedo & Ekkekakis, 2006). Additionally, interoceptive threat information will be forwarded via multiple low roads, considering sensory thalamus and further other subcortical regions (e.g. periaqueductal gray (PAG), a nucleus of the solitary tract (Acevedo & Ekkekakis, 2006; LeDoux, 1998)). According to this model, affective stimulus properties determine to recruit of input sources, finally projecting to the amygdala. The model considers a rapid and automatic threat detection potential of the amygdala for natural dangers (LeDoux, 1998), while it acts as the so-called cortical alarm system for fear (Liddell et al., 2005).

The later postulated "Two-System Framework" of LeDoux and Pine (2016) strengthened the view of multiple fear- and anxiety neural circuits that operate in parallel with respect to fear state properties. In contrast to the evolutionary driven models (Perusini & Fanselow, 2015), there is the assumption that not fear but danger is universal while the experience and response to the threat are unique (Mobbs et al., 2019). The model proposes differential brain coding mechanisms for an emotional and non-emotional fear state regarding consciousness (LeDoux & Pine, 2016). According

to this model, fear represents an unconscious state that leads to defensive responses – such that are evoked by the defensive survival circuit. In contrast, conscious emotional events lead to fearful feelings that are recruiting higher cognitive circuits (LeDoux & Pine, 2016). With respect to neural underpinnings, the amygdala complex is still assumed to be the central hub for detecting and differentiating between present and uncertain threat at an initial stage (LeDoux & Pine, 2016). Acute threat information will be initially processed within LA that either forwards information to BLA or to CeA for initiating defensive reactions (e.g. flight response). The BLA pathway projects to the BNST or directly to the NAcc that prepares defensive actions (e.g. avoidance). Uncertain threat information, captured by the BNST, could either directly evoke defensive reactions or defensive actions while bypassing the NAcc. An overview of threat-related signal cascade, postulated by LeDoux and Pine (2016), considers the BNST as a crucial structure in uncertain threat processing is depicted in Figure 1.4.

**Figure 1.4**

*Overview of Information Flow of Extended Amygdala Structures*
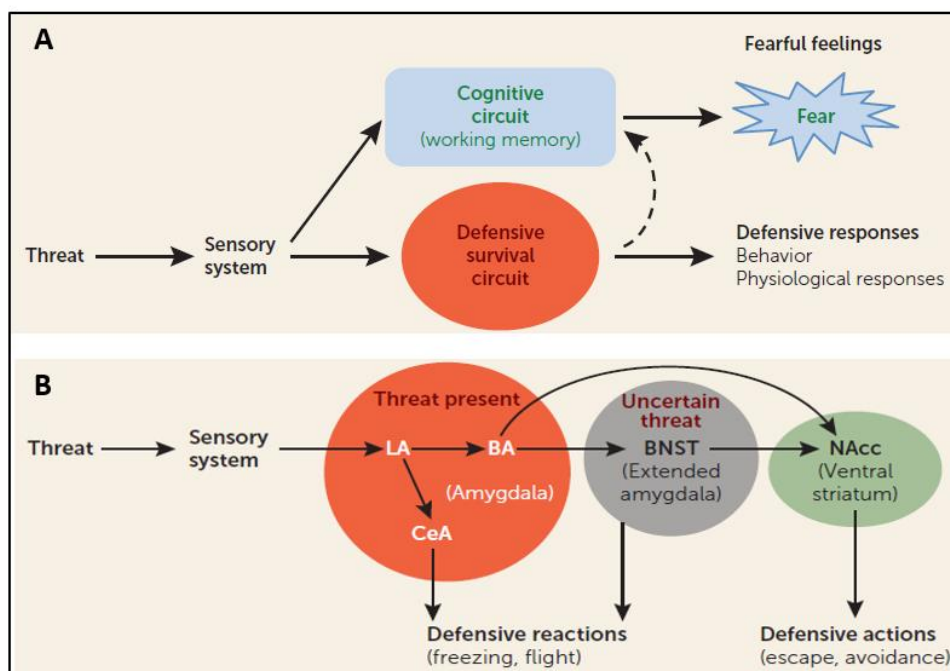


In case of an acute threat, LA immediately forwards information to CeA for initiating defensive reactions (e.g. a flight). In case of an uncertain threat, LA further forwards information either directly to the nucleus accumbens (NAcc), or by bypassing the BNST. Both routes lead to defensive actions (e.g. avoidance) modulated by the NAcc. The short route, that ends at the BNST subsequently evokes defensive reactions similar evoked as by the CeA. Figure was reprinted from "Using Neuroscience to Help Understand Fear and Anxiety: A Two-System Framework" by J.E. LeDoux and D. S. Pine, 2016, *The American Journal of Psychiatry,* 173(11), p. 2-3.

The framework of LeDoux and Pine (2016) is in concordance with published models of emotion regulation that postulate the involvement of different cortical structures operating in a network, wherein consciousness represents a key factor. What comes to explicit emotion regulation, evidence suggests an executive network that comprises frontoparietal regions such as dlPFC, ventrolateral PFC (vlPFC), dorsal anterior cingulate cortex (dACC), insula, parietal cortex and motor areas (Etkin, Büchel, & Gross, 2015). In contrast, implicit emotion regulation that is known for expiring automatically as a response to a specific stimulus, is mainly associated with ventral ACC (vACC) and ventromedial PFC (vmPFC) activity, that was found to be increased in imminent acute threat processing (Etkin et al., 2015). Further, emotional-reactivity was observed to be related to dACC, amygdala, insula and PAG activity (Etkin et al., 2015). Concomitantly with the framework of LeDoux and Pine (2016), these emotional regulation models assume a crucial role of consciousness that is not negligible.

Contradicting to this view so-called "fear-center models" (LeDoux & Pine, 2016) assume an innate operating subcortical fear system that cares both for fear and anxiety mechanisms while consciousness plays, if considered, a subordinate role (Panksepp et al., 2011; Panksepp, Knutson, & Pruitt, 2013). According to these models, the amygdala complex represents the center of an evolutionary-based fear circuit. An immediate acute threat is detected by the amygdale fear circuit which then evokes a fear state outputting information to higher anatomical targets for initiating defensive fear responses (Davis, 1992; Ohman & Mineka, 2001). The latest published neurobehavioral fear-center model by Perusini and Fanselow (2015) originates from the view that fear state represents an evolutionary driven neural-behavior system (Perusini & Fanselow, 2015). A schematic overview of this entire fear center circuit is presented in Figure 1.5. Antecedents signals enhance fear state and evoke consequences resulting in observable behavior (Mobbs et al., 2019). In this model, the BLA receives and integrates input from sensory (e.g. auditory cortex) and thalamic regions, as well as contextual input from hippocampus for modulating fear learning and renewal following extinction (Perusini & Fanselow, 2015). BLA is connected with CeA, that additional receives GABAergic (gamma aminobutyric acid) input from intercalated cell mass projections that are known to be involved in extinction learning. CeA subsequently forwards information to periaqueductal gray (PAG) and BNST for preparing fear responding. Moreover, neuromodulatory dorsal raphe nucleus inputs

the converge to BLA and PAG. Behavioral outputs are modulated by medial prefrontal cortex (mPFC) structures, such as prelimbic (PL) and infralimbic cortex (IL) structures, which are assumed to be related to fear expression after extinction (Perusini & Fanselow, 2015).

**Figure 1.5**

*Schematic Overview of an Entire Fear and Anxiety Neural Circuit*
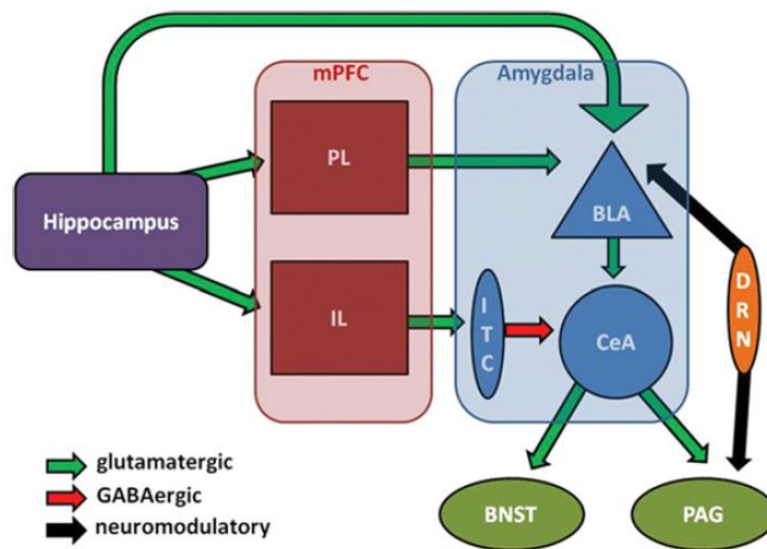


The basolateral amygdala (BLA) receives glutamatergic input (green arrows) from the hippocampus and medial prefrontal cortex (mPFC), which will be forwarded to the bed nucleus of stria terminalis (BNST) and periaqueductal gray (PAG) via central amygdala (CeA) for preparing an adequate fear response. CeA also receives direct GABAergic input (red arrow) from intercalated cell masses (ITC) that are connected to the infralimbic cortex (IL), assumed to be involved in extinction learning. Neuromodulatory inputs (black arrows) from dorsal raphe nucleus (DRN) project to BLA (e.g. serotonergic projection) and PAG for modulating defensive behaviors (e.g. freezing). Moreover, prelimbic cortex (PL) inputs to the BLA are assumed to contribute to fear response extent. Figure was reprinted from "Neurobehavioral perspectives on the distinction between fear and anxiety" by J.N. Perusini and M. S. Fanselow, 2015, Learning & Memory, 22(9), p. 418.

However, the authors assume that fear represents a post-encounter defense while anxiety is related to pre-encounter behavior (Perusini & Fanselow, 2015). Given the lack of experimental investigations that could reliably distinguish between fear and anxiety neural mechanisms, the authors conclude that it might be too early to assume differential neural networks (Perusini & Fanselow, 2015).

Taking together, a public debate still remains whether there is a common subcortical neural circuit for both fear and anxiety processes originating from a pure survival-relevant neurobiological perspective, or whether there are divergent mechanisms in

which consciousness plays a further crucial role and should be integrated into the view of parallel operating mechanisms. This debate originates from another underlying discussion about a fear definition that includes, depending on the view, a consciousness of subjective state as a further concept, whereas other perspectives define fear as an observable performed behavior (Mobbs et al., 2019). In conclusion, LeDoux and Pine (2016) assumed that subjective feeling of fear and anxiety is produced and modulated by cortical conscious networks that process in higher-order cognitive structures, such as lateral and medial prefrontal cortex and neocortex. Therefore, they are assuming separate operating neural circuits depending on threat consciousness that operate beyond the subcortical circuit (LeDoux & Pine, 2016). This view proposes for distinguishing non-emotional survival relevant fear neural mechanisms from emotional experiences that are conscious and assumed to be fundamental in patients suffering from uncontrolled fear and anxiety feelings (LeDoux, 2014). Support for this assumption is raising from an emotion research perspective in which brain processes are assumed to be able to make predictions and operating in a complex dynamic system, rather than simply responding to stimuli, while the brain is operating dynamically in a complex system (Mobbs et al., 2019). However, LeDoux assumes that this complexity of mental states could not be examined in animal models and therefore claims for considering conscious emotional aspects into fear- and anxiety models (Mobbs et al., 2019). The opposing view, that advocates for the initial fear-center view, is accepted by another group of experts in this research field (i.e. Michael Fanselow, Robert Rescorla). Given this perspective, internal feelings of fear and anxiety could be explained within the framework of behavioral and physiological responses (Fanselow & Pennington, 2017). Further, they assume that subjective feelings, as additionally considered in LeDoux´s view, are not scientifically grounded enough and should therefore not included into neurobiological models of fear and anxiety (Perusini & Fanselow, 2015). Within their view, such subjective experiences could be explained with the neurobiology of defensive behaviors (Perusini & Fanselow, 2015). Moreover, they criticize that literature selection, that is grounded the concept of LeDoux and Pine (2016), is biased and that focusing again on subjective feelings, as done in psychiatry from early beginnings would represent a retrograde step for psychiatry-related research (Fanselow & Pennington, 2017). To conclude, the ongoing

debate about neural underlying mechanisms and fear and anxiety conceptualization (Mobbs et al., 2019) highlights the need for further empirical work.

### 1.3.5  Evidence for a Neural Signature

Research has made great progress in disentangling the neural correlates of fear and anxiety. The following section presents a selection and review of the latest neuroimaging studies concerning this topic. Further, the impact of stimulus-based neural activity will be discussed.

To evoke fear- and anxiety responses while considering threat specific properties, the no (N), predictable (P) and unpredictable (U) threat task (NPU) has been found to be a suitable paradigm (Schmitz & Grillon, 2012) that is often proposed as gold-standard (Balderston et al., 2017). During the paradigm, visual cues (e.g. geometric shapes) are presented in either a predictable (fear) or unpredictable (anxiety) way while their duration is varied (short-duration, phasic (fear) vs. long-duration, sustained (anxiety); (Schmitz & Grillon, 2012). The task consists of different blocks in which either no shock (N-blocks), a shock during cue presentation (P-blocks) or a shock that might occur at any time (U-blocks) will be presented. Participants are instructed prior to the experiment and block-condition is shown prior to each block. With respect to fear condition (P ≠ N and U), Balderston and colleagues (2017) found neural pattern activity in the dmPFC and insula (fear network) that was unique for fear especially during predictable cue condition (P>U and P>N) (Balderston et al., 2017). They found another pattern of activity in the ventromedial prefrontal cortex and posterior cingulate cortex as a part of the default mode network in both fear and anxiety (P and U ≠ N), whereas there was less activity during predictable and unpredictable compared to neutral condition (P>N and U>N). The right dlPFC cluster showed similar activation pattern as the DMN, but with higher activity during the predictable and unpredictable condition compared to neutral cue trials (P>N and U>N; (Balderston et al., 2017). In conclusion, fear was found to be processed in the fear network uniquely, whereas the authors assumed that dlPFC regulates anxiety. Interestingly, BNST activity was not observed (Balderston et al., 2017).

Still, continuous threat hypervigilance and monitoring, that are common in anxiety disorder symptomatic, are rarely targeted by such paradigms using single stimulus presentation. Therefore, Somerville and colleagues (2010) investigated sustained

arousal states where participants were presented to a continuous visible stimulus line signalizing the accumulated probability for an upcoming aversive event (shock). Uprising threat probability was associated with enhanced ventrobasal forebrain (VBF)/BNST, right insula, bilateral dlPFC as well as dmPFC activity which positively correlated with participant's level of anxiety (Somerville et al., 2010). These results indicate a specialized network for continuous threat monitoring and anticipation that was found to be hyperactive in high anxious individuals.

For further investigation of the effect of threat certainty, Somerville et al. (2013) investigated fear- (predictable threat and transient-response) and anxiety-related (unpredictable threat and sustained-response) threat in a mixed block-event-related fMRI design while using different valence levels (negative, neutral). In predictable negative blocks, a descending numeric countdown reliably announced the presentation of a negative picture. During unpredictable negative blocks, a negative picture could occur randomly at any time. Neutral images were presented in the same way and block condition was announced prior to each block. The transient response related neural activity (negative > neutral pictures) was found in amygdala, extended amygdala/insula, inferior frontal gyrus, midbrain/PAG, middle frontal gyrus and visual cortex. For the amygdala, a clear preference for negative valence (negative > neutral pictures) was found, while there was no effect of predictability. Nonetheless, the interaction of valance by predictability considering IUS ratings reached significance, further indicating a key role of the amygdala in responding to unpredictable negative picture blocks in individuals with greater IU score (Somerville et al., 2013). Neural activity for sustained responses was found in the inferior frontal gyrus, the insular cortex and right VBF/BNST. Furthermore, in greater Brodmann Area 47, lateral /insula and VBF/BNST sustained activity was shown for negative (vs. neutral) and unpredictable (vs. predictable) states. Higher rates of anxiety were found for negative (vs. neutral), unpredictable (vs. predictable) and negative unpredictable (vs. neutral unpredictable) blocks indicating higher task-evoked anxiety for transient (fear) in comparison to sustained (anxiety) trials. In conclusion, Somerville and colleagues (2013) found further evidence for the amygdala-fear and VBF/BNST-anxiety relationship while IU predicted the extend of activation within the amygdala and insula, but not in the VBF/BNST complex (Somerville et al., 2013). Pedersen and colleagues (2019) used a modified version of the Somerville et al. (2013) paradigm for further

investigation of functional differences in the amygdala and BNST in transient and sustained threat responding while using a high-resolution 7-Tesla Magnetic Resonance (MR) scanner (Pedersen et al., 2019). The complete task was adapted from Sommerville et al. (2013), while a set of combined IAPS and NAPS pictures was used as a threatening stimulus. In contrast to the countdown procedure (Somerville et al., 2013), they presented a clock image prior to each picture presentation that indicated the duration of anticipation period for predictability. Results suggested that transient activation in comparison to sustained activation was found to be greater in centromedial amygdala whereas the BNST showed equal activation pattern for both conditions, which contradicts Somerville´s assumption of a structural and functional double dissociation (Pedersen et al., 2019). Moreover, the amygdala was found to be mainly involved to care for negative valanced images solely while the BNST seems to care for neutral and negative images in a similar way that may indicate that BNST is fundamental in anxious anticipation rather than in valence rating of the threat itself. Nevertheless, the authors conclude that more research is needed to disentangle temporal response patterns in both structures and to clarify under which circumstances valence modulated by predictability affects region-specific responses (Pedersen et al., 2019). To study threat anticipation and temporal dynamics of threat processing, Hudson and colleagues (2020) used horror movies as US as they are supposed to be more naturalistic, hence addressing both audio and visual modalities. During horror movie presentation, acute and sustained fear responses were evoked with transient events (sudden-jump scares) therefore creating phases of persisting sustained state (Hudson et al., 2020). The revealed pattern of activation for both fear states are shown in Figure 1.6.

**Figure 1.6**

*Neural Activity in Acute and Sustained Fear*
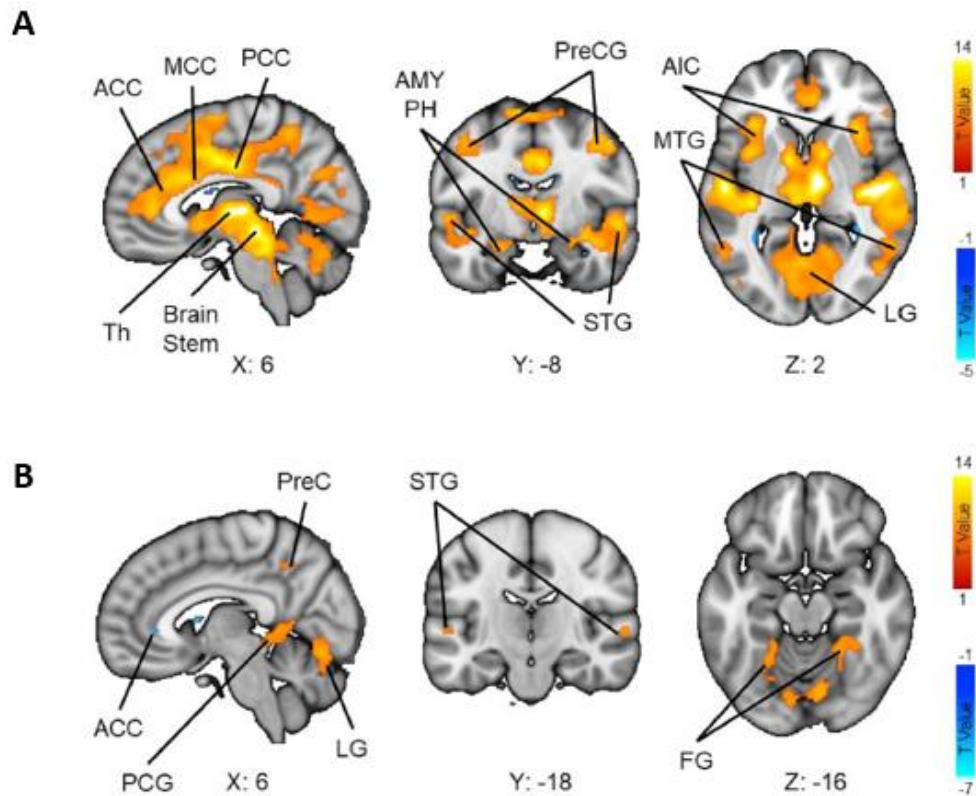


The figure represents BOLD responses to acute (A) and sustained (B) fear across horror movies. A) Acute fear was associated with neural activity in anterior cingulate cortex (ACC), middle cingulate cortex (MCC), posterior cingulate cortex (PCC), thalamus (Th), amygdala (AMY), paraHippocampus (PH), precentral Gyrus (PreCG), superior temporal gyrus (STG), anterior insula cortex (AIC), middle temporal gyrus (MTG) and lingual gyrus (LG). B) Sustained fear was associated with ACC, post-cingulate gyrus (PCG), LG, precuneus (PreC), STG and fusiform gyrus (FG) neural activity. Figure was reprinted from "Dissociable Neural Systems for Unconditioned Acute and Sustained Fear" by M. Hudson, K. Seppälä, V. Putkinen, L. Sun, E. Glerean, T. Karjalainen, H.K. Karlsson, J. Hirvonen and L. Nummenmaa, 2020, *Neuroimage,* 68(5), p. 421.

Results indicated that acute threat created a wide-spread response pattern, in which the PFC, paracentral lobule, amygdala, ACC, Insula, PAG, parahippocampus and thalamus were involved (Hudson et al., 2020). In contrast, sustained activity was found in the cingulate cortex and sensory regions (auditory and visual). The comparison of functional connectivity patterns revealed dissociable networks of acute and sustained fear. The prominence of sensory and motor areas within the fear network was assumed to serve information-gathering to solve threat uncertainty and prepare a suitable behavioral response (Hudson et al., 2020). However, these findings for acute and sustained threat processing might not be bias-free which might be related to the use of horror movies as the aversive event. For example, response might be dependent on

49

uncontrollable individual variables such as experience with horror movies and individual emotional reactions. Moreover, the use of combined sensory stimulation raises the question, whether the activation in sensory areas might reflect stimulus-based activation rather than being part of a neural activity pattern related to fear and anxiety states. Stimulus-modality driven neural activity patterns are a well-known that is related to segregation of the sensory nervous system (vision, hearing, touch, taste, and smell; (Gazzaniga et al., 2009). Nevertheless, studies revealing the role of stimulus-specific neural activation patterns in fear and anxiety mechanisms are missing and it has been suggested that a stimulus-dependent activity pattern contributes to heterogeneity in neuroimaging findings and bias interpretation of results (Sehlmeyer et al., 2009). For example, visual stimuli like an emotional face are associated with activity in the fusiform face area (FFA), emotional scenes evoke lateral occipital cortex activity and pictures showing bodily expressions are associated with fusiform as well as extrastriate body representation areas (Gazzaniga et al., 2009). Comparable results were found for auditory cortical areas which preferentially respond to emotional auditive stimuli (i.e. tones; (Gazzaniga et al., 2009). Somatosensory stimulation as aversive event (i.e. electrical stimulation) was found to be related to increased activation in left caudal dorsal ACC and motor regions (Fullana et al., 2016). Sehlmeyer and colleagues (2009) reviewed modality-specific neural activity patterns within several modalities of fear conditioning (and extinction) studies. Results indicated that the fear network (i.e. amygdala, ACC and insula) was identified reliably in most of the investigations independent of stimulus modality (Sehlmeyer et al., 2009). Additionally, tactile stimulation evoked activation patterns in frontal, occipital, motor and somatosensory cortical areas (Sehlmeyer et al., 2009). In contrast, ACC, dlPFC, thalamus, OFC as well as the occipital region showed strong activation using visual stimuli as aversive events (Sehlmeyer et al., 2009).

Nevertheless, these results must be interpreted with caution because of the low number of included studies, different stimulus categories and the comparison of both conditioning and extinction phase without considering threat of shock paradigms. However, this review indicated, that there must be a core fear network that is commonly activated across stimulus modalities. Systematic reviews investigating the neural signature of fear and anxiety are missing and limited to reviewing fear conditioning studies. But great attempts have been done while using disjunction and conjunction

analyses to investigate interactions in activity patterns for different experimental conditions, such as differences (disjunction = A ∨ B) and commonalities (conjunction = A ∧ B; for an overview see (Rudert & Lohmann, 2008). Naaz, Knight and Depue (2019) were using multimodal stimuli (audio-visual) and implemented such a conjunction analysis for evaluating neural connectivity patterns of fear (explicit threat) and anxiety (ambiguous threat). Participants were exposed to a paradigm where fearful faces, paired with a scream, were presented. During explicit threat trials the stimulus contingency was set to 100% whereas contingency in ambiguous threat trials varied across certain probabilities (80% - 40%). Moreover, the threat anticipation interval for fear (constant: 2000 ms) and anxiety (varying along 500-5000 ms) trials was differed. Fear and anxiety trials were compared to the neutral condition that comprised the same timing intervals and contingency probabilities while a neutral face was paired with chatter sound. Activation commonalities of the explicit and ambiguous threat were found the be related to the amygdala, audio-visual sensory areas, medial geniculate nucleus and right inferior frontal gyrus (Naaz et al., 2019; see Figure 1.7).

**Figure 1.7**

*Task-related Neural Activity Patterns of Explicit and Ambiguous Threat*
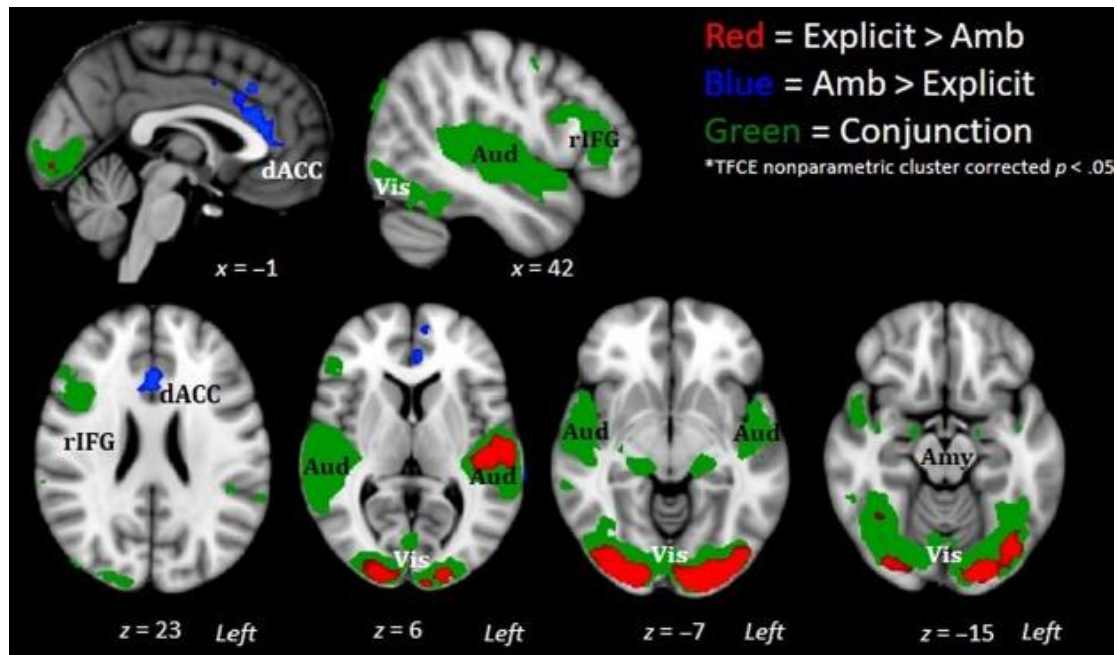


Task-related activity pattern of explicit and ambiguous threat. Comparing differences in explicit to ambiguous threat condition (explicit < ambiguous; red) revealed significant cluster activation pattern in sensory areas (auditory and visual cortex) indicating increased involvement of sensory cortices in fear. Anxiety (ambiguous > explicit; blue) showed enhanced dACC activity compared to the fear condition. Conjunction analysis (explicit ∧ ambiguous) yielded a bilateral cluster comprising the amygdala, visual and auditory areas and their relay station (e.g. medial geniculate gyrus) as well as the right inferior frontal gyrus (rIFG). Conjunction results were threshold free cluster enhancement (TFCE) corrected (*p* > .05). BNST activation pattern was not found following TFCE correction but in voxel-wise (uncorrected) conjunction. Figure was reprinted from "Explicit and Ambiguous Threat Processing: Functionally Dissociable Roles of the Amygdala and Bed Nucleus of the Stria Terminalis" by F. Naaz, L. K. Knight, and B. E. Depue, 2019, *Journal of Cognitive Neuroscience,* 31(4), p. 550.

Seed-based functional connectivity analysis revealed increased functional connectivity of BLA with the primary motor cortex (PMC) during the explicit threat. BNST showed an enhanced connection to the dorsal anterior insula in both threat conditions in comparison to BLA -indicating two different connectivity networks. Moreover, a higher state as well as trait anxiety was associated with decreased BLA-PMC connectivity. Interestingly, enhanced worry and rumination scores went along with deceased coupling strength of BNST and sagittal ACC (sgACC; (Naaz et al., 2019). In conclusion, these findings provide further evidence for the distinct neural mechanisms underlying fear (threat detection and processing; amygdala-related) and anxiety (threat monitoring and anticipation; BNST-related) and further individual differences in fear and anxiety regulation (Naaz et al., 2019). Although if threat predictability (explicit, ambiguous) was

varied, the valence dimension was not varied that was termed out to be a further criterion in disentangling fear from anxiety.

Taken together, methodological variations contribute to heterogeneity in the findings on neural representations and underlying mechanisms of fear and anxiety. The reported neural patterns leave the impression of striking results in fear circuit models and a lack of reliable biomarkers for pathological anxiety. Upcoming strategies for disentangling stimulus-based activity patterns from functional activity-based patterns should enhance the probability of finding the neural core of fear and anxiety representations. Nevertheless, these stimulus-evoked activation patterns have been shown to be a marker for threat monitoring and therefore also provide an informative value for fear and anxiety mechanisms. Shedding light into the temporal course of such activation patterns could clarify to what extent stimulus-based patterns contribute to fear and anxiety processes.

### 1.3.6  Pain – What is the Link?

Comparable with fear, acute pain is characterized as an aversive and unpleasant state that goes along with survival-relevant warning signals and contains clear sensory, cognitive and behavioral consequences (Elman & Borsook, 2018; Margoles & Weiner, 1999). Chronic pain is often linked to the concept of anxiety (Elman & Borsook, 2018) and includes e.g. physical, emotional, individual pain experiences, perceptional conditions and fluctuation of pain state over time (Margoles & Weiner, 1999). Furthermore, it is well known that emotions are modulating pain, especially negative ones. As an example, presenting unpleasant pictures was associated with reliable nociceptive flexion reflex as well as heart rate changes (Rhudy, Williams, McCabe, Nguyen, & Rambo, 2005) and was further enhanced during the unpredictable presentation (Rhudy, Williams, McCabe, Rambo, & Russell, 2006). Nevertheless, the underlying mechanisms are still not fully understood (Rhudy et al., 2006). But the number of studies using unpleasant painful electrical stimulation to elicit fear and anxiety (neural) responses (see 1.3.2) point to a further substantial relationship. Noxious stimuli recruit similar brain regions such as the amygdala, insula, ACC, and somatosensory areas, as indicated by pain signature (Figure 1.8) and further trigger pain responding (Wager et al., 2013; Zheng et al., 2020).

**Figure 1.8**

*Pain-predictive Neural Signature Patterns*
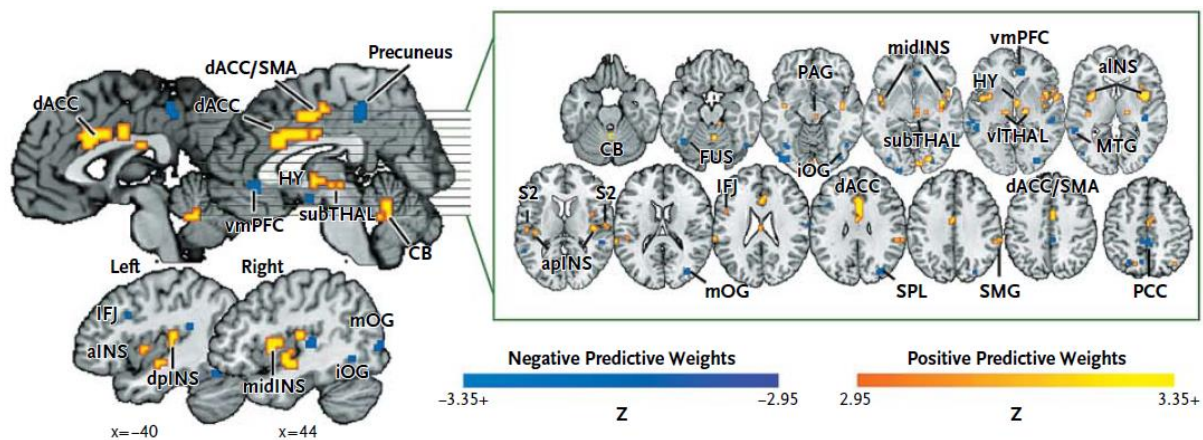


Figure 1.8 represents fMRI-based brain response maps containing voxel-based neural activity patterns with respect to negative (dark blue – bright blue) and positive (orange to yellow) pain predictions. Pain signature comprises positive weights in regions such as, e.g. bilateral dorsal posterior and anterior insula, secondary somatosensory cortex, thalamus and dorsal anterior cingulate cortex. Negative predictive weights are found in e.g. precuneus, dorsal anterior cingulate cortex and supplementary motor area as well as in ventromedial prefrontal cortex. Pain signature indicated a distributed neural activity pattern that was shown to increase (nonlinear) with enhanced stimulus intensity. (Threshold: false discovery rate was set to $q$<0.05; Abbreviations: Anterior cingulate cortex (ACC), cerebellum (CB), fusiform (FUS), hypothalamus (HY), inferior frontal junction (IFJ), insula (INS), middle temporal gyrus (MTG), occipital gyrus (OG), periaqueductal gray matter (PAG), posterior cingulate cortex (PCC), prefrontal cortex (PFC), secondary somatosensory cortex (S2), supplementary motor area (SMA); supramarginal gyrus (SMG); superior parietal lobule (SPL); temporal gyrus (TG), thalamus (THAL); anterior (a), dorsal (d), inferior (i), lateral (l), middle (m), mid-insula, posterior(p), ventral (v). Figure was reprinted from "An fMRI-Based Neurologic Signature of Physical Pain" by T.D. Wager, L. Y. Atlas, M.A. Lindquist, M. Roy, C. Woo and E. Kross, 2013, *The New England Journal of Medicine,* 368(15), p. 1391.

Interestingly, the identified pain signature (Wager et al., 2013) shows some overlap with regions found for fear and anxiety responses (see 1.3.4) but does not contain amygdala structures, although an extended amygdala pattern was formerly found to be related to pain mechanisms as well (Neugebauer, 2015). However, (Elman & Borsook, 2018)) identified distinct features between fear, acute pain, anxiety, and chronic pain specifically related to threat certainty. According to this view, fear and acute pain represent a homeostatic phasic response to an uncertain, immediate threat while defensive responses are associated with avoidance. In contrast, anxiety and chronic pain are reflecting an allostatic response state to an uncertain threat (Elman & Borsook, 2018) while defensive behavior is weakened but constantly present. With respect to pathology, the fear state was assigned to be fundamental in panic disorder (Lai, 2019) and specific phobias (Fanselow & Pennington, 2017) related to a lack in control over adequate acute responses. Chronic pain and anxiety pathology share key

symptoms mainly at the cognitive level (e.g. restlessness, distress) that may be related to increased threat attention (Jordan & Okifuji, 2011). Similarities at threat processing and cognitive level might be the reason why both conditions show high comorbidity (Bernik, Sampaio, & Gandarela, 2013). With respect to pharmacological treatment, antidepressants have been shown to have beneficial effects in anxiety disorders (Bandelow et al., 2012) as well as for treating pain-related diseases (Recla, 2010; Sansone & Sansone, 2008). Nevertheless, although commonalities in symptomatic and neural representation exist, the effect of anxiolytic medication on pain and the effect of analgesic medication on anxiety disorder symptomatic seems to be poorly investigated.

In conclusion, pain shares common features with fear and anxiety concepts at the cognitive, behavioral and neural response level. Differences in acuteness and chronification of pain- and fear-related diseases are related to distinct underlying mechanisms that respond differentially to threat properties (certainty and predictability). Although there is evidence for a unique pain signature, detecting such a neural representation for fear and anxiety is still in its beginning. Identifying the neurological signature of fear and anxiety would open an understanding of the reciprocal relationship with pain mechanisms. Regarding clinical utility, such information could yield further implications to identify a separate and common biomarker that could improve differential diagnosis and treatment recommendations.

## 2 AIMS AND STRUCTURE OF THE THESIS

The aim of this thesis is to investigate commonalities and differences of fear and anxiety circuits in the human brain. The most establish paradigm for investigating fear and anxiety in humans, the NPU-paradigm (Schmitz & Grillon, 2012), uses somatosensory aversive stimuli and investigates the startle reflex as a readout. In contrast, previous imaging studies (Somerville et al., 2013) have focused on evoking fear and anxiety by means of showing pictures. Here, we wanted to use human neuroimaging and behavioral responses as a common readout for fear and anxiety, which we evoke in different modalities in order to identify brain circuitry that processes fear and anxiety on an abstract level. To this aim we expanded the neuroimaging paradigm of Somerville and colleagues (2013) by using somatosensory and visual stimuli as aversive events. As a prerequisite, we had to establish a reliable procedure for delivering aversive somatosensory stimuli, which can also be used inside an MR scanner. This procedure and its evaluation are reported in the chapter "Behavioral Study". The main experiment, which expands Somerville's study to using visual and somatosensory stimulation is reported subsequently in the chapter "Neuroimaging Study".

# 3  BEHAVIORAL STUDY

## 3.1  Aim and Hypotheses

Cutaneous electrical stimulation allows one to assess sensory and emotional processing in healthy participants as well as in patients with neurologic and emotional dysfunctions. In present research, electrical stimulation is used for evoking e.g. anxiety, fear and pain responses in participants while experimental paradigms are presented. In this context, an electro-tactile cue serves as unconditioned stimulus (US) to activate the defensive system and to elicit unconditioned responses UR without requiring learning processes (Lonsdorf et al., 2017). Nevertheless, for evoking e.g. physiological or neural responses to fear, there is the need to calibrate suitable electrical stimulus intensity for each single subject. In these calibration procedures, participants are exposed to an electrical stimulus of different strengths and judging their sensation regarding prior set introductions. Usually for calibrating individuals' pain threshold, participants must judge the stimulus as either e.g. bearable or painful (Levine et al., 2018). Using such a procedure for detecting individual´s pain threshold is often tedious, and participants may have to be exposed to many stimuli in order to identify the proper stimulus intensity at pain threshold. Furthermore, this method requires continuous interaction in which the participants communicates numerous self-reports to the experimenter. Repetitive self-report of pain perception are known to contribute to fluctuations in pain perception (Rosier, Iadarola, & Coghill, 2002). Methodological differences may be the reason for striking differences in terms of reported reliability of stimulus intensity at pain threshold (Letzen et al., 2014; Robinson, Staud, & Price, 2013). Further, dispositional factors such as personality traits that are related to fear, anxiety and pain are known to influence what participants expect and experience in terms of pain. For example, participants with higher anxiety sensitivity showed a shorter detection latency for electrical stimulation which supports the critical role of this particular trait in the experience of pain (Esteve & Camacho, 2008). Furthermore, the "fear of pain" (FOP) trait, that describes the predisposition of how one responds to aversive unexpected experiences, is a further candidate dimension in predicting pain sensations. FOP is known to modulate avoidance tendencies (Suhr & Spickard, 2012), associated with biased pain perception as well as tolerance in

electrical and thermal pain tests (Kirwilliam & Derbyshire, 2008; Roelofs, Peters, Deutz, Spijker, & Vlaeyen, 2005). Next to such traits, the current emotional state seems to influence pain perception as well. In a previous study, lower positive affect state and depression were associated with a higher sensitivity to physical stimuli, i.e. heat and pressure (Sibille et al., 2012).

Until now it remains unclear how stable stimulation parameters are with respect to pain perception and to what extent an individual's disposition, current affect state, and measurement error contribute to fluctuations in pain perception. Taken together, we want parameters, such as stimulus intensity at pain threshold to be valid, reliable, and easy to acquire. Considering the setup of demanding pharmacological studies in which patients undergo an experimental procedure that is repeated for several weeks, there is the need for a high standardized procedure that delivers reproducible thresholds over time. Moreover, identifying a suitable electrode location for stimulus application will enhance reproducibility and cause less discomfort while setting the intensity to a minimum and keeping the validity at a maximum. Another important set of goals is to be able to determine such sensory thresholds within a reasonable amount of time and to minimize the number of unpleasant stimuli.

Therefore, the purpose of the present study was to evaluate our new developed calibration method "**ESTIMATE**" (**E**stimating **STIM**ulus p**A**in **T**hr**E**shold) in terms of test-retest reliability of stimulus intensity at pain threshold at four subsequent timepoints within three sessions using six different electrode positions at the arms and legs. We aimed at keeping the number of painful stimuli low while producing an accurate and precise measure of stimulus intensity at pain threshold. We conducted a baseline session (S1a) and repeated the entire procedure after 15 minutes (S1b), 24 hours (S2), and 168 hours (S3). Each time we also acquired state and trait variables to explain differences and eventual fluctuations in pain perception. We investigated whether (1) stimulus intensities at pain threshold remained stable over time, and whether (2) electrode location does matter with respect to reliability and validity. Additionally, we tested whether (3) personality traits such as anxiety sensitivity and fear of pain or state variables (positive and negative affect) were predicted stimulus intensity at pain threshold. Finally, we intended to assess individual aversiveness with respect to electrode locations (arm dorsal, arm ventral and legs) by questionnaire to

investigate how reported aversiveness refers to perceived intensity at pain threshold per location (4).

## 3.2 Methods

### 3.2.1 Sample Characteristics

Forty healthy subjects (31 females and 9 males, $age_{range}$ = 19 – 36 years, $age_{mean}$= 24.75; *SD* ± 4.03 years) participated in the study. Exclusion criteria were history of mental or physical illness, regular intake of medication that could have an influence on pain perception as well as the intake of analgesic medication during study days. Participants received a monetary compensation of 20,00 Euros for participation. All subjects gave written informed consent to the entire protocol that was performed in accordance with the ("World Medical Association Declaration of Helsinki: ethical principles for medical research involving human subjects", 2013) and approved by the ethics committee at the University of Regensburg.

### 3.2.2 Stimulus Material and Presentation

We delivered electrical pulse stimuli using a constant current stimulator (Digitimer DS8R, Digitimer Ltd., Welwyn Garden City, UK) equipped with Arduino® (Arduino SA, Chiasso, Switzerland) using "A Simple Framework" (ASF; Schwarzbach, 2011) to control for timing and intensity. Two durable steel disk electrodes at 8 mm diameter with 30 mm spacing were fixated with an adjustable velcro strap. The electrical stimulus consisted of subsequent single biphasic pulses with 100% recovery phase, while initial pulse strength was set to 4.7 mA. Stimulus intensity increased constantly in steps of 0.84 mA each 500 ms with an upper limit of ~70 mA (Figure 3.1).

**Figure 3.1**

*Schematic Presentation of the Pulse-width Modulation*
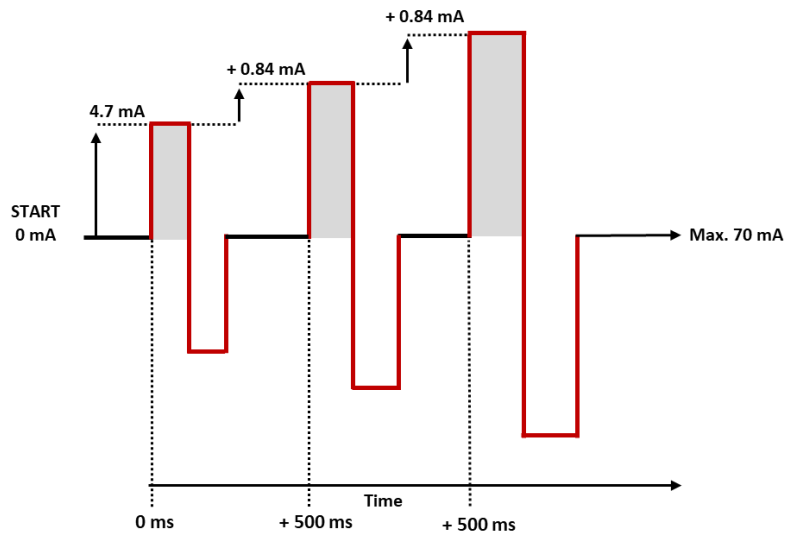


Simplified scheme of electrical stimulation. Start stimulus intensity of 4.7 mA increased every 500 ms by 0.84 mA. Each electrical stimulus (red marked bars) was presented as single biphasic pulse (gray shaded area). Maximum intensity limit was set to 70 mA.

The experiment was conducted on a 14" Sony VAIO Laptop using MATLAB R2019a (The MathWorks, Natick, USA) for stimulus delivery, visual feedback, and data analysis.

## 3.2.3 Determination of Stimulus Intensity at Pain Threshold

During stimulus presentation, participants evaluated stimulus intensity along a numeric aversiveness rating scale that went from 0 (= no sensation) to 10 (= intensity no longer tolerable) which was displayed on the computer screen throughout the entire procedure (Figure 3.2). Participants' task was to move the cursor to the right as soon as they felt the electric stimulus and to continue moving the cursor to the right (pressing the button with the right arrow) if the perceived intensity got stronger.

**Figure 3.2**

Numerical Rating Scale for Assessing Perceived Stimulus Aversiveness



While being exposed to electrical stimuli of increasing intensity, participants rated stimulus intensity along the scale indicated by button press. Participants were instructed to rate a stimulus with 0, if they did not feel it, 0.5 and 4.5 when they could feel the stimulus without perceiving it a unpleasant, between 4.5 and 5.5 when the stimulus was unpleasant but not painful, betweens 5.5 and 9.5, when stimuli were painful but still bearable, 10 if stimuli became intolerable. Stimulation was stopped automatically when participant's report reached the critical score of 10 (= pain is no longer tolerable).

Stimulus intensity was plotted against time (Figure 3.3). We computed stimulus intensity level at pain threshold as the median intensity value for aversiveness ratings that fell between 4.5 and 5.5. These values represented the intensity threshold at which the participant perceived the stimulus as bearable and not painful for a given electrode location at a given timepoint.

**Figure 3.3**

*Example Trial for Estimating Stimulus Intensity at Pain Threshold*
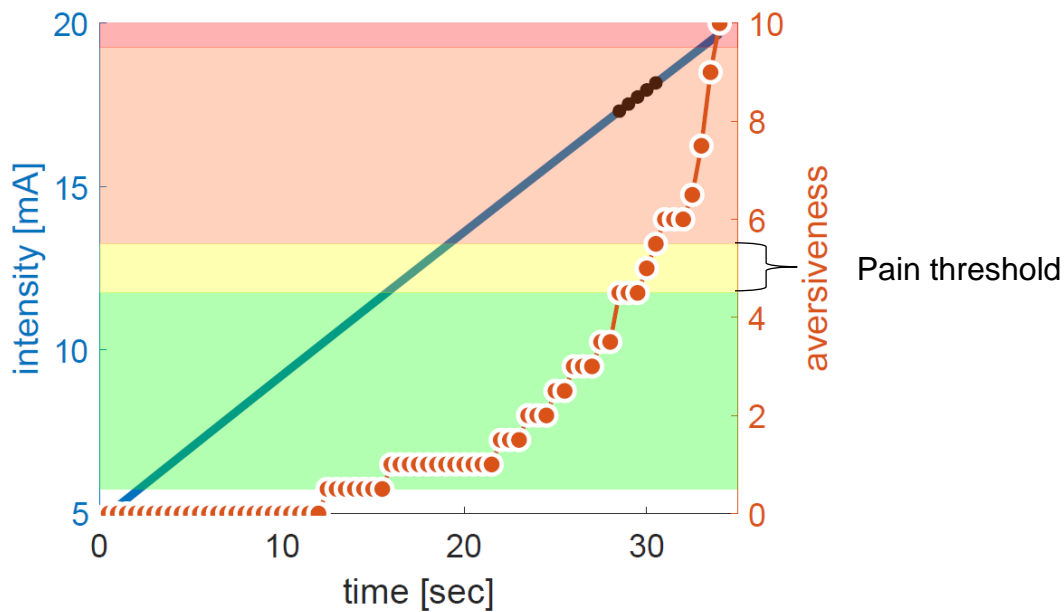


YY-plot of stimulus intensity [mA] (blue ordinate on the left) and experienced aversiveness (red ordinate on the right) ranging from 0 (=stimulus detection threshold) to 10 (= aversiveness tolerance threshold) plotted against time [seconds; sec]. The blue line depicts stimulus intensity across time. Red dots show a participant's ratings increase over time. Black dots refer to stimulus intensities whose ratings fell into the yellow corridor (i.e. when participants judged stimuli as unpleasant but not painful). The median value of the black dots (pertaining to the intensity scale) yielded stimulus intensity at pain threshold [in mA].

For assessing effects of location on aversiveness ratings, electrodes were placed on right and left body side at 3 different positions. Stimulus intensity at threshold was assessed for: arm left dorsal (ALD) and right (ARD; above the extensor carpi ulnaris muscle, right next to the ulna), arm left ventral (ALD) and right (ARD; at the medial part of the brachioradialis muscle) and at the leg left (LL) and leg right (LR) at the medial part of the tibialis anterior muscle 100 mm distal from the caudal end of the patella (Hay et al., 2016). Note that the cathode was always placed distally.

For measuring the predictive value of different trait and state variables on pain perception, participants filled in several self-report measures assessing anxiety sensitivity, fear of pain and affect characteristics. These anxiety and pain related personality dimensions as well as current affect state are known to play a crucial role in pain perception and reporting, not solely in patients suffering from anxiety disorders but also in healthy participants. We were using the following questionnaires to measure

pain and anxiety-related symptoms as well as perceived aversiveness with respect to electrode location in our healthy participants sample.

We used the ASI (Reiss et al., 1986; Reiss, 1987) beliefs about social and somatic consequences of anxiety symptoms (Peterson & Heilbronner, 1987). The questionnaire consists of 16 items that are rated along a 5-point Likert-scale (1= "very little" to 5= "very much"; total score range = 16-80) for assessing the extend of anxiety sensitivity trait. Total scores are classified in three categories representing high (≥ 23), moderate (≥ 19) and normative (≤ 18) anxiety sensitivity trait (Allan et al., 2014; Hovenkamp-Hermelink et al., 2019). Internal consistency was found to be high, while test-retest reliability was adequate and validity was estimated to be good (Reiss et al., 1986; Vujanovic, Arrindell, Bernstein, Norton, & Zvolensky, 2007).

The Fear of Pain Questionnaire (FPQ; (McNeil & Rainwater, 1998) is a widely used questionnaire consisting of 30 items for assessing the multidimensional fear of pain construct that assesses the relation of pain, fear and avoidance facets as trait. Items were rated on a 5-point Likert scale (1= not at all to 5= extreme). Therefore, higher FPQ scores represent higher disposition for fear of pain. A mean score of 77.6 ($M_{Males}$: 73.4 and $M_{Females}$: 80.7) was found in a previous study with healthy participants (Vambheim et al., 2017).

The PANAS (Watson et al., 1988) 20-item self-report questionnaire represents a valid and reliable scale for measuring positive and negative affect state (Díaz-García et al., 2020). Orthogonal subscales require scoring on a 5-point Likert-scale (1 = "very slightly or not at all", 2 = "a little", 3 = "moderately", 4 = "quite a bit", and 5 = "very much") per item, while the total score ranges from 10 - 50 (Crawford & Henry, 2004; Watson et al., 1988). Healthy participants are usually characterized with high PA and low NA which is defined as ≥ 35 on the PA and NA ≤ 18 on the NA scale (Sibille et al., 2012).

Following the last testing session (S3), participants filled in a brief questionnaire ("Aversiveness rating scale") for assessing their perceived aversiveness regarding the different electrode locations used in this experiment. Participants rated on a 5-point Likert scale (0 = not aversive at all to 5= highly aversive) their perceived aversiveness with respect to electrical stimulation at given electrode location (arm dorsal, arm ventral and legs).

### 3.2.4 Procedure

Prior to the first testing session (S1), participants completed questions about their demographic data and trait-related questionnaires (ASI-III and FPQ).

Following, participants performed an initial practice run (S1a), in which they underwent the threshold estimation procedure for each of the six locations (ALD, ARD, ALV, ARV, LL, and LR) for familiarization. Following a break of 15 minutes, the procedure was repeated for assessing pain threshold values at S1, again after 24 hours (S2), and 168 hours (S3). Electrode positions order was randomized for each subject and session. The PANAS questionnaire was filled in prior to each testing session (S1, S2 and S3). Following S3, participants rated aversiveness with respect to electrode location.

### 3.2.5 Data Analysis

We used MATLAB Release 2019a (The MathWorks, Inc., Natick, Massachusetts, United States) for extracting and analysing participants' stimulus intensity at pain threshold for each timepoint and location. Statistical analyses were performed by using MATLAB and SPSS ver. 25 (IBM Corp., Armonk, NY, United States). For determining test-retest reliability, we computed intraclass correlation coefficients (ICCs) for examining the absolute agreement of stimulus intensities at threshold across time and locations. In accordance with convention of (McGraw & Wong, 1996) and the proposed selection process by Koo and Li (2016) we calculated ICCs using a two-way mixed effects model based on mean of measurements and absolute agreement under consideration of Cronbach´s $\alpha$. We conducted separate ICC analyses to investigate stimulus intensity (1) across sessions independent of location, (2) per location across sessions and (3) per location and session. According to ICC reliability guidelines (Koo & Li, 2016) values lower than 0.5 indicate poor, between 0.5 and 0.75 moderate, between 0.75 and 0.9 good reliability. Values greater than 0.90 indicated excellent reliability. For testing mean differences with respect to stimulus amplitude at pain threshold we conducted a repeated measures analysis of variance (rmANOVA) in a mixed effects model while using "location" (ALD, ARD, ALV, ARV, LL, and LR) and "session" (S1a, S1, S2, and S3) as within-subject factors. Assessed sessions represented the repeated measures factor whereas location of electrode positions constitutes the fixed effects factor. In case of statistically significant factor effects, we

applied Bonferroni corrected pairwise comparisons for post-hoc testing. Item responses for each questionnaire were summed up to total score per construct, in which higher scores indicating higher expression of the representing construct. Pearson´s correlation coefficient ($r$) was calculated for addressing the relationship between personality variables, aversiveness rating and stimulus intensity at pain threshold across subjects.

## 3.3 Results

Mean stimulus intensity at pain threshold across session and location was 17.4 mA ($SD$ ± 0.11 mA). A detailed overview of sample mean values (mA) with respect to location and session is represented in Table 7.1 in the appendix. Sample characteristics of anxiety sensitivity, fear of pain as well as positive and negative affect can be found in Table 3.1. Our sample showed normal score in anxiety sensitivity (Allan et al., 2014; Hovenkamp-Hermelink et al., 2019), while scores for fear of pain trait were a little higher than in the sample of healthy participants from (Vambheim et al., 2017). Considering scores for positive and negative affect state, we found an atypical affect style pattern represented with low positive while showing normal negative affect scores (Sibille et al., 2012).

**Table 3.1**

*Sample Characteristics with respect to Psychometric Outcome Measures*

| Questionnaire | *M* | | *SD* | |
|---|---|---|---|---|
| ASI | 20.90 | | 9.27 | |
| FPQ | 81.45 | | 18.31 | |
| PANAS | Positive affect | Negative affect | Positive Affect | Negative Affect |
| S1 | 30.87 | 14.72 | 5.75 | 5.14 |
| S2 | 30.95 | 13.70 | 5.64 | 5.13 |
| S3 | 30.70 | 15.77 | 8.11 | 5.98 |

*Note.* Questionnaires: ASI = Anxiety Sensitivity Index, FPQ = Fear of Pain Questionnaire and PANAS = Positive and Negative Affect Schedule. Session: S1 = day 1; S2: deltaT = 24 hours/1 day, S3 = 168h/1 day.

Our primary concern was whether stimulus intensity at pain threshold is a reliable, i.e. stable, measure. To this aim we computed test-retest reliability using ICCs between different testing sessions: within session 1 (S1a and S1, deltaT=15 min), between

session 1 and 2 (deltaT=24 hours/1 day) as well as between session 1 and 3 (deltaT=168 hours/7 days). Figure 3.4 provides an overview of ICC results considering different sessions and locations

**Figure 3.4**

*Results of ICC for Stimulus Intensity at Pain Threshold*
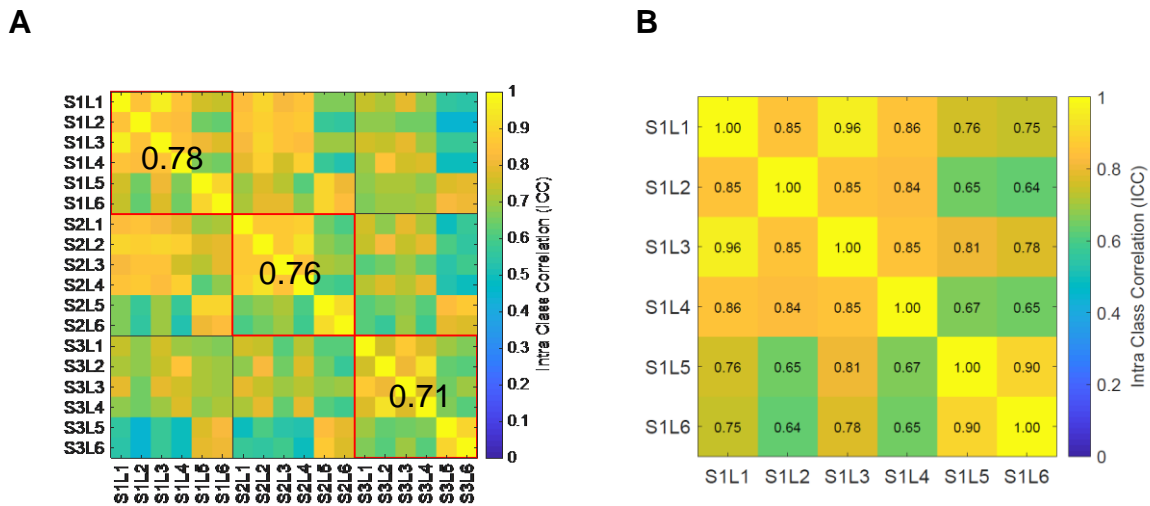


A) Different cells (colored outlines) represent pairwise intra-class-correlations (ICC) of stimulus intensity at pain threshold for different sessions and electrode positions. Red boxes denote the pattern off ICCs within session (S1, S2 and S3; consistency), off-diagonal boxes (black frames) denote the pattern off ICCs between sessions (S1-S2, S1-S3 and S2-S3, test-retest reliability). Black numbers represent ICC scores (S1, S1 − S2 and S1 − S3). All cells show similar patterns (see panel B for a detailed explanation), but with a stronger expression within than between sessions. B) Pairwise ICC of stimulus intensity at pain threshold for session 1 (S1). The four by four matrix in the upper left quadrant depicts high ICCs for the dorsal and ventral sides of the arms. The two-by-two matrix in the lower right depicts high ICCs between left and right legs. ICC values are shown for each cell. (Location coding: L1 = "arm left dorsal", L2 = "arm left ventral", L3 = "arm right dorsal", L4 = "arm left ventral", L5 = "leg left" and L6 = "leg right").

Test-retest reliability of stimulus intensity at pain threshold was good for the first (ICC$_{S1}$ = 0.78; 95% confidence interval ranging from 0.671 to 0.868) and and the second session 24 hours later (ICC$_{S1-S2}$ = 0.76, 95% confidence interval ranging from 0.666 to 0.843; $t(5) = 1.08$, $p = .329$). After 168 hours, ICC was moderate (ICC$_{S1-S3}$ = 0.71, 95% confidence interval ranging from 0.605 to 0.806). Testing for differences revealed that test-retest reliability of intensity at pain threshold decreased over time ($F(2, 10) = 15.797$, $p < .001$, partial $\eta^2 = .760$). While reliability of the estimated intensity did not decrease after 24 hours ($t(5) = 1.08$, $p < .329$), it was significantly decreased following 168 hours to initial testing ($t(5) = 6.03$, $p < .01$). A decline in test-retest reliability was further observed when comparing ICCs from S2 to S3 corresponding to a time period of 144 hours (S2 - S3; $t(5) = 3.97$, $p < .05$).

Additionally, we wanted to elaborate if different locations show different stability of pain threshold over time. The time course of test-retest reliabilities for each specific location with regard to the comparison of sessions (S1 = S1a vs. S1; S2 = S1 vs. S2; S3 = S1 vs. S3) is displayed in Figure 3.5 while confidence intervals are represented in Table 7.2 in the appendix.

**Figure 3.5**

*Time Course of Test-Retest Reliability with Respect to Location*
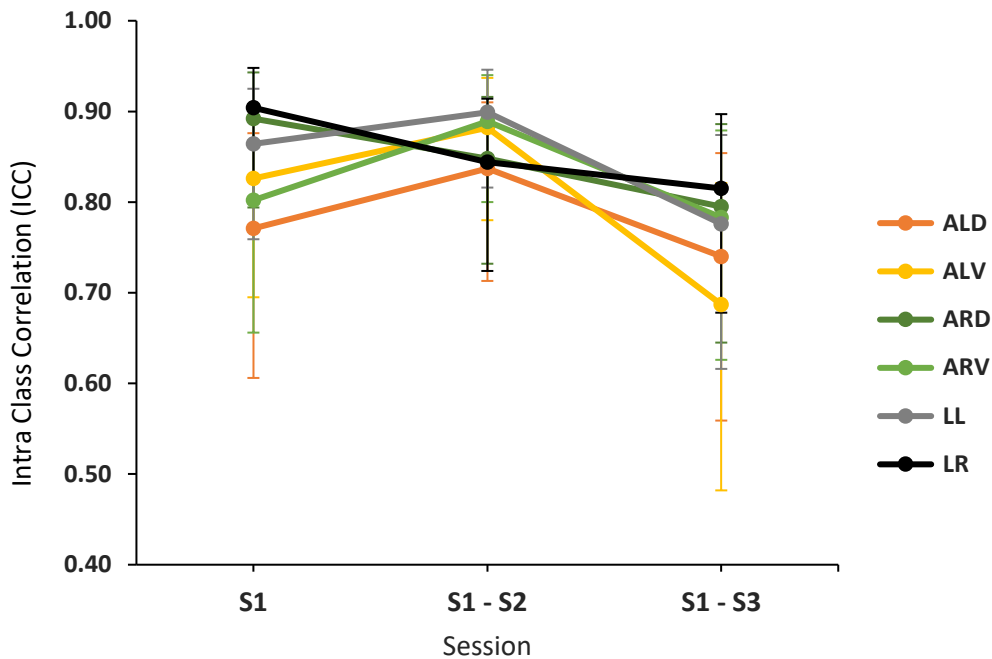


Test-retest reliability (ICC) across sessions (S1a - S1, S1- S2 and S1 – S3) for each location. Reproducibility was good for all locations within S1 (deltaT = 15 min). After 24 hours (S1 – S2), results indicated that location "leg left" shows excellent, while the remaining locations furthermore continuously showed good stability. After 168 hours (S1 – S3) results showed moderate reliabilities for "arm left dorsal" and "arm left ventral" location while the other locations still showed good stability of pain threshold perception over time.(Location coding: ALD= "arm left dorsal", ALV = "arm left ventral", ARD = "arm right dorsal", ALV = "arm left ventral", LL = "leg left" and LR = "leg right". Error bars represent standard error of the mean (SEM).

Within the first session (S1a – S1) all locations showed a high stability of intensity at pain threshold demonstrated by good reliabilities (ALD: ICC = 0.77; ALV: ICC = 0.83, ARD: ICC = 0.89; ARV: ICC = 0.80; LL: ICC = 0.86) while location "leg right" showed excellent reliability (ICC = 0.90). Following 24 hours (S1 vs. S2) we found excellent reliability for location 'leg left' (ICC= 0.90). Follow up testing 24 hours later showed good test-retest reliabilities as well, when comparing S1 and S2 (ALD, ICC= 0.84; ALV, ICC = 0.88; ARD, ICC = 0.85; ARV, ICC=0.89; LL, ICC = 0.90; LR, ICC=0.85). After 168 hours (S1 vs. S3) ICC indicated good (ARD, ICC = 0.80; ARV, ICC=0.78; LL, ICC=0.78; LR, ICC=0.81) to moderate reliabilities (ALD, ICC= 0.74; ALV, ICC = 0.68). Results indicated that there was no difference in stability of intensity at pain threshold over time when regarding location as a further factor ($F$(5, 10) = 1.673, $p$ = .228 , partial $\eta^2$ = .455). Taken together, results indicated that the reproducibility of stimulus intensity

at pain threshold decreased over time (>24 hours). But when considering location as an additional variable, decline over time was not statistically significant.

Figure 3.6 shows that stimulus intensity at pain threshold was different for different body parts (main effect "location": $F(5, 195) = 14.152$, $p < .001$, partial $\eta^2 = .266$). Overall, stimulus intensity at pain threshold was stable over time (main effect "session": $F(1.50, 41.31) = 0.988$, $p = .358$, partial $\eta^2 = .025$). Pairwise post-hoc testing revealed that stimulating the arms yielded higher sensitivity to electrical currents in comparison to stimulating the legs.

**Figure 3.6**

*Mean Stimulus Intensity (in mA) at Pain Threshold by Session*
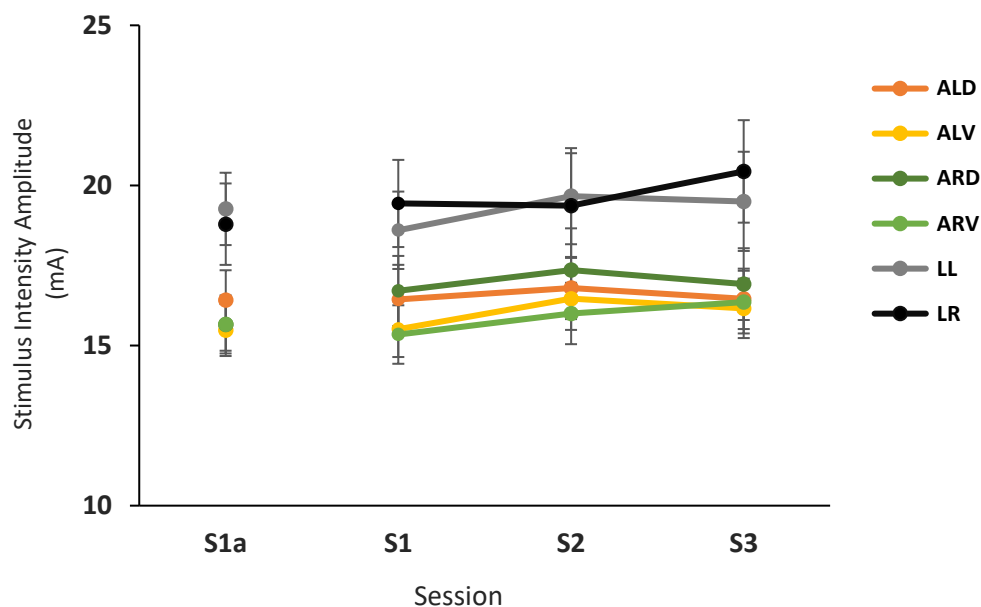


Stimulus intensity at pain threshold (in mA) as a function of session (S1a, S1: deltaT = 15min, S2: deltaT = 24 hours/1day, S3: deltaT = 168hours/1 week) and location ("arm left dorsal" (ALD), "arm left ventral" (ALV), "arm right dorsal" (ARD), "arm right ventral" (ARV), "leg left" (LL), "leg right" (LR)). Significantly higher sensitivity to stimulus intensity was found for the arms in comparison to the legs. Error bars represent standard errors.

Since we were hypothesizing that personality traits and states contribute to fluctuations in pain perception, we correlated mean intensity amplitudes (in mA) with scores from psychological questionnaires. Correlation of ASI with stimulus intensity at pain threshold across locations and timepoints showed a negative relation in a way that higher AS was associated with lower intensities at pain threshold. Nevertheless, this comparison did not reach statistical significance level ($r = -.261$, $p = .104$; Figure 3.7).

**Figure 3.7**

*Correlation of Anxiety Sensitivity Trait with Stimulus Intensity at Pain Threshold*
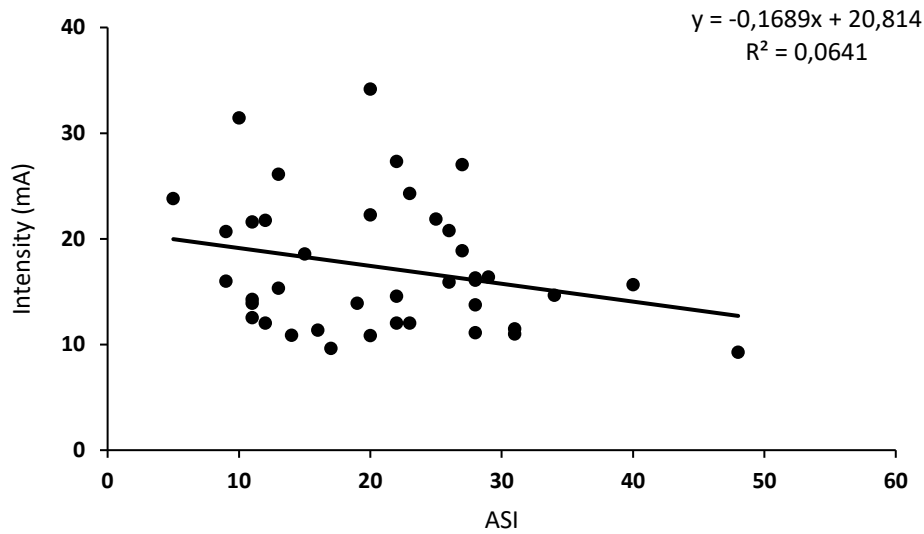


Relation (Pearson correlation coefficient) of anxiety sensitivity (measured with ASI) trait with stimulus intensity at pain threshold. The analysis yielded a negative correlation of ASI score with stimulus intensity at pain threshold across sessions and locations, in a way that lower anxiety sensitivity was associated with intensity at threshold. But this correlation did not reach statistical significance.

For investigating the impact of fear of pain trait we correlated scores of fear of pain questionnaire with stimulus intensity at threshold and observed no statistically significant correlation ($r = -.06$, $p = .694$; Figure 3.8).

**Figure 3.8**

*Correlation of Fear of Pain Trait with Stimulus Intensity at Pain Threshold*
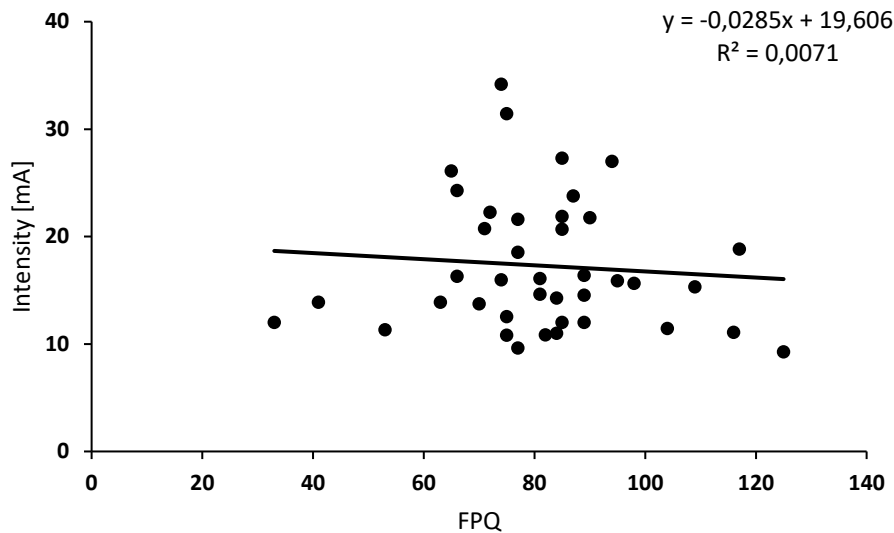


Relation of fear of pain trait (measured with FPQ) with stimulus intensity at pain threshold. Fear of pain was found to be unrelated to stimulus intensity at pain threshold across locations over time.

For interpreting the predictive value of current emotional state on pain threshold amplitude we initially wanted to figure out how positive and negative affect are related to each other within and across testing sessions. Considering positive affect measured at the first session, we found that PA was able to predict positive affect state following 24 and 168 hours (S1$_{PA}$ vs. S2 $_{PA}$: $r = .621$, $p < .001$; S1$_{PA}$ vs. S3 $_{PA}$: $r = .639$, $p < .001$). Moreover, positive affect at session 2 was associated with positive affect at session 3 (S2 $_{PA}$ vs. S3 $_{PA}$: $r = .584$, $p < .001$). This finding indicates a relation of positive affect over one-week testing period. With respect to time course of negative affect state, we found a similar pattern (S1 $_{NA}$ vs. S2 $_{NA}$: $r = .810$, $p < .001$; S1 $_{NA}$ vs. S3 $_{NA}$: $r = .412$, $p < .01$), although negative affect at session 2 could not predict negative affect for session 3. When comparing scores of positive to scores of negative affect, we could not find any significant correlation, indicating that positive and negative affect states represent distinctive and independent dimensions (Figure 3.9).

**Figure 3.9**

Correlation of PANAS Subscales with Respect to Testing Sessions
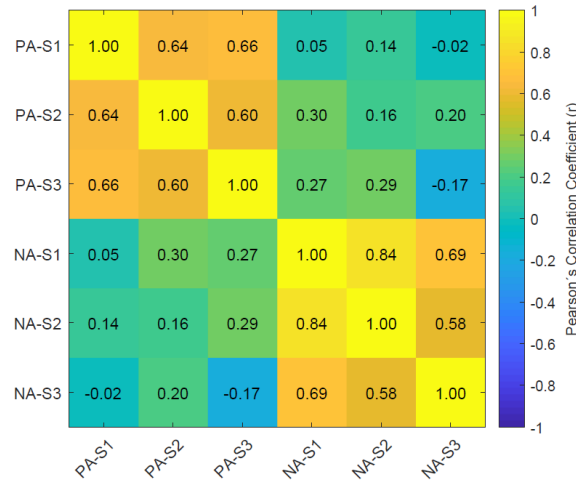


Correlation matrix depicts the relation of positive (PA) and negative affect (NA; both measured with PANAS) within and between testing sessions (S1, S2 and S3). Patterns denote, high within affect pattern considering each negative and positive affect across sessions. However, a relation of positive with negative affect was not found indicating distinct opposing dimensions.

Further, we wanted to investigate the influence of positive and negative affect on pain threshold intensity with respect to session and location. Therefore, we correlated positive and negative affect scores (PA $_{S1}$, PA $_{S2}$, PA $_{S3}$, NA $_{S1}$, NA $_{S2}$, NA $_{S3}$) with pain threshold intensity per location regarding each session (ALD $_{S1}$, ALV $_{S1}$, ARD $_{S1}$, ALV $_{S1}$, LL $_{S1}$, LR $_{S1}$, …, LR $_{S3}$). All comparisons are visualized in Figure 3.10.

**Figure 3.10**

*Correlations of PANAS Subscales with Intensity at Pain Threshold within Locations*
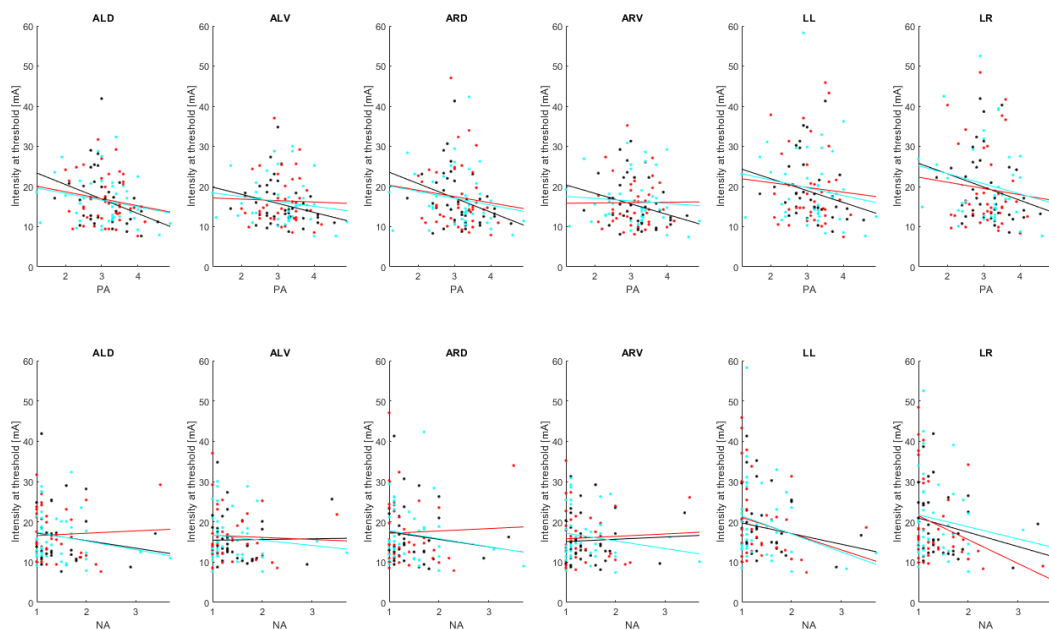


Subplots depict relation of PANAS subscales (positive (PA; first row) and negative affect (NA; second row)) with intensity at threshold (in mA) for each location (Location coding: ALD= "arm left dorsal", ALV = "arm left ventral", ARD = "arm right dorsal", ALV = "arm left ventral", LL = "leg left" and LR = "leg right") and session (S1= black, S2=red and S3=cyan). Increased positive affect at session 1 was able to predict lower pain threshold intensities within the third session. When negative affect in session 1 was enhanced, there were found significant lower pain thresholds at "leg right" position in session 2 and at "leg left" within session 3.

We found that higher positive affect in the first session was associated with lower pain threshold in "arm left ventral" location at session three (PA $_{S1}$ vs. ALD $_{S3}$, $r = -.313$, $p = .05$). In contrast, higher negative affect measured in the first session was found to be related to lower pain threshold intensities at "leg right" in session 2 (NA $_{S1}$ vs. LL $_{S2}$, $r = -.343$, $p = .05$) and "leg left" location at session 3 (NA $_{S1}$ vs. LR $_{S3}$, $r = -.317$, $p = .05$). Although, these relations are very specific and selective for single locations and sessions, we assume that an influence of affect might be relevant when assessing pain stimulus intensities.

Furthermore, we explored which location ("arm dorsal", "arm ventral" and "legs") causes less discomfort considering self-reported perceived aversiveness retrospectively. Therefore, we initially compared aversiveness rating scores that were assessed following the last session to receive information about participants individual' perception. We found that locations "arms ventral" ($M = 3.65;$ $SD = 1.09$) were

perceived as more aversive than the "arms dorsal" ($M = 2.80$; $SD = 1.06$; $t(39) = 3.98$, $p < .001$) and "legs" ($M = 2.13$; $SD = 1.09$; $t(39) = 6.21$, $p < .001$). Moreover, receiving electrical stimuli at the "arm outer sites" was perceived as more aversive than at the "legs" ($t(39) = 3.08$, $p < .01$) indicating that the application of stimuli at the legs was less unpleasant in comparison to the arms.

Furthermore, we correlated aversiveness rating scores with intensity at pain threshold (in mA) per location to get information about the relation of reported and perceived aversiveness. An overview of the relationship between aversiveness rating and intensity threshold across sessions is provided in Figure 3.11.

**Figure 3.11**

*Correlations of Aversiveness Rating with Location*
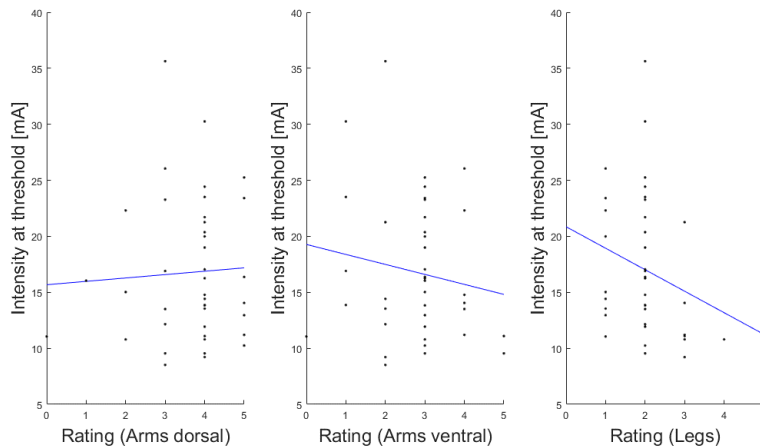


Line plots are displaying the correlation (blue lines) of location-specific rating (arms dorsal, arms ventral and legs) with mean stimulus amplitude across sessions while each dot represents a total score of one participant. Higher perceived aversiveness in "arms dorsal" location was related to higher pain intensity at threshold. In contrast, "arms ventral" and "legs" condition shows inverse patterns in a way that higher aversiveness corresponded to higher pain sensitivity at pain threshold. Nevertheless, these patterns did not reach level of statistical significance.

With respect to "arms dorsal" location we found that higher perceived aversiveness came along with higher pain intensity at threshold. In contrast, we found an opposed pattern for "arms ventral" and "legs" location. Both locations showed that higher aversiveness corresponded to higher pain sensitivity at threshold. However, only the correlation with "legs" and pain intensity amplitude reached level of statistical significance ($r = -.438$, $p < .01$). These results indicated that perceived pain and reported pain does not necessarily agree.

## 3.4 Discussion

Standardized procedures that reliably measure pain perception thresholds allow one to investigate emotional states and neurological dysfunctions in experimental studies as well as in clinical settings. Information about stability or inconsistencies in pain perception have implications for highly demanding clinical studies, i.e. pharmacological studies in which participants will be measured repeatedly over weeks. Irrespective of particular context, parameters such as stimulus intensity at pain threshold should be valid, reliable, and easy to acquire. For addressing these aspects there was the aim to discuss study results with respect to the proposed new developed calibration method "**ESTIMATE**" (**E**stimating **STIM**ulus p**A**in **T**hr**E**shold). This procedure was designed i.e. for assessing pain sensitivity across multiple sessions while minimizing interaction between participant and experimenter and to keep the number of painful stimuli low.

However, a major issue in estimating the stimulus intensity at pain thresholds are fluctuations in pain perception (Robinson et al., 2013) for which the underlying reasons andtemporal dynamics are not yet fully understood. Previous studies revealed that procedural variations but also inconsistencies in individuals´ self-report (Rosier et al., 2002) are contributing to instability of estimating stimulus intensity at pain threshold. Further, there is evidence that personality traits related to pain and fear as well as current affective state contribute to pain perception (Finan & Garland, 2015; George & Hirsh, 2009). Therefore, we wanted to address how stable stimulus intensities at pain threshold are while considering multiple testing sessions, controlling for methodological variance (i.e., participant-experimenter interaction and electrode location) and considering dispositional and situational factors with respect to personality states and traits.

Given our main research purpose, stability of stimulus intensity at pain threshold was addressed with determining test-retest reliability of electrical stimulus intensities over time (15 min, 24 hours, and 7 days). The phenomenon that pain experience is non-static and fluctuates over time (Robinson et al., 2013) is already well-known, but the time course of pain perception inconsistencies was not addressed. We discovered good test-retest reliability of stimulus intensity at pain threshold for the ESTIMATE procedure across locations after a time period of 15 minutes and 24 hours. Nevertheless, stability of our estimates decreased after 7 days (~ 168 hours).

Since we were assuming that the use of different locations had contributed to inconsistencies in studies of pain (Letzen et al., 2014; Robinson et al., 2013) we controlled for commonly used locations (Hay et al., 2016; Tabbert et al., 2005).

We found that within a given session there was a high agreement between stimulus intensities at pain threshold among different electrode locations (Figure 3.4). This means that despite individual differences, there is a consistency that reflects that each participant has some stable internal threshold. Furthermore, we found that these results were stable over minutes, hours, and even days, although declining over time. Stability was not substantially affected by location of stimulation (Figure 3.5), however participants showed higher sensitivities when stimulated on the arm compared to the leg (Figure 3.6). Thus, we can conclude that stimulating the arms can be used for aversive stimulation resulting in lower dosage without negatively affecting validity and reliability.

Eventually, retest-reliability declines after several days. We were able to explain part of the effects using psychological state variables (Figure 3.9). Psychological trait variables did not substantially explain the data. Taken together, this means that repeated measurement designs with aversive stimuli are possible and can yield stable results. In order to keep validity high across longer timeframes (i.e. more than 24 hours), we recommend to gather a new estimate for stimulus intensity at pain threshold. In that context, we believe that our ESTIMATE procedure is a fast and reliable tool for repeated-measurement designs that involve aversive stimuli.

# 4 NEUROIMAGING STUDY

## 4.1 Aim and Hypotheses

The aim of our neuroimaging study was to investigate commonalities and differences of fear and anxiety circuits in the human brain, by identifying brain regions that exhibit differential neural responses to the emotional states of fear and anxiety and to investigate to which degree these brain responses would depend on the sensory modality in which the fear- and anxiety evoking stimuli had been presented.

To this aim, we adapted the threat anticipation paradigm of Somerville and colleagues (2013) that had been designed to allow modeling fear as transient and anxiety as sustained mental and neural processes. We expanded this paradigm by stimulating participants in two modalities: vision (as in the original paradigm) and somatosensation using transcutaneous electrical stimulation. Using different kinds of stimulus modalities allowed us to address the question of whether there are modality-general representations of fear and anxiety, i.e. higher-level representations of negative emotions that abstract away from the sensory source. The adapted experiment therefore followed a three-factorial 2x2x2 design with stimulus- "modality" (visual, somatosensory), "predictability" (predictable, unpredictable), and "valence" (negative, neutral) as within-subject factors. Obviously, we expected to see modality-specific brain activity due to segregation of the sensory nervous systems into vision, hearing, touch, taste, and smell (Friston, 2010; Gazzaniga et al., 2009). Additionally, we predicted to find brain responses in structures identified in the pain matrix (Wager et al., 2013) involved in noxious stimulus processing since they are recruiting similar brain regions as found for fear and anxiety processing.

However, we also know that there are multisensory areas in the human brain (Stein & Meredith, 1994) and there is agreement in the field that complex cognition relies on integrating information from different sources (Cohen & D'Esposito, 2016). However, there is little knowledge in terms of multisensory aspects of fear and anxiety, or whether fear and anxiety are differentially organized in terms of multisensory integration. To further elaborate that point, let's recall how the field operationalizes fear as a transient response to a concrete and existing threat and anxiety as an emotional state in which one is afraid that something aversive might happen (LeDoux & Pine, 2016). Fear is therefore much more concrete, which may be efficiently encoded in modality-specific

brain representations, since they would use the knowledge in which modality the aversive stimulus occurs. Anxiety, instead, may have a more abstract character, in the sense that there may even be an uncertainty with respect to what the aversive event might be. The particular question, we want to address here is, whether therefore, the brain systems that distinguish fear and anxiety (Somerville et al., 2013) operate on a different level of abstraction. In concrete terms, we will ask whether the fear-system can distinguish between the underlying modality of threat whereas the anxiety system abstracts away from the sensory origin of threat.

In the context of our experiment, the first step consists in distinguishing the neural systems for fear and anxiety by identifying brain areas that exhibit transient responses to aversive stimuli (i.e. they process fear) and areas that exhibit sustained responses to periods in which participants expect aversive (unpredictable negative) events. In the second step, we investigate modality-specificity of the previously identified brain systems. We expect that both systems (fear and anxiety) are sensitive to valence (main effect "valence"). In the context of our factorial design ("modality", "predictability", "valence"), a modality specific system should exhibit a statistical interaction of the factors "predictability" and "valence" with the factor "modality". Instead, in a modality-agnostic system, any effects of "predictability" and "valence" should be statistically indistinguishable for different modalities.

Figure 4.1 and Figure 4.2 below show a graphical depiction of our hypotheses pertaining to the influence of our experimental manipulations on the BOLD amplitude in different systems processing fear and anxiety.

**Figure 4.1**

*Illustration of Hypotheses Concerning the Influence of Experimental Manipulations on the BOLD Amplitude in Systems that Process Fear*
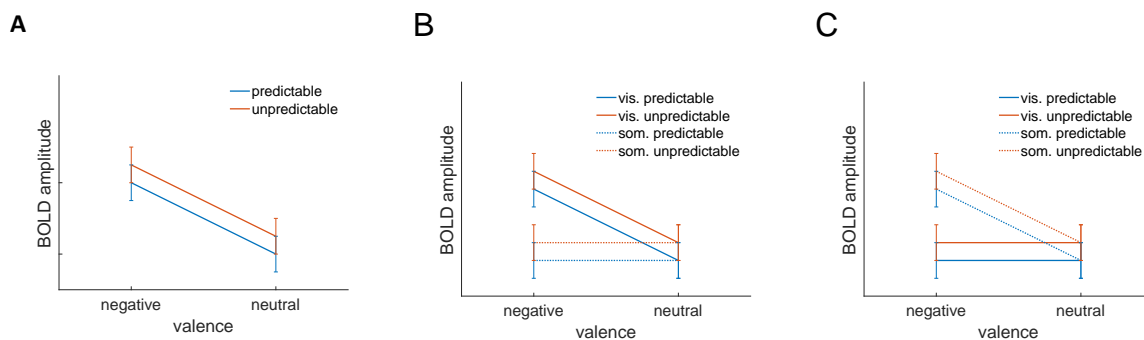


Panel A) Based on the findings of Somerville et al. (2013) a neural system that processes fear should exhibit a higher transient BOLD response for negative than for neutral stimuli. Predictability should have no systematic effect. Panels B and C) A two-way interaction would show that if fear is a modality specific process, we expect some brain regions to show this effect only for one stimulus modality, but not the other.

**Figure 4.2**

*Illustration of Hypotheses Concerning the Influence of Experimental Manipulations on the BOLD Amplitude in Systems that Process Anxiety*
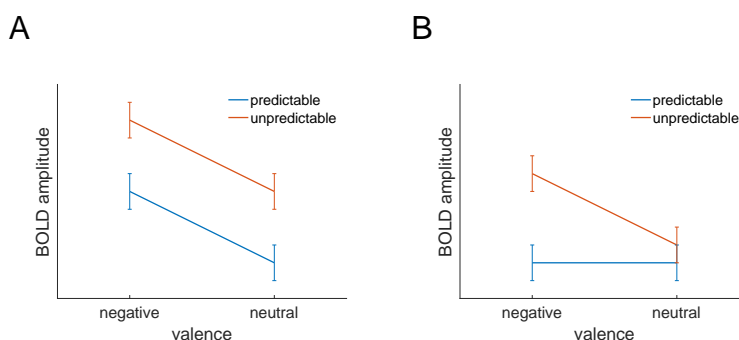


Based on theoretical considerations anxiety (LeDoux & Pine, 2016; Somerville et al., 2013) is tightly linked to predictability of threat. Panel A) main effects of predictability and valence: anxiety-related brain systems may show an increased BOLD signal when threatening stimuli occur whereas unpredictable stimuli (due to uncertainty) may yield stronger amplitudes. Panel B) Expecting negative may not trigger anxiety related processing unless the threat is unpredictable. In this case one we would observe a main effect of predictability in addition to an interaction of valence with predictability. If this process of gating-threat-by-predictability were also modality specific, we would observe brain areas showing pattern A in one and pattern B in the other stimulus modality, which statistically constitutes a three-way interaction of modality, valence, and predictability.

Additionally, we expected that neural responses to fear and anxiety in the amygdala would be highly dependent on individual differences in psychological disposition (i.e. personality traits) and affect states (i.e. anxiety, positive and negative affect) as indicated in previous studies (Barrett, Bliss-Moreau, Duncan, Rauch, & Wright, 2007; Porta-Casteràs et al., 2020). To this aim, we explored correlations of psychological

dimensions with both transient (fear) and sustained (anxiety) responses in the amygdala that would yield information about the impact and direction of effect of these traits and states.

We collected task-evoked anxiety ratings as described in Somerville et al. (2013) and expected that differences of threat manipulation would also affect participants' self-report such that participants would report higher states of anxiety in "negative" blocks compared to "neutral" blocks (main effect of "valence") and that reported anxiety would be modulated by predictability" (unpredictable > predictable). We expected predictability to play a larger role for negative than neutral stimuli (interaction of the factors "valence" and "predictability").

## 4.2 Methods

Study procedures and experimental methods were full in accordance with the Declaration of Helsinki ("World Medical Association Declaration of Helsinki: ethical principles for medical research involving human subjects", 2014) and approved by the ethics committee at the University of Regensburg.

### 4.2.1 Sample characteristics

We investigated 44 participants while seven needed to be excluded due to technical issues. Further, two participants were excluded showing specific phobia symptoms (claustrophobia and spider phobia). Finally, 35 healthy volunteers (12 ♂; 5 left-handed; $age_{mean}$= 23.77; SD ± 3.31 years) were included into data. We excluded participants based on a history of mental or physical illness, regular intake of medication (e.g. analgesic medication) as it might impact pain perception. Participants were recruited from the University of Regensburg and received 20.00 Euro as well as their anatomical brain images as compensation.

To investigate the effect of personality traits and current affect state on task-evoked anxiety rating and emotional brain state, we used self-report questionnaires for obtaining sample characteristics related to these psychological variables. Sample characteristics with respect to psychometric outcome variables are displayed in Table 4.1.

**Table 4.1**

*Sample Characteristics with Respect to Psychometric Outcome Measures*

| Questionnaire | *M* | *SD* |
|---|---|---|
| ASI | 16.68 | 9.61 |
| IUS | 44.68 | 12.15 |
| PANAS | | |
| Positive Affect | 33.71 | 6.02 |
| Negative Affect | 13.02 | 4.08 |
| STAI-S | | |
| Pre | 35.97 | 4.80 |
| Post | 37.74 | 6.95 |

*Note.* ASI = Anxiety Sensitivity Index; IUS = Intolerance to Uncertainty Scale; PANAS = Positive And Negative Affect Schedule; STAI-S = State Anxiety Inventory.

Regarding trait anxiety sensitivity and intolerance to uncertainty, our sample showed normative score (see chapter 3.2.1). With respect to affect state, our results indicated an atypical healthy participant affect style pattern with respect to relatively low positive affect value. Nevertheless, our sample showed significant higher positive ($M = 33.71$, $SD = 6.02$) than negative affect scores ($M = 13.02$, $SD = 4.08$; $t(34) = 16.468$, $p < .001$) while both affect dimensions were not related to each other ($r = -.045$, $p = .797$). The lack of a relationship between positive and negative affect demonstrates independent opposing dimensions. Given averaged state anxiety scores for both timepoints (pre vs. post experiment; $M = 36.85$; $SD = 4.53$), our sample showed typical healthy participant scores. Further, we found no difference between pre ($M = 35.97$; $SD = 4.80$) and post ($M = 37.74$; $SD = 6.95$) experiment scores ($t(34) = -1.348$, $p = .187$), which indicates stability of state anxiety across time while not being influenced by our experimental paradigm and fMRI scanning procedure.

Additionally, we analyzed psychometric data with respect to between state and trait pattern for examining a relationship of different psychological variables. The correlation matrix in Figure 4.3. Higher IU came along with increased AS trait ($r = .617$, $p < .001$) indicating a dispositional relationship for evaluating ambiguous situations as potentially threatening and fearing the experience of anxiety-related bodily symptoms. Further, higher AS predicted increased negative affect state ($r = .522$, $p < .001$), while IU did

not. However, we found a relationship of ASI ($r$ = .521, $p$ < .001) and IUS ($r$ = .428, $p$ < .01) with respect to STAI-S across time points (averaged for pre and post assessment). These results indicate that both, increased trait anxiety and uncertainty, come along with higher state anxiety. Our within affect state comparison revealed a positive relation of state anxiety and negative affect ($r$ = .627, $p$ < .001). Positive affect was found to be independent from the remaining other trait and state variables.

**Figure 4.3**

*Correlations of Trait and State Variables*

A

B
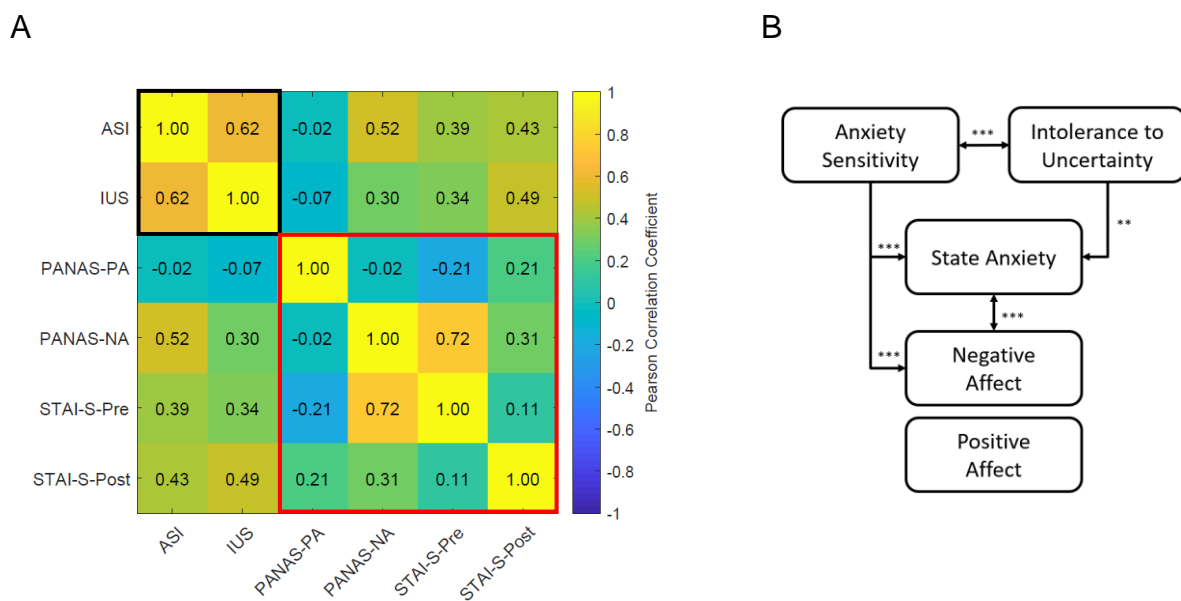


A) Colored outlines display Pearson Correlation Coefficient scores within trait (black box) and state variables (red box). Warmer colors of a cell represent higher correlation. The analysis revealed a significant moderate relationship between the AS and IU trait indicating that in our sample higher AS is accompanied with higher score IUS. Further, an increased AS score predicted higher negative affect state while IU trait did not. Considering affect state measures, the higher negative affect came along with increased state anxiety indicated by high positive correlation. Figure (B) represents an overview of significant correlations of state and trait variables based on Pearson Correlation scores displayed in figure A. In conclusion, traits are highly correlated with each other and with state anxiety. Further, anxiety sensitivity predicted negative affect state, while intolerance to uncertainty did not. Higher negative affect was related to increased state anxiety while positive affect did not show any relationship with respect to states and traits (Significance level: *** = $p$ < .001 and ** = $p$ < .01).

In conclusion, assessed anxiety-related traits show high within correlation and were further positively related to anxiety state. The AS trait was positively related with a persistent state of negative affect while IU was not. We found the negative affect state to be positively correlated with state anxiety, reflecting a relationship within aversive affect states. Lastly, the positive affect appears to be independent from anxiety-related emotional traits and states.

## 4.2.2 Stimulus Material and Presentation

We used visual stimuli from the Nencki Affective Picture System (NAPS; (Marchewka et al., 2014)). The pictures within this database are categorized into five classes: animals, faces, objects, people and landscapes. For the purpose of our study, we chose horizontal stimuli and selected them with respect to following criteria:

Within a preliminary study ($N = 5$) pictures were rated with respect to location ("indoors" vs. "outdoors" vs. "ambiguous") to obtain suitable categories for our paradigm task. The results indicate that the landscape category lacked enough indoors pictures and was excluded alongside "ambiguous" rated pictures. Moreover, we excluded pictures of the "people" category, in which a face was dominantly displayed to avoid overlap with pictures of the "face" category. Additionally, we selected images were selected based on their valence score. These values were already determined in a previous study while evaluating stimulus properties (Marchewka et al., 2014); see chapter 1.3.2). We created different stimulus categories containing neutral ($valence_{range}= 0 - 3$) and negative ($valence_{range}= 5.6 - 8$) images. Finally, we stratified pictures into image subsets with respect to content (animals, faces, objects, and people), location (indoors, outdoors), valence (negative, neutral) and predictability (predictable vs. unpredictable). Prior to paradigm start, such a subset was randomly compiled and stratified in a way that mean valence was comparable within negative and within neutral condition.

Somatosensory stimuli consisted of a single biphasic pulse with a stimulus duration of 500 ms (see 3.2.2 for an illustration). For training, we applied the stimulation electrode on the dorsal side of the non-dominant arm and, prior to fMRI scanning, on a ventral position for the final calibration using our STEP procedure. With respect to the experimental design of our neuroimaging paradigm, different stimulus intensities were chosen for having complementary valence dimensions (negative, neutral) as for the pictures. **Figure 4.4** shows a psychometric function for one participant.

**Figure 4.4**

*Example Trial of Threshold Calibration Procedure*
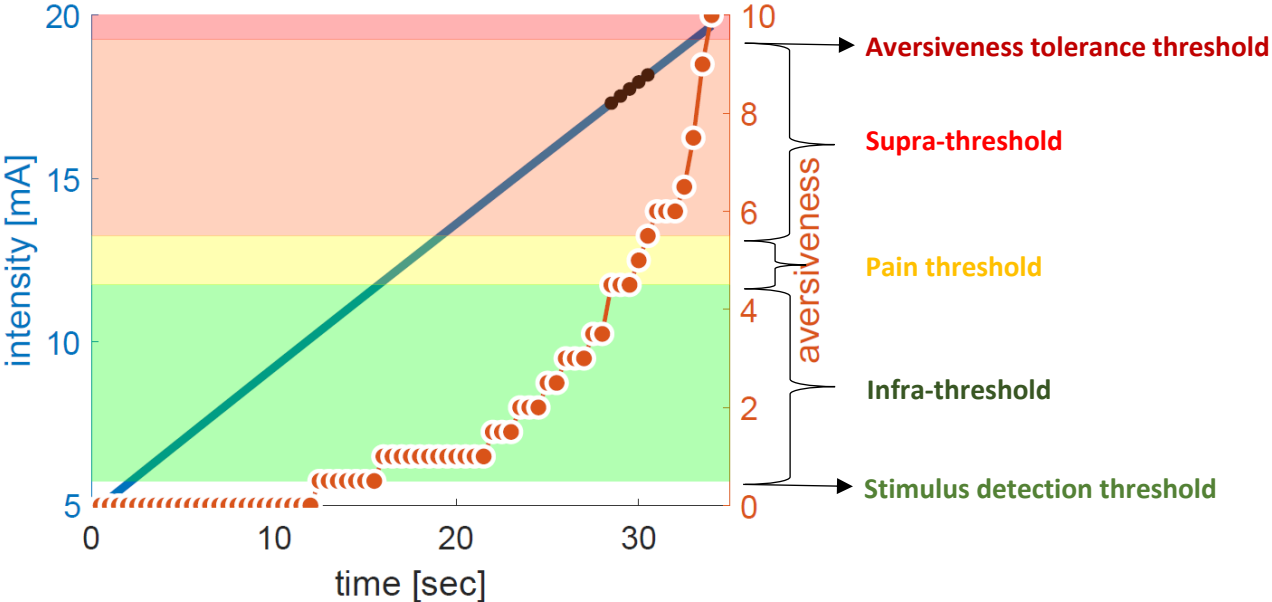


Figure represents an example trial of individual calibrated thresholds within STEP procedure trial. Time (in sec) is displayed at the x-axis, intensity of stimulus (mA; y-axis)) are plotted against aversiveness rating scale (right vertical axis). Each dot (red) represents an applied stimulus intensity, the blue line displays slope of intensity and intensitiy values at pain threshold are represented with black dots. Different thresholds, depending on aversiveness rating are depicted at figure right side (stimulus detection threshold: *aversiveness* = 0.5; infra-threshold: *aversiveness$_{Med}$* = 0.5 − 4.5; pain threshold: *aversiveness$_{Med}$* = 4.5 − 5.5; pain threshold: *aversiveness$_{Med}$ = 4.5 − 5.5;* supra-threshold: *aversiveness$_{Med}$* = 5.5 − 9.5 and aversiveness tolerance threshold: *aversiveness$_{Med}$* = 10.0). Median of infra-threshold was used as neutral valent intensity level while median intensity at pain threshold was used for negative valence category.

High intensity value, that served as negative valent stimulus, corresponded to intensity at pain threshold (Aversiveness$_{Med}$ = 4.5 – 5.5). Neutral valent stimulus intensity was extracted from infra-threshold median (Aversiveness$_{Med}$ = 0.5 – 4.5). Sample mean of weak intensity was ~ 14 mA (weak$_{range}$ = 9.80 - 20.79 mA) while strong intensity mean was 20.87 mA (strong$_{range}$ = 12.80 - 37.45 mA).

Further, we implemented a blocks with somatosensory stimulation, but kept the paradigm comparable to the visual one

The experiment was created and presented with MATLAB R2019a (The MathWorks, Natick, USA) using "A Simple Framework" (ASF; (Schwarzbach, 2011) supported with "Psychophysics toolbox" (Brainard, 1997). Visual stimuli were displayed with a video projector (PROPixx, VPixx Technologies Inc., Canada; resolution: 1024 x 768, frame rate: 60 Hz,) through a translucent screen to a mirror attached at the scanner head coil. Electric pulse stimulus was produced and elicited with a MRI compatible multimode, discrete pulse, constant current stimulator (Digitimer DS8R, Digitimer Ltd., Welwyn Garden City, UK) using Arduino® (Arduino SA, Chiasso, Switzerland).


## 4.2.3 Data Acquisition

We conducted our MRI experiment at the University of Regensburg, Germany using a 3-Tesla MRI scanner (Magnetom Prisma; Siemens, Erlangen, Germany) equipped with a 64-channel head coil. At the beginning of each scanning session, structural images were acquired using a T1-weighted magnetization-prepared rapid gradient-echo (MPRAGE; (Mugler & Brookeman, 1990)) sequence (field of view (FOV) = 250 x 250 mm$^2$, isotropic voxel resolution (VR) = 1 x 1 x 1mm$^3$, repetition time (TR) = 1910 ms, echo time (TE) = 3.67 ms, flip angle (FA) = 9°, and slice thickness = 2.5 mm) that lasted 4:27 min. Two runs of functional images were acquired with T2*-weighted echo-planar imaging (EPI) sequence using a 4-fold multi band acceleration (Seidel, Levine, Tahedl, & Schwarzbach, 2020; Setsompop et al., 2012) with 60 slices per volume (FOV = 240 x 240 mm$^2$, VR = 2.5 x 2.5 x 2.5 mm$^3$, without inter slice gap, TR = 2000 ms, TE = 30 ms, FA = 75°, and slice thickness = 2.5 mm) lasting 22:22 min each. Further a field mapping sequence (2:20 min) was assessed (60 slices/volume, FOV = 240 x 240 mm$^2$, VR = 2.5 x 2.5 x 2.5 mm$^3$, without inter slice gap, TR = 715 ms, TE$_1$ = 5.81, TE$_2$

=8.27, FA = 40°, and slice thickness = 2.50 mm) for acquiring further information about $B_0$ inhomogeneities (Jenkinson & Chappell, 2018).

We used psychological questionnaires for exploring sample characteristics with respect to affect and anxiety state as well as trait variables and for investigating their impact on dependent variables.

For measuring intolerance to uncertainty, participants filled in the 18-item German IU scale, which is comparable to the original versions (Gerlach, Andor, & Patzelt, 2008). The IUS exists in a 27-item (Michel Dugas et al., 1997), 17-item (Carleton, Norton, & Asmundson, 2007) and 12-item version (Carleton et al., 2007). Items are rated on a 5-point Likert-scale (1= "not at all characteristic of me" to 5 = "entirely characteristic of me") where higher values represent higher intolerance to uncertainty disposition (Carleton et al., 2007).

The 20-item STAI-S (Spielberger, 1983) was assessed for measuring the level of perceived anxiety with respect to e.g. apprehension, nervousness, worry and autonomic arousal dimension. Items of this questionnaire are self-evaluable by participants given a 4-point Likert-scale (1= "not at all", 2 = "somewhat", 3 = "moderately so", 4 = "very much so"). Scores can range from 20 to 80 points, whereby a higher score represents a higher state anxiety level (Gustafson et al., 2020) and cut-off values (≥ 40) represent clinically relevant anxiety scores (Addolorato et al., 1999; Knight, Waal-Manning, & Spears, 1983).

Behavioral responses, such as accuracy rate and respective response time, were collected in each trial for each participant. We used task-evoked anxiety ratings measured with a visual NRS for "nervousness" (1= "not nervous at all" to 9= "extremely nervous") for each condition following each experimental run for retrospectively assessing task-evoked anxiety level with respect to experimental conditions and to evaluate suitability of paradigm at self-report level. Additionally, we were assessing positive and negative affect state while using the PANAS (Watson et al., 1988) and anxiety sensitivity trait measured with the ASI (Reiss et al., 1986; Reiss, 1987). Descriptions and psychometric properties of both questionnaires could be found in chapter 3.2.3

## 4.2.4 Design and Procedure

To evoke transient and sustained responses, we adapted the task structure used in the study of (Somerville et al., 2013)) in its fundamentals for our present study to disentangle both kinds of responses. Although, for our "fear vs. anxiety" paradigm we were using a different image stimulus set and somatosensory stimuli to additionally investigate the influence of stimulus modality on dependent variables (see section 3.2.2). Thus, the paradigm was presented in a mixed block event design to distinguish trial-related responses (transient) and overall block activity (sustained). To assess fear and anxiety responses, target stimulus valence (negative vs. neutral) was varied within subjects and target stimulus onset was varied within subjects to manipulate predictability (predictable vs. unpredictable). Given this experimental design, task conditions were assigned with respect to different valence and predictability levels, as previously used in the (Somerville et al., 2013)) work. In blocks of electrical-stimulation, intensity was varied (high (= negative) vs. low (= neutral)) to yield valence dimensions (negative vs. neutral) comparable to picture stimuli (see chapter 4.2.2). A schematic overview of different block types and event timings is depicted in Figure 4.5.

**Figure 4.5**

*Schematic Overview of the Experimental Paradigm*
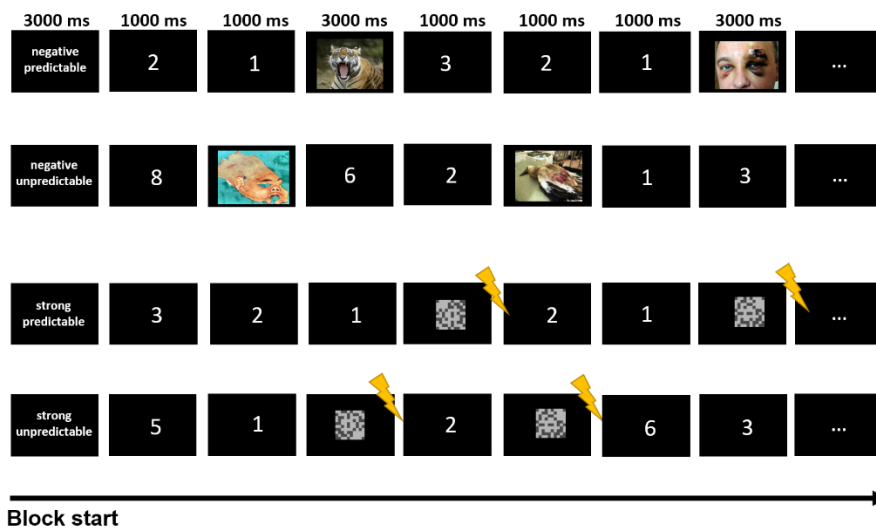


Block types were varying with respect to conditions: modality (picture vs. electric shock), valence (negative vs. neutral (pictures), weak vs. strong (electrical stimulation)) and predictability (predictable vs. unpredictable). The upcoming block type was announced (3000 ms) prior to each block containing 8 trials. A trial consisted of either a predictable countdown or an unpredictable order of digits that announced the target onset. In predictable trials, countdown started with any number ranging from 1-8, reached number one and subsequently the visual stimulus (picture vs. matrix) was presented. In zap trials the electric stimulus was applied following pixel matrix offset. In unpredictable trials, countdown numbers were shuffled and visual stimuli (picture vs. matrix) could be presented at any time. Target images were presented for 3000 ms (including application of electric stimulus in zap trials). Distractor numbers (1-8) were shown for 1000 ms, whereby trial duration was variable with respect to the shown numbers (4 sec – 11 sec). Eight trials were presented within one block with a 16 sec break between blocks. One run consisted of 8 Blocks (64 trials) while all conditions were shown two times. Whole run duration was ~ 22 min.

In predictable trials, the occurrence of the aversive event was announced with digits decreasing in a numeric order (countdown), while length was randomized between 1 - 8 digits. In unpredictable trials numbers were shuffled while an aversive event could be presented at any time. Finally, the experimental paradigm consisted of 8 different block types (conditions) with respect to the factors "modality" (pictures, electrical-stimulation (zaps)), "valence" (negative, neutral) and "predictability" (predictable, unpredictable): "Picture Negative Predictable" (PicNegPred), "Picture Negative Unpredictable" (PicNegUnpr), "Picture Neutral Predictable" (PicNeuPred), "Picture Neutral Unpredictable" (PicNeuUnpr), "Zap Negative Predictable" (ZapNegPred), "Zap Negative Unpredictable" (ZapNegUnpr), "Zap Neutral Predictable" (Zap Neu Pred), and "Zap Neutral Unpredictable" (ZapNeuUnpr).

At the beginning of the session, participants received a detailed written study instruction containing all relevant information for the experimental trial. Following signature of the consent form, participants filled in psychometric questionnaires to assess state (PANAS and STAI-S) and trait (ASI and IUS) variables. After that, participants underwent the "ESTIMATE" procedure (see chapter 3.2.3) to calibrate individual intensity parameters. After completion of the procedure, Participants were prepared for the MRI examination. In the scanner they completed two experimental runs of the so-called "fear vs. anxiety" paradigm. Following the (Somerville et al., 2013) study, we presented a task-evoked anxiety rating, in which the participants were asked to verbally indicate their level of nervousness concerning each of the 8 conditions (e.g. "How nervous did you feel during the block – "unpredictable negative" ?") while a numerical rating scale was presented (1 = "not nervous at all" to 9 = "extremely nervous") after each run. During MRI examination heart and respiratory rate parameter were continuously measured while responses were collected. Note that RT, accuracy, respiratory and pulse rate data was assessed during the scanning session, but analysis of these parameter was not part of this thesis. To focus participants attention to the target stimulus and acquire behavioral data that allowed us to evaluate suitability of paradigm, we implemented two kinds of decision tasks dependent on stimulus modality. In picture trials, the task of the participants was the same as in the Somerville et al. (2013) investigation, namely to evaluate the target picture with respect to an indoors-outdoors focus ("Was this picture shown an indoor or outdoor scene?"). Response was collected with a button box attached at the participant´s dominant hand. Participants indicated their decision with the index (indoors) or middle finger (outdoors). In trials with electrical stimulation modality, a matrix containing bright and dark gray pixels was presented following digit presentation. In these trials, participants indicated, whether the pixel matrix contained a higher number of bright (index finger button) or dark gray (middle finger) pixels. After matrix offset, the somatosensory stimulus was applied. Following the MRI session, participants completed the post-testing state anxiety questionnaire (STAI-S), were debriefed and thanked for their participation. They received a compensation of 20.00 € and their anatomical images on disk. An overview of the whole experimental procedure is represented in **Figure 4.6**.

**Figure 4.6**

*Schematic Overview of the Experimental Procedure*
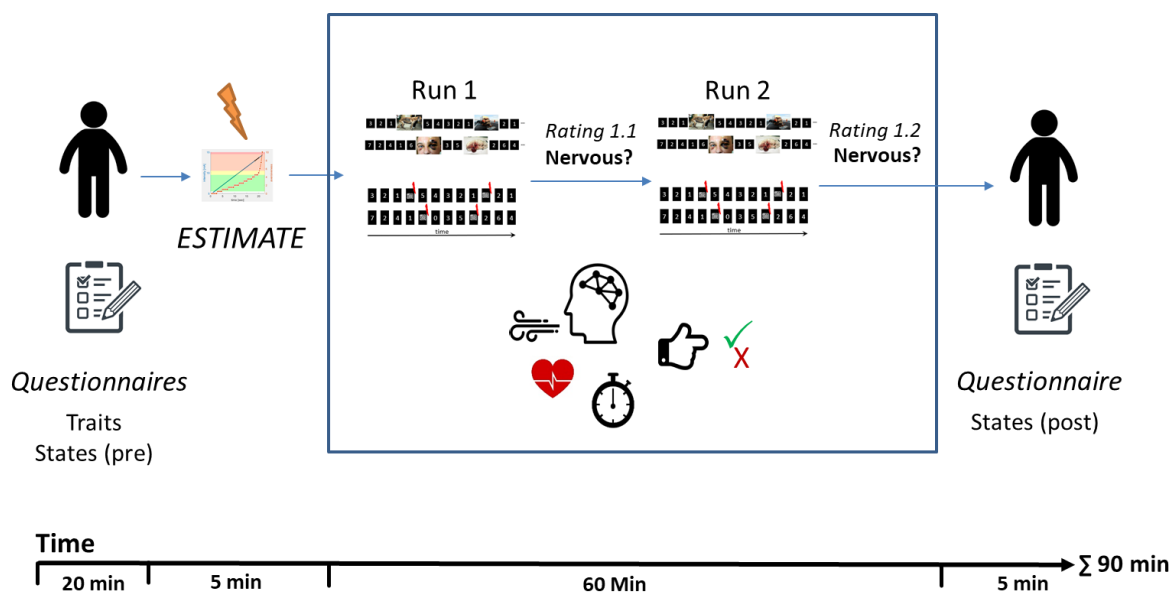


Figure represents a schematic overview of the whole experimental procedure that was conducted in one session lasting ~1,5 hours in total. Participants filled out informed consent and pre-testing questionnaires (state and trait scales). The STEP-procedure was performed to establish participants individual zap intensities (weak and strong). Neuroimaging procedure (blue box) consisted of two experimental runs containing the 8 experimental blocks. Following both runs, a numerical scale was presented while participants were asked to rate their level of nervousness (task-evoked anxiety rating). Parallel to neuroimaging data acquisition, physiological parameters (heart and respiratory rate), RT and accuracy rate were obtained. After the scanning session, participants were asked to fill in a post-scanning questionnaire (STAI-S-post).

## 4.2.5 Data Analysis

We were using FMRIB Software Library (FSL; (Smith et al., 2004) for neuroimaging data preprocessing. First, structural scans (T1-weighted images) were preprocessed with "fsl_anat" preprocessing pipeline ("fsl_anat - FslWiki", 2020) including transferring, orienting and registering images to standard space (FSL´s MNI152_T1_2mm standard template), cropping, bias-field correction, brain extraction, tissue-type and subcortical structure segmentation while using FSL FLIRT (FMRIB's Linear Image Registration Tool; (Jenkinson, 2002; Jenkinson & Smith, 2001). Functional images were preprocessed in the same way as anatomical scans while using FSL FEAT (FMRI Expert Analysis Tool) pipeline (Woolrich, Ripley, Brady, & Smith, 2001) for modeling fMRI data analysis based on general linear modelling (GLM). Within this process, slice timing was corrected for MB sequences (MB = 4) controlling for inherent sampling offsets in EPI sequence acquisition. Further, FSL FLIRT was used for co-registering

functional images to reference T1-image as well as for $B_0$-distortion and motion correction. Motion correction parameter estimates were further used in GLM analysis as predictors correcting for spatial displacements. Following slice-timing, distortion and motion correction, spatial smoothing with 5 mm by full width at half maximum (FWHM) was performed for revealing the local weighted average neighborhood activation of each voxel (Jenkinson & Chappell, 2018). We were applying high-pass temporal filtering cutoff for removing low-frequency artefacts. Following, ICA (independent component analysis) with FSL AROMA (Automatic Removal Of Motion Artifacts) pipeline was performed for identifying and removing non-neuronal denoised signal (i.e. physiological signals, motion artifacts) from fMRI data (Jenkinson & Chappell, 2018). Analysis pipeline was adapted in its fundamentals from the analysis strategy of Somerville et al. (2013). Within first-level analysis, GLM was modelled for each subject and each run for estimating stimulus response with respect to neural activity. We were setting up explanatory variables (EVs), containing a time course description for each voxel, for receiving parameter estimates that were needed for condition contrasting and running statistical analysis. Performing higher-level analysis, results of first-level analysis were combined for both runs (Woolrich, Behrens, Beckmann, Jenkinson, & Smith, 2004).

For receiving statistical parameter estimate (PE) image maps for each voxel, condition based EVs were modelled (PicNegPred, PicNegUnpr, PicNeuPred, PicNeuUnpr, ZapNegPred, ZapNegUnpr, ZapNeuPred and ZapNeuUnpr) separately for transient and sustained responses. Panel A in Figure 4.7 represents an example of the design matrix while a cut-out is displayed in panel B. For sustained responses, 8 predictors were modelled containing neural responses for whole block duration. Considering transient responses, 80 predictors were modelled along each TR of 2 seconds (T0 – T9) resulting in 10 predictors per condition. Transient responses were modeled with a finite impulse response (FIR), i.e. predictors that represent trial onsets (time 0) were shifted by one TR for 9 more TRs yielding a FIR-model with ten predictors (0-9) that covered a 20 sec period (or 10 TRs). Following, predictors for T2 – T5 were chosen for the final FIR-model which corresponds to calculating the area under the curve (AUC). Additionally, occurrence of on- and offset cues were modelled as confounds and additional predictors within design matrix.

**Figure 4.7**

*Design Matrix for Modelling Transient and Sustained Responses*

**A**
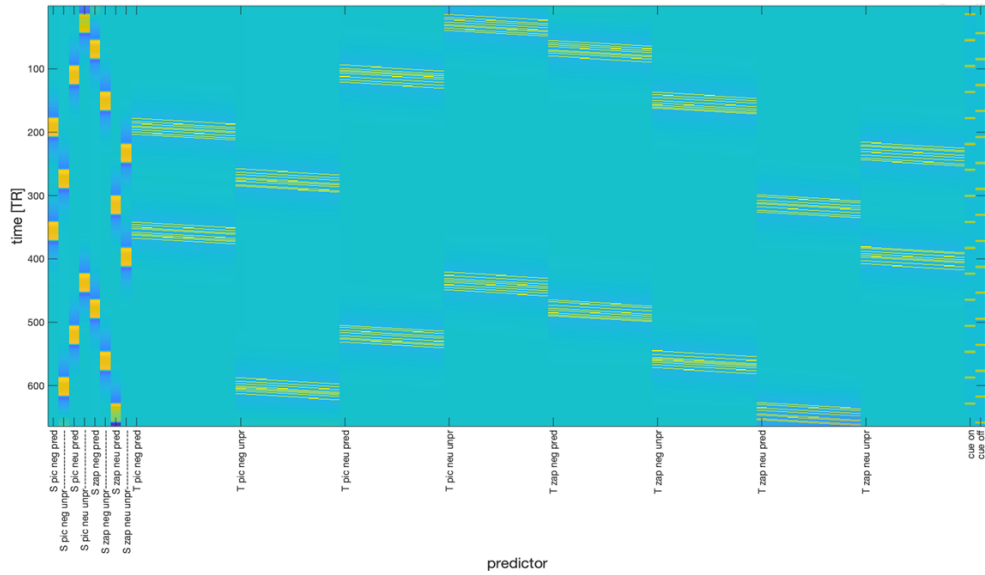


**B**
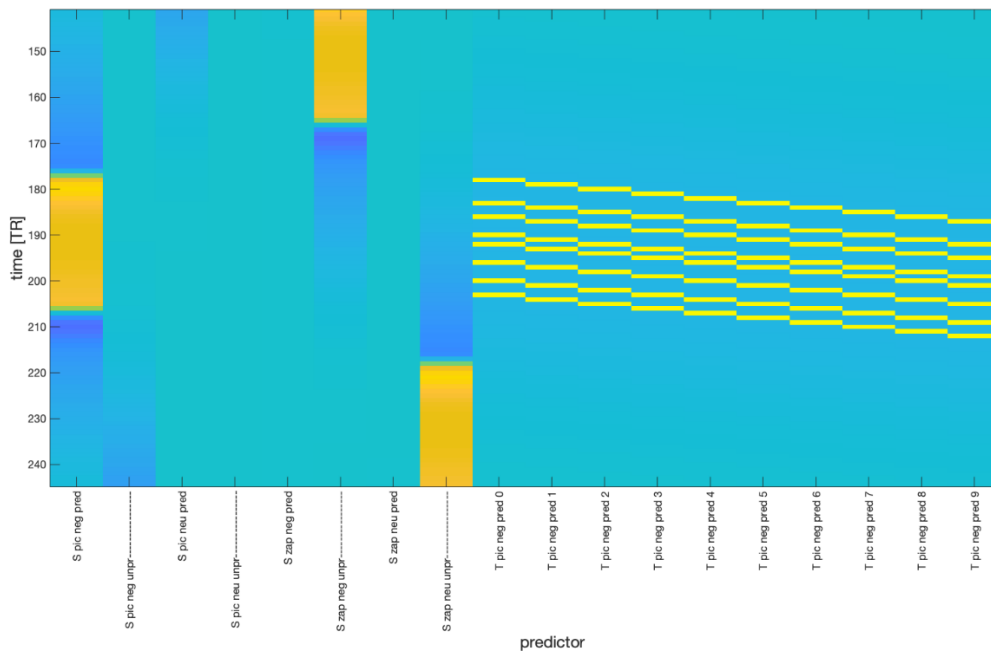


A) Example design matrix of one run. All design matrices contain 90 predictors (columns) over time (rows). The first 8 predictors model the sustained responses (S), i.e. entire blocks of conditions that extend over ~ 140 seconds each. The next 80 predictors model transient responses. The last two predictors modeled the occurrence of on- and offset cues that were presented visually at the beginning and end of each block. B) Cut-out from design matrix above demonstrating the modeling of sustained responses (first column: "S pic neg pred") and transient responses of the 8 trials that occurred during that block ("T pic neg pred 0"). Transient responses were modeled with a finite impulse response (FIR), i.e. predictors that represent trial onsets (time 0) were shifted by one TR for 9 more TRs yielding a FIR-model with ten predictors (0-9) that covered a 20 second period (or 10 TRs).

Resulting PE maps for transient (FIR parameter estimates) and sustained responses (blockwise PE) per subject and condition was used for repeated measures statistical analysis at group-level. Analysis was performed with MATLAB-based MRM (multivariate and repeated measures) toolbox (McFarquhar et al., 2016). For each kind of modality type (pictures vs. electrical stimulation), hypotheses testing was performed calculating a three-way rmANOVA while specifying "modality" (pictures, electrical stimulation (zaps)),"predictability" (pred, unpred), and "valence" (neg, neu) as within-subject factors. Uncorrected thresholding, approximate $p$-value calculation ($p < .001$), and false discovery rate correction method was set as inference statistics settings for exploring main effect of "modality", "valence" and "predictability" as well as the two- and three way interaction of interaction effect "modality*valence", "modality*predictability", "valence*predictability", and "modality*valence*predictability". For investigating brain systems involved in transient and sustained responses within, across and between stimulus modality, mass univariate $t$-test were performed on statistical parameter maps (SPM) resulted from MRM analysis. Separately, SPMs of picture trials and electrical stimulation were tested against null which yields information about stimulus-specific neural activity. SPM of the ME of "modality" resulting from the three-way ANOVA was used for exploring commonalities (minimal $t$-conjuction = pictures ∧ electrical stimulation) and differences (disjunction = pictures ∨ electrical stimulation) between stimulus modalities. Resulting SPMs were thresholded at $t = 3.347934$ (corresponding to $p < .001$).

Specific ROIs were defined that were shown to be involved in fear and anxiety processing according to literature and for ROIs that showed up in the whole brain analyses. With respect to transient responses, there was the aim to target areas that are known to play a crucial role in the fear network as well as during acute threat i.e., the amygdala, thalamus, insular cortex, hippocampus, parahippocampal gyrus, cingulate cortex, inferior frontal gyrus as well as middle frontal gyrus (Balderston et al., 2017; Hudson et al., 2020; Naaz et al., 2019; Somerville et al., 2010; Somerville et al., 2013). Considering sustained responses, regions responding to anxiety in unpredictable threat processing mainly frontal regions responses, such as superior and inferior frontal gyrus, insular cortex, brain stem, as well as cingulate cortex (Hudson et al., 2020; Somerville et al., 2010) were investigated. For exploring differences and

93

commonalities in threat processing in all regions contributing to acute and certain threat processing were analyzed in both transient and sustained responses.

ROI masks were selected from the Harvard-Oxford cortical and subcortical structural atlases (Desikan et al., 2006; Frazier et al., 2005; Goldstein et al., 2007; Makris et al., 2006). Harvard-Oxford cortical atlas was used for extracting masks of middle frontal gyrus, insular cortex, inferior frontal gyrus, frontal pole, frontal medial cortex, and superior frontal gyrus while Harvard-Oxford subcortical atlas was used for creating amygdala (left and right), thalamus (left and right), hippocampus (left and right), parahippocampal gyrus, and paracingulate gyrus masks.

Statistical analysis for hypotheses testing on these specific ROIs was performed with "ezANOVA statistics software" (Lawrence, 2015) which provides the opportunity for calculating confidence intervals (95%) according to procedure proposed by (Loftus & Masson, 1994) which is an appropriate way in repeated measures designs. For average BOLD amplitudes of each ROI, a three-way ANOVA considering three within factors ("modality" (pictures, electrical stimulation), "valence" (negative, neutral), and "predictability" (predictable, unpredictable)) was performed.

Considering questionnaire data, single item values of each participant for each questionnaire were summed up to a final score per scale and averaged across sample for obtaining affect sample characteristics. For investigating a pattern in personality trait and state dimensions, the relationship of personality state and trait variables questionnaires were correlated with each other (Pearson´s correlation coefficient analysis). Following, questionnaire data was correlated with BOLD signal amplitudes within the amygdala in both transient and sustained responses with respect to experimental conditions for exploring any relation.

Task-evoked anxiety rating responses was averaged for each participant across runs. For each dependent variable, 2x2 rmANOVAs were calculated for each type of stimulus modality (predictability*valence) separately while a further 2x2x2 rmANOVA (predictability*valence*stimulus) was conducted. In case of significant main and interaction effects, post-hoc comparisons were performed for yielding information about effect direction. Statistical analyses of behavioral and psychometric data was performed using SPSS software (IBM Corp. Released 2019. IBM SPSS Statistics for Windows, Version 25.0. Armonk, NY: IBM Corp.).

## 4.3 Results

Results part is structed as two main chapters with respect to transient (fear) and sustained (anxiety) neural responses. For each kind of responses, results of thresholded statistical parameter maps will be reported that was performed yielding response-specific patterns corresponding to our first analysis step. Following, results of ROI analyses will be presented while presenting results rmANOVA representing the second step of our analysis strategy. Subsequently, results of the correlation analyses with respect to individual differences in personality traits and affect states will be reported. At the end of the results chapter, behavioral data will be presented that was analyzed as a manipulation check which will provide information about suitability of paradigm and would give implication for interpreting the neural results.

### 4.3.1 Transient Responses to Fear

### 4.3.1.1  Whole Brain Analysis

Transient responses were estimated from statistical parameter maps of the AUC for time period of 4-12 seconds after stimulus onset resulting from a finite impulse response (FIR) analysis. Results of whole brain analysis for transient responses are presented in Figure 4.8. With respect to AUC (activity against null) BOLD amplitude in picture blocks (A), we found a strong increase of bilateral visual cortex, supplementary motor area, the posterior part of paracingulate cortex, insular cortex, brain stem, superior frontal gyrus, thalamus and the amygdala. Given blocks with electrical stimulation (B), results indicated strong bilateral BOLD response in visual cortex the posterior aspect of paracingulate cortex, brain stem, superior frontal gyrus, thalamus, while amygdala response was absent. Comparison of differences in BOLD response between stimulus modalities (C) revealed higher BOLD responses in visual cortex and the amygdala, whereas electrical stimulation produced higher amplitudes in somatosensory areas. Considering commonalities (D), minimal *t*-conjuction between picture and electrical stimulation yielded accordance in both stimulus modalities in visual cortex, brain stem, middle frontal gyrus, the posterior aspect of paracingulate cortex and in thalamic nuclei.

**Figure 4.8**

*Statistical Parameter Maps of the Area Under the Curve for Transient Responses*
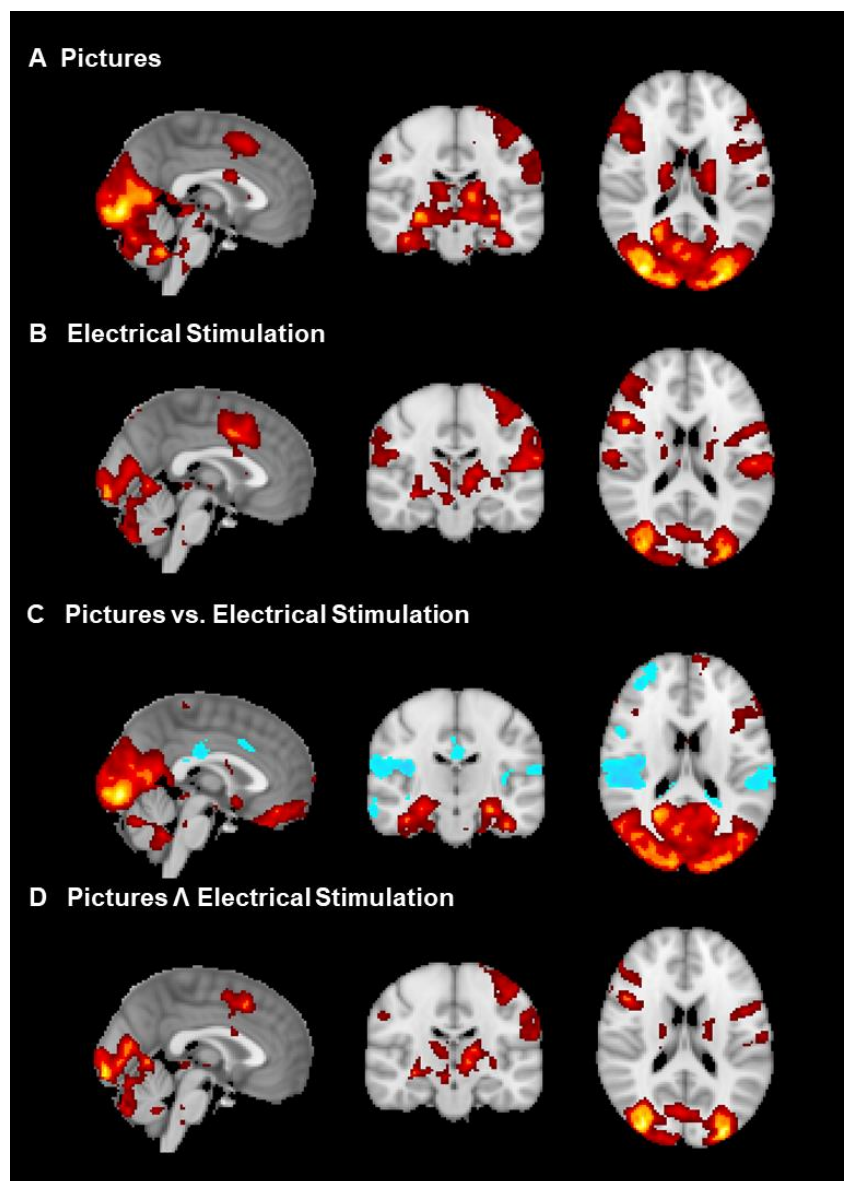


Statistical parameter maps of the area under the curve (AUC) 4-12 seconds after stimulus onset resulting from a finite impulse response (FIR) analysis (hot colors in A), B), and D): regions that show increased BOLD amplitude with respect to analysis; hot colors in C): increased BOLD amplitude within picture trials; cold colors in C): increased BOLD amplitude within electrical-simulation trials). A) AUC in picture trials (activity against null) revealed a strong increase of bilateral visual cortex, supplementary motor area, posterior part of paracingulate cortex, insular cortex, brain stem, superior frontal gyrus, thalamus and the amygdala. B) Trials with electrical stimulation also yielded strong bilateral BOLD responses in visual cortex the posterior aspect of paracingulate cortex, brain stem, superior frontal gyrus, thalamus, but not in the amygdala. C) Voxelwise comparison of BOLD differences between stimulus modalities. Picture trials yielded higher BOLD amplitudes in visual cortex and the amygdala, whereas electrical stimulation produced higher responses in somatosensory areas. D) SPM of the minimal t-conjunction between picture- and somatosensory stimulation revealed commonalities in visual cortex, brain stem, middle frontal gyrus, the posterior aspect of paracingulate cortex and in thalamic nuclei. All maps are thresholded at $t$ = 3.347934, corresponding to $p < .001$.

## 4.3.1.2  Region of Interest Analysis

Region of interest (ROI) analysis was conducted for exploring the effects of the factorial study design in predefined ROIs that selected according to literature as well as for regions that show up in the whole-brain analysis with respect to transient responses.

### 4.3.1.2.1 Left Amygdala

Table 7.4 in the appendix and panel A in **Figure 4.9** depict the average BOLD signal in left amygdala as a function of valence and predictability. Table 7.5 in the appendix reports a corresponding three-factorial within-subjects ANOVA (modality vs. valence vs. predictability). Unpredictably occurring stimuli yielded a higher BOLD response than predictably occurring stimuli (ME "predictability": $F(1, 34) = 10.5$, $p < .01$). Panels B and C show that pictures yielded stronger responses than electrical stimulation (ME "modality": $F(1, 34) = 85.8$, $p < .001$), but statistically these patterns did not differ as there were no statistically significant two-way or three-way interactions between modality, predictability, and valence.

**Figure 4.9**

*Average BOLD Signal in the Left Amygdala for Transient Responses*
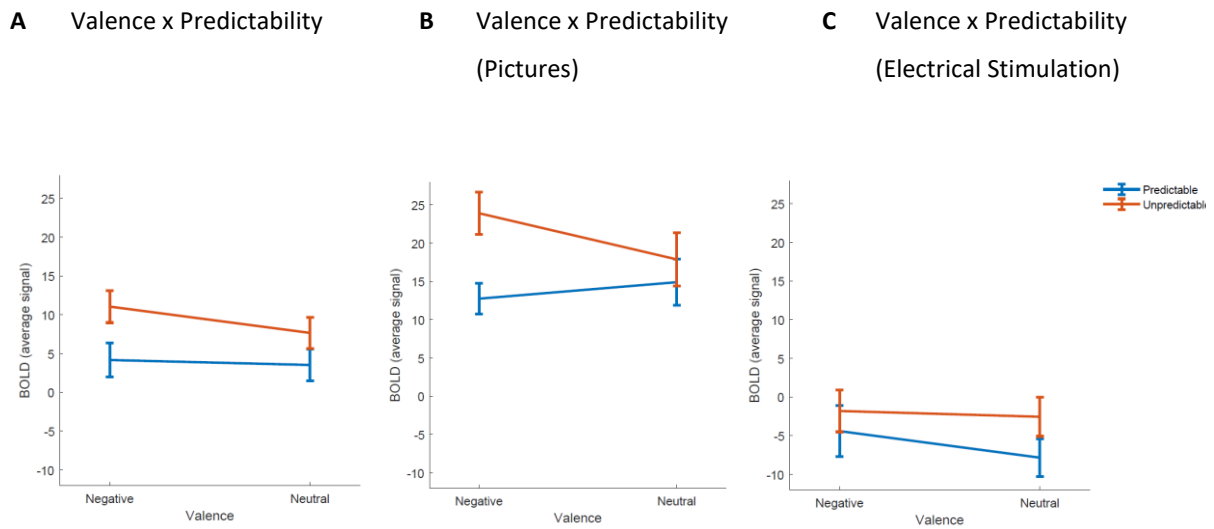


Average BOLD signal in the left amygdala A) across modality: unpredictably occurring stimuli yield a higher BOLD response than predictably occurring stimuli (ME "predictability": $F_{(1, 34)}$= 10.5, $p < .01$). Error bars depict the standard error of the mean. Panels B) and C) illustrate that pictures yielded stronger responses than electrical stimulation (ME "modality": $F_{(1, 34)}$= 85.8, $p < .001$), but statistically these patterns did not differ as there were no statistically significant two-way or three-way interactions between modality, predictability, and valence.

## 4.3.1.2.2   Right Amygdala

Table 7.6 in the appendix and panel A in Figure 4.10 depict the average BOLD signal in right amygdala as a function of valence and predictability. Table 7.7 in the appendix reports a corresponding three-factorial within-subjects ANOVA. Unpredictably occurring stimuli yielded a marginally higher BOLD response than predictably occurring stimuli (ME "predictability": $F(1,34) = 4.67$, $p < .05$). Panels B and C show that pictures yielded stronger responses than electrical stimulation (ME "modality": $F(1, 34)= 101.00$, $p < .001$), but statistically these patterns did not differ as there were no statistically significant two-way or three-way interactions between modality, predictability, and valence.

**Figure 4.10**

*Average BOLD Signal in the Right Amygdala for Transient Responses*

**A**   Valence x Predictability

**B**   Valence x Predictability (Pictures)

**C**   Valence x Predictability (Electrical Stimulation)



Average BOLD signal in the right amygdala A) across modality: unpredictably occurring stimuli yielded a marginally higher BOLD response than predictably occurring stimuli (main effect "predictability": $F(1,34) = 4.67$, $p < .05$). Error bars depict the standard error of the mean. Panels B) and C) illustrate that pictures yielded stronger responses than electrical stimulation (ME "modality": $F(1, 34)= 101.00$, $p < .001$), but statistically these patterns did not differ as there were no statistically significant two-way or three-way interactions between modality, predictability, and valence.

## 4.3.1.2.3 Left Thalamus

Table 7.8 in the appendix and panel A in Figure 4.11 depict the average BOLD signal in left thalamus as a function of valence and predictability. Table 7.9 in the appendix reports a corresponding three-factorial within-subjects ANOVA. Unpredictably occurring stimuli yielded a higher BOLD response than predictably occurring stimuli (ME "predictability": $F(1, 34)= 6.20$, $p < 0.05$). Panels B and C show that pictures yielded stronger responses than electrical stimulation (main effect "modality": $F(1, 34) = 68.7$, $p < .001$), but statistically these patterns did not differ as there were no statistically significant two-way or three-way interactions between modality, predictability, and valence.

**Figure 4.11**

*Average BOLD Signal in the Left Thalamus for Transient Responses*

**A**    Valence x Predictability

**B**    Valence x Predictability
(Pictures)

**C**    Valence x Predictability
(Electrical Stimulation)



Average BOLD signal in the left thalamus A) across modality: unpredictably occurring stimuli yield a higher BOLD response than predictably occurring stimuli (ME "predictability": $F(1, 34)= 6.20$, $p < 0.05$). Error bars depict the standard error of the mean. Panels B) and C) illustrate that pictures yielded stronger responses than electrical stimulation (ME "modality": $F(1, 34) = 68.7$, $p < .001$), but statistically these patterns did not differ as there were no statistically significant two-way or three-way interactions between modality, predictability, and valence.

## 4.3.1.2.4 Right Thalamus

Table 7.10 in the appendix and panel A in Figure 4.12 depict the average BOLD signal in right thalamus as a function of valence and predictability. Table 7.11 in the appendix reports a corresponding three-factorial within-subjects ANOVA. Unpredictably occurring stimuli yielded a higher BOLD response than predictably occurring stimuli but this effect did not reach level of statistical significance. Panels B and C show that pictures yielded stronger responses than electrical stimulation (ME "modality": $F(1, 34)$ = 66.8, $p < .001$), but statistically these patterns did not differ as there were no statistically significant two-way or three-way interactions between modality, predictability, and valence.

**Figure 4.12**

*Average BOLD Signal in the Right Thalamus for Transient Responses*

**A** Valence x Predictability    **B** Valence x Predictability (Pictures)    **C** Valence x Predictability (Electrical Stimulation)



Average BOLD signal in the right Thalamus A) across modality: unpredictably occurring stimuli yielded a marginally higher BOLD response than predictably occurring stimuli but this effect did not reach level of statistical significance. Error bars depict the standard error of the mean. Panels B) and C) illustrate that pictures yielded stronger responses than electrical stimulation (ME "modality": $F(1, 34) = 66.8$, $p < .001$) , but statistically these patterns did not differ as there were no statistically significant two-way or three-way interactions between modality, predictability, and valence.

## 4.3.1.2.5 Left Hippocampus

Table 7.12 in the appendix and panel A in Figure 4.13 depict the average BOLD signal in left hippocampus as a function of valence and predictability. Table 7.13 in the appendix reports a corresponding three-factorial within-subjects ANOVA. Unpredictably occurring stimuli yielded a higher BOLD response than predictably occurring stimuli (ME "predictability": $F(1, 34)= 9.50$, $p < .01$). Panels B and C show that pictures yielded stronger responses than electrical stimulation (main effect "modality": $F(1, 34) = 116.00$, $p < .001$), but statistically these patterns did not differ as there were no statistically significant two-way or three-way interactions between modality, predictability, and valence.

**Figure 4.13**

*Average BOLD Signal in the Left Hippocampus for Transient Responses*

| **A** Valence x Predictability | **B** Valence x Predictability (Pictures) | **C** Valence x Predictability (Electrical Stimulation) |



Average BOLD signal in the left hippocampus A) across modality: unpredictably occurring stimuli yield a higher BOLD response than predictably occurring stimuli (ME "predictability": $F(1, 34)= 9.50$, $p < 0.01$). Error bars depict the standard error of the mean. Panels B) and C) illustrate that pictures yielded stronger responses than electrical stimulation (ME "modality": $F(1, 34) = 116.00$, $p < .001$), but statistically these patterns did not differ as there were no statistically significant two-way or three-way interactions between modality, predictability, and valence.

### 4.3.1.2.6 Right Hippocampus

Table 7.14 in the appendix and panel A in Figure 4.14 depict the average BOLD signal in right hippocampus as a function of valence and predictability. Table 7.15 in the appendix reports a corresponding three-factorial within-subjects ANOVA. Unpredictably occurring stimuli yielded a higher BOLD response than predictably occurring stimuli (ME "predictability": $F(1, 34)= 6.10$, $p < .05$). Panels B and C show that pictures yielded stronger responses than electrical stimulation (ME "modality": $F(1, 34) = 120.00$, $p < .001$), but statistically these patterns did not differ as there were no statistically significant two-way or three-way interactions between modality, predictability, and valence.

**Figure 4.14**

*Average BOLD Signal in the Right Hippocampus for Transient Responses*

| A | Valence x Predictability | B | Valence x Predictability (Pictures) | C | Valence x Predictability (Electrical Stimulation) |
|---|---|---|---|---|---|



Average BOLD signal in the right hippocampus A) across modality: unpredictably occurring stimuli yield a higher BOLD response than predictably occurring stimuli (ME "predictability": $F(1, 34)= 6.10$, $p < .05$). Error bars depict the standard error of the mean. Panels B) and C) illustrate that pictures yielded stronger responses than electrical stimulation (ME "modality": $F(1, 34) = 120.00$, $p < .001$), but statistically these patterns did not differ as there were no statistically significant two-way or three-way interactions between modality, predictability, and valence.

### 4.3.1.2.7 Parahippocampal Gyrus

**Table 7.16** in the appendix and panel A in Figure 4.15 depict the average BOLD signal in parahippocampal gyrus as a function of valence and predictability. Table 7.17 in the appendix reports a corresponding three-factorial within-subjects ANOVA. Unpredictably occurring stimuli yielded a higher BOLD response than predictably occurring stimuli (ME "predictability": $F(1, 34)= 10.2$, $p < .01$). Panels B and C show that pictures yielded stronger responses than electrical stimulation (ME "modality": $F(1, 34) = 137.00$, $p < .001$), but statistically these patterns did not differ as there were no statistically significant two-way or three-way interactions between modality, predictability, and valence.

**Figure 4.15**

*Average BOLD Signal in Parahippocampal Gyrus for Transient Responses*

**A** Valence x Predictability    **B** Valence x Predictability (Pictures)    **C** Valence x Predictability (Electrical Stimulation)
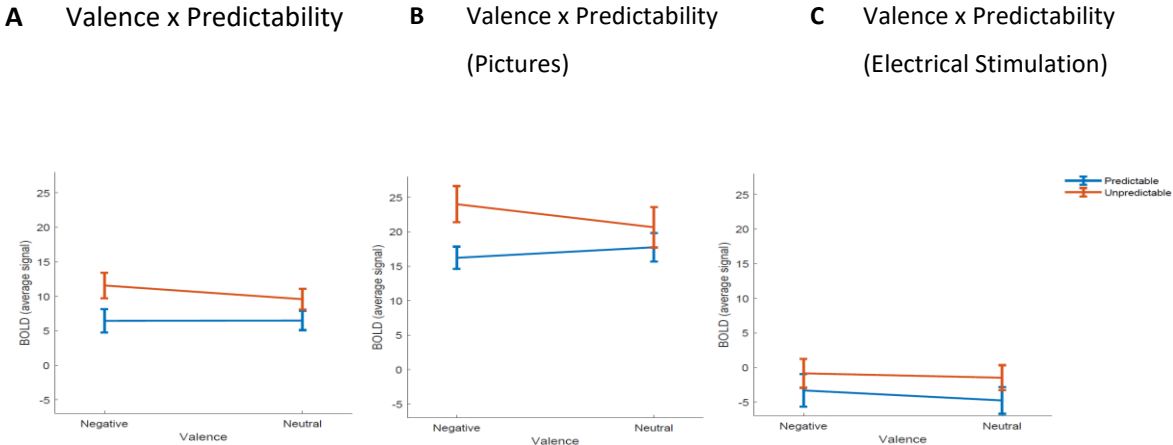


Average BOLD signal in the parahippocampal gyrus A) across modality: unpredictably occurring stimuli yield a higher BOLD response than predictably occurring stimuli (ME "predictability": $F(1, 34)= 10.2$, $p < .01$).. Error bars depict the standard error of the mean. Panels B) and C) illustrate that pictures yielded stronger responses than electrical stimulation (ME "modality": $F(1, 34) = 137.00$, $p < .001$), but statistically these patterns did not differ as there were no statistically significant two-way or three-way interactions between modality, predictability, and valence.

### 4.3.1.2.8 Brain Stem

Table 7.18 in the appendix and panel A in Figure 4.16 depict the average BOLD signal in brain stem as a function of valence and predictability. Table 7.19 in the appendix reports a corresponding three-factorial within-subjects ANOVA. Unpredictably occurring stimuli yielded a higher BOLD response than predictably occurring stimuli but this effect did not reach level of statistical significance. Panels B and C show that pictures yielded stronger responses than electrical stimulation (ME "modality": $F(1, 34)$ = 82.5, $p < .001$), but statistically these patterns did not differ as there were no statistically significant two-way or three-way interactions between modality, predictability, and valence.

**Figure 4.16**

*Average BOLD Signal in the Brain Stem for Transient Responses*

**A**  Valence x Predictability      **B**  Valence x Predictability      **C**  Valence x Predictability

(Pictures)                          (Electrical Stimulation)
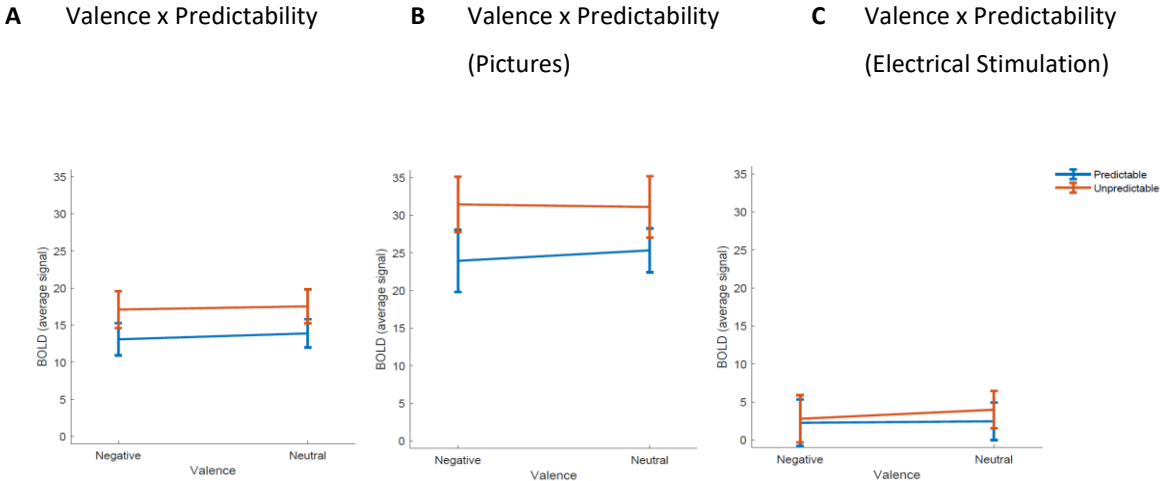


Average BOLD signal in the brain stem A) across modality: unpredictably occurring stimuli yield a higher BOLD response than predictably occurring stimuli but this effect did not reach level of statistical significance. Error bars depict the standard error of the mean. Panels B) and C) illustrate that pictures yielded stronger responses than electrical stimulation (ME "modality": $F(1, 34) = 82.5$, $p < .001$), but statistically these patterns did not differ as there were no statistically significant two-way or three-way interactions between modality, predictability, and valence.

### 4.3.1.2.9 Paracingulate Gyrus

Table 7.20 in the appendix and panel A in Table 7.21 depict the average BOLD signal in paracingulate gyrus as a function of valence and predictability. Table 7.21 in the appendix reports a corresponding three-factorial within-subjects ANOVA. Unpredictably occurring stimuli yielded a higher BOLD response than predictably occurring stimuli (ME "predictability": $F(1, 34)= 5.50$, $p < .05$). Panels B and C show that pictures yielded stronger responses than electrical stimulation (ME "modality": $F(1, 34) = 22.60$, $p < .001$), but statistically these patterns did not differ as there were no statistically significant two-way or three-way interactions between modality, predictability, and valence.

**Figure 4.17**

*Average BOLD Signal in Paracingulate Gyrus for Transient Responses*
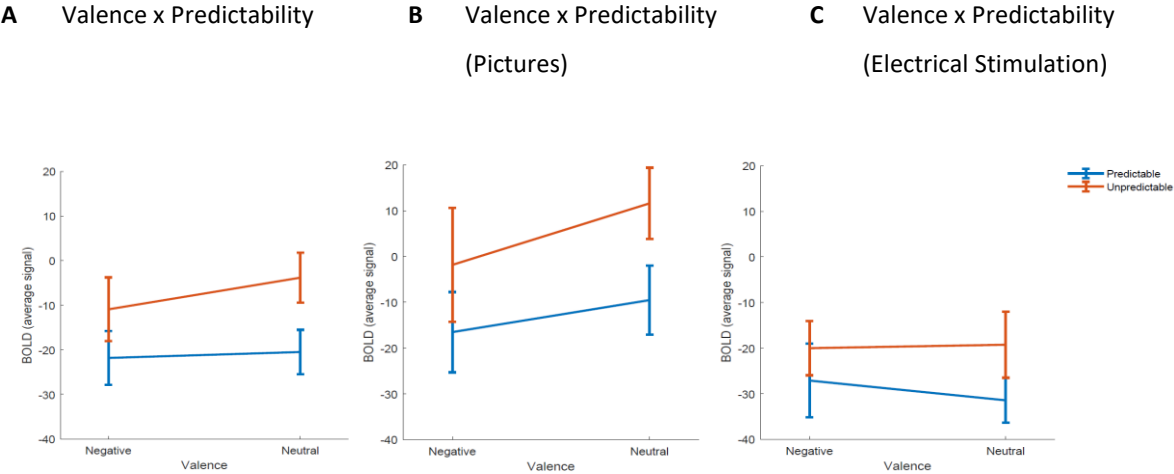
| **A** Valence x Predictability | **B** Valence x Predictability (Pictures) | **C** Valence x Predictability (Electrical Stimulation) |



Average BOLD signal in the paracingulate gyrus A) across modality: unpredictably occurring stimuli yield a higher BOLD response than predictably occurring stimuli (ME "predictability": $F(1, 34)= 5.50$, $p < .05$). Error bars depict the standard error of the mean. Panels B) and C) illustrate that pictures yielded stronger responses than electrical stimulation (ME "modality": $F(1, 34) = 22.6$, $p < .001$), but statistically these patterns did not differ as there were no statistically significant two-way or three-way interactions between modality, predictability, and valence.

#### 4.3.1.2.10    Insular Cortex

Table 7.22 in the appendix and panel A in Figure 4.18 depict the average BOLD signal in insular cortex as a function of valence and predictability. Table 7.23 in the appendix reports a corresponding three-factorial within-subjects ANOVA. Unpredictably occurring stimuli yielded a higher BOLD response than predictably occurring stimuli but this effect did not reach level of statistical significance. Panels B and C show that electrical stimulation yielded stronger responses than pictures (ME "modality": $F(1, 34)$ = 40.80, $p < .001$), but statistically these patterns did not differ as there were no statistically significant two-way or three-way interactions between modality, predictability, and valence.

**Figure 4.18**

*Average BOLD Signal in the Insular Cortex for Transient Responses*

| **A** Valence x Predictability | **B** Valence x Predictability (Pictures) | **C** Valence x Predictability (Electrical Stimulation) |
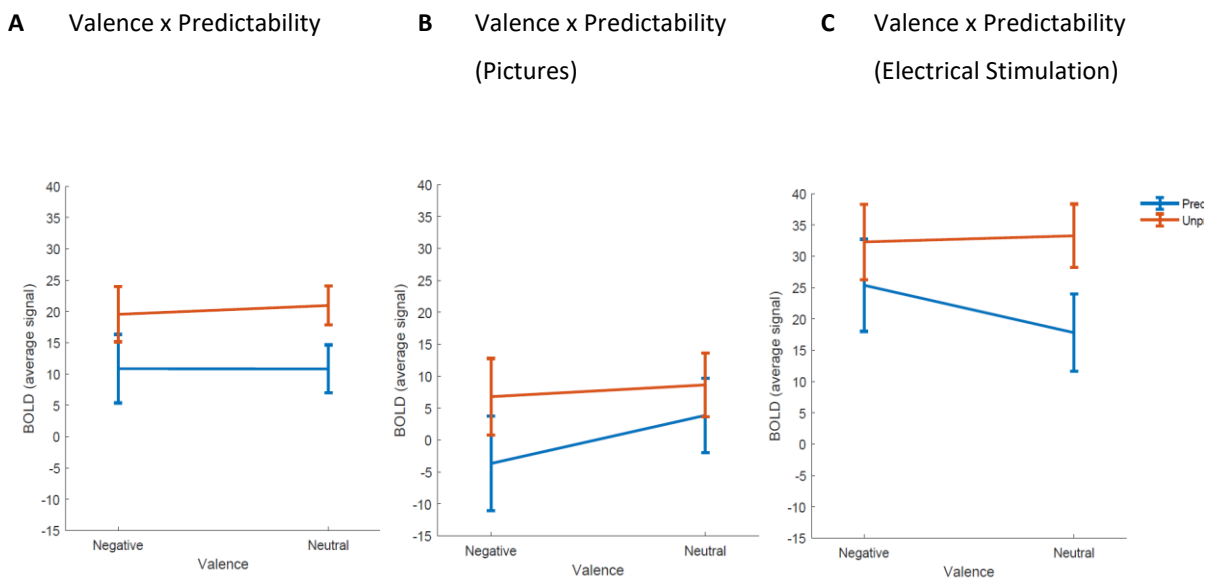


Average BOLD signal in the insular cortex A) across modality: unpredictably occurring stimuli yield a higher BOLD response than predictably occurring stimuli but this effect did not reach level of statistical significance. Error bars depict the standard error of the mean. Panels B) and C) illustrate that electrical stimulation yielded stronger responses than pictures (ME "modality": $F(1, 34)$ = 40.80, $p < .001$), but statistically these patterns did not differ as there were no statistically significant two-way or three-way interactions between modality, predictability, and valence.

### 4.3.1.2.11    Frontal Pole

Table 7.24 in the appendix and panel A in Figure 4.19 depict the average BOLD signal in frontal gyrus as a function of valence and predictability. Table 7.25 in the appendix reports a corresponding three-factorial within-subjects ANOVA. Unpredictably occurring stimuli yielded a higher BOLD response than predictably occurring stimuli (ME "predictability": $F(1, 34) = 4.99$, $p < .05$). Panels B and C show that pictures yielded stronger responses than electrical stimulation (ME "modality": $F(1, 34) = 17.90$, $p < .001$), but statistically these patterns did not differ as there were no statistically significant two-way or three-way interactions between modality, predictability, and valence.

**Figure 4.19**

*Average BOLD Signal in Frontal Pole for Transient Responses*

| **A** Valence x Predictability | **B** Valence x Predictability (Pictures) | **C** Valence x Predictability (Electrical Stimulation) |



Average BOLD signal in the paracingulate gyrus A) across modality: unpredictably occurring stimuli yield a higher BOLD response than predictably occurring stimuli (ME "predictability": $F(1, 34)= 4.99$, $p < .05$). Error bars depict the standard error of the mean. Panels B) and C) illustrate that pictures yielded stronger responses than electrical stimulation (ME "modality": $F(1, 34) = 17.9$, $p < .001$), but statistically these patterns did not differ as there were no statistically significant two-way or three-way interactions between modality, predictability, and valence.

### 4.3.1.2.12    Middle Frontal Gyrus

Table 7.26 in the appendix and panel A in **Figure 4.20** depict the average BOLD signal in middle frontal gyrus as a function of valence and predictability. Table 7.27 in the appendix reports a corresponding three-factorial within-subjects ANOVA. Unpredictably occurring stimuli yielded a higher BOLD response than predictably occurring stimuli across stimulus modality. But these effects did not reach level of statistical significance. Panels B and C show that pictures yielded stronger responses than electrical stimulation (ME "modality": $F(1, 34) = 24.50$, $p < .001$). Considering electrical stimulation, unpredictability came along with lower BOLD amplitude compared to predictable timings in negative valent stimuli. But statistically these patterns did not differ as there were no statistically significant two-way or three-way interactions between modality, predictability, and valence.

**Figure 4.20**

*Average BOLD Signal in the Middle Frontal Gyrus for Transient Responses*

**A**    Valence x Predictability        **B**    Valence x Predictability        **C**    Valence x Predictability
                                                    (Pictures)                                        (Electrical Stimulation)
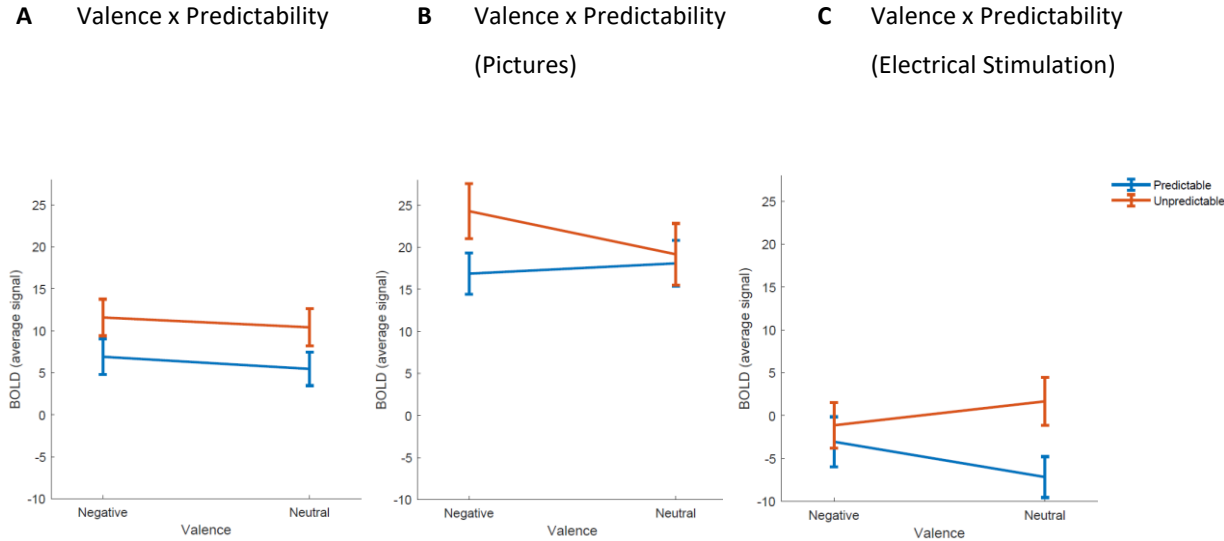


Average BOLD signal in the middle frontal gyrus A) across modality: unpredictably occurring stimuli yield a higher BOLD response than predictably occurring stimuli but this effect did not reach level of statistical significance. Error bars depict the standard error of the mean. Panels B) and C) illustrate that pictures yielded stronger responses than electrical stimulation (ME "modality": $F(1, 34) = 24.50$, $p < .001$), but statistically these patterns did not differ as there were no statistically significant two-way or three-way interactions between modality, predictability, and valence.

### 4.3.1.2.13    Inferior Frontal Gyrus

Table 7.28 in the appendix and panel A in Figure 4.21 depict the average BOLD signal in inferior frontal gyrus as a function of valence and predictability. Table 7.29 in the appendix reports a corresponding three-factorial within-subjects ANOVA. Unpredictably occurring stimuli yielded a higher BOLD response than predictably occurring stimuli (ME "predictability": $F(1, 34)= 4.19$, $p < .05$). Panels B and C show that pictures yielded stronger responses than electrical stimulation (ME "modality": $F(1, 34) = 45.60$, $p < .001$). While in picture blocks unpredictability came along with higher BOLD response regardless of valence, there was found that predictable negative trials evoked stronger responses than unpredictable negative trials. But statistically these patterns did not differ as there were no statistically significant two-way or three-way interactions between modality, predictability, and valence.

**Figure 4.21**

*Average BOLD Signal in the Inferior Frontal Gyrus for Transient Responses*

**A**    Valence x Predictability          **B**    Valence x Predictability          **C**    Valence x Predictability
                                                    (Pictures)                                    (Electrical Stimulation)
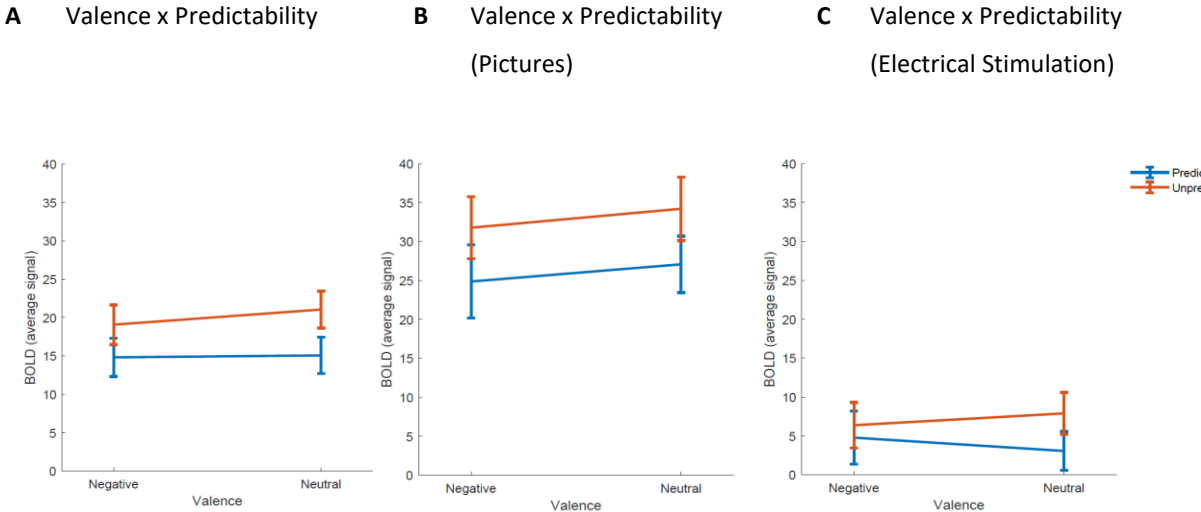


Average BOLD signal in the inferior frontal gyrus A) across modality: unpredictably occurring stimuli yield a higher BOLD response than predictably occurring stimuli (ME "predictability": $F(1, 34)= 4.19$, $p < .05$). Error bars depict the standard error of the mean. Panels B) and C) illustrate that pictures yielded stronger responses than electrical stimulation (ME "modality": $F(1, 34) = 45.6$, $p < .001$), but statistically these patterns did not differ as there were no statistically significant two-way or three-way interactions between modality, predictability, and valence.

### 4.3.1.2.14    Frontal medial cortex

Table 7.30 in the appendix and panel A in Figure 4.22 depict the average BOLD signal in the frontal medial cortex as a function of valence and predictability. Table 7.31 in the appendix reports a corresponding three-factorial within-subjects ANOVA. Unpredictably occurring stimuli yielded a higher BOLD response than predictably occurring stimuli (ME "predictability": $F(1, 34)= 4.69$, $p < .05$). Panels B and C show that pictures yielded stronger responses than electrical stimulation (ME "modality": $F(1, 34) = 63.30$, $p < .001$), but statistically these patterns did not differ as there were no statistically significant two-way or three-way interactions between modality, predictability, and valence.

**Figure 4.22**

*Average BOLD Signal in the Inferior Frontal Medial Cortex for Transient Responses*

**A**    Valence x Predictability          **B**    Valence x Predictability          **C**    Valence x Predictability
                                              (Pictures)                         (Electrical Stimulation)
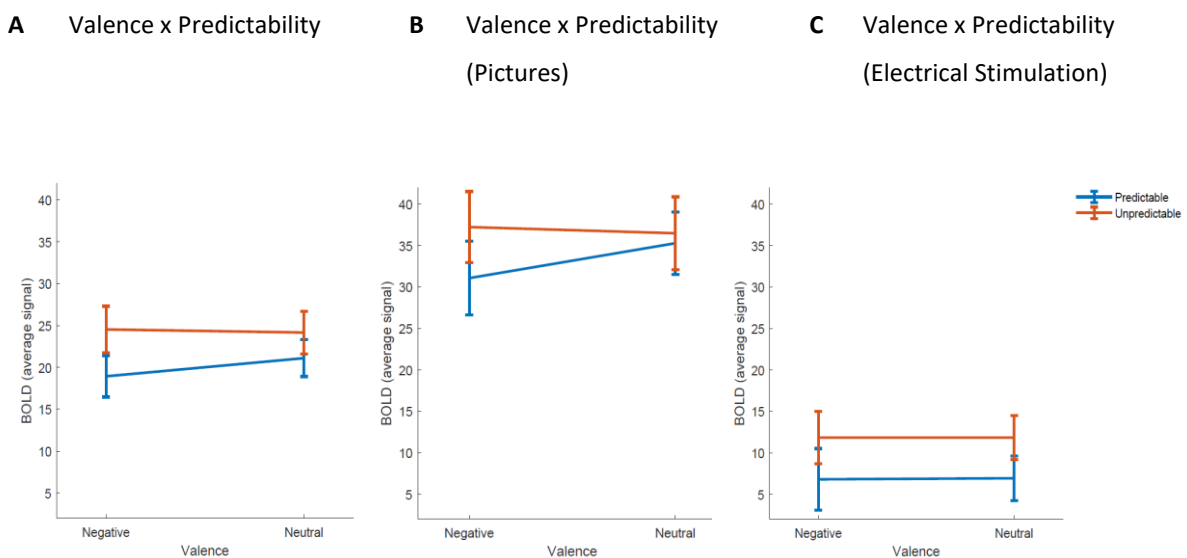


Average BOLD signal in the inferior frontal gyrus A) across modality: unpredictably occurring stimuli yield a higher BOLD response than predictably occurring stimuli (ME "predictability": $F(1, 34)= 4.69$, $p < .05$). Error bars depict the standard error of the mean. Panels B) and C) illustrate that pictures yielded stronger responses than electrical stimulation (ME "modality": $F(1, 34) = 63.30$, $p < .001$), but statistically these patterns did not differ as there were no statistically significant two-way or three-way interactions between modality, predictability, and valence.

### 4.3.1.2.15    Superior Frontal Gyrus

Table 7.32 in the appendix and panel A in Figure 4.23 depict the average BOLD signal in the superior frontal gyrus as a function of valence and predictability. Table 7.33 in the appendix reports a corresponding three-factorial within-subjects ANOVA. Unpredictably occurring stimuli yielded a higher BOLD response than predictably occurring stimuli (ME "predictability": $F(1, 34)= 5.10$, $p < .05$). Panels B and C show that pictures yielded stronger responses than electrical stimulation (ME "modality": $F(1, 34) = 45.80$, $p < .001$), but statistically these patterns did not differ as there were no statistically significant two-way or three-way interactions between modality, predictability, and valence.

**Figure 4.23**

*Average BOLD Signal in the Superior Frontal Gyrus for Transient Responses*

**A**    Valence x Predictability        **B**    Valence    x    Predictability   **C**    Valence    x    Predictability
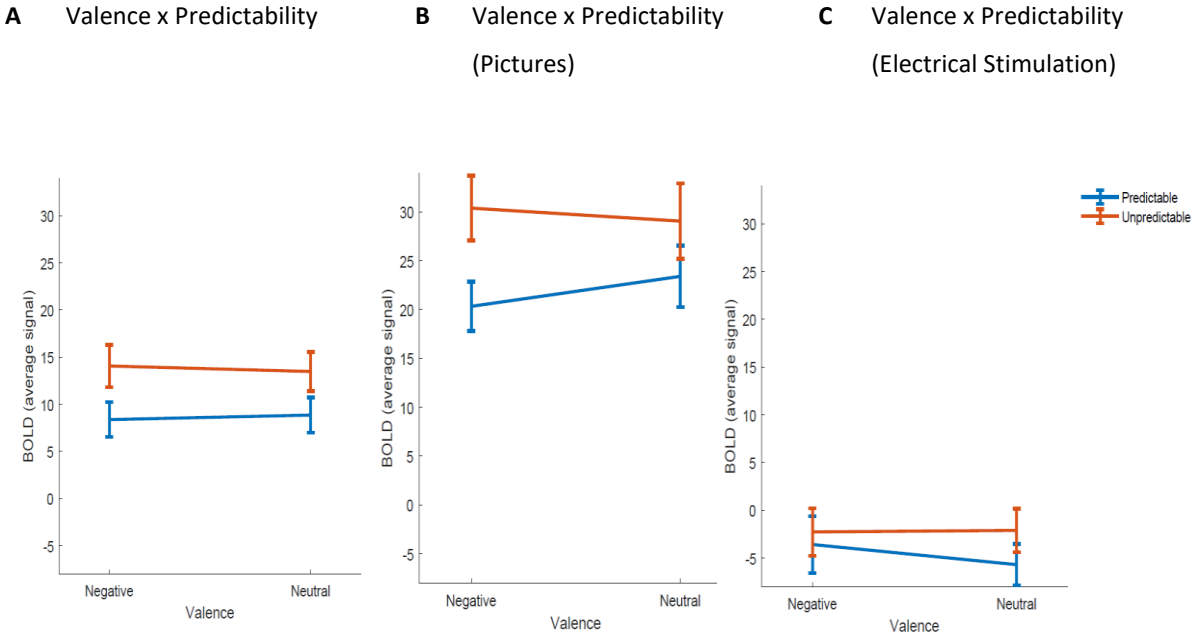                                                  (Pictures)                                  (Electrical Stimulation)
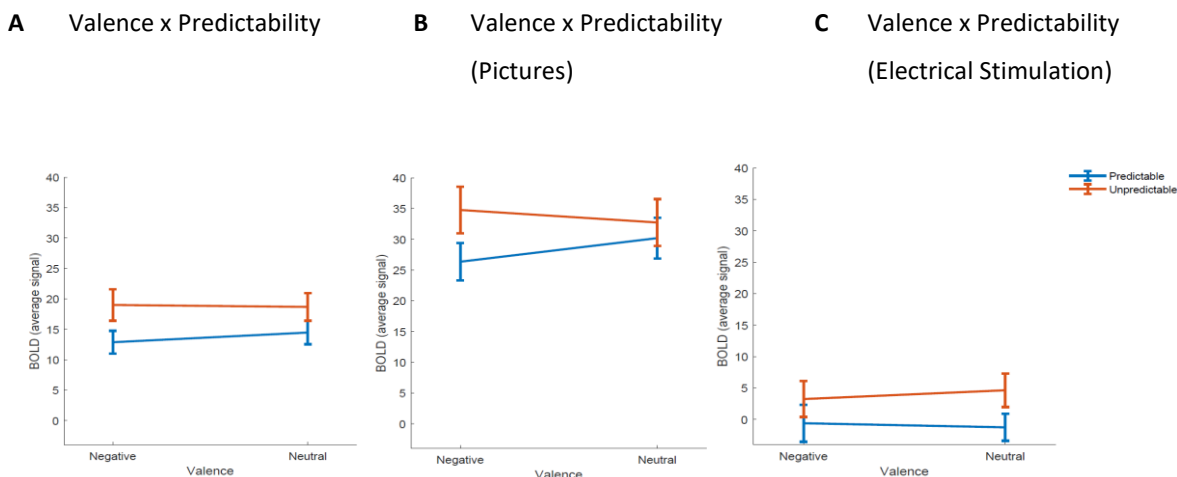


Average BOLD signal in the superior frontal gyrus A) across modality: unpredictably occurring stimuli yield a higher BOLD response than predictably occurring stimuli (ME "predictability": $F(1, 34)= 5.10$, $p < .05$). Error bars depict the standard error of the mean. Panels B) and C) illustrate that pictures yielded stronger responses than electrical stimulation (ME "modality": $F(1, 34) = 45.80$, $p < .001$), but statistically these patterns did not differ as there were no statistically significant two-way or three-way interactions between modality, predictability, and valence.

### 4.3.1.2.16 Individual Differences in Transient Responses within the Amygdala

Table 7.34, Table 7.35, and Table 7.36 in the appendix and in Figure 4.24 are displaying pairwise Pearson correlations for questionnaire data with average BOLD signal within the left amygdala for transient responses.

**Figure 4.24**

*Correlation of Questionnaire data with Average BOLD Signal Within the Left Amygdala for Transient Responses*
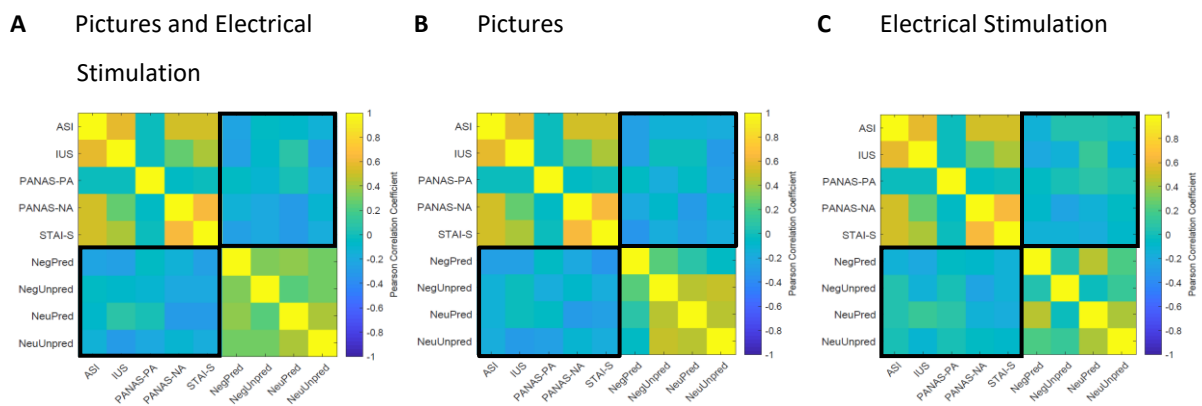


Different cells (colored outlines) represent pairwise correlations of questionnaires and BOLD amplitude within the left amygdala for transient responses across stimulus modalities (panel A) within picture (panel B) and electrical stimulation trials (anel C) while warmer colors represent higher Pearson Correlation Coefficient. Black frames represent correlations between questionnaires and BOLD amplitude with respect to conditions. Results indicated no significant relationship of questionnaire data across, and within both stimulus modalities

Considering the correlations of questionnaire data for personality traits and affect states with average BOLD signal within the left amygdala with respect to transient responses across stimulus modality (panel A), for picture stimuli (panel B) and electrical stimulation trials (panel C) there were found no significant correlations.

Table 7.37, Table 7.38, and Table 7.39 in the appendix and Figure 4.25 are displaying pairwise Pearson correlations for questionnaire data with average BOLD signal within the right amygdala for transient responses.

**Figure 4.25**

*Correlation of Questionnaire data with Average BOLD Signal Within the Right Amygdala for Transient Responses*

**A**  Pictures and Electrical Stimulation     **B**  Pictures     **C**  Electrical Stimulation



Different cells (colored outlines) represent pairwise correlations of questionnaires and BOLD amplitude within the right amygdala for transient responses across stimulus modalities (panel A) within picture (panel B) and electrical stimulation trials (panel C) while warmer colors represent higher Pearson Correlation Coefficient. Black frames represent correlations between questionnaires and BOLD amplitude with respect to conditions. Results indicated that higher negative affect was significantly related to decreased BOLD amplitude in negative unpredictable trials across stimulus modalities (panel A). Considering trials with picture stimulus modality (panel (B), negative affect was significantly positively related with BOLD signal in negative predictable trials but significantly negative correlated with negative unpredictable trials. Regarding electrical stimulation stimulus modality (panel C), higher anxiety sensitivity was able to predict lower BOLD amplitudes in negative predictable trials.

With respect to correlations of questionnaire data for personality traits and affect states with average BOLD signal within the right amygdala considering transient responses across stimulus modality (panel A) there was that higher negative affect was significantly related to decreased responding in negative unpredictable trials ($r = -.409$, $p < .05$). Within picture stimulus trials (panel B) heightened negative affect was associated with increased BOLD amplitude in negative predictable ($r = .367$, $p < .05$). but decreased BOLD response in negative unpredictable trials ($r = -.334$, $p < .05$). Regarding electrical stimulation trials, higher anxiety sensitivity trait predicted decreased BOLD amplitudes in negative predictable trials ($r = -.346$, $p < .05$).

## 4.3.2 Sustained Responses to Anxiety

### 4.3.2.1  Whole Brain Analysis

Sustained responses were estimated from statistical parameter maps considering whole block duration. Results of whole brain analysis for sustained responses are displayed in Figure 4.26.

Considering BOLD amplitude in sustained responses (activity against null) in picture blocks (A), there was strong increase of bilateral visual cortex, inferior frontal gyrus, insular and cingulate gyrus, bilateral hippocampus, parahippocampal gyrus and left amygdala. B) Blocks with electrical stimulation yielded increased BOLD amplitudes in bilateral visual cortex, hippocampus, insular cortex, somatosensory cortex and amygdala. Comparison of differences in BOLD response between stimulus modalities (C) revealed for picture blocks higher amplitudes in visual cortex as well as in bilateral hippocampus, whereas electrical stimulation produced higher responses in somatosensory, cingulate as well es insular cortex and cerebellum. Considering commonalities (D), minimal *t*-conjuction between picture and electrical stimulation yielded accordance in visual cortex, frontal cortex, paracingulate gyrus, precentral gyrus, and insular cortex.

**Figure 4.26**

*Statistical Parameter Maps for Sustained Responses*
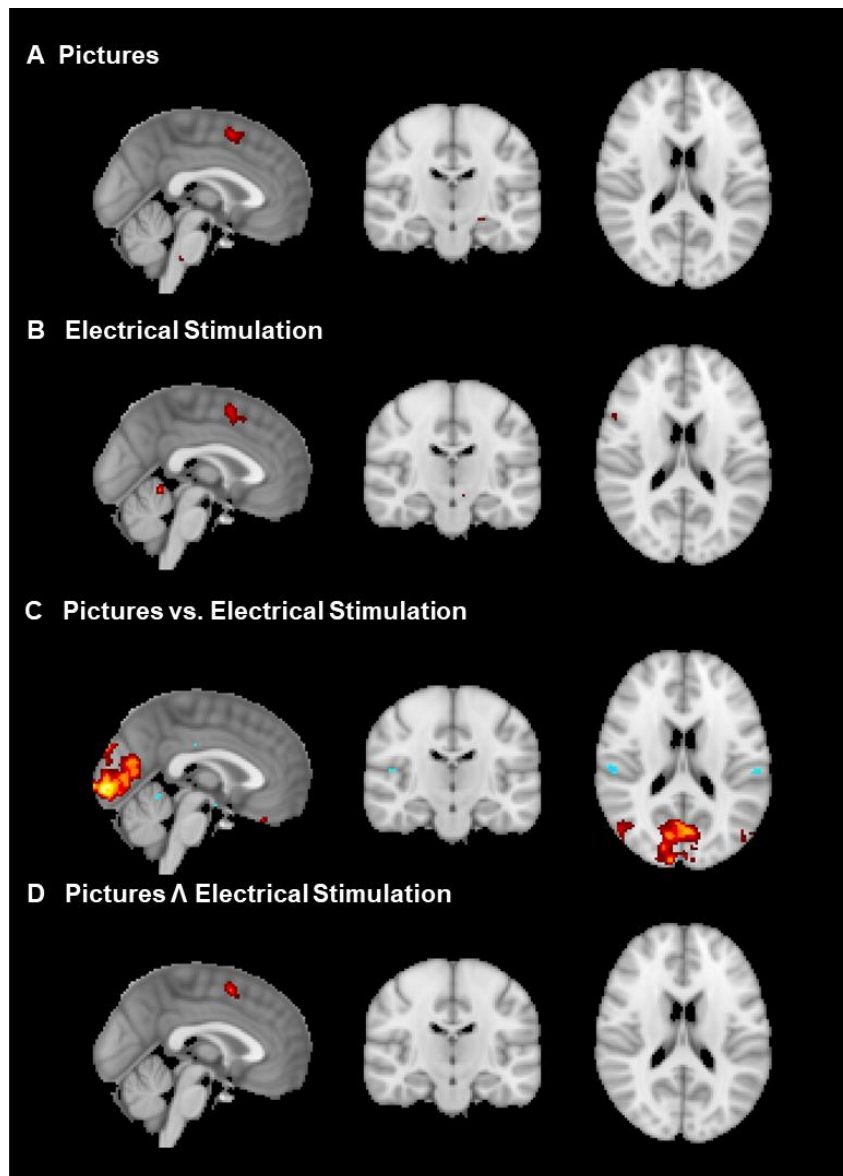


Statistical parameter maps of whole block duration representing sustained responses. (hot colors in A), B), and D): regions that show increased BOLD amplitude with respect to analysis; hot colors in C): increased BOLD amplitude within picture trials; cold colors in C): increased BOLD amplitude within electrical Stimulation trials). A) BOLD amplitudes in picture trials (activity against null) were increased in bilateral visual cortex, inferior frontal gyrus, insular and paracingulate gyrus, bilateral hippocampus, parahippocampal gyrus, and left amygdala. B) Trials with electrical stimulation also yielded strong bilateral BOLD responses in bilateral visual cortex, hippocampus, somatosensory cortex, cerebellum and amygdala. C) Voxelwise comparison of BOLD differences between stimulus modalities. Picture trials yielded higher BOLD amplitudes in visual cortex as well as in bilateral hippocampus, whereas electrical stimulation produced higher responses in somatosensory, cingulate as well es insular cortex and cerebellum. D) SPM of the minimal t-conjunction between picture- and somatosensory stimulation revealed commonalities in visual cortex, paracingulate gyrus and insular cortex. All maps are thresholded at $t$ = 3.347934, corresponding to $p < .001$.

## 4.3.2.2  Region of Interest Analysis

ROI analysis was conducted for exploring the effects of the factorial study design in predefined ROIs that were selected according to literature as well as for regions that show up in the whole-brain analysis with respect to sustained responses.

### 4.3.2.2.1 Left Amygdala

With respect to sustained responses in left amygdala there were found no significant main effects or interactions considering experimental conditions.

### 4.3.2.2.2 Right Amygdala

Table 7.40 in the appendix and panel A in Figure 4.27 depict the average BOLD signal in right amygdala as a function of valence and predictability. Table 7.41 in the appendix reports a corresponding three-factorial within-subjects ANOVA. Panels B and C show that electrical stimulation yielded stronger responses than pictures (ME "modality": $F(1, 34) = 19.40$, $p < .001$). Further, there was found that negative predictable pictures evoked higher BOLD amplitudes than negative unpredictable pictures while for neutral valent pictures the effect of predictability was inversely. But statistically these patterns did not differ as there were no statistically significant two-way or three-way interactions between modality, predictability, and valence.

**Figure 4.27**

*Average BOLD Signal in the Right Amygdala for Sustained Responses*
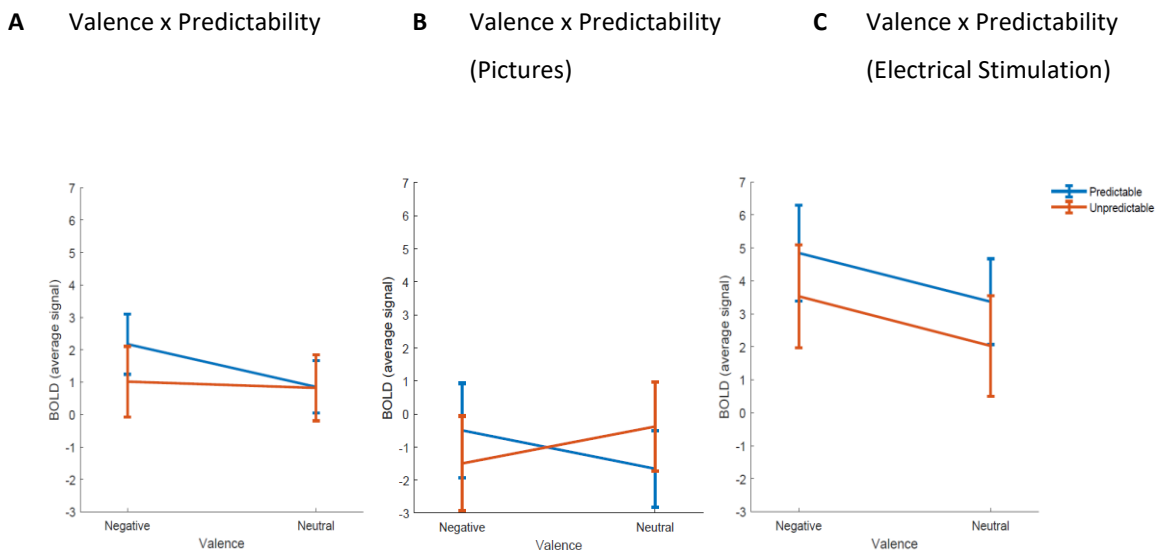
**A**  Valence x Predictability    **B**  Valence x Predictability    **C**  Valence x Predictability

(Pictures)                                  (Electrical Stimulation)
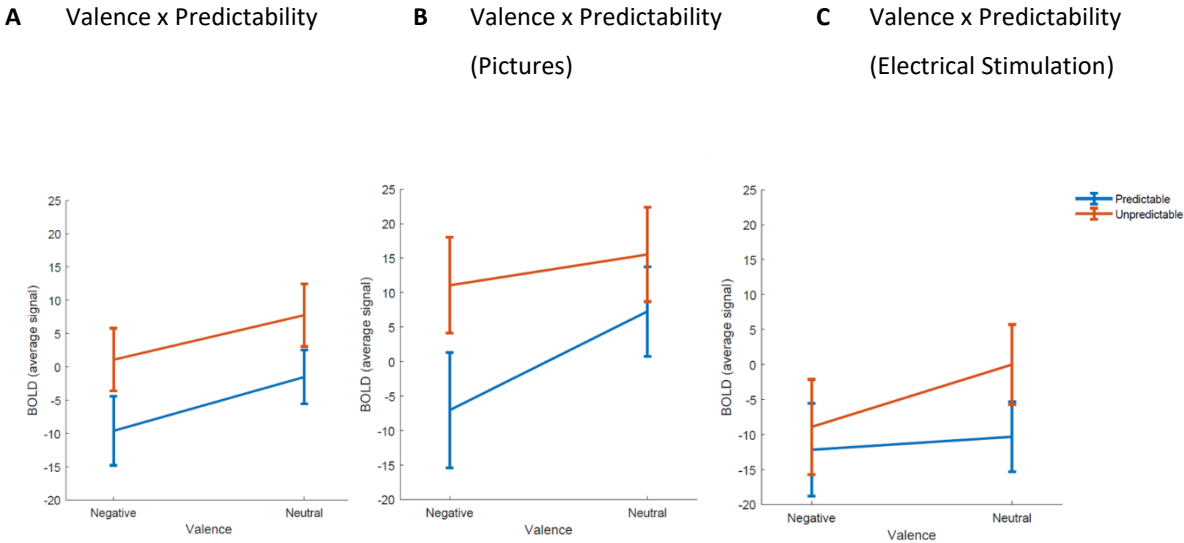


Average BOLD signal in the right amygdala A) across modality: unpredictably occurring stimuli yield a higher BOLD response than predictably occurring stimuli but this effect did not reach level of statistical significance. Error bars depict the standard error of the mean. Panels B) and C) illustrate that electrical stimulation yielded stronger responses than pictures (ME "modality": $F(1, 34) = 19.4$, $p < .001$). Further, there was found that negative predictable pictures evoked higher BOLD amplitudes than negative unpredictable pictures while for neutral valent pictures the effect of predictability was inversely. But statistically these patterns did not differ as there were no statistically significant two-way or three-way interactions between modality, predictability, and valence.

### 4.3.2.2.3 Left Thalamus

Table 7.42 in the appendix and panel A in Figure 4.28 depict the average BOLD signal in left thalamus as a function of valence and predictability. Table 7.43 in the appendix reports a corresponding three-factorial within-subjects ANOVA. Predictably occurring stimuli yielded a higher BOLD response than unpredictably occurring stimuli (ME "predictability": $F(1, 34)= 4.59$, $p < .05$). Panels B and C show that pictures yielded stronger responses than electrical stimulation (ME "modality": $F(1, 34) = 13.00$, $p < .001$), but statistically these patterns did not differ as there were no statistically significant two-way or three-way interactions between modality, predictability, and valence.

**Figure 4.28**

*Average BOLD Signal in the Left Thalamus for Sustained Responses*

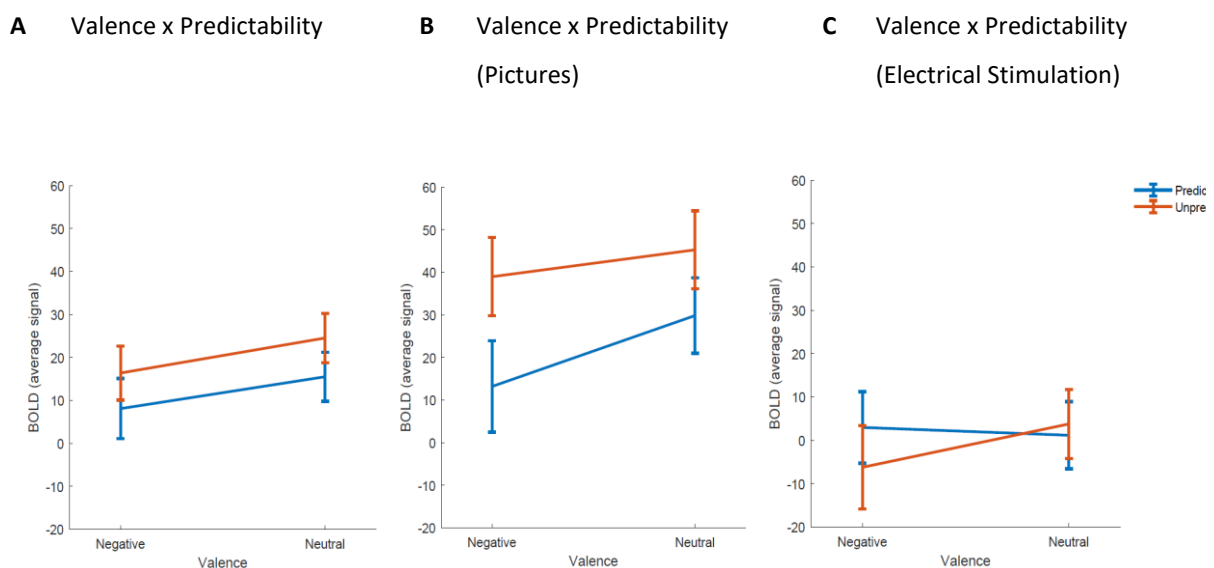| **A** | Valence x Predictability | **B** | Valence x Predictability (Pictures) | **C** | Valence x Predictability (Electrical Stimulation) |
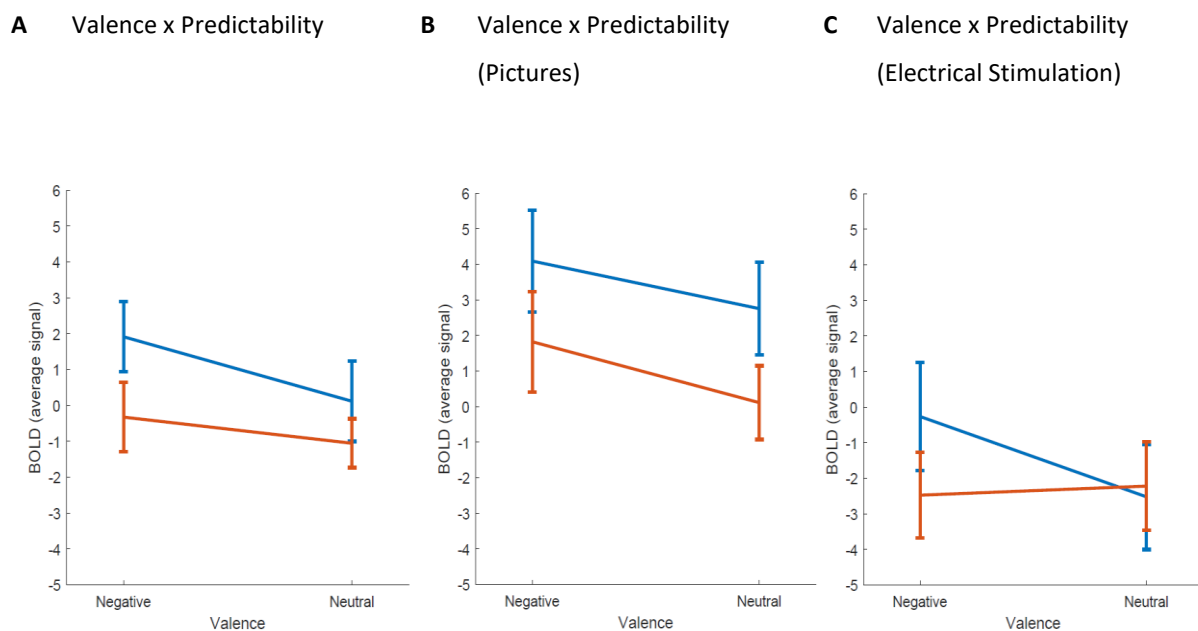


Average BOLD signal in the left thalamus A) across modality: predictable occurring stimuli yield a higher BOLD response than unpredictably occurring stimuli (ME "predictability": $F(1, 34)= 4.59$, $p < .05$). Error bars depict the standard error of the mean. Panels B) and C) illustrate that pictures yielded stronger responses than electrical stimulation (ME "modality": $F(1, 34) = 13.00$, $p < .001$), but statistically these patterns did not differ as there were no statistically significant two-way or three-way interactions between modality, predictability, and valence.

#### 4.3.2.2.4  Right Thalamus

Table 7.44 in the appendix and panel A in Figure 4.29 depict the average BOLD signal in right thalamus as a function of valence and predictability. Table 7.45 in the appendix reports a corresponding three-factorial within-subjects ANOVA. Predictably occurring stimuli yielded a higher BOLD response than unpredictably occurring stimuli but this effect did not reach level of statistical significance. Panels B and C show that pictures yielded stronger responses than electrical stimulation (ME "modality": $F(1, 34) = 21.90$, $p < .001$), but statistically these patterns did not differ as there were no statistically significant two-way or three-way interactions between modality, predictability, and valence.

**Figure 4.29**

*Average BOLD signal in right thalamus for sustained responses*
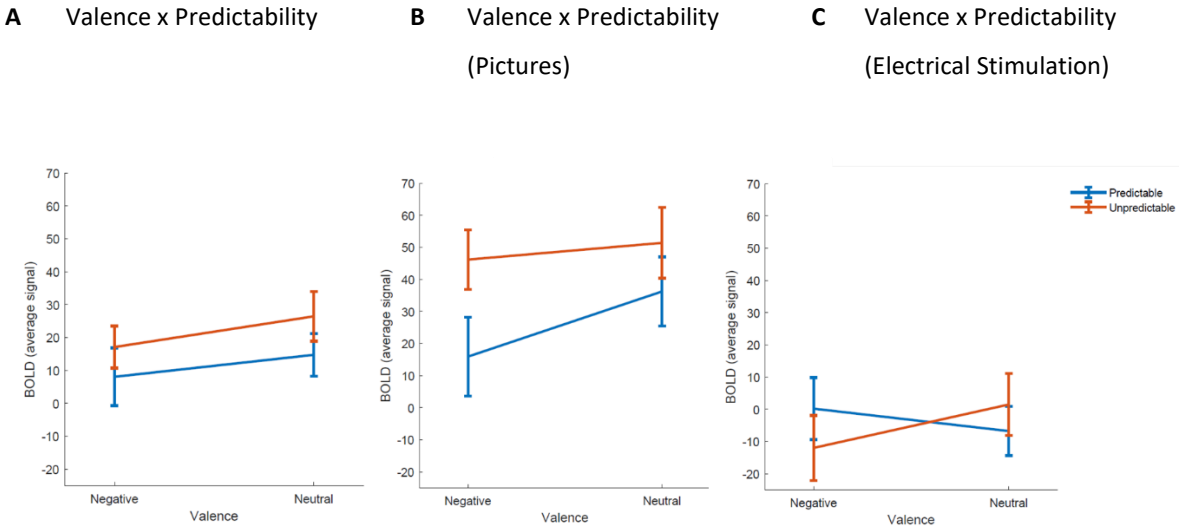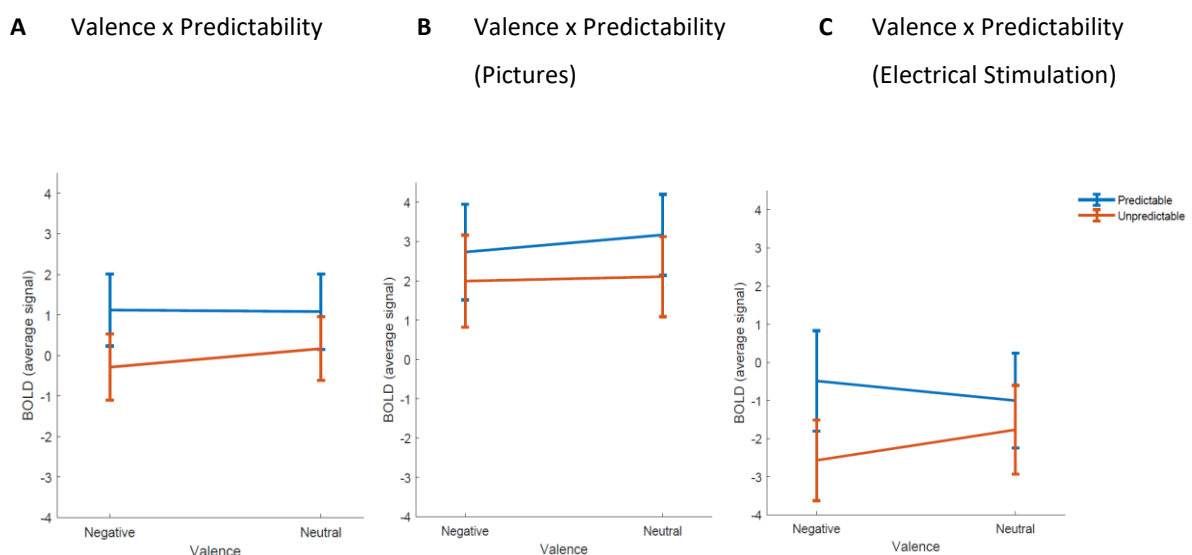


Average BOLD signal in the right thalamus A) across modality: predictably occurring stimuli yield a higher BOLD response than unpredictably occurring stimuli but this effect did not reach level of statistical significance. Error bars depict the standard error of the mean. Panels B) and C) illustrate that pictures yielded stronger responses than electrical stimulation (ME "modality": $F(1, 34) = 21.90$, $p < .001$), but statistically these patterns did not differ as there were no statistically significant two-way or three-way interactions between modality, predictability, and valence.

### 4.3.2.2.5 Left Hippocampus

Table 7.46 in the appendix and panel A in Figure 4.30 depict the average BOLD signal in left hippocampus as a function of valence and predictability. Table 7.47 in the appendix reports a corresponding three-factorial within-subjects ANOVA. Predictably occurring stimuli yielded a higher BOLD response than unpredictably occurring stimuli but this effect did not reach level of statistical significance. Panels B and C show that pictures yielded stronger responses than electrical stimulation (ME "modality": $F_{(1, 34)}$ = 24.50, $p < .001$), but statistically these patterns did not differ as there were no statistically significant two-way or three-way interactions between modality, predictability, and valence.

**Figure 4.30**

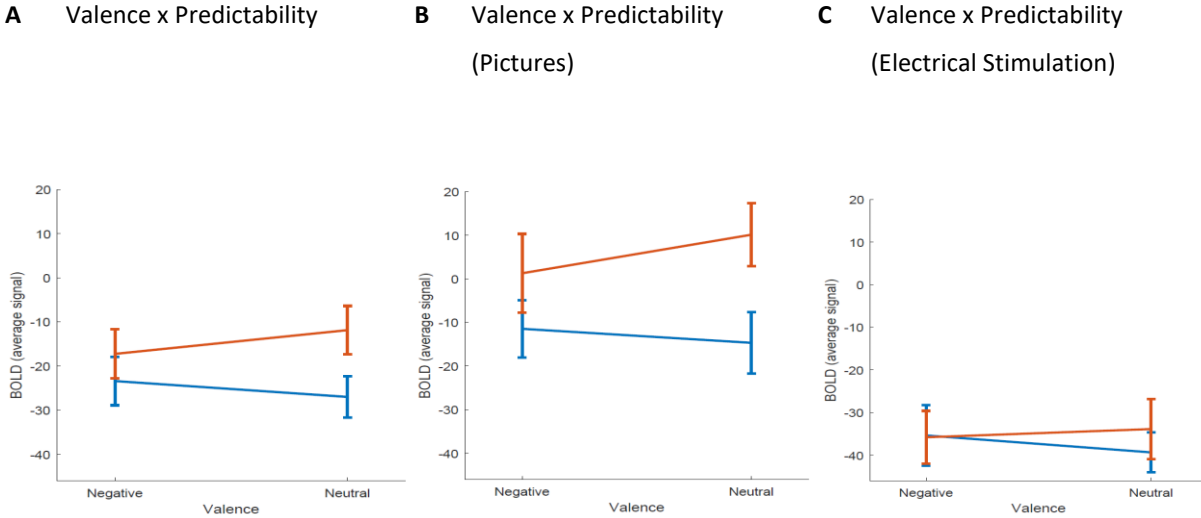*Average BOLD Signal in the Left Hippocampus for Sustained Responses*
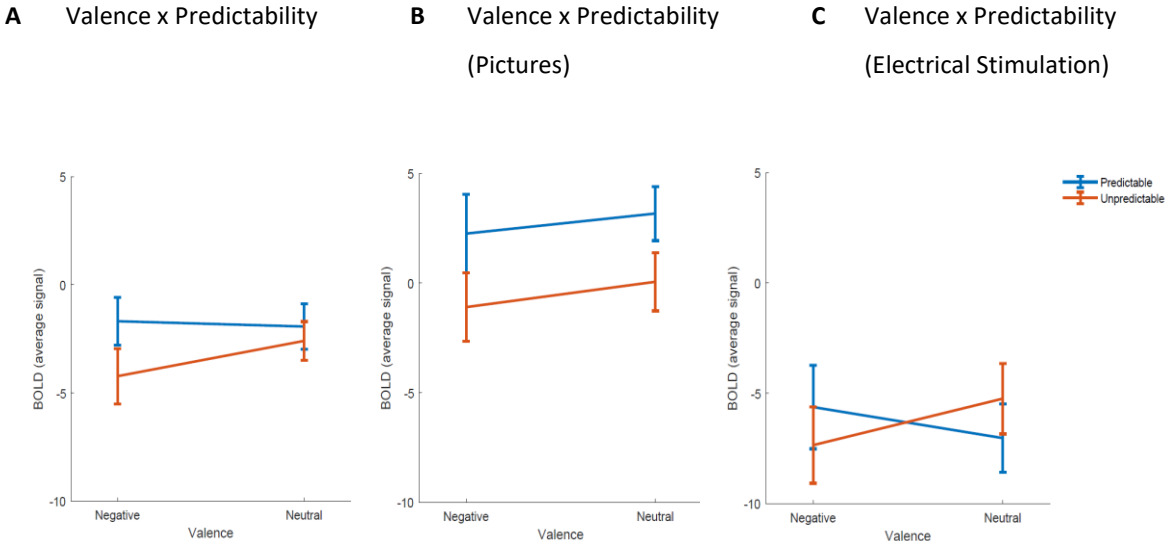


Average BOLD signal in the left hippocampus A) across modality: predictably occurring stimuli yield a higher BOLD response than unpredictably occurring stimuli but this effect did not reach level of statistical significance. Error bars depict the standard error of the mean. Panels B) and C) illustrate that pictures yielded stronger responses than electrical stimulation (ME "modality": $F_{(1, 34)}$ = 24.50, $p < .001$), but statistically these patterns did not differ as there were no statistically significant two-way or three-way interactions between modality, predictability, and valence.

### 4.3.2.2.6 Right Hippocampus

Table 7.48 in the appendix and panel A in Figure 4.31 depict the average BOLD signal in right hippocampus as a function of valence and predictability. Table 7.49 in the appendix reports a corresponding three-factorial within-subjects ANOVA. Predictably occurring stimuli yielded a higher BOLD response than unpredictably occurring stimuli (ME "predictability": $F(1, 34) = 6.27$, $p < .05$). Panels B and C show that pictures yielded stronger responses than electrical stimulation (ME "modality": $F(1, 34) = 26.7$, $p < .001$), but statistically these patterns did not differ as there were no statistically significant two-way or three-way interactions between modality, predictability, and valence.

**Figure 4.31**

*Average BOLD Signal in the Right Hippocampus for Sustained Responses*
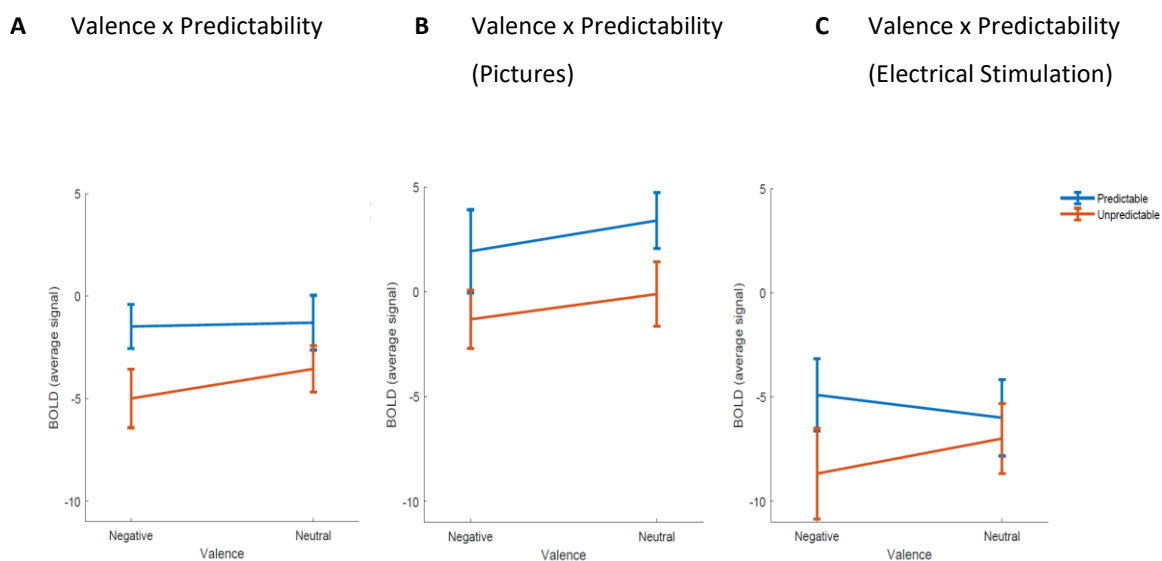
**A**  Valence x Predictability

**B**  Valence x Predictability (Pictures)
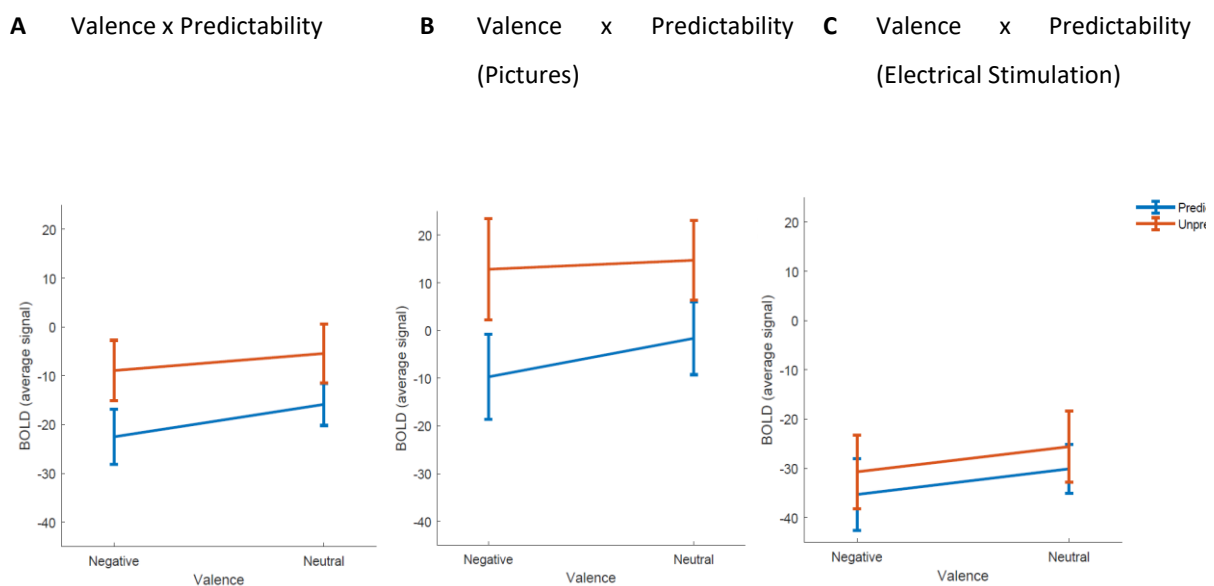
**C**  Valence x Predictability (Electrical Stimulation)



Average BOLD signal in the right hippocampus A) across modality: predictably occurring stimuli yield a higher BOLD response than unpredictably occurring stimuli (ME "predictability": $F(1, 34) = 6.27$, $p < .05$). Error bars depict the standard error of the mean. Panels B) and C) illustrate that pictures yielded stronger responses than electrical stimulation (ME "modality": $F(1, 34) = 26.7$, $p < .001$), but statistically these patterns did not differ as there were no statistically significant two-way or three-way interactions between modality, predictability, and valence.

### 4.3.2.2.7 Parahippocampal Gyrus

Table 7.50 in the appendix and panel A in Figure 4.32 depict the average BOLD signal in parahippocampal gyrus as a function of valence and predictability. Table 7.51 in the appendix reports a corresponding three-factorial within-subjects ANOVA. Panels B and C show that pictures yielded stronger responses than electrical stimulation (ME "modality": $F(1, 34) = 19.3$, $p < .001$). Further, there was found a significant two-way interaction of "modality*predictability" ($F(1, 34) = 5.47$, $p < .05$) that indicated that parahippocampal gyrus responds differently with respect to predictable and unpredictable timing dependent on stimulus modality.

**Figure 4.32**

*Average BOLD Signal in the Parahippocampal Gyrus for Sustained Responses*
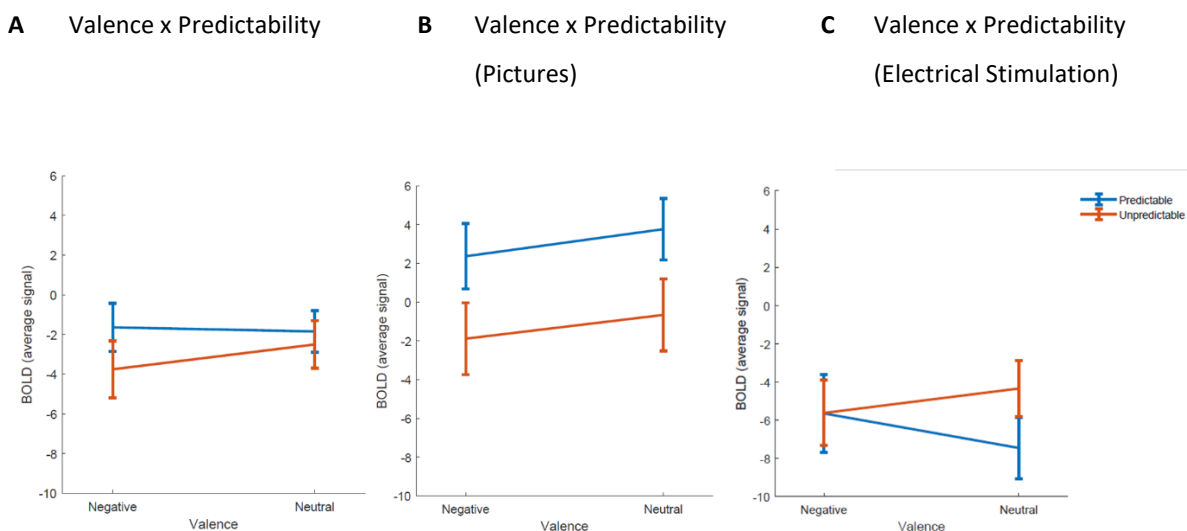


Average BOLD signal in the right hippocampus A) across modality: predictably occurring stimuli yield a higher BOLD response than unpredictably occurring stimuli, but this effect did not reach level of statistical significance. Error bars depict the standard error of the mean. Panels B) and C) illustrate that pictures yielded stronger responses than electrical stimulation (ME "modality": $F(1, 34) = 26.7$, $p < .001$). Further, there was found a significant two-way interaction of "modality*predictability" (F(1, 34) = 5.47, p < .05) that indicated that parahippocampal gyrus responds differently with respect to predictable and unpredictable timing, dependent on stimulus modality.

**4.3.2.2.8  Brain Stem**

With respect to sustained responses within the brain stem there were found no significant main effects or interactions considering experimental conditions.

**4.3.2.2.9 Paracingulate Gyrus**

With respect to sustained responses within the paracingulate gyrus there were found no significant main effects or interactions with respect to experimental conditions.

### 4.3.2.2.10 Insular Cortex

Table 7.52 in the appendix and panel A in Figure 4.33 depict the average BOLD signal in insular cortex as a function of valence and predictability. Table 7.53 in the appendix reports a corresponding three-factorial within-subjects ANOVA. Predictably occurring stimuli yielded a higher BOLD response than unpredictably occurring stimuli especially in negative valent stimuli, but this effect did not reach level of statistical significance. Panels B and C show that electrical stimulation yielded stronger responses than pictures (ME "modality": $F(1, 34) = 28.90$, $p < .001$), but statistically these patterns did not differ as there were no statistically significant two-way or three-way interactions between modality, predictability, and valence.

**Figure 4.33**

*Average BOLD Signal in the Insular Cortex for Sustained Responses*
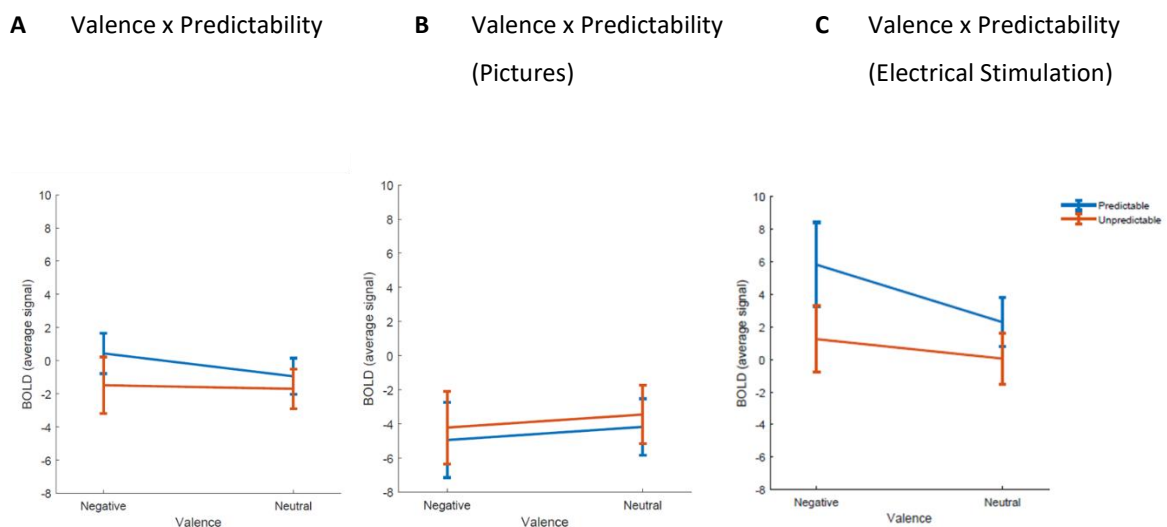
| **A** Valence x Predictability | **B** Valence x Predictability (Pictures) | **C** Valence x Predictability (Electrical Stimulation) |



Average BOLD signal in the left hippocampus A) across modality: predictably occurring stimuli yield a marginally higher BOLD response than unpredictably occurring stimuli but this effect did not reach level of statistical significance. Error bars depict the standard error of the mean. Panels B) and C) illustrate that electrical stimulation yielded stronger responses than pictures (ME "modality": $F(1, 34) = 28.90$, $p < .001$), but statistically these patterns did not differ as there were no statistically significant two-way or three-way interactions between modality, predictability, and valence.

### 4.3.2.2.11    Frontal pole

Table 7.54 in the appendix and panel A in Figure 4.34 depict the average BOLD signal in the frontal pole as a function of valence and predictability. Table 7.55 in the appendix reports a corresponding three-factorial within-subjects ANOVA. Panels B and C show that electrical stimulation yielded stronger responses than pictures (ME "modality": $F(1, 34) = 13.80$, $p < .001$), but statistically these patterns did not differ as there were no statistically significant two-way or three-way interactions between modality, predictability, and valence.

**Figure 4.34**

*Average BOLD Signal in the Frontal Pole for Sustained Responses*
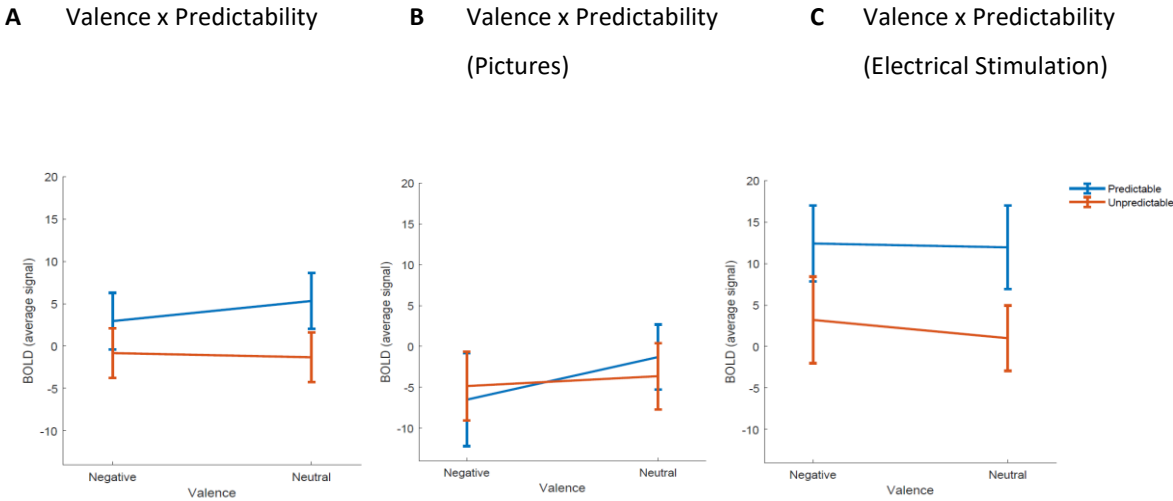
**A**  Valence x Predictability

**B**  Valence x Predictability (Pictures)

**C**  Valence x Predictability (Electrical Stimulation)



Average BOLD signal in the frontal pole A) across modality: predictably occurring stimuli yield a higher BOLD response than unpredictably occurring stimuli but this effect did not reach level of statistical significance. Error bars depict the standard error of the mean. Panels B) and C) illustrate that electrical stimulation yielded stronger responses than pictures (ME "modality": $F(1, 34) = 13.80$, $p < .001$), but statistically these patterns did not differ as there were no statistically significant two-way or three-way interactions between modality, predictability, and valence.

### 4.3.2.2.12 Middle Frontal Gyrus

Table 7.56 in the appendix and panel A in Table 7.57 depict the average BOLD signal in middle frontal gyrus as a function of valence and predictability. Table 7.57 in the appendix reports a corresponding three-factorial within-subjects ANOVA. Results further showed a significant two-way interaction of "valence*predictability" ($F(1, 34)=$ 14.50, $p < .001$) which points to differential responding of middle frontal gyrus with respect to predictability as a function of valence across modalities. Panels B and C show that BOLD amplitude for electrical stimulation was significantly different from pictures (ME "modality": $F(1, 34)= 11.80$, $p < .001$) but this effect could further not be specified since there were no statistically significant two-way or three-way interactions between modality, predictability, and valence.

**Figure 4.35**

*Average BOLD Signal in the Middle Frontal Gyrus for Sustained Responses*
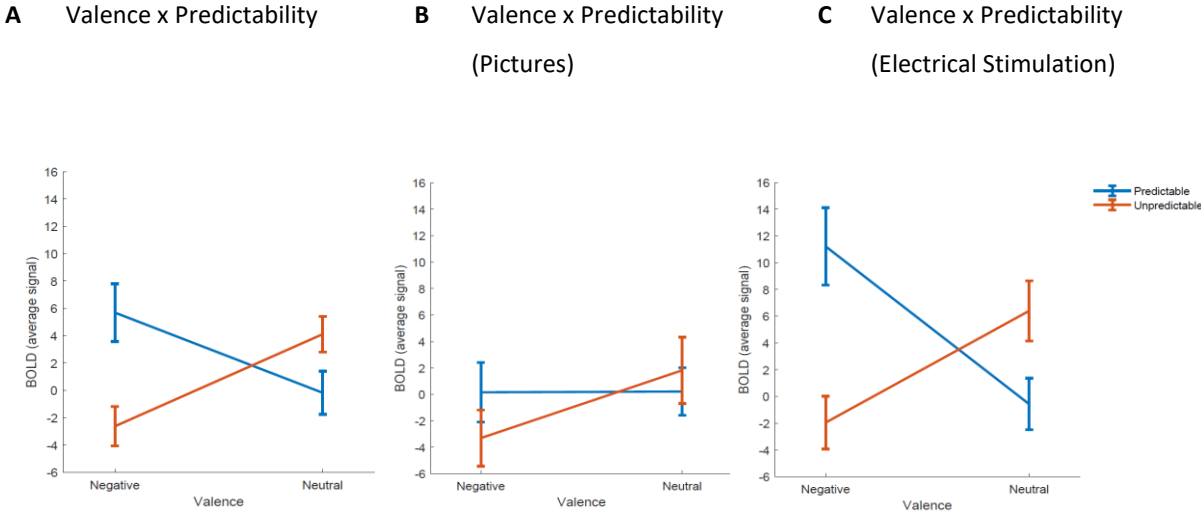
| **A** Valence x Predictability | **B** Valence x Predictability (Pictures) | **C** Valence x Predictability (Electrical Stimulation) |



Average BOLD signal in the frontal pole A) across modality: results indicated significant two-way interaction of "valence*predictability" ($F(1, 34)= 14.50$, $p < .001$) which points to differential responding of middle frontal gyrus with respect to predictability as a function of valence across modalities Error bars depict the standard error of the mean. Panels B) and C) illustrate that the pattern of BOLD amplitudes differs between modalities (ME "modality": $F(1, 34) = 11.80$, $p < .001$), but statistically these patterns did not differ as there were no statistically significant two-way or three-way interactions between modality, predictability, and valence.

### 4.3.2.2.13    Inferior frontal Gyrus

Table 7.58 in the appendix and panel A in Figure 4.36 depict the average BOLD signal in insular cortex as a function of valence and predictability. Table 7.59 in the appendix reports a corresponding three-factorial within-subjects ANOVA. Panels B and C show that electrical stimulation yielded stronger responses than pictures (ME "modality": $F(1, 34) = 20.4$, $p < .001$). Further there was found a significant two-way interaction of "modality*predictability" ($F(1, 34) = 7.93$, $p < .01$) in a way that different levels of predictability evoke different pattern of BOLD amplitude within the inferior frontal gyrus depending on stimulus modality.

**Figure 4.36**

*Average BOLD Signal in the Inferior Frontal Gyrus for Sustained Responses*

| **A** Valence x Predictability | **B** Valence x Predictability (Pictures) | **C** Valence x Predictability (Electrical Stimulation) |
|---|---|---|
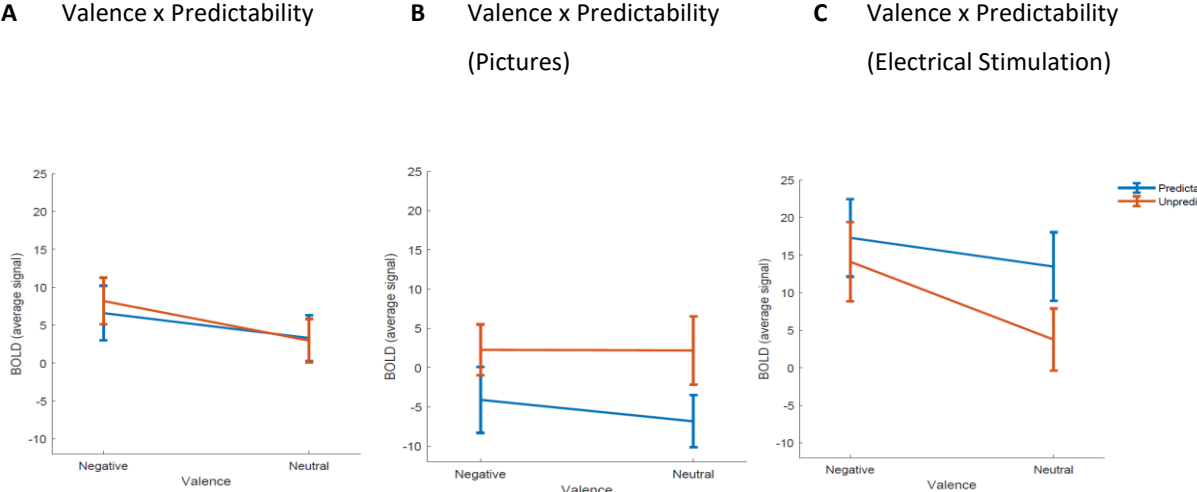


Average BOLD signal in the inferior frontal gyrus A) across modality: "modality*predictability" ($F(1, 34) = 7.93$, $p < .01$) different levels of predictability evoke different pattern of BOLD amplitude within the inferior frontal gyrus depending on stimulus modality ("modality*predictability" ($F(1, 34) = 7.93$, $p < .01$). Error bars depict the standard error of the mean. Panels B) and C) illustrate that electrical stimulation yielded stronger responses than pictures (ME "modality": $F(1, 34) = 28.90$, $p < .001$).

### 4.3.2.2.14    Frontal medial cortex

Table 7.60 in the appendix and panel A in Figure 4.37 depict the average BOLD signal in the frontal medial cortex as a function of valence and predictability. Table 7.61 in the appendix reports a corresponding three-factorial within-subjects ANOVA. predictability. Predictably occurring stimuli yielded a higher BOLD response than unpredictably occurring stimuli but this effect did not reach level of statistical significance. Panels B and C show that pictures yielded stronger responses than electrical stimulation (ME "modality": $F(1, 34) = 19.60$, $p < .001$), but statistically these patterns did not differ as there were no statistically significant two-way or three-way interactions between modality, predictability, and valence.

**Figure 4.37**

*Average BOLD Signal in the Frontal Medial Cortex for Sustained Responses*

| **A** Valence x Predictability | **B** Valence x Predictability (Pictures) | **C** Valence x Predictability (Electrical Stimulation) |
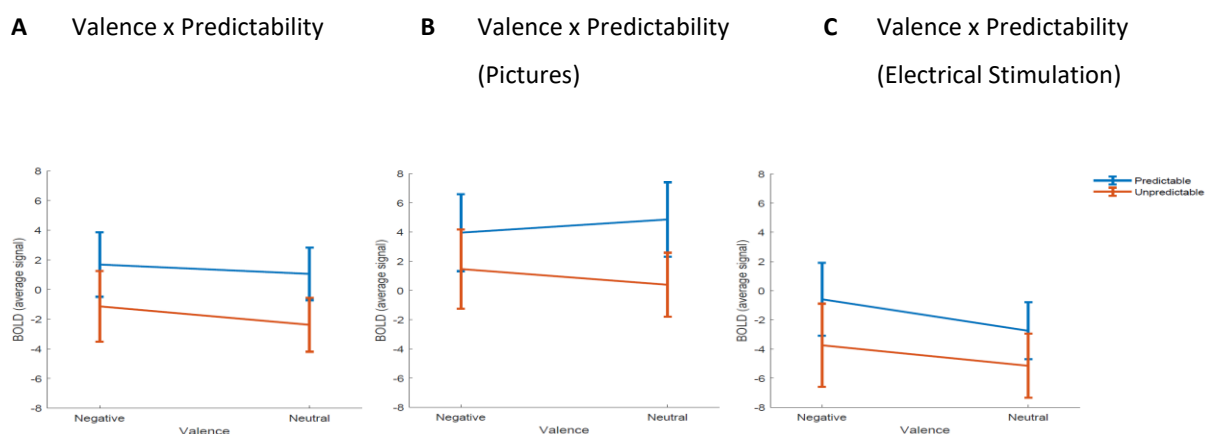


Average BOLD signal in the frontal medial cortex A) across modality: predictably occurring stimuli yield a higher BOLD response than unpredictably occurring stimuli but this effect did not reach level of statistical significance. Error bars depict the standard error of the mean. Panels B) and C) illustrate that electrical stimulation yielded stronger responses than pictures (ME "modality": $F(1, 34) = 19.60$, $p < .001$), but statistically these patterns did not differ as there were no statistically significant two-way or three-way interactions between modality, predictability, and valence.

### 4.3.2.2.15 Superior frontal gyrus

Table 7.62 in the appendix and panel A in Figure 4.38 depict the average BOLD signal in middle superior frontal gyrus as a function of valence and predictability. Table 7.63 in the appendix reports a corresponding three-factorial within-subjects ANOVA. Results indicated a significant two-way interaction of "valence*predictability" ($F(1, 34)=$ 7.59, $p < .001$) which points to differential responding of middle frontal gyrus with respect to predictability as a function of valence across modalities. Panels B and C show that BOLD amplitude for electrical stimulation was significantly different from pictures (ME "modality": $F(1, 34)= 16.20, p < .001$).

**Figure 4.38**

*Average BOLD Signal in the Superior Frontal Cortex for Sustained Responses*
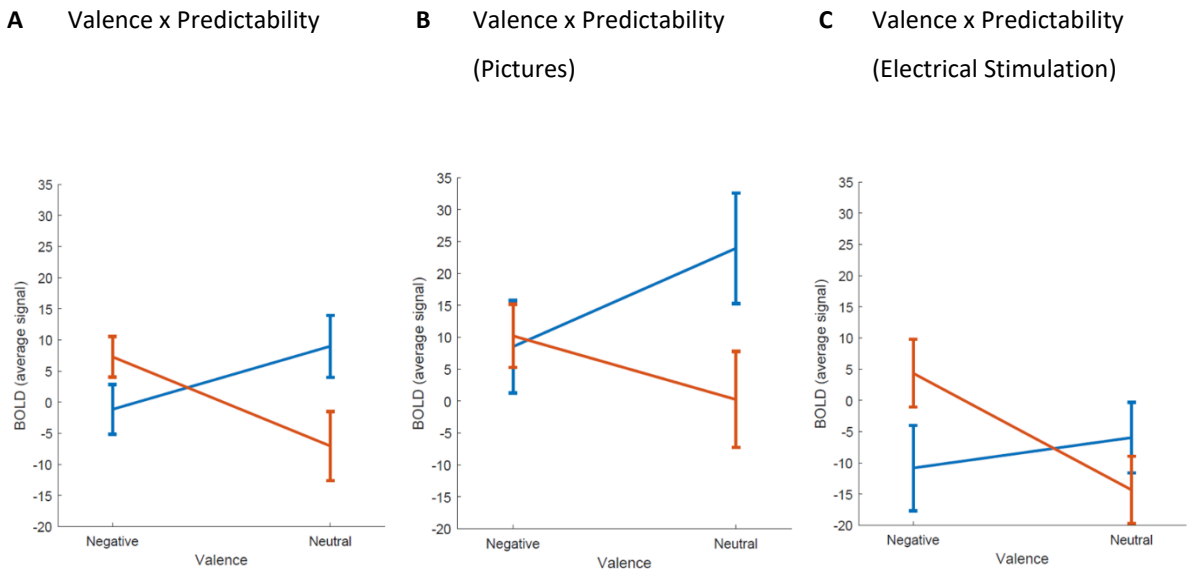


| **A** Valence x Predictability | **B** Valence x Predictability (Pictures) | **C** Valence x Predictability (Electrical Stimulation) |

Average BOLD signal in the frontal pole A) across modality: results indicated significant two-way interaction of "valence*predictability" ($F(1, 34)= 7.59, p < .001$) which points to differential responding of the superior frontal gyrus with respect to predictability as a function of valence across modalities Error bars depict the standard error of the mean. Panels B) and C) illustrate that the pattern of BOLD amplitudes differs between modalities (ME "modality": $F(1, 34) = 16.20, p < .001$), but statistically these patterns did not differ as there were no statistically significant two-way or three-way interactions between modality, predictability, and valence.

#### 4.3.2.2.16 Individual Differences in Sustained Responses Within the Amygdala

Table 7.64, Table 7.65, and Table 7.66 in the appendix and in Figure 4.39 are displaying pairwise Pearson correlations for questionnaire data with average BOLD signal within the right amygdala for sustained responses.

**Figure 4.39**

*Correlation of Questionnaire data with Average BOLD Signal Within the Right Amygdala for Sustained Responses*

| **A** Pictures and Electrical Stimulation | **B** Pictures | **C** Electrical Stimulation |
|---|---|---|



Different cells (colored outlines) represent pairwise correlations of questionnaires and BOLD amplitude within the right amygdala for sustained responses across stimulus modalities (panel A) within picture (panel B) and electrical stimulation trials (panel C) while warmer colors represent higher Pearson Correlation Coefficient. Black frames represent correlations between questionnaires and conditions while red boxes denote significant correlations. Results indicated that higher positive affect was significantly related to increased BOLD amplitude in negative predictable across stimulus modalities (panel A). Considering trials with picture stimulus modality (panel (B), negative affect was significantly positively related with BOLD signal in neutral predictable trials. Given electrical stimulation stimulus modality (panel C), increased anxiety sensitivity significantly decreased BOLD signal in neutral unpredictable trials. Further, heightened negative affect was able to predict significantly lower BOLD amplitudes in neutral unpredictable trials.

With respect to correlations of questionnaire data for personality traits and affect states with average BOLD signal within the right amygdala considering sustained responses across stimulus modality (panel A) there was that higher positive affect was significantly related to increased responding in negative predictable trials ($r = .357$, $p < .05$). Within picture stimulus trials (panel B) heightened negative affect was associated with increased BOLD amplitude in neutral predictable ($r = .395$, $p < .05$) trials. Considering electrical stimulation (panel C), higher anxiety sensitivity trait was able to predict lower BOLD amplitudes in neutral unpredictable trials ($r = -.432$, $p <$

.01). Additionally, higher negative affect was significantly associated with increased BOLD amplitudes with respect to neutral unpredictable trials ($r$ = -.351, $p$ < .05).

### 4.3.3 Task-evoked Anxiety Rating

Given the main purpose of the present study that was the investigation of differences and commonalities in fear and anxiety systems, there was the aim to behavioral data (task-evoked anxiety) as manipulation check for suitability of experimental conditions. Further, there was the aim to investigate to what extend personality traits and states are related to nervousness rating. These analysis comprise a comparison across (pictures and electrical stimulation) and within each stimulus modality type (pictures, electrical stimulation).

Sample characteristics of task-evoked anxiety rating with respect to picture and electrical stimuli could be drawn from Table 7.67 in appendix. Results of three-way rmANOVA (modality*valence*predictability) as a function of modality, valence, and predictability are displayed in **Figure 4.40** while results of rmANOVA could be extracted from Table 7.68 in the appendix.

**Figure 4.40**

*Overview of Task-evoked Anxiety Rating Results with respect to Block Type across Modality*
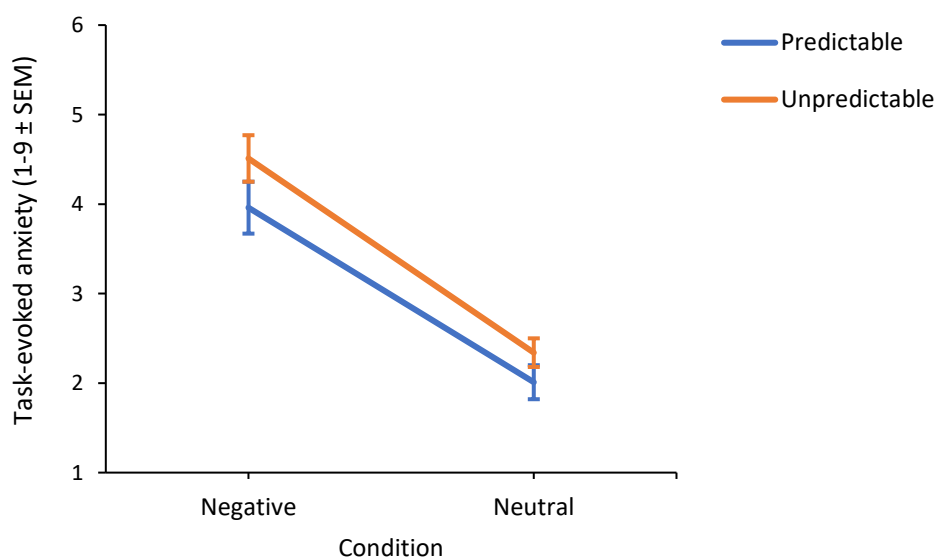


Average task-evoked anxiety rating results across modality (pictures and electrical stimulation) as a function of valence (negative vs. neutral) and predictability (predictable (blue) and unpredictable (orange)). Error bars depict the standard error of the mean. Negative valent trials evoked significantly higher task-evoked anxiety compared to neutral trials especially in unpredictable compared to predictable trials.

Analysis revealed significant main effects for all factors ("modality": $F(1, 34) = 6.897$, $p < .05$, partial $\eta^2 = .169$, "valence": $F(1, 34) = 93.076$, p < .001, partial $\eta^2 = .732$, and "predictability": $F(1, 34) = 28.635$, $p < .001$, partial $\eta^2 = .457$). Further, there were found significant two-way interactions for "modality*predictability" ($F(1, 34) = 4.354$, $p < .05$, partial $\eta^2 = .114$) and "valence*predictability" ($F(1, 34) = 8.080$, $p < .01$, partial $\eta^2 = .192$). Nevertheless, the interaction of "modality*valence" and the three-way interaction ("modality*valence*predictability") did not reach level of statistical significance. Results of significant post-hoc comparisons for significant main and interaction effects could be drawn from Table 7.69 in the appendix. Electrical stimulation stimulus trials evoked significantly higher anxiety compared to picture trials. Further, negative valent stimuli came along with significantly higher anxiety compared to neutral stimuli while unpredictable blocks evoked significantly higher anxiety compared to predictable blocks in both modality types. Given the significant "modality* predictability" interaction, all post-hoc t-tests reached level of statistical significance. Unpredictable electrical stimulation blocks came along with significantly higher aversive rating, while predictable picture trials were rated as least anxiety evoking (zaps unpr > zaps pred > pics unpr > pics pred). With respect to the "predictability*valence" interaction, post-hoc t-tests indicated significantly higher task-evoked anxiety rating scores in unpredictable negative blocks while predictable neutral was less anxiety evoking (NegUnpr > NeuUnpr > NegPred> NeuPred).

Results of two-way rmANOVAs with respect to stimulus modality could be drawn from Table 7.70 in the appendix and are visualized in Figure 4.41. Considering results of task-evoked anxiety rating within picture blocks, there was found a significant main effect for the factor "predictability" ($F(1, 34) = 18.04$, $p < .001$, partial $\eta^2 = .347$) and "valence" ($F(1, 34) = 74.67$, $p < .001$, partial $\eta^2 = .687$) while the interaction did not reach level of statistical significance. Post-hoc t-testing for exploring direction of main effects in pictures (Table 7.71 in the appendix), showed that negative pictures evoked significant higher anxiety compared to neutral pictures and in unpredictable compared to predictable blocks. With respect to electrical stimulation blocks (Table 7.72 in the appendix), analysis of task-evoked anxiety rating results revealed significant main effect for the factors "predictability" ($F(1, 34) = 30.048$, $p < .001$, partial $\eta^2 = .469$) and "valence" ($F(1, 34) = 62.806$, $p < .001$, partial $\eta^2 = .649$) while the valence by predictability interaction was statistical significant as well ($F(1, 34) = 11.156$, $p < .01$,

partial $\eta^2$ = .247). All post-hoc *t*-test comparisons for the main and interaction effects (**Table 7.72** in the appendix) reached level of statistical significance. Trials within unpredictable electrical stimulation blocks were rated as more aversive than in predictable blocks while negative electrical stimuli came along with higher score in anxiety rating in comparison to neutral electrical stimuli. Analysis of interaction direction revealed significantly greater anxiety in unpredictable blocks with negative zap intensity while predictable neutral blocks showed lowest task-evoked anxiety score (NegUnpr > NegPred > NeuUnpr > NeuPred).

**Figure 4.41**

*Overview of Task-evoked Anxiety Rating Results with respect to Experimental Condition within Modality*
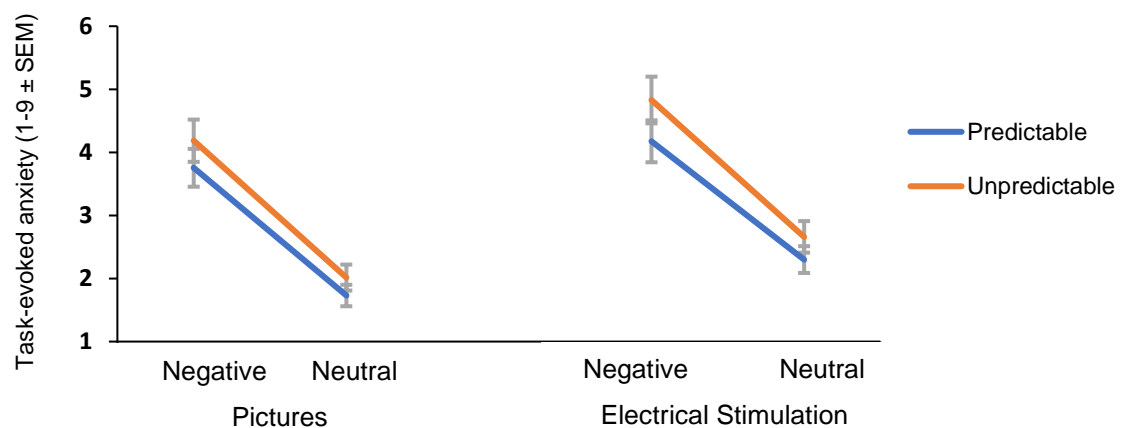


The line plot gives information about task-evoked anxiety assessed with nervousness rating (1= "not nervous at all" to 9= "extremely nervous") in predictable (blue) and unpredictable (orange) blocks with respect to modality (pictures vs. electrical stimulation) and valence (negative vs. neutral ) while error bars represent SEM. Negative pictures evoked significantly greater anxiety compared to neutral valent pictures. Further, significantly higher task-evoked anxiety was found in unpredictable than in predictable picture blocks. Same pattern of results was found for electrical stimulation blocks (negative > neutral; unpredictable > predictable) while additionally a significant "valence*predictability" interaction (NegUnpr > NegPred > NeuUnpr > NeuPred) was observed. Given these results, our paradigm was able to evoke differences in fear and anxiety responses measured with retrospective self-report in both modalities while a predictability by valence relationship was found for electrical stimulation blocks solely.

For investigating the effect of trait and state variables on task-evoked anxiety rating scores, psychological questionnaires were correlated with anxiety scores across stimulus modalities (pictures and electrical stimulation) as well as within each stimulus modality type. Results of Pearson correlation analyses across stimulus modalities

(Table 7.73 in the appendix) as well as for picture (Table 7.74 in the appendix) and electrical stimulation blocks (Table 7.75 in the appendix) are presented in the appendix, while results are depicted in Figure 4.42.

**Figure 4.42**

*Correlations of Questionnaires and Task-evoked Anxiety Rating in Picture and Electrical Stimulation Blocks*

**A**      Pictures and Electrical Stimulation
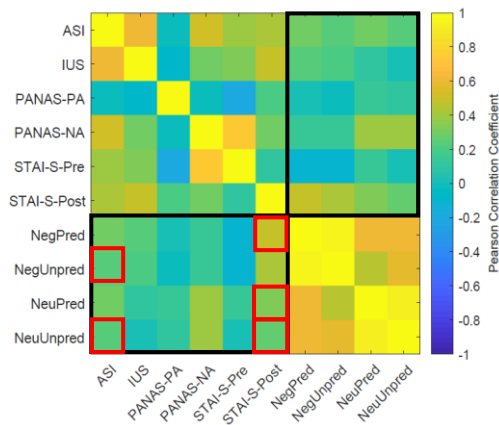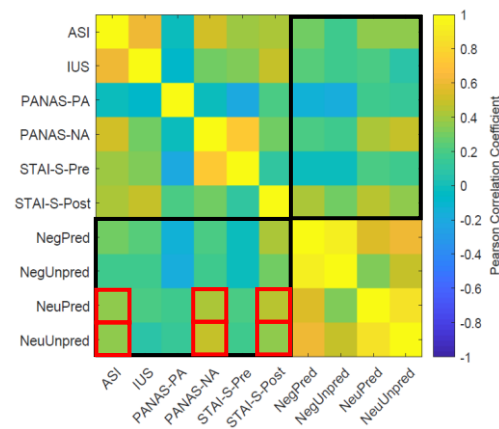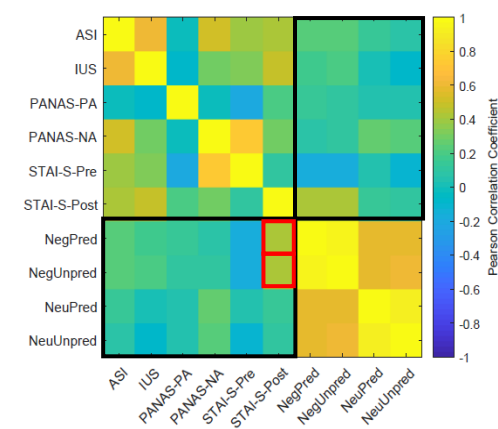


**B**      Pictures



**C**      Electrical Stimulation



Different cells (colored outlines) represent pairwise correlations of questionnaires and task-evoked anxiety rating across stimulus modalities (panel A) within picture (panel B) and electrical stimulation blocks (panel C) while warmer colors represent higher Pearson Correlation Coefficient. Black frames represent correlations between questionnaires and conditions while red boxes denote significant correlations. Given the effect of trait and state variables on task-evoked anxiety rating across modalities (panel A) there was found that higher anxiety sensitivity. Higher negative affect was significantly related to increased anxiety in negative unpredictable and neutral unpredictable blocks. Further, higher anxiety in negative predictable, negative unpredictable, and neutral unpredictable blocks predicted higher state anxiety following the experiment. In picture blocks (panel B), higher anxiety sensitivity trait and negative affect state was significantly associated with higher scores in task-evoked anxiety rating in neutral predictable and neutral unpredictable blocks. Further, both conditions evoked significantly higher post-experimental state anxiety. With respect to electrical stimulation (panel C), there was found that negative predictable and negative unpredictable conditions were significantly related to higher state anxiety following the experiment.

135

First, with respect to trait variables, we found that IU was not related to task-evoked anxiety across and in both kinds of stimulus modality at all. Given the impact of state and trait variables across stimulus modalities (panel A) there was found that anxiety sensitivity predicted significantly higher anxiety in negative unpredictable ($r = .341$, $p < .05$) as well as neutral unpredictable blocks ($r = .352$, $p < .05$). Further, higher negative affect was found to be significantly related to higher anxiety in negative unpredictable ($r = .480$, $p < .01$) and neutral unpredictable blocks ($r = .497$, $p < .01$) as well. Additionally, higher anxiety in negative predictable ($r = .411$, $p < .05$), negative unpredictable ($r = .446$, $p < .01$), and neutral unpredictable blocks ($r = .396$, $p < .05$). evoked significantly higher post-experimental state anxiety. Regarding picture blocks (panel B), higher anxiety sensitivity trait individuals showed increased task-evoked anxiety rating in neutral predictable ($r = .341$, $p < .05$) and neutral unpredictable blocks ($r = .352$, $p < .05$). Considering the influence of state variables on task evoked anxiety rating in picture modality, results indicated that increased negative affect score significantly increased task-evoked anxiety in neutral predictable ($r = .480$, $p < .01$) and neutral unpredictable picture blocks ($r = .497$, $p < .01$). Further, higher anxiety in neutral predictable ($r = .446$, $p < .01$) and neutral unpredictable blocks ($r = .396$, $p < .05$) indicated significantly higher state anxiety following the experiment. With respect to electrical stimulation blocks (panel C), there was found that increased anxiety score in negative predictable ($r = .446$, $p < .01$) and negative unpredictable blocks ($r = .422$, $p < .05$) was significantly associated with higher state anxiety following the experiment.

# 5  DISCUSSION

The purpose of the present neuroimaging study was to investigate commonalities and differences of neural systems involved in transient (fear) and sustained (anxiety) responses and to which degree responses of these systems represented abstract, i.e. modality-independent processes. To this aim, we extended a previously published paradigm for evoking and disentangling fear and anxiety (Sommerville at al., 2013) and exposed participants to stimuli from two modalities (visual and somatosensory), which were predictable or unpredictable, and which were neutral or aversive, using a fully factorial 2x2x2 within subject design.

**Modality Specificity**. As expected, we found modality-specific neural activation pattern, corresponding to visual and somatosensory modality because of the functional segregation of sensory of the nervous system (Gazzaniga et al., 2009). We identified brain regions highly associated with somatosensory and motor areas pain corresponding to pain perception (Wager et al., 2013) while visual stimuli evoked strong responses in occipital regions.

**Separate Systems for Fear and Anxiety**. Importantly, we showed that there are distinguishable brain systems that code for fear and anxiety processes (LeDoux & Pine, 2016). Brain stem, middle frontal gyrus, the posterior aspect of the paracingulate cortex and bilateral thalamus exhibited strong transient response pattern to aversive events representing a neural system that codes for acute and imminent threat, i.e. fear. On the other hand, paracingulate gyrus, precentral gyrus, and insular cortex showed strong sustained responses, thereby prepresenting a neural system that codes for anxiety.

**A Common Core of Fear and Anxiety**. However, the analysis for transient as well as for the sustained responses revealed an overlap of fear- and anxiety related processes in the posterior aspect of the cingulate cortex. We hypothesize that such common processes are those that regulate fear and anxiety.

**Met and Unmet Expectations**. Based on previous experiments (see 1.3.5) we set out with a couple of hypotheses in which we predicted that we would observe effects of modality, predictability, and valence, as well as interactions at least between valence and predictability. As summarized above, there were substantial effects of modality. We also observed effects of predictability in sustained responses in bilateral

hippocampus and left thalamus. Such findings are consistent with the idea of attentional processing leading to increased activity for expected stimuli (Kastner, Pinsk, Weerd, Desimone, & Ungerleider, 1999; LaBerge, 1997). However, there were surprisingly few effects of valence, which we considered a main experimental variable in our logic. There was no region that exhibited a main effect of valence. We argued in the introduction that the more important contribution of valence would be in its interaction with predictability, since a dual systems account of fear and anxiety posits that threat leads to fear whether expected or not, whereas an uncertainty of threat is the defining feature of anxiety (Grillon et al., 2004). In agreement with that prediction we found that the (retrospectively assessed) nervousness ratings of our participants where substantially increased for blocks with unpredictable negative stimuli with respect to the three other conditions (predictable negative, unpredictable and predictable neutral). Furthermore, we observed this interaction also in sustained responses of the brain in the midfrontal and the inferior frontal gyri. However, the lack of interactions between valence and predictability in other parts of the neural systems for fear and anxiety needs explanation. We cannot exclude that our design lacked the necessary power for this particular set of statistical tests. Somerville and colleagues (2013) presented a figure (3b) suggesting the presence of such an interaction, but they neither reported how they identified that region nor did they present a pertaining statistical analysis. Assuming that they did report a robust effect, we have to acknowledge that we only tested 35 participants in contrast to their large sample of 61 subjects.

Another possibility is that our stimuli were simply too weak. We need to point out here that we did not use the same pictures as Somerville and colleagues, who used the IAPS (Lang, 2005). We instead, used the Nencki Affective Picture System (NAPS) (Marchewka et al., 2014) actually because we felt that the by now slightly dated IAPS lacked the potential to evoke emotions. In our stimulus selection we took utmost care of selecting a large number of pictures with strong differences in valence between the neutral and the negative category. Furthermore, we also failed to yield effects of valence in the somatosensory modality despite our participants having rated the stronger stimuli as highly aversive. We therefore offer an alternative explanation in which we suggest that what we observe in the fMRI data may not necessarily be the neural correlate of evoked emotions but of emotion-regulation. Emotion regulation may

kick in too fast for the BOLD response to capture the original emotion or actually even before the supposedly emotion-evoking event occurs, i.e. as soon as the participants see the block instruction. However, our participants did report feeling these emotions when we asked them how nervous they felt in the respective experimental conditions. But since these reports where acquired retrospectively at the end of a 22 min long experimental run, they may reflect the participants' respective understanding of the experiment, but not their actual evoked emotions.

An interesting alternative explanation is based on the idea that different participants may have very different brain- and emotional reactions to the very same stimulus material (Levine, Wackerle, Rupprecht, & Schwarzbach, 2018b). Their study showed that the average brain response of a group of participants to emotionally charged stimuli was located in the lateral occipital temporal cortex (LOTC), reflecting perceptual rather than affective processes. When taking the participants' behavioral ratings into account, the authors showed with a representational similarity analysis that individualized affective spaces were represented in the insula. Thus, our failure to find stronger effects of valence may be due to the approach of reporting group averages and not taking individual affective spaces into account.

**How do you feel?** Within the context of regulation, we were interested in the relation between intolerance for uncertainty (IUS) and amygdala activity, which, in contrast to Somerville (2013), we did not find. Beyond IUS, we looked at other psychological trait- and state variables and found some indication that the neural system for fear and anxiety may react differentially to threats depending on the affect-state of the participant. In participants with negative affect-state the fear (i.e. transient) response of the amygdala was low when the participant was exposed to negative unpredictable (i.e. the most aversive) stimuli, which we interpret as a successful protection of the fear system. When participants were in a positive state, announcing a series of aversive events, did lead to a higher sustained activity in the amygdala. These results should be taken with a grain of salt until replicated. However, they may point us to interesting future research questions on the state-dependency of processing emotionally charged stimuli. We believe that such an individualized approach may constitute a major contribution of psychological research on precision psychiatry in the sense that on the one hand we hope that brain responses to particular stimuli will eventually become

biomarkers, but on the other hand we have to stress that these responses may be state dependent.

# 6 CONCLUSION

We developed a fast and reliable method for estimating stimulus intensity at pain threshold. We found high consistency of such estimates across stimulation site, indicating that the somatosensory pain threshold is a tangible variable of an individual, which can be assessed irrespective of body location. We furthermore found that stimulus intensity at pain threshold is relatively stable in the range of 24 hours but can substantially change after a week. This was backed by the finding that state variables were able to predict stimulus intensity at pain threshold whereas trait variables were not. In the neuroimaging study we found modality specific and modality general processing of fear and anxiety. We furthermore found commonalities between fear- and anxiety- processing neural systems, which we interpreted as common control systems. Also, in processing of fear and anxiety state variables may have an important modulatory effect in the sense of being in a good mood affects how we worry and being in a bad mood may make us less fearful. In our view, the modulatory role of individual affective spaces and of psychological states may have been understated in the literature.

# 7 APPENDIX

**Table 7.1**

*Means and Standard Deviations with Respect to Stimulus Intensity Values (mA) given Location and Session*

| Location/Session | mA | | | | | | | |
|---|---|---|---|---|---|---|---|---|
| | S1a | | S1 | | S2 | | S3 | |
| | $M \pm$ SD | | $M \pm$ SD | | $M \pm$ SD | | $M \pm$ SD | |
| ALD | 16.42 ± | 0.93 | 16.44 ± | 1.09 | 16.80 ± | 0.97 | 16.46 ± | 0.94 |
| ALV | 15.48 ± | 0.81 | 15.51 ± | 0.87 | 16.46 ± | 0.98 | 16.16 ± | 0.93 |
| ARD | 15.66 ± | 0.91 | 16.70 ± | 1.09 | 17.36 ± | 1.30 | 16.92 ± | 1.12 |
| ARV | 15.66 ± | 0.82 | 15.34 ± | 0.91 | 16.00 ± | 0.96 | 16.36 ± | 0.98 |
| LL | 19.27 ± | 1.13 | 18.60 ± | 1.21 | 19.66 ± | 1.50 | 19.50 ± | 1.55 |
| LR | 18.79 ± | 1.27 | 19.44 ± | 1.36 | 19.37 ± | 1.64 | 20.44 ± | 1.60 |

*Note.* Location: ALD= "arm left dorsal", ALV = "arm left ventral", ARD = "arm right dorsal", ALV = "arm left ventral", LL = "leg left" and LR = "leg right". Session: S1a = Practice, S1 = day 1; S2: deltaT = 24hs/1day, S3 = 168h/1 day. Confidence interval (95%) with lower limit (LL) and upper limit (UL).

**Table 7.2**

*Confidence Intervals (95%) for ICCs Considering Sessions and Locations*

| Location | S1 | | S2 | | S3 | |
|---|---|---|---|---|---|---|
| | 95% CI | | 95% CI | | 95% CI | |
| | LL | UL | LL | UL | LL | UL |
| ALD | 0.165 | 0.105 | 0.124 | 0.073 | 0.181 | 0.114 |
| ALV | 0.131 | 0.078 | 0.102 | 0.055 | 0.205 | 0.134 |
| ARD | 0.098 | 0.051 | 0.116 | 0.068 | 0.15 | 0.091 |
| ARV | 0.146 | 0.088 | 0.089 | 0.051 | 0.157 | 0.096 |
| LL | 0.105 | 0.061 | 0.083 | 0.047 | 0.16 | 0.098 |
| LR | 0.077 | 0.044 | 0.12 | 0.07 | 0.137 | 0.082 |

*Note.* Location: ALD= "arm left dorsal", ALV = "arm left ventral", ARD = "arm right dorsal", ALV = "arm left ventral", LL = "leg left" and LR = "leg right". Session: S1 = Practice to day 1; S2: deltaT = 24hs/1day, S3 = 168h/1 day. Confidence interval (95%) with lower limit (LL) and upper limit (UL).

**Table 7.3**

*Sample Characteristics with Respect to Psychometric Outcome Measures*

| Questionnaire | *M* | *SD* |
|---|---|---|
| ASI | *16.68* | *9.61* |
| IUS | *44.68* | *12.15* |
| PANAS | | |
|   Positive Affect | *33.71* | *6.02* |
|   Negative Affect | *13.02* | *4.08* |
| STAI-S | | |
|   Pre | *35.97* | *4.80* |
|   Post | *37.74* | *6.95* |

*Note.* ASI = Anxiety Sensitivity Index; IUS = Intolerance to Uncertainty Scale; PANAS = Positive And Negative Affect Schedule; STAI-S = State Anxiety Inventory.

**Table 7.4**

*Descriptive Statistics of the Average BOLD Response in the Left Amygdala as a Function of Stimulus Modality for Transient Responses*

| | MOD | pics | pics | pics | pics | zaps | zaps | zaps | zaps |
|---|---|---|---|---|---|---|---|---|---|
| | VAL | neg | neg | neu | neu | neg | neg | neu | neu |
| | PRED | pred | unpr | pred | unpr | pred | unpr | pred | unpr |
| *M* | | 12.76 | 23.92 | 14.91 | 17.89 | -4.40 | -1.80 | -7.83 | -2.54 |
| *SD* | | 10.55 | 11.38 | 14.91 | 18.27 | 15.26 | 16.21 | 12.49 | 13.21 |
| *SEM* | | 1.78 | 1.92 | 2.52 | 3.09 | 2.58 | 2.74 | 2.11 | 2.23 |
| *Var* | | 111.30 | 129.54 | 222.33 | 333.62 | 232.74 | 262.65 | 156.07 | 174.37 |
| *CI95%* | | 5.07 | 5.07 | 5.07 | 5.07 | 5.07 | 5.07 | 5.07 | 5.07 |
| *Skew* | | -0.517 | 0.996 | 0.797 | 1.361 | 0.410 | -0.111 | -0.132 | 0.371 |
| *zSkew* | | -1.249 | 2.405 | 1.925 | 3.287 | 0.990 | -0.269 | -0.318 | 0.895 |

*Note.* Modality (MOD: pictures (pics), electrical stimulation (zaps)), valence (VAL: negative (neg), neutral (neu)), and predictability (PRED: predictable (pred), unpredictable (unpr)). *M* = Mean, *SD* = standard deviation, *SEM* = standard error *Var* = variance, *CI95%* = 95% confidence interval, *Skew* = skewness, and *zSkew* = *z*-score of the skew. *N* = 35.

**Table 7.5**

*Repeated Measures ANOVA for Average BOLD response in the Left Amygdala with Factors Stimulus Modality, Valence, and Predictability for Transient Responses*

|  | df | F | p | SS | MSE |
|---|---|---|---|---|---|
| MOD | 1,34 | 85.8 | <0.000001 | 32396.53 | 377.62 |
| VAL | 1,34 | 1.21 | <0.279615 | 283.84 | 235.13 |
| PRED | 1,34 | 10.5 | <0.002645 | 2125.49 | 201.97 |
| MOD*VAL | 1,34 | 0.002 | <0.966544 | 0.39 | 219.25 |
| MOD*PRED | 1,34 | 0.619 | <0.436749 | 171.29 | 276.58 |
| VAL*PRED | 1,34 | 0.741 | <0.395401 | 132.01 | 178.17 |
| MOD*VAL*PRED | 1,34 | 3.86 | <0.057805 | 516.23 | 133.90 |

*Note.* Modality (MOD: pictures, electrical stimulation), valence (VAL: negative, neutral), and predictability (PRED: predictable, unpredictable). Df = degrees of freedom, F = F-statistic, p = p-value, SS = sum of squares, and MSE = mean squared error. N = 35.

**Table 7.6**

*Descriptive Statistics of the Average BOLD Response in the Right Amygdala as a Function of Stimulus Modality for Transient Responses*

| MOD | pics | pics | pics | pics | zaps | zaps | zaps | zaps |
|---|---|---|---|---|---|---|---|---|
| VAL | neg | neg | neu | neu | neg | neg | neu | neu |
| PRED | pred | unpr | pred | unpr | pred | unpr | pred | unpr |
| *M* | 16.86 | 24.29 | 18.08 | 19.16 | -3.05 | -1.13 | -7.16 | 1.66 |
| *SD* | 13.13 | 14.63 | 11.29 | 18.48 | 15.19 | 16.89 | 12.65 | 16.23 |
| *SEM* | 2.22 | 2.47 | 1.91 | 3.12 | 2.57 | 2.85 | 2.14 | 2.74 |
| *Var* | 172.32 | 213.95 | 127.56 | 341.52 | 230.70 | 285.27 | 159.94 | 263.49 |
| *CI95%* | 5.34 | 5.34 | 5.34 | 5.34 | 5.34 | 5.34 | 5.34 | 5.34 |
| *Skew* | 0.203 | 0.083 | 0.625 | 0.641 | -0.206 | -0.814 | -0.990 | 1.101 |
| *zSkew* | 0.489 | 0.201 | 1.509 | 1.548 | -0.498 | -1.965 | -2.391 | 2.659 |

*Note.* Modality (MOD: pictures (pics), electrical stimulation (zaps)), valence (VAL: negative (neg), neutral (neu)), and predictability (PRED: predictable (pred), unpredictable (unpr)). *M* = Mean, *SD* = standard deviation, *SEM* = standard error *Var* = variance, *CI95%* = 95% confidence interval, *Skew* = skewness, and *zSkew* = z-score of the skew. *N* = 35.

**Table 7.7**

*Repeated Measures ANOVA for Average BOLD response in the Right Amygdala with Factors Stimulus Modality, Valence, and Predictability for Transient Responses*

| | df | F | p | SS | MSE |
|---|---|---|---|---|---|
| MOD | 1,34 | 101.00 | <0.000001 | 33945.13 | 334.65 |
| VAL | 1,34 | 0.721 | <0.401641 | 119.36 | 165.46 |
| PRED | 1,34 | 4.67 | <0.037776 | 1621.67 | 347.05 |
| MOD*VAL | 1,34 | 0.153 | <0.698228 | 29.15 | 190.68 |
| MOD*PRED | 1,34 | 0.072 | <0.790339 | 21.76 | 303.00 |
| VAL*PRED | 1,34 | 0.006 | <0.937352 | 1.32 | 210.80 |
| MOD*VAL*PRED | 1,34 | 3.16 | <0.084481 | S767.84 | 243.11 |

*Note.* Modality (MOD: pictures, electrical stimulation), valence (VAL: negative, neutral), and predictability (PRED: predictable, unpredictable). *Df* = degrees of freedom, *F* = F-statistic, *p* = p-value, *SS* = sum of squares, and *MSE* = mean squared error. *N* = 35.

**Table 7.8**

*Descriptive Statistics of the Average BOLD Response in the Left Thalamus as a Function of Stimulus Modality for Transient Responses*

| | MOD | pics | pics | pics | pics | zaps | zaps | zaps | zaps |
|---|---|---|---|---|---|---|---|---|---|
| | VAL | neg | neg | neu | neu | neg | neg | neu | neu |
| | PRED | pred | unpr | pred | unpr | pred | unpr | pred | unpr |
| M | | 24.86 | 31.76 | 27.06 | 34.19 | 4.77 | 6.37 | 3.06 | 7.88 |
| SD | | 24.84 | 19.23 | 15.56 | 18.82 | 18.96 | 16.19 | 13.41 | 14.84 |
| SEM | | 4.20 | 3.25 | 2.63 | 3.18 | 3.20 | 2.74 | 2.27 | 2.51 |
| Var | | 617.11 | 369.93 | 242.08 | 354.03 | 359.32 | 262.23 | 179.85 | 220.21 |
| CI95% | | 6.43 | 6.43 | 6.43 | 6.43 | 6.43 | 6.43 | 6.43 | 6.43 |
| Skew | | 1.247 | 0.661 | 0.425 | 0.569 | -0.880 | 0.467 | 0.431 | 0.212 |
| zSkew | | 3.011 | 1.596 | 1.027 | 1.375 | -2.126 | 1.128 | 1.042 | 0.513 |

*Note.* Modality (MOD: pictures (pics), electrical stimulation (zaps)), valence (VAL: negative (neg), neutral (neu)), and predictability (PRED: predictable (pred), unpredictable (unpr)). *M* = Mean, *SD* = standard deviation, *SEM* = standard error *Var* = variance, *CI95%* = 95% confidence interval, *Skew* = skewness, and *zSkew* = z-score of the skew. *N* = 35.

**Table 7.9**

*Repeated Measures ANOVA for Average BOLD response in the Right Amygdala with Factors Stimulus Modality, Valence, and Predictability for Transient Responses*

|  | *df* | *F* | *p* | *SS* | *MSE* |
|---|---|---|---|---|---|
| MOD | 1,34 | 68.7 | <0.000001 | 40137.73 | 584.42 |
| VAL | 1,34 | 0.350 | <0.557750 | 86.27 | 246.13 |
| PRED | 1,34 | 6.20 | <0.017831 | 1830.49 | 295.28 |
| MOD*VAL | 1,34 | 0.306 | <0.583564 | 101.95 | 332.81 |
| MOD*PRED | 1,34 | 0.496 | <0.485866 | 253.08 | 509.79 |
| VAL*PRED | 1,34 | 0.240 | <0.627631 | 52.24 | 218.02 |
| MOD*VAL*PRED | 1,34 | 0.094 | <0.760727 | 39.42 | 418.30 |

*Note.* Modality (MOD: pictures, electrical stimulation), valence (VAL: negative, neutral), and predictability (PRED: predictable, unpredictable). *Df* = degrees of freedom, *F* = F-statistic, *p* = p-value, *SS* = sum of squares, and *MSE* = mean squared error. *N* = 35.

**Table 7.10**

*Descriptive Statistics of the Average BOLD Response in the Right Thalamus as a Function of Stimulus Modality for Transient Responses*

| MOD | pics | pics | pics | pics | zaps | zaps | zaps | zaps |
|---|---|---|---|---|---|---|---|---|
| VAL | neg | neg | neu | neu | neg | neg | neu | neu |
| PRED | pred | unpr | pred | unpr | pred | unpr | pred | unpr |
| *M* | 31.06 | 37.22 | 35.26 | 36.47 | 6.80 | 11.83 | 6.92 | 11.84 |
| *SD* | 22.58 | 20.84 | 15.94 | 20.94 | 20.88 | 18.16 | 16.93 | 15.47 |
| *SEM* | 3.82 | 3.52 | 2.69 | 3.54 | 3.53 | 3.07 | 2.86 | 2.61 |
| *Var* | 509.85 | 434.24 | 254.20 | 438.58 | 435.80 | 329.63 | 286.76 | 239.28 |
| *CI95%* | 6.82 | 6.82 | 6.82 | 6.82 | 6.82 | 6.82 | 6.82 | 6.82 |
| *Skew* | 0.723 | 0.208 | 0.089 | 0.227 | -0.842 | 0.581 | -0.404 | 0.228 |
| *zSkew* | 1.745 | 0.503 | 0.214 | 0.549 | -2.033 | 1.404 | -0.975 | 0.551 |

*Note.* Modality (MOD: pictures (pics), electrical stimulation (zaps)), valence (VAL: negative (neg), neutral (neu)), and predictability (PRED: predictable (pred), unpredictable (unpr)). *M* = Mean, *SD* = standard deviation, *SEM* = standard error *Var* = variance, *CI95%* = 95% confidence interval, *Skew* = skewness, and *zSkew* = z-score of the skew. *N* = 35.

**Table 7.11**

*Repeated Measures ANOVA for Average BOLD response in the Right Thalamus with Factors Stimulus Modality, Valence, and Predictability for Transient Responses*

|  | df | F | p | SS | MSE |
|---|---|---|---|---|---|
| MOD | 1,34 | 66.8 | <0.000001 | 46073.99 | 689.97 |
| VAL | 1,34 | 0.315 | <0.578463 | 56.51 | 179.56 |
| PRED | 1,34 | 3.16 | <0.084190 | 1311.22 | 414.33 |
| MOD*VAL | 1,34 | 0.173 | <0.679699 | 48.46 | 279.40 |
| MOD*PRED | 1,34 | 0.050 | <0.823688 | 29.25 | 580.18 |
| VAL*PRED | 1,34 | 0.425 | <0.518905 | 112.67 | 265.20 |
| MOD*VAL*PRED | 1,34 | 0.196 | <0.660504 | 102.03 | 519.70 |

*Note.* Modality (MOD: pictures, electrical stimulation), valence (VAL: negative, neutral), and predictability (PRED: predictable, unpredictable). *Df* = degrees of freedom, *F* = F-statistic, *p* = p-value, *SS* = sum of squares, and *MSE* = mean squared error. *N* = 35.

**Table 7.12**

*Descriptive Statistics of the Average BOLD Response in the Left Hippocampus as a Function of Stimulus Modality for Transient Responses*

| MOD | pics | pics | pics | pics | zaps | zaps | zaps | zaps |
|---|---|---|---|---|---|---|---|---|
| VAL | neg | neg | neu | neu | neg | neg | neu | neu |
| PRED | pred | unpr | pred | unpr | pred | unpr | pred | unpr |
| *M* | 20.33 | 30.38 | 23.40 | 29.06 | -3.58 | -2.26 | -5.68 | -2.10 |
| *SD* | 14.00 | 14.07 | 14.76 | 18.96 | 15.64 | 14.28 | 12.33 | 13.10 |
| *SEM* | 2.37 | 2.38 | 2.49 | 3.20 | 2.64 | 2.41 | 2.08 | 2.22 |
| *Var* | 195.94 | 197.93 | 217.78 | 359.34 | 244.45 | 203.96 | 152.14 | 171.73 |
| *CI95%* | 5.26 | 5.26 | 5.26 | 5.26 | 5.26 | 5.26 | 5.26 | 5.26 |
| *Skew* | 0.942 | 0.716 | 0.041 | 0.691 | 0.222 | -0.396 | 0.188 | -0.003 |
| *zSkew* | 2.275 | 1.730 | 0.100 | 1.670 | 0.536 | -0.956 | 0.454 | -0.006 |

*Note.* Modality (MOD: pictures (pics), electrical stimulation (zaps)), valence (VAL: negative (neg), neutral (neu)), and predictability (PRED: predictable (pred), unpredictable (unpr)). *M* = Mean, *SD* = standard deviation, *SEM* = standard error *Var* = variance, *CI95%* = 95% confidence interval, *Skew* = skewness, and *zSkew* = *z*-score of the skew. *N* = 35.

**Table 7.13**

*Repeated Measures ANOVA for Average BOLD response in the Left Hippocampus with Factors Stimulus Modality, Valence, and Predictability for Transient Responses*

|  | *df* | *F* | *p* | *SS* | *MSE* |
|---|---|---|---|---|---|
| MOD | 1,34 | 116 | <0.000001 | 59669.68 | 514.74 |
| VAL | 1,34 | 0.001 | <0.975154 | 0.20 | 198.67 |
| PRED | 1,34 | 9.50 | <0.004064 | 1858.30 | 195.69 |
| MOD*VAL | 1,34 | 0.294 | <0.591480 | 59.47 | 202.60 |
| MOD*PRED | 1,34 | 1.54 | <0.223332 | 510.66 | 331.92 |
| VAL*PRED | 1,34 | 0.147 | <0.704121 | 19.79 | 134.95 |
| MOD*VAL*PRED | 1,34 | 1.18 | <0.285524 | 193.94 | 164.72 |

*Note.* Modality (MOD: pictures, electrical stimulation), valence (VAL: negative, neutral), and predictability (PRED: predictable, unpredictable). *Df* = degrees of freedom, *F* = F-statistic, *p* = p-value, *SS* = sum of squares, and *MSE* = mean squared error. *N* = 35.

**Table 7.14**

*Descriptive Statistics of the Average BOLD Response in the Right Hippocampus as a Function of Stimulus Modality for Transient Responses*

| MOD | pics | pics | pics | pics | zaps | zaps | zaps | zaps |
|---|---|---|---|---|---|---|---|---|
| VAL | neg | neg | neu | neu | neg | neg | neu | neu |
| PRED | pred | unpr | pred | unpr | pred | unpr | pred | unpr |
| *M* | 26.35 | 34.77 | 30.19 | 32.73 | -0.61 | 3.23 | -1.26 | 4.63 |
| *SD* | 15.45 | 16.29 | 13.86 | 18.00 | 17.20 | 16.03 | 14.08 | 15.54 |
| *SEM* | 2.61 | 2.75 | 2.34 | 3.04 | 2.91 | 2.71 | 2.38 | 2.63 |
| *Var* | 238.71 | 265.44 | 192.06 | 324.08 | 295.93 | 256.88 | 198.20 | 241.34 |
| *CI95%* | 5.65 | 5.65 | 5.65 | 5.65 | 5.65 | 5.65 | 5.65 | 5.65 |
| *Skew* | 1.237 | 0.469 | -0.144 | 0.574 | -0.670 | 0.155 | -0.402 | 0.877 |
| *zSkew* | 2.988 | 1.133 | -0.347 | 1.387 | -1.618 | 0.374 | -0.972 | 2.118 |

*Note.* Modality (MOD: pictures (pics), electrical stimulation (zaps)), valence (VAL: negative (neg), neutral (neu)), and predictability (PRED: predictable (pred), unpredictable (unpr)). *M* = Mean, *SD* = standard deviation, *SEM* = standard error *Var* = variance, *CI95%* = 95% confidence interval, *Skew* = skewness, and *zSkew* = z-score of the skew. *N* = 35.

**Table 7.15**

*Repeated Measures ANOVA for Average BOLD response in the Right Hippocampus with Factors Stimulus Modality, Valence, and Predictability for Transient Responses*

|  | df | F | p | SS | MSE |
|---|---|---|---|---|---|
| MOD | 1,34 | 120 | <0.000001 | 60966.57 | 510.15 |
| VAL | 1,34 | 0.183 | <0.671379 | 28.29 | 154.44 |
| PRED | 1,34 | 6.10 | <0.018686 | 1874.09 | 307.18 |
| MOD*VAL | 1,34 | 0.026 | <0.872155 | 4.83 | 183.56 |
| MOD*PRED | 1,34 | 0.016 | <0.899130 | 6.50 | 398.37 |
| VAL*PRED | 1,34 | 0.384 | <0.539471 | 63.92 | 166.35 |
| MOD*VAL*PRED | 1,34 | 0.937 | <0.339892 | 274.15 | 292.59 |

*Note.* Modality (MOD: pictures, electrical stimulation), valence (VAL: negative, neutral), and predictability (PRED: predictable, unpredictable). *Df* = degrees of freedom, *F* = F-statistic, *p* = p-value, *SS* = sum of squares, and *MSE* = mean squared error. *N* = 35.

**Table 7.16**

*Descriptive Statistics of the Average BOLD Response in the Parahippocampal Gyrus as a Function of Stimulus Modality for Transient Responses*

| MOD | pics | pics | pics | pics | zaps | zaps | zaps | zaps |
|---|---|---|---|---|---|---|---|---|
| VAL | neg | neg | neu | neu | neg | neg | neu | neu |
| PRED | pred | unpr | pred | unpr | pred | unpr | pred | unpr |
| *M* | 16.22 | 24.00 | 17.74 | 20.65 | -3.33 | -0.86 | -4.78 | -1.50 |
| *SD* | 7.35 | 10.46 | 9.99 | 15.44 | 11.17 | 12.52 | 9.72 | 10.62 |
| *SEM* | 1.24 | 1.77 | 1.69 | 2.61 | 1.89 | 2.12 | 1.64 | 1.80 |
| *Var* | 54.05 | 109.39 | 99.88 | 238.41 | 124.80 | 156.64 | 94.50 | 112.84 |
| *CI95%* | 3.97 | 3.97 | 3.97 | 3.97 | 3.97 | 3.97 | 3.97 | 3.97 |
| *Skew* | -0.111 | 0.387 | -0.011 | 0.681 | -0.192 | -0.298 | -0.588 | 0.058 |
| *zSkew* | -0.269 | 0.936 | -0.027 | 1.645 | -0.463 | -0.719 | -1.421 | 0.140 |

*Note.* Modality (MOD: pictures (pics), electrical stimulation (zaps)), valence (VAL: negative (neg), neutral (neu)), and predictability (PRED: predictable (pred), unpredictable (unpr)). *M* = Mean, *SD* = standard deviation, *SEM* = standard error *Var* = variance, *CI95%* = 95% confidence interval, *Skew* = skewness, and *zSkew* = z-score of the skew. *N* = 35.

**Table 7.17**

*Repeated Measures ANOVA for Average BOLD response in the Parahippocampal Gyrus with Factors Stimulus Modality, Valence, and Predictability for Transient Responses*

|  | df | F | p | SS | MSE |
|---|---|---|---|---|---|
| MOD | 1,34 | 137 | <0.000001 | 34709.82 | 252.88 |
| VAL | 1,34 | 0.562 | <0.458416 | 66.50 | 118.23 |
| PRED | 1,34 | 10.2 | <0.003015 | 1183.68 | 115.97 |
| MOD*VAL | 1,34 | 0.002 | <0.963242 | 0.28 | 131.10 |
| MOD*PRED | 1,34 | 0.698 | <0.409450 | 106.79 | 153.10 |
| VAL*PRED | 1,34 | 0.626 | <0.434160 | 71.82 | 114.66 |
| MOD*VAL*PRED | 1,34 | 1.35 | <0.253583 | 141.07 | 104.59 |

*Note.* Modality (MOD: pictures, electrical stimulation), valence (VAL: negative, neutral), and predictability (PRED: predictable, unpredictable). *Df* = degrees of freedom, *F* = F-statistic, *p* = p-value, *SS* = sum of squares, and *MSE* = mean squared error. *N* = 35.

**Table 7.18**

*Descriptive Statistics of the Average BOLD Response in the Brain Stem as a Function of Stimulus Modality for Transient Responses*

| MOD | pics | pics | pics | pics | zaps | zaps | zaps | zaps |
|---|---|---|---|---|---|---|---|---|
| VAL | neg | neg | neu | neu | neg | neg | neu | neu |
| PRED | pred | unpr | pred | unpr | pred | unpr | pred | unpr |
| M | 23.93 | 31.42 | 25.32 | 31.09 | 2.24 | 2.77 | 2.44 | 3.96 |
| SD | 22.11 | 18.21 | 14.04 | 21.04 | 18.40 | 17.00 | 13.06 | 13.64 |
| SEM | 3.74 | 3.08 | 2.37 | 3.56 | 3.11 | 2.87 | 2.21 | 2.31 |
| Var | 489.02 | 331.43 | 197.15 | 442.70 | 338.63 | 288.85 | 170.49 | 186.14 |
| CI95% | 6.23 | 6.23 | 6.23 | 6.23 | 6.23 | 6.23 | 6.23 | 6.23 |
| Skew | 1.255 | 0.997 | 0.179 | 1.082 | -0.796 | 0.512 | -0.220 | -0.315 |
| zSkew | 3.032 | 2.408 | 0.431 | 2.614 | -1.922 | 1.236 | -0.531 | -0.761 |

*Note.* Modality (MOD: pictures (pics), electrical stimulation (zaps)), valence (VAL: negative (neg), neutral (neu)), and predictability (PRED: predictable (pred), unpredictable (unpr)). *M* = Mean, *SD* = standard deviation, *SEM* = standard error *Var* = variance, *CI95%* = 95% confidence interval, *Skew* = skewness, and *zSkew* = z-score of the skew. *N* = 35.

**Table 7.19**

*Repeated Measures ANOVA for Average BOLD response in the Brain Stem with Factors Stimulus Modality, Valence, and Predictability for Transient Responses*

|  | df | F | p | SS | MSE |
|---|---|---|---|---|---|
| MOD | 1,34 | 82.5 | <0.000001 | 44059.97 | 533.91 |
| VAL | 1,34 | 0.164 | <0.688105 | 26.18 | 159.71 |
| PRED | 1,34 | 2.64 | <0.113270 | 1027.05 | 388.65 |
| MOD*VAL | 1,34 | 0.002 | <0.967030 | 0.50 | 287.64 |
| MOD*PRED | 1,34 | 1.01 | <0.322550 | 549.65 | 545.46 |
| VAL*PRED | 1,34 | 0.010 | <0.920667 | 2.37 | 235.83 |
| MOD*VAL*PRED | 1,34 | 0.111 | <0.741187 | 32.51 | 293.20 |

*Note.* Modality (MOD: pictures, electrical stimulation), valence (VAL: negative, neutral), and predictability (PRED: predictable, unpredictable). *Df* = degrees of freedom, *F* = F-statistic, *p* = p-value, *SS* = sum of squares, and *MSE* = mean squared error. *N* = 35.

**Table 7.20**

*Descriptive Statistics of the Average BOLD Response in the Paracingulate Cortex as a Function of Stimulus Modality for Transient Responses*

| MOD | pics | pics | pics | pics | zaps | zaps | zaps | zaps |
|---|---|---|---|---|---|---|---|---|
| VAL | neg | neg | neu | neu | neg | neg | neu | neu |
| PRED | pred | unpr | pred | unpr | pred | unpr | pred | unpr |
| *M* | -16.52 | -1.84 | -9.54 | 11.58 | -27.11 | -20.00 | -31.43 | -19.25 |
| *SD* | 48.88 | 63.94 | 35.18 | 44.34 | 40.13 | 33.94 | 27.16 | 38.74 |
| *SEM* | 8.26 | 10.81 | 5.95 | 7.49 | 6.78 | 5.74 | 4.59 | 6.55 |
| *Var* | 2388.82 | 4088.18 | 1237.42 | 1965.68 | 1610.78 | 1151.61 | 737.90 | 1500.51 |
| *CI95%* | 15.27 | 15.27 | 15.27 | 15.27 | 15.27 | 15.27 | 15.27 | 15.27 |
| *Skew* | 1.022 | -1.798 | 0.374 | 0.586 | -0.588 | -0.042 | 0.361 | -0.792 |
| *zSkew* | 2.469 | -4.343 | 0.903 | 1.416 | -1.420 | -0.101 | 0.872 | -1.914 |

*Note.* Modality (MOD: pictures (pics), electrical stimulation (zaps)), valence (VAL: negative (neg), neutral (neu)), and predictability (PRED: predictable (pred), unpredictable (unpr)). *M* = Mean, *SD* = standard deviation, *SEM* = standard error *Var* = variance, *CI95%* = 95% confidence interval, *Skew* = skewness, and *zSkew* = z-score of the skew. *N* = 35.

**Table 7.21**

*Repeated Measures ANOVA for Average BOLD response in the Paracingulate Cortex with Factors Stimulus Modality, Valence, and Predictability for Transient Responses*

|  | *df* | *F* | *p* | *SS* | *MSE* |
|---|---|---|---|---|---|
| MOD | 1,34 | 22.6 | <0.000036 | 29043.57 | 1287.08 |
| VAL | 1,34 | 0.599 | <0.444364 | 1238.51 | 2068.14 |
| PRED | 1,34 | 5.50 | <0.024975 | 13269.69 | 2412.09 |
| MOD*VAL | 1,34 | 1.97 | <0.169406 | 2514.58 | 1275.76 |
| MOD*PRED | 1,34 | 0.350 | <0.558046 | 1192.93 | 3408.70 |
| VAL*PRED | 1,34 | 0.315 | <0.578185 | 580.95 | 1843.08 |
| MOD*VAL*PRED | 1,34 | 0.003 | <0.953568 | 8.21 | 2386.04 |

*Note.* Modality (MOD: pictures, electrical stimulation), valence (VAL: negative, neutral), and predictability (PRED: predictable, unpredictable). *Df* = degrees of freedom, *F* = F-statistic, *p* = p-value, *SS* = sum of squares, and *MSE* = mean squared error. *N* = 35.

**Table 7.22**

*Descriptive Statistics of the Average BOLD Response in the Insular Cortex as a Function of Stimulus Modality for Transient Responses*

| MOD | pics | pics | pics | pics | zaps | zaps | zaps | zaps |
|---|---|---|---|---|---|---|---|---|
| VAL | neg | neg | neu | neu | neg | neg | neu | neu |
| PRED | pred | unpr | pred | unpr | pred | unpr | pred | unpr |
| *M* | -3.67 | 6.79 | 3.86 | 8.63 | 25.37 | 32.29 | 17.80 | 33.26 |
| *SD* | 36.77 | 32.11 | 32.55 | 26.48 | 36.52 | 32.76 | 31.99 | 29.58 |
| *SEM* | 6.22 | 5.43 | 5.50 | 4.48 | 6.17 | 5.54 | 5.41 | 5.00 |
| *Var* | 1352.04 | 1030.79 | 1059.33 | 701.36 | 1333.88 | 1073.03 | 1023.05 | 874.68 |
| *CI95%* | 11.58 | 11.58 | 11.58 | 11.58 | 11.58 | 11.58 | 11.58 | 11.58 |
| *Skew* | 1.706 | 1.142 | 0.792 | 0.155 | -0.874 | -0.828 | -0.628 | 1.496 |
| *zSkew* | 4.121 | 2.759 | 1.913 | 0.376 | -2.112 | -2.001 | -1.518 | 3.613 |

*Note.* Modality (MOD: pictures (pics), electrical stimulation (zaps)), valence (VAL: negative (neg), neutral (neu)), and predictability (PRED: predictable (pred), unpredictable (unpr)). *M* = Mean, *SD* = standard deviation, *SEM* = standard error *Var* = variance, *CI95%* = 95% confidence interval, *Skew* = skewness, and *zSkew* = *z*-score of the skew. *N* = 35.

**Table 7.23**

*Repeated Measures ANOVA for Average BOLD response in the Insular Cortex with Factors Stimulus Modality, Valence, and Predictability for Transient Responses*

|  | df | F | p | SS | MSE |
|---|---|---|---|---|---|
| MOD | 1,34 | 40.8 | <0.000001 | 37914.84 | MSe=928.71 |
| VAL | 1,34 | 0.059 | <0.809632 | 33.67 | 571.20 |
| PRED | 1,34 | 3.83 | <0.058525 | 6189.86 | 1615.22 |
| MOD*VAL | 1,34 | 0.683 | <0.414389 | 1113.43 | 1630.71 |
| MOD*PRED | 1,34 | 0.176 | <0.677514 | 223.51 | 1270.30 |
| VAL*PRED | 1,34 | 0.045 | <0.834099 | 35.62 | 799.60 |
| MOD*VAL*PRED | 1,34 | 0.543 | <0.466441 | 885.62 | 1632.42 |

*Note.* Modality (MOD: pictures, electrical stimulation), valence (VAL: negative, neutral), and predictability (PRED: predictable, unpredictable). *Df* = degrees of freedom, *F* = F-statistic, *p* = p-value, *SS* = sum of squares, and *MSE* = mean squared error. *N* = 35.

**Table 7.24**

*Descriptive Statistics of the Average BOLD Response in the Frontal Pole as a Function of Stimulus Modality for Transient Responses*

| MOD | pics | pics | pics | pics | zaps | zaps | zaps | zaps |
|---|---|---|---|---|---|---|---|---|
| VAL | neg | neg | neu | neu | neg | neg | neu | neu |
| PRED | pred | unpr | pred | unpr | pred | unpr | pred | unpr |
| *M* | -7.03 | 11.06 | 7.27 | 15.53 | -12.18 | -8.91 | -10.32 | 0.01 | -7.03 |
| *SD* | 45.21 | 40.69 | 30.44 | 39.02 | 32.28 | 33.65 | 27.80 | 29.64 | 45.21 |
| *SEM* | 7.64 | 6.88 | 5.15 | 6.60 | 5.46 | 5.69 | 4.70 | 5.01 | 7.64 |
| *Var* | 2043.50 | 1655.97 | 926.60 | 1522.83 | 1042.05 | 1132.22 | 772.85 | 878.43 | 2043.50 |
| *CI95%* | 12.58 | 12.58 | 12.58 | 12.58 | 12.58 | 12.58 | 12.58 | 12.58 | 12.58 |
| *Skew* | 0.193 | -0.379 | 0.830 | 1.499 | 0.393 | -1.109 | 0.235 | -0.458 | 0.193 |
| *zSkew* | 0.465 | -0.916 | 2.004 | 3.621 | 0.950 | -2.679 | 0.568 | -1.107 | 0.465 |

*Note.* Modality (MOD: pictures (pics), electrical stimulation (zaps)), valence (VAL: negative (neg), neutral (neu)), and predictability (PRED: predictable (pred), unpredictable (unpr)). *M* = Mean, *SD* = standard deviation, *SEM* = standard error *Var* = variance, *CI95%* = 95% confidence interval, *Skew* = skewness, and *zSkew* = z-score of the skew. *N* = 35.

**Table 7.25**

*Repeated Measures ANOVA for Average BOLD response in the Frontal Pole with Factors Stimulus Modality, Valence, and Predictability for Transient Responses*

|  | df | F | p | SS | MSE |
|---|---|---|---|---|---|
| MOD | 1,34 | 17.9 | <0.000163 | 14833.38 | 826.39 |
| VAL | 1,34 | 2.59 | <0.117007 | 3817.56 | 1475.79 |
| PRED | 1,34 | 4.99 | <0.032113 | 6979.44 | 1397.54 |
| MOD*VAL | 1,34 | 0.180 | <0.674121 | 280.92 | 1561.41 |
| MOD*PRED | 1,34 | 0.340 | <0.563871 | 712.66 | 2098.15 |
| VAL*PRED | 1,34 | 0.042 | <0.838496 | 33.93 | 804.38 |
| MOD*VAL*PRED | 1,34 | 0.689 | <0.412166 | 1248.32 | 1810.77 |

*Note.* Modality (MOD: pictures, electrical stimulation), valence (VAL: negative, neutral), and predictability (PRED: predictable, unpredictable). *Df* = degrees of freedom, *F* = F-statistic, *p* = p-value, *SS* = sum of squares, and *MSE* = mean squared error. *N* = 35.

**Table 7.26**

*Descriptive Statistics of the Average BOLD Response in the Middle Frontal Gyrus as a Function of Stimulus Modality for Transient Responses*

| MOD | pics | pics | pics | pics | zaps | zaps | zaps | zaps |
|---|---|---|---|---|---|---|---|---|
| VAL | neg | neg | neu | neu | neg | neg | neu | neu |
| PRED | pred | unpr | pred | unpr | pred | unpr | pred | unpr |
| *M* | 13.19 | 38.96 | 29.82 | 45.26 | 2.97 | -6.22 | 1.16 | 3.76 |
| *SD* | 56.82 | 51.47 | 40.33 | 52.00 | 38.03 | 52.31 | 42.17 | 39.91 |
| *SEM* | 9.60 | 8.70 | 6.82 | 8.79 | 6.43 | 8.84 | 7.13 | 6.75 |
| *Var* | 3228.70 | 2648.90 | 1626.14 | 2704.40 | 1446.55 | 2736.17 | 1778.65 | 1593.11 |
| *CI95%* | 16.79 | 16.79 | 16.79 | 16.79 | 16.79 | 16.79 | 16.79 | 16.79 |
| *Skew* | 0.441 | -0.477 | 0.939 | 1.180 | 0.484 | -1.071 | -0.185 | -0.086 |
| *zSkew* | 1.065 | -1.152 | 2.267 | 2.851 | 1.170 | -2.586 | -0.446 | -0.208 |

*Note.* Modality (MOD: pictures (pics), electrical stimulation (zaps)), valence (VAL: negative (neg), neutral (neu)), and predictability (PRED: predictable (pred), unpredictable (unpr)). *M* = Mean, *SD* = standard deviation, *SEM* = standard error *Var* = variance, *CI95%* = 95% confidence interval, *Skew* = skewness, and *zSkew* = z-score of the skew. *N* = 35.

**Table 7.27**

*Repeated Measures ANOVA for Average BOLD response in the Middle Frontal Gyrus with Factors Stimulus Modality,*

*Valence, and Predictability for Transient Responses*

|  | df | F | p | SS | MSE |
|---|---|---|---|---|---|
| MOD | 1,34 | 24.5 | <0.000020 | 68965.53 | 2814.98 |
| VAL | 1,34 | 1.48 | <0.232442 | 4237.14 | 2866.56 |
| PRED | 1,34 | 3.69 | <0.063191 | 5242.84 | 1421.21 |
| MOD*VAL | 1,34 | 0.367 | <0.548751 | 953.43 | 2598.99 |
| MOD*PRED | 1,34 | 2.67 | <0.111299 | 10001.08 | 3741.73 |
| VAL*PRED | 1,34 | 0.005 | <0.941368 | 9.38 | 1708.19 |
| MOD*VAL*PRED | 1,34 | 0.821 | <0.371360 | 2142.73 | 2610.96 |

*Note.* Modality (MOD: pictures, electrical stimulation), valence (VAL: negative, neutral), and predictability (PRED: predictable, unpredictable). *Df* = degrees of freedom, *F* = F-statistic, *p* = p-value, *SS* = sum of squares, and *MSE* = mean squared error. *N* = 35.

**Table 7.28**

*Descriptive Statistics of the Average BOLD Response in the Inferior Frontal Gyrus as a Function of Stimulus Modality for*

*Transient Responses*

| MOD | pics | pics | pics | pics | zaps | zaps | zaps | zaps |
|---|---|---|---|---|---|---|---|---|
| VAL | neg | neg | neu | neu | neg | neg | neu | neu |
| PRED | pred | unpr | pred | unpr | pred | unpr | pred | unpr |
| *M* | 15.92 | 46.17 | 36.22 | 51.38 | 0.20 | -11.97 | -6.75 | 1.49 |
| *SD* | 61.84 | 57.81 | 47.52 | 58.72 | 38.71 | 54.76 | 43.96 | 46.43 |
| *SEM* | 10.45 | 9.77 | 8.03 | 9.93 | 6.54 | 9.26 | 7.43 | 7.85 |
| *Var* | 3823.92 | 3342.11 | 2257.93 | 3448.33 | 1498.75 | 2999.07 | 1932.19 | 2155.51 |
| *CI95%* | 18.46 | 18.46 | 18.46 | 18.46 | 18.46 | 18.46 | 18.46 | 18.46 |
| *Skew* | -0.148 | -0.382 | 1.243 | 1.315 | 0.570 | -1.408 | -0.314 | -0.180 |
| *zSkew* | -0.356 | -0.922 | 3.001 | 3.176 | 1.377 | -3.400 | -0.759 | -0.434 |

*Note.* Modality (MOD: pictures (pics), electrical stimulation (zaps)), valence (VAL: negative (neg), neutral (neu)), and predictability (PRED: predictable (pred), unpredictable (unpr)). *M* = Mean, *SD* = standard deviation, *SEM* = standard error *Var* = variance, *CI95%* = 95% confidence interval, *Skew* = skewness, and *zSkew* = *z*-score of the skew. *N* = 35.

**Table 7.29**

*Repeated Measures ANOVA for Average BOLD response in the Inferior Frontal Gyrus with Factors Stimulus Modality, Valence, and Predictability for Transient Responses*

|  | *df* | *F* | *p* | *SS* | *MSE* |
|---|---|---|---|---|---|
| MOD | 1,34 | 45.6 | <0.000001 | 121621.16 | 2668.15 |
| VAL | 1,34 | 1.11 | <0.299652 | 4482.30 | 4040.50 |
| PRED | 1,34 | 4.19 | <0.048438 | 7526.28 | 1795.96 |
| MOD*VAL | 1,34 | 0.372 | <0.546049 | 1576.62 | 4239.88 |
| MOD*PRED | 1,34 | 2.54 | <0.120366 | 10655.96 | 4197.99 |
| VAL*PRED | 1,34 | 0.061 | <0.806132 | 123.86 | 2024.61 |
| MOD*VAL*PRED | 1,34 | 2.21 | <0.146104 | 5511.04 | 2490.75 |

*Note.* Modality (MOD: pictures, electrical stimulation), valence (VAL: negative, neutral), and predictability (PRED: predictable, unpredictable). *Df* = degrees of freedom, *F* = F-statistic, *p* = p-value, *SS* = sum of squares, and *MSE* = mean squared error. *N* = 35.

**Table 7.30**

*Descriptive Statistics of the Average BOLD Response in the Frontal Medial Cortex as a Function of Stimulus Modality for Transient Responses*

| MOD | pics | pics | pics | pics | zaps | zaps | zaps | zaps |
|---|---|---|---|---|---|---|---|---|
| VAL | neg | neg | neu | neu | neg | neg | neu | neu |
| PRED | pred | unpr | pred | unpr | pred | unpr | pred | unpr |
| *M* | -11.46 | 1.28 | -14.67 | 10.11 | -35.35 | -35.78 | -39.32 | -33.86 | -11.46 |
| *SD* | 32.50 | 44.89 | 32.22 | 39.20 | 34.82 | 34.26 | 26.57 | 34.28 | 32.50 |
| *SEM* | 5.49 | 7.59 | 5.45 | 6.63 | 5.89 | 5.79 | 4.49 | 5.79 | 5.49 |
| *Var* | 1056.50 | 2014.69 | 1038.31 | 1536.80 | 1212.18 | 1173.75 | 706.22 | 1174.91 | 1056.50 |
| *CI95%* | 12.54 | 12.54 | 12.54 | 12.54 | 12.54 | 12.54 | 12.54 | 12.54 | 12.54 |
| *Skew* | 0.075 | -1.164 | 0.474 | 0.337 | -0.894 | -0.746 | 0.291 | -0.713 | 0.075 |
| *zSkew* | 0.180 | -2.811 | 1.145 | 0.815 | -2.160 | -1.801 | 0.703 | -1.721 | 0.180 |

*Note.* Modality (MOD: pictures (pics), electrical stimulation (zaps)), valence (VAL: negative (neg), neutral (neu)), and predictability (PRED: predictable (pred), unpredictable (unpr)). *M* = Mean, *SD* = standard deviation, *SEM* = standard error *Var* = variance, *CI95%* = 95% confidence interval, *Skew* = skewness, and *zSkew* = *z*-score of the skew. *N* = 35.

**Table 7.31**

*Repeated Measures ANOVA for Average BOLD response in the Frontal Medial Cortex with Factors Stimulus Modality, Valence, and Predictability for Transient Responses*

|  | df | F | p | SS | MSE |
|---|---|---|---|---|---|
| MOD | 1,34 | 63.3 | <0.000001 | 73442.80 | 1159.80 |
| VAL | 1,34 | 0.042 | <0.839016 | 56.03 | 1337.05 |
| PRED | 1,34 | 4.69 | <0.037399 | 7921.51 | 1688.16 |
| MOD*VAL | 1,34 | 0.240 | <0.627334 | 257.75 | 1073.83 |
| MOD*PRED | 1,34 | 2.30 | <0.138647 | 4618.21 | 2008.23 |
| VAL*PRED | 1,34 | 1.14 | <0.294194 | 1406.37 | 1238.96 |
| MOD*VAL*PRED | 1,34 | 0.118 | <0.733851 | 165.39 | 1407.33 |

*Note.* Modality (MOD: pictures, electrical stimulation), valence (VAL: negative, neutral), and predictability (PRED: predictable, unpredictable). *Df* = degrees of freedom, *F* = F-statistic, *p* = p-value, *SS* = sum of squares, and *MSE* = mean squared error. *N* = 35.

**Table 7.32**

*Descriptive Statistics of the Average BOLD Response in the Superior Frontal Gyrus as a Function of Stimulus Modality for Transient Responses*

| MOD | pics | pics | pics | pics | zaps | zaps | zaps | zaps |
|---|---|---|---|---|---|---|---|---|
| VAL | neg | neg | neu | neu | neg | neg | neu | neu |
| PRED | pred | unpr | pred | unpr | pred | unpr | pred | unpr |
| *M* | -9.73 | 12.83 | -1.65 | 14.72 | -35.32 | -30.72 | -30.12 | -25.61 | -9.73 |
| *SD* | 48.80 | 60.01 | 40.79 | 46.69 | 40.31 | 43.48 | 29.29 | 38.97 | 48.80 |
| *SEM* | 8.25 | 10.14 | 6.89 | 7.89 | 6.81 | 7.35 | 4.95 | 6.59 | 8.25 |
| *Var* | 2381.64 | 3601.10 | 1663.52 | 2179.83 | 1624.72 | 1890.60 | 857.97 | 1518.44 | 2381.64 |
| *CI95%* | 15.80 | 15.80 | 15.80 | 15.80 | 15.80 | 15.80 | 15.80 | 15.80 | 15.80 |
| *Skew* | -0.506 | -0.463 | 0.339 | 1.358 | -0.520 | -0.267 | 0.890 | -0.791 | -0.506 |
| *zSkew* | -1.222 | -1.119 | 0.819 | 3.280 | -1.256 | -0.646 | 2.151 | -1.910 | -1.222 |

*Note.* Modality (MOD: pictures (pics), electrical stimulation (zaps)), valence (VAL: negative (neg), neutral (neu)), and predictability (PRED: predictable (pred), unpredictable (unpr)). *M* = Mean, *SD* = standard deviation, *SEM* = standard error *Var* = variance, *CI95%* = 95% confidence interval, *Skew* = skewness, and *zSkew* = z-score of the skew. *N* = 35.

**Table 7.33**

*Repeated Measures ANOVA for Average BOLD response in the Superior Frontal Gyrus with Factors Stimulus Modality, Valence, and Predictability for Transient Responses*

|  | df | F | p | SS | MSE |
|---|---|---|---|---|---|
| MOD | 1,34 | 45.8 | <0.000001 | 83234.07 | 1817.42 |
| VAL | 1,34 | 0.728 | <0.399395 | 1797.23 | 2467.58 |
| PRED | 1,34 | 5.10 | <0.030391 | 10091.44 | 1977.05 |
| MOD*VAL | 1,34 | 0.001 | <0.987643 | 0.51 | 2080.84 |
| MOD*PRED | 1,34 | 1.36 | <0.251293 | 3887.27 | 2853.86 |
| VAL*PRED | 1,34 | 0.075 | <0.785342 | 172.78 | 2292.56 |
| MOD*VAL*PRED | 1,34 | 0.073 | <0.788441 | 163.01 | 2228.53 |

*Note.* Modality (MOD: pictures, electrical stimulation), valence (VAL: negative, neutral), and predictability (PRED: predictable, unpredictable). *Df* = degrees of freedom, *F* = F-statistic, *p* = p-value, *SS* = sum of squares, and *MSE* = mean squared error. *N* = 35.

**Table 7.34**

*Correlations Between Questionnaires and Transient Responses within Right Amygdala across Stimulus Modalities*

| Variable | | ASI | IUS | PANAS-PA | PANAS-NA | STAI-S | NegPred | NegUnpr | NeuPred | NeuUnpr |
|---|---|---|---|---|---|---|---|---|---|---|
| ASI | r | 1 | | | | | | | | |
| | p | | | | | | | | | |
| | N | 35 | | | | | | | | |
| IUS | r | .590** | 1 | | | | | | | |
| | p | 0.000 | | | | | | | | |
| | N | 35 | 35 | | | | | | | |
| PANAS-PA | r | -0.020 | -0.017 | 1 | | | | | | |
| | p | 0.907 | 0.925 | | | | | | | |
| | N | 35 | 35 | 35 | | | | | | |
| PANAS-NA | r | .519** | 0.251 | -0.045 | 1 | | | | | |
| | p | 0.001 | 0.145 | 0.797 | | | | | | |
| | N | 35 | 35 | 35 | 35 | | | | | |
| STAI-S | r | .521** | .428* | -0.005 | .627** | 1 | | | | |
| | p | 0.001 | 0.010 | 0.978 | 0.000 | | | | | |
| | N | 35 | 35 | 35 | 35 | 35 | | | | |
| NegPred | r | -0.235 | -0.263 | -0.062 | -0.153 | -0.261 | 1 | | | |
| | p | 0.174 | 0.127 | 0.725 | 0.379 | 0.129 | | | | |
| | N | 35 | 35 | 35 | 35 | 35 | 35 | | | |
| NegUnpr | r | -0.048 | -0.087 | -0.108 | -0.200 | -0.207 | 0.329 | 1 | | |
| | p | 0.785 | 0.620 | 0.537 | 0.248 | 0.233 | 0.053 | | | |
| | N | 35 | 35 | 35 | 35 | 35 | 35 | 35 | | |
| NeuPred | r | -0.079 | 0.076 | 0.009 | -0.298 | -0.297 | .351* | 0.244 | 1 | |
| | p | 0.651 | 0.666 | 0.958 | 0.082 | 0.083 | 0.039 | 0.159 | | |
| | N | 35 | 35 | 35 | 35 | 35 | 35 | 35 | 35 | |
| NeuUnpr | r | -0.146 | -0.311 | -0.205 | -0.114 | -0.182 | 0.311 | 0.282 | .420* | 1 |
| | p | 0.404 | 0.069 | 0.237 | 0.515 | 0.295 | 0.069 | 0.101 | 0.012 | |
| | N | 35 | 35 | 35 | 35 | 35 | 35 | 35 | 35 | 35 |

*Note.* Questionnaires (ASI: Anxiety Sensitivity Index, IUS: Intolerance to Uncertainty Scale, PANAS-PA: Positive Affect Schedule, PANAS-NA: Negative Affect Schedule, and STAI-S: State Anxiety Inventory (pre and post). Modality (zaps and pics), Valence (negative (neg), neutral (neu)), and predictability (predictable (pred), unpredictable(unpr)). *R* = correlation coefficient (Pearson), *p* = *p*-value, and *N* = number of subjects. Significance level: *** = $p < .001$, ** = $p < .01$, and * = $p < .05$.

**Table 7.35**

*Correlations Between Questionnaires and Transient Responses within Right Amygdala for Picture Stimulus Blocks*

| Variable | | ASI | IUS | PANAS-PA | PANAS-NA | STAI-S | PicsNegPred | PicsNegUnpr | PicsNeuPred | PicsNeuUnpr |
|---|---|---|---|---|---|---|---|---|---|---|
| | | | | | **Pearson Correlations** | | | | | |
| ASI | r | 1 | | | | | | | | |
| | p | | | | | | | | | |
| | N | 35 | | | | | | | | |
| IUS | r | .590** | 1 | | | | | | | |
| | p | 0.000 | | | | | | | | |
| | N | 35 | 35 | | | | | | | |
| PANAS-PA | r | -0.020 | -0.017 | 1 | | | | | | |
| | p | 0.907 | 0.925 | | | | | | | |
| | N | 35 | 35 | 35 | | | | | | |
| PANAS-NA | r | .519** | 0.251 | -0.045 | 1 | | | | | |
| | p | 0.001 | 0.145 | 0.797 | | | | | | |
| | N | 35 | 35 | 35 | 35 | | | | | |
| STAI-S | r | .521** | .428* | -0.005 | .627** | 1 | | | | |
| | p | 0.001 | 0.010 | 0.978 | 0.000 | | | | | |
| | N | 35 | 35 | 35 | 35 | 35 | | | | |
| PicsNegPred | r | -0.275 | -0.252 | -0.050 | -0.218 | -0.320 | 1 | | | |
| | p | 0.109 | 0.144 | 0.777 | 0.209 | 0.061 | | | | |
| | N | 35 | 35 | 35 | 35 | 35 | 35 | | | |
| PicsNegUnpr | r | -0.132 | -0.003 | -0.186 | -0.067 | -0.165 | 0.243 | 1 | | |
| | p | 0.450 | 0.984 | 0.284 | 0.702 | 0.345 | 0.160 | | | |
| | N | 35 | 35 | 35 | 35 | 35 | 35 | 35 | | |
| PicsNeuPred | r | -0.152 | -0.001 | -0.045 | -0.299 | -0.258 | 0.080 | .456** | 1 | |
| | p | 0.383 | 0.996 | 0.797 | 0.081 | 0.135 | 0.649 | 0.006 | | |
| | N | 35 | 35 | 35 | 35 | 35 | 35 | 35 | 35 | |
| PicsNeuUnpr | r | -0.184 | -0.290 | -0.253 | -0.095 | -0.163 | -0.058 | .486** | .441** | 1 |
| | p | 0.291 | 0.092 | 0.143 | 0.587 | 0.349 | 0.739 | 0.003 | 0.008 | |
| | N | 35 | 35 | 35 | 35 | 35 | 35 | 35 | 35 | 35 |

*Note.* Questionnaires (ASI: Anxiety Sensitivity Index, IUS: Intolerance to Uncertainty Scale, PANAS-PA: Positive Affect Schedule, PANAS-NA: Negative Affect Schedule, and STAI-S: State Anxiety Inventory (pre and post). Modality (pictures(pics)), Valence (negative (neg), neutral (neu)), and predictability (predictable (pred), unpredictable(unpr)). *R* = correlation coefficient (Pearson), *p* = *p*-value, and *N* = number of subjects. Significance level: *** = *p* < .001, ** = *p* < .01, and * = *p* < .05.

**Table 7.36**

*Correlations Between Questionnaires and Transient Responses within Right Amygdala for Electrical Stimulation Blocks*

| Variable | | ASI | IUS | PANAS-PA | PANAS-NA | STAI-S | ZapsNegPred | ZapsNegUnpr | ZapsNeuPred | ZapsNeuUnpr |
|---|---|---|---|---|---|---|---|---|---|---|
| | | | | | | Pearson Correlations | | | | |
| ASI | r | 1 | | | | | | | | |
| | p | | | | | | | | | |
| | N | 35 | | | | | | | | |
| IUS | r | .590** | 1 | | | | | | | |
| | p | 0.000 | | | | | | | | |
| | N | 35 | 35 | | | | | | | |
| PANAS-PA | r | -0.020 | -0.017 | 1 | | | | | | |
| | p | 0.907 | 0.925 | | | | | | | |
| | N | 35 | 35 | 35 | | | | | | |
| PANAS-NA | r | .519** | 0.251 | -0.045 | 1 | | | | | |
| | p | 0.001 | 0.145 | 0.797 | | | | | | |
| | N | 35 | 35 | 35 | 35 | | | | | |
| STAI-S | r | .521** | .428* | -0.005 | .627** | 1 | | | | |
| | p | 0.001 | 0.010 | 0.978 | 0.000 | | | | | |
| | N | 35 | 35 | 35 | 35 | 35 | | | | |
| ZapsNegPred | r | -0.146 | -0.197 | -0.052 | -0.072 | -0.154 | 1 | | | |
| | p | 0.403 | 0.257 | 0.767 | 0.682 | 0.378 | | | | |
| | N | 35 | 35 | 35 | 35 | 35 | 35 | | | |
| ZapsNegUnpr | r | 0.061 | -0.129 | 0.025 | -0.238 | -0.149 | 0.048 | 1 | | |
| | p | 0.726 | 0.460 | 0.887 | 0.168 | 0.394 | 0.786 | | | |
| | N | 35 | 35 | 35 | 35 | 35 | 35 | 35 | | |
| ZapsNeuPred | r | 0.055 | 0.127 | 0.071 | -0.128 | -0.179 | .462** | -0.011 | 1 | |
| | p | 0.753 | 0.467 | 0.686 | 0.462 | 0.304 | 0.005 | 0.950 | | |
| | N | 35 | 35 | 35 | 35 | 35 | 35 | 35 | 35 | |
| ZapsNeuUnpr | r | 0.021 | -0.096 | 0.022 | -0.050 | -0.065 | 0.207 | 0.133 | .435** | 1 |
| | p | 0.904 | 0.584 | 0.901 | 0.776 | 0.711 | 0.234 | 0.445 | 0.009 | |
| | N | 35 | 35 | 35 | 35 | 35 | 35 | 35 | 35 | 35 |

*Note.* Questionnaires (ASI: Anxiety Sensitivity Index, IUS: Intolerance to Uncertainty Scale, PANAS-PA: Positive Affect Schedule, PANAS-NA: Negative Affect Schedule, and STAI-S: State Anxiety Inventory (pre and post). Modality (electrical stimulation (zaps)), Valence (negative (neg), neutral (neu)), and predictability (predictable (pred), unpredictable(unpr)). *R* = correlation coefficient (Pearson), *p* = *p*-value, and *N* = number of subjects. Significance level: *** = $p < .001$, ** = $p < .01$, and * = $p < .05$.

**Table 7.37**

*Correlations Between Questionnaires and Transient Responses within Left Amygdala across Stimulus Modalities*

| Variable | | ASI | IUS | PANAS-PA | PANAS-NA | STAI-S | NegPred | NegUnpr | NeuPred | NeuUnpr |
|---|---|---|---|---|---|---|---|---|---|---|
| | | | | | **Pearson Correlations** | | | | | |
| ASI | r | 1 | | | | | | | | |
| | p | | | | | | | | | |
| | N | 35 | | | | | | | | |
| IUS | r | .590** | 1 | | | | | | | |
| | p | 0.000 | | | | | | | | |
| | N | 35 | 35 | | | | | | | |
| PANAS-PA | r | -0.020 | -0.017 | 1 | | | | | | |
| | p | 0.907 | 0.925 | | | | | | | |
| | N | 35 | 35 | 35 | | | | | | |
| PANAS-NA | r | .519** | 0.251 | -0.045 | 1 | | | | | |
| | p | 0.001 | 0.145 | 0.797 | | | | | | |
| | N | 35 | 35 | 35 | 35 | | | | | |
| STAI-S | r | .521** | .428* | -0.005 | .627** | 1 | | | | |
| | p | 0.001 | 0.010 | 0.978 | 0.000 | | | | | |
| | N | 35 | 35 | 35 | 35 | 35 | | | | |
| NegPred | r | -0.203 | -0.206 | 0.067 | 0.061 | 0.005 | 1 | | | |
| | p | 0.243 | 0.236 | 0.703 | 0.726 | 0.977 | | | | |
| | N | 35 | 35 | 35 | 35 | 35 | 35 | | | |
| NegUnpr | r | -0.306 | -0.094 | 0.049 | **-.409*** | -0.313 | -0.042 | 1 | | |
| | p | 0.073 | 0.591 | 0.780 | 0.015 | 0.068 | 0.810 | | | |
| | N | 35 | 35 | 35 | 35 | 35 | 35 | 35 | | |
| NeuPred | r | -0.186 | 0.039 | -0.150 | -0.141 | -0.307 | .542** | 0.324 | 1 | |
| | p | 0.284 | 0.822 | 0.389 | 0.418 | 0.073 | 0.001 | 0.058 | | |
| | N | 35 | 35 | 35 | 35 | 35 | 35 | 35 | 35 | |
| NeuUnpr | r | -0.269 | -0.274 | -0.233 | 0.028 | -0.142 | 0.068 | 0.291 | 0.288 | 1 |
| | p | 0.118 | 0.111 | 0.178 | 0.874 | 0.415 | 0.697 | 0.090 | 0.094 | |
| | N | 35 | 35 | 35 | 35 | 35 | 35 | 35 | 35 | 35 |

*Note.* Questionnaires (ASI: Anxiety Sensitivity Index, IUS: Intolerance to Uncertainty Scale, PANAS-PA: Positive Affect Schedule, PANAS-NA: Negative Affect Schedule, and STAI-S: State Anxiety Inventory (pre and post). Modality (zaps and pics), Valence (negative (neg), neutral (neu)), and predictability (predictable (pred), unpredictable(unpr)). *R* = correlation coefficient (Pearson), *p* = *p*-value, and *N* = number of subjects. Significance level: *** = $p < .001$, ** = $p < .01$, and * = $p < .05$.

**Table 7.38**

*Correlations Between Questionnaires and Transient Responses within Left Amygdala for Picture Stimulus Modality*

| Variable | | ASI | IUS | PANAS-PA | PANAS-NA | STAI-S | PicsNegPred | PicsNegUnpr | PicsNeuPred | PicsNeuUnpr |
|---|---|---|---|---|---|---|---|---|---|---|
| | | | | | **Pearson Correlations** | | | | | |
| ASI | r | 1 | | | | | | | | |
| | p | | | | | | | | | |
| | N | 35 | | | | | | | | |
| IUS | r | .590** | 1 | | | | | | | |
| | p | 0.000 | | | | | | | | |
| | N | 35 | 35 | | | | | | | |
| PANAS-PA | r | -0.020 | -0.017 | 1 | | | | | | |
| | p | 0.907 | 0.925 | | | | | | | |
| | N | 35 | 35 | 35 | | | | | | |
| PANAS-NA | r | .519** | 0.251 | -0.045 | 1 | | | | | |
| | p | 0.001 | 0.145 | 0.797 | | | | | | |
| | N | 35 | 35 | 35 | 35 | | | | | |
| STAI-S | r | .521** | .428* | -0.005 | .627** | 1 | | | | |
| | p | 0.001 | 0.010 | 0.978 | 0.000 | | | | | |
| | N | 35 | 35 | 35 | 35 | 35 | | | | |
| PicsNegPred | r | 0.065 | -0.027 | 0.059 | .367* | 0.128 | 1 | | | |
| | p | 0.710 | 0.877 | 0.735 | 0.030 | 0.464 | | | | |
| | N | 35 | 35 | 35 | 35 | 35 | 35 | | | |
| PicsNegUnpr | r | -0.308 | 0.025 | -0.157 | -.334* | -0.288 | 0.063 | 1 | | |
| | p | 0.072 | 0.885 | 0.368 | 0.050 | 0.093 | 0.721 | | | |
| | N | 35 | 35 | 35 | 35 | 35 | 35 | 35 | | |
| PicsNeuPred | r | -0.178 | -0.032 | -0.238 | -0.092 | -0.239 | .359* | .520** | 1 | |
| | p | 0.305 | 0.853 | 0.169 | 0.601 | 0.166 | 0.034 | 0.001 | | |
| | N | 35 | 35 | 35 | 35 | 35 | 35 | 35 | 35 | |
| PicsNeuUnpr | r | -0.197 | -0.297 | -0.190 | 0.069 | -0.111 | 0.184 | 0.261 | .482** | 1 |
| | p | 0.257 | 0.083 | 0.275 | 0.696 | 0.524 | 0.290 | 0.131 | 0.003 | |
| | N | 35 | 35 | 35 | 35 | 35 | 35 | 35 | 35 | 35 |

*Note.* Questionnaires (ASI: Anxiety Sensitivity Index, IUS: Intolerance to Uncertainty Scale, PANAS-PA: Positive Affect Schedule, PANAS-NA: Negative Affect Schedule, and STAI-S: State Anxiety Inventory (pre and post). Modality (pictures(pics)), Valence (negative (neg), neutral (neu)), and predictability (predictable (pred), unpredictable(unpr)). *R* = correlation coefficient (Pearson), *p* = *p*-value, and *N* = number of subjects. Significance level: *** = $p < .001$, ** = $p < .01$, and * = $p < .05$.

**Table 7.39**

*Correlations Between Questionnaires and transient responses within Left Amygdala for Electrical Stimulation Blocks*

| Variable | | ASI | IUS | PANAS-PA | PANAS-NA | STAI-S | ZapsNegPred | ZapsNegUnpr | ZapsNeuPred | ZapsNeuUnpr |
|---|---|---|---|---|---|---|---|---|---|---|
| | | | | | **Pearson Correlations** | | | | | |
| ASI | r | 1 | | | | | | | | |
| | p | | | | | | | | | |
| | N | 35 | | | | | | | | |
| IUS | r | .590** | 1 | | | | | | | |
| | p | 0.000 | | | | | | | | |
| | N | 35 | 35 | | | | | | | |
| PANAS-PA | r | -0.020 | -0.017 | 1 | | | | | | |
| | p | 0.907 | 0.925 | | | | | | | |
| | N | 35 | 35 | 35 | | | | | | |
| PANAS-NA | r | .519** | 0.251 | -0.045 | 1 | | | | | |
| | p | 0.001 | 0.145 | 0.797 | | | | | | |
| | N | 35 | 35 | 35 | 35 | | | | | |
| STAI-S | r | .521** | .428* | -0.005 | .627** | 1 | | | | |
| | p | 0.001 | 0.010 | 0.978 | 0.000 | | | | | |
| | N | 35 | 35 | 35 | 35 | 35 | | | | |
| ZapsNegPred | r | -.346* | -0.273 | 0.047 | -0.219 | -0.100 | 1 | | | |
| | p | 0.042 | 0.112 | 0.791 | 0.207 | 0.569 | | | | |
| | N | 35 | 35 | 35 | 35 | 35 | 35 | | | |
| ZapsNegUnpr | r | -0.125 | -0.187 | 0.275 | -0.262 | -0.160 | -0.312 | 1 | | |
| | p | 0.474 | 0.283 | 0.110 | 0.129 | 0.360 | 0.068 | | | |
| | N | 35 | 35 | 35 | 35 | 35 | 35 | 35 | | |
| ZapsNeuPred | r | -0.104 | 0.103 | 0.023 | -0.130 | -0.235 | .389* | -0.180 | 1 | |
| | p | 0.550 | 0.557 | 0.895 | 0.456 | 0.173 | 0.021 | 0.300 | | |
| | N | 35 | 35 | 35 | 35 | 35 | 35 | 35 | 35 | |
| ZapsNeuUnpr | r | -0.169 | -0.046 | -0.121 | -0.045 | -0.080 | -0.066 | 0.270 | -0.161 | 1 |
| | p | 0.331 | 0.791 | 0.487 | 0.797 | 0.648 | 0.708 | 0.117 | 0.355 | |
| | N | 35 | 35 | 35 | 35 | 35 | 35 | 35 | 35 | 35 |

*Note.* Questionnaires (ASI: Anxiety Sensitivity Index, IUS: Intolerance to Uncertainty Scale, PANAS-PA: Positive Affect Schedule, PANAS-NA: Negative Affect Schedule, and STAI-S: State Anxiety Inventory (pre and post). Modality (Electrical stimulation (zaps)), Valence (negative (neg), neutral (neu)), and predictability (predictable (pred), unpredictable(unpr)). *R* = correlation coefficient (Pearson), *p* = *p*-value, and *N* = number of subjects. Significance level: *** = *p* < .001, ** = *p* < .01, and * = *p* < .05.

**Table 7.40**

*Descriptive Statistics of the Average BOLD Response in the Right Amygdala as a Function of Stimulus Modality for Sustained Responses*

| | MOD | pics | pics | pics | pics | zaps | zaps | zaps | zaps |
|---|---|---|---|---|---|---|---|---|---|
| | VAL | neg | neg | neu | neu | neg | neg | neu | neu |
| | PRED | pred | unpr | pred | unpr | pred | unpr | pred | unpr |
| *M* | | -0.50 | -1.50 | -1.66 | -0.38 | 4.84 | 3.53 | 3.37 | 2.03 |
| *SD* | | 7.71 | 7.28 | 6.09 | 6.91 | 7.48 | 8.64 | 7.35 | 7.84 |
| *SEM* | | 1.30 | 1.23 | 1.03 | 1.17 | 1.26 | 1.46 | 1.24 | 1.32 |
| *Var* | | 59.45 | 52.99 | 37.06 | 47.71 | 55.88 | 74.69 | 54.05 | 61.40 |
| *CI95%* | | 2.65 | 2.65 | 2.65 | 2.65 | 2.65 | 2.65 | 2.65 | 2.65 |
| *Skew* | | 0.268 | -0.206 | -0.926 | 0.104 | 0.068 | -0.167 | 0.396 | 0.819 |
| *zSkew* | | 0.647 | -0.498 | -2.237 | 0.251 | 0.164 | -0.404 | 0.957 | 1.979 |

*Note.* Modality (MOD: pictures (pics), electrical stimulation (zaps)), valence (VAL: negative (neg), neutral (neu)), and predictability (PRED: predictable (pred), unpredictable (unpr)). *M* = Mean, *SD* = standard deviation, *SEM* = standard error *Var* = variance, *CI95%* = 95% confidence interval, *Skew* = skewness, and *zSkew* = z-score of the skew. *N* = 35.

**Table 7.41**

*Repeated Measures ANOVA for Average BOLD response in the Right Amygdala with Factors Stimulus Modality, Valence, and Predictability for Sustained Responses*

| | *df* | *F* | *p* | *SS* | *MSE* |
|---|---|---|---|---|---|
| MOD | 1,34 | 19.4 | <0.000102 | 1387.30 | 71.68 |
| VAL | 1,34 | 1.00 | <0.323544 | 39.94 | 39.81 |
| PRED | 1,34 | 0.429 | <0.516933 | 24.64 | 57.45 |
| MOD*VAL | 1,34 | 0.539 | <0.467715 | 37.67 | 69.84 |
| MOD*PRED | 1,34 | 0.617 | <0.437508 | 37.56 | 60.85 |
| VAL*PRED | 1,34 | 0.407 | <0.527893 | 22.12 | 54.39 |
| MOD*VAL*PRED | 1,34 | 0.260 | <0.613500 | 23.18 | 89.21 |

*Note.* Modality (MOD: pictures, electrical stimulation), valence (VAL: negative, neutral), and predictability (PRED: predictable, unpredictable). *Df* = degrees of freedom, *F* = F-statistic, *p* = p-value, *SS* = sum of squares, and *MSE* = mean squared error. *N* = 35.

**Table 7.42**

*Descriptive Statistics of the Average BOLD Response in the Left Thalamus as a Function of Stimulus Modality for Sustained Responses*

| | MOD | pics | pics | pics | pics | zaps | zaps | zaps | zaps |
|---|---|---|---|---|---|---|---|---|---|
| | VAL | neg | neg | neu | neu | neg | neg | neu | neu |
| | PRED | pred | unpr | pred | unpr | pred | unpr | pred | unpr |
| *M* | | 4.09 | 1.82 | 2.75 | 0.11 | -0.26 | -2.48 | -2.52 | -2.22 |
| *SD* | | 8.56 | 7.52 | 6.85 | 6.08 | 7.58 | 5.62 | 6.90 | 7.66 |
| *SEM* | | 1.45 | 1.27 | 1.16 | 1.03 | 1.28 | 0.95 | 1.17 | 1.29 |
| *Var* | | 73.25 | 56.54 | 46.87 | 37.01 | 57.52 | 31.56 | 47.58 | 58.66 |
| *CI95%* | | 2.55 | 2.55 | 2.55 | 2.55 | 2.55 | 2.55 | 2.55 | 2.55 |
| *Skew* | | 0.299 | -0.710 | -1.279 | -0.075 | 0.865 | 0.313 | 0.267 | -0.576 |
| *zSkew* | | 0.723 | -1.714 | -3.089 | -0.180 | 2.088 | 0.756 | 0.646 | -1.392 |

*Note.* Modality (MOD: pictures (pics), electrical stimulation (zaps)), valence (VAL: negative (neg), neutral (neu)), and predictability (PRED: predictable (pred), unpredictable (unpr)). *M* = Mean, *SD* = standard deviation, *SEM* = standard error *Var* = variance, *CI95%* = 95% confidence interval, *Skew* = skewness, and *zSkew* = *z*-score of the skew. *N* = 35.

**Table 7.43**

*Repeated Measures ANOVA for Average BOLD response in the Left Thalamus with Factors Stimulus Modality, Valence, and Predictability for Sustained Responses*

| | *df* | *F* | *p* | *SS* | *MSE* |
|---|---|---|---|---|---|
| MOD | 1,34 | 13.0 | <0.000975 | 1156.61 | 88.76 |
| VAL | 1,34 | 1.79 | <0.190125 | 111.49 | 62.37 |
| PRED | 1,34 | 4.59 | <0.039304 | 203.59 | 44.31 |
| MOD*VAL | 1,34 | 0.113 | <0.738448 | 4.78 | 42.19 |
| MOD*PRED | 1,34 | 0.674 | <0.417425 | 39.35 | 58.39 |
| VAL*PRED | 1,34 | 0.363 | <0.550711 | 19.99 | 55.04 |
| MOD*VAL*PRED | 1,34 | 0.629 | <0.433376 | 36.41 | 57.92 |

*Note.* Modality (MOD: pictures, electrical stimulation), valence (VAL: negative, neutral), and predictability (PRED: predictable, unpredictable). *Df* = degrees of freedom, *F* = F-statistic, *p* = p-value, *SS* = sum of squares, and *MSE* = mean squared error. *N* = 35.

**Table 7.44**

*Descriptive Statistics of the Average BOLD Response in the Right Thalamus as a Function of Stimulus Modality for Sustained Responses*

| | MOD | pics | pics | pics | pics | zaps | zaps | zaps | zaps |
|---|---|---|---|---|---|---|---|---|---|
| | VAL | neg | neg | neu | neu | neg | neg | neu | neu |
| | PRED | pred | unpr | pred | unpr | pred | unpr | pred | unpr |
| *M* | | 2.73 | 1.99 | 3.17 | 2.10 | -0.49 | -2.57 | -1.00 | -1.77 |
| *SD* | | 6.51 | 6.43 | 5.42 | 5.34 | 7.34 | 5.82 | 6.31 | 6.38 |
| *SEM* | | 1.10 | 1.09 | 0.92 | 0.90 | 1.24 | 0.98 | 1.07 | 1.08 |
| *Var* | | 42.44 | 41.35 | 29.32 | 28.49 | 53.81 | 33.93 | 39.78 | 40.68 |
| *CI95%* | | 2.22 | 2.22 | 2.22 | 2.22 | 2.22 | 2.22 | 2.22 | 2.22 |
| *Skew* | | -0.541 | -0.229 | -0.285 | -0.188 | 0.901 | -0.125 | 0.558 | 0.142 |
| *zSkew* | | -1.306 | -0.554 | -0.688 | -0.455 | 2.176 | -0.301 | 1.348 | 0.343 |

*Note.* Modality (MOD: pictures (pics), electrical stimulation (zaps)), valence (VAL: negative (neg), neutral (neu)), and predictability (PRED: predictable (pred), unpredictable (unpr)). *M* = Mean, *SD* = standard deviation, *SEM* = standard error *Var* = variance, *CI95%* = 95% confidence interval, *Skew* = skewness, and *zSkew* = *z*-score of the skew. *N* = 35.

**Table 7.45**

*Repeated Measures ANOVA for Average BOLD response in the Left Thalamus with Factors Stimulus Modality, Valence, and Predictability for Sustained Responses*

| | *df* | *F* | *p* | *SS* | *MSE* |
|---|---|---|---|---|---|
| MOD | 1,34 | 21.9 | <0.000044 | 1095.82 | 49.95 |
| VAL | 1,34 | 0.067 | <0.796739 | 3.05 | 45.27 |
| PRED | 1,34 | 1.61 | <0.213780 | 94.46 | 58.85 |
| MOD*VAL | 1,34 | 0.012 | <0.912140 | 0.30 | 24.32 |
| MOD*PRED | 1,34 | 0.084 | <0.774226 | 4.76 | 56.93 |
| VAL*PRED | 1,34 | 0.118 | <0.732953 | 4.31 | 36.38 |
| MOD*VAL*PRED | 1,34 | 0.308 | <0.582494 | 11.74 | 38.11 |

*Note.* Modality (MOD: pictures, electrical stimulation), valence (VAL: negative, neutral), and predictability (PRED: predictable, unpredictable). *Df* = degrees of freedom, *F* = F-statistic, *p* = p-value, *SS* = sum of squares, and *MSE* = mean squared error. *N* = 35.

**Table 7.46**

*Descriptive Statistics of the Average BOLD Response in the Left Hippocampus as a Function of Stimulus Modality for Sustained Responses*

| | MOD | pics | pics | pics | pics | zaps | zaps | zaps | zaps |
|---|---|---|---|---|---|---|---|---|---|
| | VAL | neg | neg | neu | neu | neg | neg | neu | neu |
| | PRED | pred | unpr | pred | unpr | pred | unpr | pred | unpr |
| *M* | | 2.26 | -1.09 | 3.17 | 0.06 | -5.62 | -7.35 | -7.03 | -5.24 |
| *SD* | | 11.48 | 8.39 | 7.56 | 8.08 | 9.30 | 8.14 | 6.83 | 8.85 |
| *SEM* | | 1.94 | 1.42 | 1.28 | 1.37 | 1.57 | 1.38 | 1.15 | 1.50 |
| *Var* | | 131.68 | 70.33 | 57.12 | 65.27 | 86.42 | 66.26 | 46.63 | 78.30 |
| *CI95%* | | 3.09 | 3.09 | 3.09 | 3.09 | 3.09 | 3.09 | 3.09 | 3.09 |
| *Skew* | | -0.793 | -0.900 | -0.254 | 0.513 | 0.523 | -0.037 | 0.612 | 0.670 |
| *zSkew* | | -1.915 | -2.174 | -0.613 | 1.240 | 1.263 | -0.090 | 1.478 | 1.618 |

*Note.* Modality (MOD: pictures (pics), electrical stimulation (zaps)), valence (VAL: negative (neg), neutral (neu)), and predictability (PRED: predictable (pred), unpredictable (unpr)). *M* = Mean, *SD* = standard deviation, *SEM* = standard error *Var* = variance, *CI95%* = 95% confidence interval, *Skew* = skewness, and *zSkew* = z-score of the skew. *N* = 35.

**Table 7.47**

*Repeated Measures ANOVA for Average BOLD response in the Left Hippocampus with Factors Stimulus Modality, Valence, and Predictability for Sustained Responses*

| | *df* | *F* | *p* | *SS* | *MSE* |
|---|---|---|---|---|---|
| MOD | 1,34 | 24.5 | <0.000020 | 3840.34 | 157.04 |
| VAL | 1,34 | 0.406 | <0.528145 | 33.56 | 82.60 |
| PRED | 1,34 | 2.14 | <0.152791 | 179.34 | 83.85 |
| MOD*VAL | 1,34 | 0.172 | <0.681016 | 8.14 | 47.32 |
| MOD*PRED | 1,34 | 2.23 | <0.144925 | 186.40 | 83.74 |
| VAL*PRED | 1,34 | 1.18 | <0.285484 | 61.50 | 52.22 |
| MOD*VAL*PRED | 1,34 | 0.492 | <0.487858 | 46.84 | 95.23 |

*Note.* Modality (MOD: pictures, electrical stimulation), valence (VAL: negative, neutral), and predictability (PRED: predictable, unpredictable). *Df* = degrees of freedom, *F* = F-statistic, *p* = p-value, *SS* = sum of squares, and *MSE* = mean squared error. *N* = 35.

**Table 7.48**

*Descriptive Statistics of the Average BOLD Response in the Right Hippocampus as a Function of Stimulus Modality for Sustained Responses*

| | MOD | pics | pics | pics | pics | zaps | zaps | zaps | zaps |
|---|---|---|---|---|---|---|---|---|---|
| | VAL | neg | neg | neu | neu | neg | neg | neu | neu |
| | PRED | pred | unpr | pred | unpr | pred | unpr | pred | unpr |
| *M* | | 1.93 | -1.31 | 3.40 | -0.11 | -4.90 | -8.68 | -6.00 | -7.00 |
| *SD* | | 11.48 | 7.78 | 6.90 | 8.75 | 9.75 | 9.54 | 7.46 | 8.41 |
| *SEM* | | 1.94 | 1.32 | 1.17 | 1.48 | 1.65 | 1.61 | 1.26 | 1.42 |
| *Var* | | 131.86 | 60.60 | 47.65 | 76.60 | 94.98 | 91.01 | 55.67 | 70.80 |
| *CI95%* | | 3.16 | 3.16 | 3.16 | 3.16 | 3.16 | 3.16 | 3.16 | 3.16 |
| *Skew* | | -0.292 | -0.423 | -0.823 | -0.166 | 1.651 | -0.528 | -0.323 | 2.217 |
| *zSkew* | | -0.706 | -1.021 | -1.989 | -0.401 | 3.987 | -1.276 | -0.781 | 5.354 |

*Note.* Modality (MOD: pictures (pics), electrical stimulation (zaps)), valence (VAL: negative (neg), neutral (neu)), and predictability (PRED: predictable (pred), unpredictable (unpr)). *M* = Mean, *SD* = standard deviation, *SEM* = standard error *Var* = variance, *CI95%* = 95% confidence interval, *Skew* = skewness, and *zSkew* = *z*-score of the skew. *N* = 35.

**Table 7.49**

*Repeated Measures ANOVA for Average BOLD response in the Right Hippocampus with Factors Stimulus Modality, Valence, and Predictability for Sustained Responses*

| | df | F | p | SS | MSE |
|---|---|---|---|---|---|
| MOD | 1,34 | 26.7 | <0.000011 | 4063.18 | 152.42 |
| VAL | 1,34 | 0.843 | <0.364986 | 46.34 | 54.96 |
| PRED | 1,34 | 6.27 | <0.017223 | 581.32 | 92.68 |
| MOD*VAL | 1,34 | 0.370 | <0.546857 | 18.90 | 51.03 |
| MOD*PRED | 1,34 | 0.170 | <0.682736 | 17.14 | 100.87 |
| VAL*PRED | 1,34 | 0.333 | <0.567970 | 27.63 | 83.10 |
| MOD*VAL*PRED | 1,34 | 0.427 | <0.517629 | 40.22 | 94.10 |

*Note.* Modality (MOD: pictures, electrical stimulation), valence (VAL: negative, neutral), and predictability (PRED: predictable, unpredictable). *Df* = degrees of freedom, *F* = F-statistic, *p* = p-value, *SS* = sum of squares, and *MSE* = mean squared error. *N* = 35.

**Table 7.50**

*Descriptive Statistics of the Average BOLD Response in the Parahippocampal Gyrus as a Function of Stimulus Modality for Sustained Responses*

| | MOD | pics | pics | pics | pics | zaps | zaps | zaps | zaps |
|---|---|---|---|---|---|---|---|---|---|
| | VAL | neg | neg | neu | neu | neg | neg | neu | neu |
| | PRED | pred | unpr | pred | unpr | pred | unpr | pred | unpr |
| *M* | | 2.36 | -1.89 | 3.76 | -0.66 | -5.65 | -5.62 | -7.45 | -4.34 |
| *SD* | | 9.82 | 9.13 | 9.57 | 9.94 | 10.02 | 7.77 | 7.57 | 8.04 |
| *SEM* | | 1.66 | 1.54 | 1.62 | 1.68 | 1.69 | 1.31 | 1.28 | 1.36 |
| *Var* | | 96.48 | 83.35 | 91.50 | 98.83 | 100.31 | 60.43 | 57.32 | 64.70 |
| *CI95%* | | 3.22 | 3.22 | 3.22 | 3.22 | 3.22 | 3.22 | 3.22 | 3.22 |
| *Skew* | | 0.588 | -0.910 | 0.547 | 0.118 | -0.417 | -0.330 | -0.029 | 0.191 |
| *zSkew* | | 1.420 | -2.197 | 1.320 | 0.285 | -1.007 | -0.797 | -0.070 | 0.462 |

*Note.* Modality (MOD: pictures (pics), electrical stimulation (zaps)), valence (VAL: negative (neg), neutral (neu)), and predictability (PRED: predictable (pred), unpredictable (unpr)). *M* = Mean, *SD* = standard deviation, *SEM* = standard error *Var* = variance, *CI95%* = 95% confidence interval, *Skew* = skewness, and *zSkew* = *z*-score of the skew. *N* = 35.


**Table 7.51**

*Repeated Measures ANOVA for Average BOLD response in the Parahippocampal Gyrus with Factors Stimulus Modality, Valence, and Predictability for Sustained Responses*

| | *df* | *F* | *p* | *SS* | *MSE* |
|---|---|---|---|---|---|
| MOD | 1,34 | 19.3 | <0.000104 | 3104.51 | 161.03 |
| VAL | 1,34 | 0.211 | <0.648781 | 19.21 | 90.95 |
| PRED | 1,34 | 1.60 | <0.214083 | 134.25 | 83.75 |
| MOD*VAL | 1,34 | 0.719 | <0.402471 | 43.37 | 60.34 |
| MOD*PRED | 1,34 | 5.47 | <0.025398 | 610.00 | 111.58 |
| VAL*PRED | 1,34 | 0.637 | <0.430406 | 37.13 | 58.31 |
| MOD*VAL*PRED | 1,34 | 0.534 | <0.470036 | 46.41 | 86.96 |

*Note.* Modality (MOD: pictures, electrical stimulation), valence (VAL: negative, neutral), and predictability (PRED: predictable, unpredictable). *Df* = degrees of freedom, *F* = F-statistic, *p* = p-value, *SS* = sum of squares, and *MSE* = mean squared error. *N* = 35.

**Table 7.52**

*Descriptive Statistics of the Average BOLD Response in the Insular Cortex as a Function of Stimulus Modality for Sustained Responses*

| | MOD | pics | pics | pics | pics | zaps | zaps | zaps | zaps |
|---|---|---|---|---|---|---|---|---|---|
| | VAL | neg | neg | neu | neu | neg | neg | neu | neu |
| | PRED | pred | unpr | pred | unpr | pred | unpr | pred | unpr |
| *M* | | -4.95 | -4.21 | -4.17 | -3.45 | 5.82 | 1.25 | 2.29 | 0.05 |
| *SD* | | 13.07 | 10.88 | 8.41 | 8.95 | 13.76 | 9.53 | 8.54 | 9.46 |
| *SEM* | | 2.21 | 1.84 | 1.42 | 1.51 | 2.33 | 1.61 | 1.44 | 1.60 |
| *Var* | | 170.80 | 118.46 | 70.67 | 80.09 | 189.24 | 90.85 | 72.94 | 89.43 |
| *CI95%* | | 3.74 | 3.74 | 3.74 | 3.74 | 3.74 | 3.74 | 3.74 | 3.74 |
| *Skew* | | -2.511 | 0.175 | -0.246 | 0.261 | 1.896 | 0.046 | 0.547 | 0.187 |
| *zSkew* | | -6.066 | 0.422 | -0.595 | 0.631 | 4.580 | 0.110 | 1.322 | 0.452 |

*Note.* Modality (MOD: pictures (pics), electrical stimulation (zaps)), valence (VAL: negative (neg), neutral (neu)), and predictability (PRED: predictable (pred), unpredictable (unpr)). *M* = Mean, *SD* = standard deviation, *SEM* = standard error *Var* = variance, *CI95%* = 95% confidence interval, *Skew* = skewness, and *zSkew* = *z*-score of the skew. *N* = 35.

**Table 7.53**

*Repeated Measures ANOVA for Average BOLD response in the Insular Cortex with Factors Stimulus Modality, Valence, and Predictability for Sustained Responses*

| | *df* | *F* | *p* | *SS* | *MSE* |
|---|---|---|---|---|---|
| MOD | 1,34 | 28.9 | <0.000006 | 3001.48 | 104.02 |
| VAL | 1,34 | 0.360 | <0.552533 | 44.71 | 124.22 |
| PRED | 1,34 | 1.44 | <0.238874 | 125.65 | 87.42 |
| MOD*VAL | 1,34 | 1.53 | <0.224680 | 171.72 | 112.28 |
| MOD*PRED | 1,34 | 2.12 | <0.154660 | 299.40 | 141.30 |
| VAL*PRED | 1,34 | 0.263 | <0.611405 | 23.77 | 90.41 |
| MOD*VAL*PRED | 1,34 | 0.108 | <0.744271 | 24.10 | 222.85 |

*Note.* Modality (MOD: pictures, electrical stimulation), valence (VAL: negative, neutral), and predictability (PRED: predictable, unpredictable). *Df* = degrees of freedom, *F* = F-statistic, *p* = p-value, *SS* = sum of squares, and *MSE* = mean squared error. *N* = 35.

**Table 7.54**

*Descriptive Statistics of the Average BOLD Response in the Frontal Pole as a Function of Stimulus Modality for Sustained Responses*

| | MOD | pics | pics | pics | pics | zaps | zaps | zaps | zaps |
|---|---|---|---|---|---|---|---|---|---|
| | VAL | neg | neg | neu | neu | neg | neg | neu | neu |
| | PRED | pred | unpr | pred | unpr | pred | unpr | pred | unpr |
| *M* | -6.51 | -4.85 | -1.30 | -3.64 | 12.41 | 3.21 | 11.95 | 1.01 | -6.51 |
| *SD* | 28.52 | 23.69 | 19.08 | 21.11 | 25.68 | 27.24 | 26.61 | 24.47 | 28.52 |
| *SEM* | 4.82 | 4.00 | 3.22 | 3.57 | 4.34 | 4.61 | 4.50 | 4.14 | 4.82 |
| *Var* | 813.22 | 561.06 | 364.02 | 445.50 | 659.50 | 742.21 | 708.28 | 598.76 | 813.22 |
| *CI95%* | 8.81 | 8.81 | 8.81 | 8.81 | 8.81 | 8.81 | 8.81 | 8.81 | 8.81 |
| *Skew* | 0.501 | 0.020 | 0.107 | 0.112 | 2.295 | 0.441 | -0.210 | 0.942 | 0.501 |
| *zSkew* | 1.210 | 0.049 | 0.259 | 0.271 | 5.543 | 1.065 | -0.506 | 2.274 | 1.210 |

*Note.* Modality (MOD: pictures (pics), electrical stimulation (zaps)), valence (VAL: negative (neg), neutral (neu)), and predictability (PRED: predictable (pred), unpredictable (unpr)). *M* = Mean, *SD* = standard deviation, *SEM* = standard error *Var* = variance, *CI95%* = 95% confidence interval, *Skew* = skewness, and *zSkew* = *z*-score of the skew. *N* = 35.

**Table 7.55**

*Repeated Measures ANOVA for Average BOLD response in the Frontal Pole with Factors Stimulus Modality, Valence, and Predictability for Sustained Responses*

| | *df* | *F* | *p* | *SS* | *MSE* |
|---|---|---|---|---|---|
| MOD | 1,34 | 13.8 | <0.000720 | 8810.19 | 637.12 |
| VAL | 1,34 | 0.171 | <0.681505 | 61.69 | 360.03 |
| PRED | 1,34 | 2.71 | <0.109234 | 1896.05 | 700.88 |
| MOD*VAL | 1,34 | 0.466 | <0.499653 | 360.50 | 774.32 |
| MOD*PRED | 1,34 | 1.91 | <0.175713 | 1659.27 | 867.64 |
| VAL*PRED | 1,34 | 0.257 | <0.615331 | 144.15 | 560.50 |
| MOD*VAL*PRED | 1,34 | 0.023 | <0.881156 | 22.51 | 992.06 |

*Note.* Modality (MOD: pictures, electrical stimulation), valence (VAL: negative, neutral), and predictability (PRED: predictable, unpredictable). *Df* = degrees of freedom, *F* = F-statistic, *p* = p-value, *SS* = sum of squares, and *MSE* = mean squared error. *N* = 35.

**Table 7.56**

*Descriptive Statistics of the Average BOLD Response in the Middle Frontal Gyrus as a Function of Stimulus Modality for Sustained Responses*

| | MOD | pics | pics | pics | pics | zaps | zaps | zaps | zaps |
|---|---|---|---|---|---|---|---|---|---|
| | VAL | neg | neg | neu | neu | neg | neg | neu | neu |
| | PRED | pred | unpr | pred | unpr | pred | unpr | pred | unpr |
| *M* | | 0.16 | -3.30 | 0.21 | 1.81 | 11.22 | -1.95 | -0.57 | 6.40 |
| *SD* | | 12.39 | 12.53 | 9.42 | 12.16 | 14.60 | 10.73 | 9.54 | 15.16 |
| *SEM* | | 2.09 | 2.12 | 1.59 | 2.05 | 2.47 | 1.81 | 1.61 | 2.56 |
| *Var* | | 153.52 | 156.91 | 88.77 | 147.80 | 213.09 | 115.17 | 90.95 | 229.79 |
| *CI95%* | | 4.36 | 4.36 | 4.36 | 4.36 | 4.36 | 4.36 | 4.36 | 4.36 |
| *Skew* | | 1.774 | -0.090 | -0.172 | -0.459 | 1.123 | -0.503 | 0.154 | 1.322 |
| *zSkew* | | 4.284 | -0.218 | -0.416 | -1.109 | 2.712 | -1.214 | 0.371 | 3.193 |

*Note.* Modality (MOD: pictures (pics), electrical stimulation (zaps)), valence (VAL: negative (neg), neutral (neu)), and predictability (PRED: predictable (pred), unpredictable (unpr)). *M* = Mean, *SD* = standard deviation, *SEM* = standard error *Var* = variance, *CI95%* = 95% confidence interval, *Skew* = skewness, and *zSkew* = z-score of the skew. *N* = 35.

**Table 7.57**

*Repeated Measures ANOVA for Average BOLD response in the Middle Frontal Gyrus with Factors Stimulus Modality, Valence, and Predictability for Sustained Responses*

| | *df* | *F* | *p* | *SS* | *MSE* |
|---|---|---|---|---|---|
| MOD | 1,34 | 11.8 | <0.001579 | 1149.65 | 97.45 |
| VAL | 1,34 | 0.079 | <0.780645 | 13.25 | 168.15 |
| PRED | 1,34 | 1.55 | <0.221619 | 284.68 | 183.64 |
| MOD*VAL | 1,34 | 2.31 | <0.137943 | 324.13 | 140.43 |
| MOD*PRED | 1,34 | 0.312 | <0.580236 | 82.80 | 265.55 |
| VAL*PRED | 1,34 | 14.5 | <0.000564 | 2775.64 | 191.69 |
| MOD*VAL*PRED | 1,34 | 6.66 | <0.014318 | 993.72 | 149.10 |

*Note.* Modality (MOD: pictures, electrical stimulation), valence (VAL: negative, neutral), and predictability (PRED: predictable, unpredictable). *Df* = degrees of freedom, *F* = F-statistic, *p* = p-value, *SS* = sum of squares, and *MSE* = mean squared error. *N* = 35.

**Table 7.58**

*Descriptive Statistics of the Average BOLD Response in the Inferior Frontal Gyrus as a Function of Stimulus Modality for Sustained Responses*

| | MOD | pics | pics | pics | pics | zaps | zaps | zaps | zaps |
|---|---|---|---|---|---|---|---|---|---|
| | VAL | neg | neg | neu | neu | neg | neg | neu | neu |
| | PRED | pred | unpr | pred | unpr | pred | unpr | pred | unpr |
| *M* | | -4.11 | 2.26 | -6.84 | 2.18 | 17.30 | 14.12 | 13.47 | 3.75 |
| *SD* | | 20.11 | 18.54 | 16.81 | 22.26 | 26.49 | 26.78 | 25.40 | 23.07 |
| *SEM* | | 3.40 | 3.13 | 2.84 | 3.76 | 4.48 | 4.53 | 4.29 | 3.90 |
| *Var* | | 404.33 | 343.79 | 282.62 | 495.63 | 701.94 | 717.41 | 645.07 | 532.25 |
| *CI95%* | | 8.09 | 8.09 | 8.09 | 8.09 | 8.09 | 8.09 | 8.09 | 8.09 |
| *Skew* | | 0.207 | 0.771 | 0.360 | -0.372 | 2.026 | 0.445 | -0.028 | -0.165 |
| *zSkew* | | 0.499 | 1.862 | 0.869 | -0.899 | 4.894 | 1.075 | -0.068 | -0.398 |

*Note.* Modality (MOD: pictures (pics), electrical stimulation (zaps)), valence (VAL: negative (neg), neutral (neu)), and predictability (PRED: predictable (pred), unpredictable (unpr)). *M* = Mean, *SD* = standard deviation, *SEM* = standard error *Var* = variance, *CI95%* = 95% confidence interval, *Skew* = skewness, and *zSkew* = *z*-score of the skew. *N* = 35.

**Table 7.59**

*Repeated Measures ANOVA for Average BOLD response in the Inferior Frontal Gyrus with Factors Stimulus Modality, Valence, and Predictability for Sustained Responses*

| | *df* | *F* | *p* | *SS* | *MSE* |
|---|---|---|---|---|---|
| MOD | 1,34 | 20.4 | <0.000073 | 13307.36 | 653.49 |
| VAL | 1,34 | 2.40 | <0.130501 | 1265.25 | 526.92 |
| PRED | 1,34 | 0.041 | <0.841677 | 27.14 | 669.81 |
| MOD*VAL | 1,34 | 0.967 | <0.332355 | 567.34 | 586.65 |
| MOD*PRED | 1,34 | 7.93 | <0.008026 | 3501.75 | 441.44 |
| VAL*PRED | 1,34 | 0.152 | <0.699134 | 65.86 | 433.52 |
| MOD*VAL*PRED | 1,34 | 0.456 | <0.504254 | 369.58 | 811.19 |

*Note.* Modality (MOD: pictures, electrical stimulation), valence (VAL: negative, neutral), and predictability (PRED: predictable, unpredictable). *Df* = degrees of freedom, *F* = F-statistic, *p* = p-value, *SS* = sum of squares, and *MSE* = mean squared error. *N* = 35.

**Table 7.60**

*Descriptive Statistics of the Average BOLD Response in the Frontal Medial Cortex as a Function of Stimulus Modality for Sustained Responses*

| | MOD | pics | pics | pics | pics | zaps | zaps | zaps | zaps |
|---|---|---|---|---|---|---|---|---|---|
| | VAL | neg | neg | neu | neu | neg | neg | neu | neu |
| | PRED | pred | unpr | pred | unpr | pred | unpr | pred | unpr |
| *M* | 3.95 | 1.46 | 4.85 | 0.39 | -0.59 | -3.75 | -2.75 | -5.15 | 3.95 |
| *SD* | 13.34 | 13.58 | 14.52 | 10.88 | 12.19 | 12.49 | 11.25 | 10.40 | 13.34 |
| *SEM* | 2.25 | 2.30 | 2.45 | 1.84 | 2.06 | 2.11 | 1.90 | 1.76 | 2.25 |
| *Var* | 177.89 | 184.48 | 210.73 | 118.38 | 148.66 | 155.91 | 126.56 | 108.18 | 177.89 |
| *CI95%* | 4.42 | 4.42 | 4.42 | 4.42 | 4.42 | 4.42 | 4.42 | 4.42 | 4.42 |
| *Skew* | 0.885 | -0.156 | 0.046 | -1.002 | 0.627 | -0.482 | -1.060 | 0.944 | 0.885 |
| *zSkew* | 2.137 | -0.377 | 0.111 | -2.420 | 1.515 | -1.165 | -2.559 | 2.280 | 2.137 |

*Note.* Modality (MOD: pictures (pics), electrical stimulation (zaps)), valence (VAL: negative (neg), neutral (neu)), and predictability (PRED: predictable (pred), unpredictable (unpr)). *M* = Mean, *SD* = standard deviation, *SEM* = standard error *Var* = variance, *CI95%* = 95% confidence interval, *Skew* = skewness, and *zSkew* = z-score of the skew. *N* = 35.

**Table 7.61**

*Repeated Measures ANOVA for Average BOLD response in the Frontal Medial Cortex with Factors Stimulus Modality, Valence, and Predictability for Sustained Responses*

| | *df* | *F* | *p* | *SS* | *MSE* |
|---|---|---|---|---|---|
| MOD | 1,34 | 19.6 | <0.000092 | 2294.55 | 116.83 |
| VAL | 1,34 | 0.249 | <0.621232 | 61.15 | 245.91 |
| PRED | 1,34 | 2.21 | <0.146043 | 684.58 | 309.31 |
| MOD*VAL | 1,34 | 0.309 | <0.581720 | 50.20 | 162.29 |
| MOD*PRED | 1,34 | 0.064 | <0.801486 | 8.64 | 134.55 |
| VAL*PRED | 1,34 | 0.042 | <0.838259 | 6.53 | 154.34 |
| MOD*VAL*PRED | 1,34 | 0.303 | <0.585859 | 32.54 | 107.55 |

*Note.* Modality (MOD: pictures, electrical stimulation), valence (VAL: negative, neutral), and predictability (PRED: predictable, unpredictable). *Df* = degrees of freedom, *F* = F-statistic, *p* = p-value, *SS* = sum of squares, and *MSE* = mean squared error. *N* = 35.

**Table 7.62**

*Descriptive Statistics of the Average BOLD Response in the Superior Frontal Gyrus as a Function of Stimulus Modality for Sustained Responses*

| | MOD | pics | pics | pics | pics | zaps | zaps | zaps | zaps |
|---|---|---|---|---|---|---|---|---|---|
| | VAL | neg | neg | neu | neu | neg | neg | neu | neu |
| | PRED | pred | unpr | pred | unpr | pred | unpr | pred | unpr |
| *M* | 8.52 | 10.21 | 23.93 | 0.25 | -10.83 | 4.35 | -5.97 | -14.33 | 8.52 |
| *SD* | 41.89 | 29.32 | 43.73 | 38.70 | 37.38 | 29.53 | 31.91 | 31.08 | 41.89 |
| *SEM* | 7.08 | 4.96 | 7.39 | 6.54 | 6.32 | 4.99 | 5.39 | 5.25 | 7.08 |
| *Var* | 1755.05 | 859.80 | 1912.03 | 1498.05 | 1396.96 | 872.25 | 1018.09 | 965.86 | 1755.05 |
| *CI95%* | 12.77 | 12.77 | 12.77 | 12.77 | 12.77 | 12.77 | 12.77 | 12.77 | 12.77 |
| *Skew* | 0.734 | 1.873 | 1.509 | -1.482 | -0.812 | 1.158 | -0.740 | 0.149 | 0.734 |
| *zSkew* | 1.772 | 4.524 | 3.644 | -3.580 | -1.960 | 2.798 | -1.787 | 0.361 | 1.772 |

*Note.* Modality (MOD: pictures (pics), electrical stimulation (zaps)), valence (VAL: negative (neg), neutral (neu)), and predictability (PRED: predictable (pred), unpredictable (unpr)). *M* = Mean, *SD* = standard deviation, *SEM* = standard error *Var* = variance, *CI95%* = 95% confidence interval, *Skew* = skewness, and *zSkew* = *z*-score of the skew. *N* = 35.

**Table 7.63**

*Repeated Measures ANOVA for Average BOLD response in the Superior Frontal Gyrus with Factors Stimulus Modality, Valence, and Predictability for Sustained Responses*

| | *df* | *F* | *p* | *SS* | *MSE* |
|---|---|---|---|---|---|
| MOD | 1,34 | 16.2 | <0.000306 | 21241.90 | 1314.77 |
| VAL | 1,34 | 0.275 | <0.603211 | 306.61 | 1113.79 |
| PRED | 1,34 | 0.714 | <0.404138 | 1008.01 | 1412.46 |
| MOD*VAL | 1,34 | 1.17 | <0.287556 | 1622.46 | 1389.89 |
| MOD*PRED | 1,34 | 1.61 | <0.213395 | 3630.49 | 2257.84 |
| VAL*PRED | 1,34 | 7.59 | <0.009343 | 10464.10 | 1377.89 |
| MOD*VAL*PRED | 1,34 | 0.010 | <0.919546 | 14.62 | 1411.46 |

*Note.* Modality (MOD: pictures, electrical stimulation), valence (VAL: negative, neutral), and predictability (PRED: predictable, unpredictable). *Df* = degrees of freedom, *F* = F-statistic, *p* = p-value, *SS* = sum of squares, and *MSE* = mean squared error. *N* = 35.

**Table 7.64**

*Correlations Between Questionnaires and Sustained Responses within Right Amygdala across Stimulus Modalities*

| Variable | | ASI | IUS | PANAS-PA | PANAS-NA | STAI-S | NegPred | NegUnpr | NeuPred | NeuUnpr |
|---|---|---|---|---|---|---|---|---|---|---|
| | | | | | | **Pearson Correlations** | | | | |
| ASI | r | 1 | | | | | | | | |
| | p | | | | | | | | | |
| | N | 35 | | | | | | | | |
| IUS | r | .590** | 1 | | | | | | | |
| | p | 0.000 | | | | | | | | |
| | N | 35 | 35 | | | | | | | |
| PANAS-PA | r | -0.020 | -0.017 | 1 | | | | | | |
| | p | 0.907 | 0.925 | | | | | | | |
| | N | 35 | 35 | 35 | | | | | | |
| PANAS-NA | r | .519** | 0.251 | -0.045 | 1 | | | | | |
| | p | 0.001 | 0.145 | 0.797 | | | | | | |
| | N | 35 | 35 | 35 | 35 | | | | | |
| STAI-S | r | .521** | .428* | -0.005 | .627** | 1 | | | | |
| | p | 0.001 | 0.010 | 0.978 | 0.000 | | | | | |
| | N | 35 | 35 | 35 | 35 | 35 | | | | |
| NegPred | r | -0.194 | -0.105 | **.357*** | 0.086 | -0.007 | 1 | | | |
| | p | 0.264 | 0.549 | 0.035 | 0.624 | 0.968 | | | | |
| | N | 35 | 35 | 35 | 35 | 35 | 35 | | | |
| NegUnpr | r | 0.066 | -0.228 | -0.092 | 0.117 | -0.122 | 0.114 | 1 | | |
| | p | 0.705 | 0.187 | 0.599 | 0.502 | 0.486 | 0.516 | | | |
| | N | 35 | 35 | 35 | 35 | 35 | 35 | 35 | | |
| NeuPred | r | -0.249 | -0.256 | 0.293 | -0.028 | -0.035 | .392* | 0.125 | 1 | |
| | p | 0.150 | 0.138 | 0.088 | 0.874 | 0.841 | 0.020 | 0.476 | | |
| | N | 35 | 35 | 35 | 35 | 35 | 35 | 35 | 35 | |
| NeuUnpr | r | -0.271 | -0.086 | 0.046 | -0.002 | -0.155 | .392* | 0.208 | 0.192 | 1 |
| | p | 0.115 | 0.624 | 0.794 | 0.991 | 0.375 | 0.020 | 0.231 | 0.270 | |
| | N | 35 | 35 | 35 | 35 | 35 | 35 | 35 | 35 | 35 |

*Note.* Questionnaires (ASI: Anxiety Sensitivity Index, IUS: Intolerance to Uncertainty Scale, PANAS-PA: Positive Affect Schedule, PANAS-NA: Negative Affect Schedule, and STAI-S: State Anxiety Inventory (pre and post). Modality (pictures, electrical stimulation), Valence (negative (neg), neutral (neu)), and predictability (predictable (pred), unpredictable(unpr)). *R* = correlation coefficient (Pearson), *p* = *p*-value, and *N* = number of subjects. Significance level: *** = $p < .001$, ** = $p < .01$, and * = $p < .05$.

**Table 7.65**

*Correlations Between Questionnaires and Sustained Responses within Right Amygdala for Picture Stimulus Modality*

| Variable | | ASI | IUS | PANAS-PA | PANAS-NA | STAI-S | PicsNegPred | PicsNegUnpr | PicsNeuPred | PicsNeuUnpr |
|---|---|---|---|---|---|---|---|---|---|---|
| | | | | | | **Pearson Correlations** | | | | |
| ASI | r | 1 | | | | | | | | |
| | p | | | | | | | | | |
| | N | 35 | | | | | | | | |
| IUS | r | .590** | 1 | | | | | | | |
| | p | 0.000 | | | | | | | | |
| | N | 35 | 35 | | | | | | | |
| PANAS-PA | r | -0.020 | -0.017 | 1 | | | | | | |
| | p | 0.907 | 0.925 | | | | | | | |
| | N | 35 | 35 | 35 | | | | | | |
| PANAS-NA | r | .519** | 0.251 | -0.045 | 1 | | | | | |
| | p | 0.001 | 0.145 | 0.797 | | | | | | |
| | N | 35 | 35 | 35 | 35 | | | | | |
| STAI-S | r | .521** | .428* | -0.005 | .627** | 1 | | | | |
| | p | 0.001 | 0.010 | 0.978 | 0.000 | | | | | |
| | N | 35 | 35 | 35 | 35 | 35 | | | | |
| PicsNegPred | r | -0.064 | -0.057 | 0.151 | 0.024 | 0.071 | 1 | | | |
| | p | 0.714 | 0.743 | 0.387 | 0.890 | 0.685 | | | | |
| | N | 35 | 35 | 35 | 35 | 35 | 35 | | | |
| PicsNegUnpr | r | 0.043 | -0.220 | 0.076 | 0.003 | -0.165 | 0.047 | 1 | | |
| | p | 0.806 | 0.204 | 0.666 | 0.987 | 0.344 | 0.791 | | | |
| | N | 35 | 35 | 35 | 35 | 35 | 35 | 35 | | |
| PicsNeuPred | r | -0.117 | -0.151 | 0.117 | -0.197 | -0.126 | 0.174 | 0.158 | 1 | |
| | p | 0.504 | 0.387 | 0.503 | 0.258 | 0.470 | 0.318 | 0.365 | | |
| | N | 35 | 35 | 35 | 35 | 35 | 35 | 35 | 35 | |
| PicsNeuUnpr | r | 0.079 | 0.100 | -0.101 | .395* | 0.114 | 0.274 | 0.272 | -0.037 | 1 |
| | p | 0.651 | 0.567 | 0.563 | 0.019 | 0.513 | 0.112 | 0.114 | 0.834 | |
| | N | 35 | 35 | 35 | 35 | 35 | 35 | 35 | 35 | 35 |

*Note.* Questionnaires (ASI: Anxiety Sensitivity Index, IUS: Intolerance to Uncertainty Scale, PANAS-PA: Positive Affect Schedule, PANAS-NA: Negative Affect Schedule, and STAI-S: State Anxiety Inventory (pre and post). Modality (pictures (pics)), Valence (negative (neg), neutral (neu)), and predictability (predictable (pred), unpredictable(unpr)). *R* = correlation coefficient (Pearson), *p* = *p*-value, and *N* = number of subjects. Significance level: *** = $p < .001$, ** = $p < .01$, and * = $p < .05$.

**Table 7.66**

*Correlations Between Questionnaires and Sustained Responses within Right Amygdala for Zap Stimulus Modality*

| Variable | | ASI | IUS | PANAS-PA | PANAS-NA | STAI-S | ZapsNegPred | ZapsNegUnpr | ZapsNeuPred | ZapsNeuUnpr |
|---|---|---|---|---|---|---|---|---|---|---|
| | | | | | Pearson Correlations | | | | | |
| ASI | r | 1 | | | | | | | | |
| | p | | | | | | | | | |
| | N | 35 | | | | | | | | |
| IUS | r | .590** | 1 | | | | | | | |
| | p | 0.000 | | | | | | | | |
| | N | 35 | 35 | | | | | | | |
| PANAS-PA | r | -0.020 | -0.017 | 1 | | | | | | |
| | p | 0.907 | 0.925 | | | | | | | |
| | N | 35 | 35 | 35 | | | | | | |
| PANAS-NA | r | .519** | 0.251 | -0.045 | 1 | | | | | |
| | p | 0.001 | 0.145 | 0.797 | | | | | | |
| | N | 35 | 35 | 35 | 35 | | | | | |
| STAI-S | r | .521** | .428* | -0.005 | .627** | 1 | | | | |
| | p | 0.001 | 0.010 | 0.978 | 0.000 | | | | | |
| | N | 35 | 35 | 35 | 35 | 35 | | | | |
| ZapsNegPred | r | -0.185 | -0.078 | 0.308 | 0.086 | -0.079 | 1 | | | |
| | p | 0.286 | 0.657 | 0.072 | 0.624 | 0.654 | | | | |
| | N | 35 | 35 | 35 | 35 | 35 | 35 | | | |
| ZapsNegUnpr | r | 0.053 | -0.116 | -0.198 | 0.161 | -0.018 | -0.064 | 1 | | |
| | p | 0.763 | 0.507 | 0.255 | 0.356 | 0.917 | 0.715 | | | |
| | N | 35 | 35 | 35 | 35 | 35 | 35 | 35 | | |
| ZapsNeuPred | r | -0.206 | -0.184 | 0.261 | 0.141 | 0.069 | 0.113 | 0.068 | 1 | |
| | p | 0.236 | 0.291 | 0.130 | 0.420 | 0.694 | 0.519 | 0.698 | | |
| | N | 35 | 35 | 35 | 35 | 35 | 35 | 35 | 35 | |
| ZapsNeuUnpr | r | -.432** | -0.203 | 0.150 | -.351* | -0.307 | 0.212 | -0.148 | 0.268 | 1 |
| | p | 0.010 | 0.242 | 0.390 | 0.039 | 0.073 | 0.222 | 0.396 | 0.120 | |
| | N | 35 | 35 | 35 | 35 | 35 | 35 | 35 | 35 | 35 |

*Note.* Questionnaires (ASI: Anxiety Sensitivity Index, IUS: Intolerance to Uncertainty Scale, PANAS-PA: Positive Affect Schedule, PANAS-NA: Negative Affect Schedule, and STAI-S: State Anxiety Inventory (pre and post). Modality (electrical stimulation (zaps)), Valence (negative (neg), neutral (neu)), and predictability (predictable (pred), unpredictable(unpr)). *R* = correlation coefficient (Pearson), *p* = *p*-value, and *N* = number of subjects. Significance level: *** = *p* < .001, ** = *p* < .01, and * = *p* < .05.

**Table 7.67**

*Sample Characteristics of Task-evoked Anxiety Rating with Respect to Modality, Valence and, Predictability*

| MOD | VAL | PRED | *N* | *M* | *SD* | *SEM* |
|---|---|---|---|---|---|---|
| pics and | neg | pred | 35 | 3.96 | 1.55 | 0.26 |
| zaps | neg | unpr | 35 | 4.51 | 1.72 | 0.29 |
| | neu | pred | 35 | 2.01 | 0.92 | 0.16 |
| | neu | unpr | 35 | 2.34 | 1.10 | 0.19 |
| pics | neg | pred | 35 | 3.76 | 1.62 | 0.27 |
| | neg | unpr | 35 | 4.19 | 1.84 | 0.31 |
| | neu | pred | 35 | 1.73 | 0.97 | 0.16 |
| | neu | unpr | 35 | 2.01 | 1.10 | 0.19 |
| zaps | neg | pred | 35 | 4.17 | 1.86 | 0.31 |
| | neg | unpr | 35 | 4.83 | 2.10 | 0.36 |
| | neu | pred | 35 | 2.30 | 1.18 | 0.20 |
| | neu | unpr | 35 | 2.66 | 1.40 | 0.24 |

*Note.* Modality (MOD: pictures (pics), electrical stimulation (zaps)), valence (VAL: negative (neg), neutral (neu)), and predictability (PRED: predictable (pred), unpredictable(unpr)). *N* = number of subjects, *M* = Mean, *SD* = standard deviation, and *SEM* = standard error of mean.

**Table 7.68**

*Repeated Measures ANOVA for Task-evoked Anxiety Rating with Factors Stimulus Modality, Valence, and Predictability*

| Effect | *df* | *F* | *p* | *η²* |
|---|---|---|---|---|
| MOD | 1,34 | 6.897 | <0.013 | .169 |
| VAL | 1,34 | 93.076 | <0.000 | .732 |
| PRED | 1,34 | 28.635 | <0.000 | .457 |
| MOD*VAL | 1,34 | 0.094 | <0.761 | .003 |
| MOD*PRED | 1,34 | 4.354 | <0.045 | .114 |
| VAL*PRED | 1,34 | 8.080 | <0.008 | .192 |
| MOD*VAL*PRED | 1,34 | 1.135 | <0.294 | .032 |

*Note.* Modality (MOD: pictures, electrical stimulation), valence (VAL: negative, neutral), and predictability (PRED: predictable, unpredictable). *Df* = degrees of freedom, *F* = F-statistic, *p* = p-value, and *η²* = partial eta squared.

**Table 7.69**

*Significant Post-hoc Comparisons of Repeated Measures ANOVA for Task-evoked Anxiety Rating with Factors Stimulus Modality, Valence, and Predictability*

| Effect | Condition | *M* | *SD* | *df* | *t-test* |
|---|---|---|---|---|---|
| MOD | pics | 2.92 | 1.19 | 34 | -2.626* |
|  | zaps | 3.48 | 1.46 |  |  |
| VAL | neg | 4.23 | 1.60 | 34 | 9.648*** |
|  | neu | 2.17 | 0.98 |  |  |
| PRED | pred | 2.98 | 1.12 | 34 | -5.351*** |
|  | unpr | 3.42 | 1.17 |  |  |
| MOD*PRED | pics unpr | 3.10 | 1.29 | 34 | 2.737** |
|  | zaps unpr | 3.74 | 1.59 |  |  |
|  | pics pred | 2.74 | 1.16 | 34 | 2.437* |
|  | zaps pred | 3.24 | 1.38 |  |  |
|  | zaps unpr | 3.74 | 1.59 | 34 | 4.258*** |
|  | pics pred | 2.74 | 1.16 |  |  |
| VAL*PRED | neg pred | 3.96 | 1.55 | 34 | 9.624*** |
|  | neu pred | 2.01 | 0.92 |  |  |
|  | neg unpr | 4.51 | 1.72 | 34 | 9.411*** |
|  | neu unpr | 2.34 | 1.10 |  |  |
|  | neu pred | 2.01 | 0.92 | 34 | -10.018*** |
|  | neg unpr | 4.51 | 1.72 |  |  |
|  | neu unpr | 2.34 | 1.10 | 34 | -7.912*** |
|  | neg pred | 3.96 | 1.55 |  |  |

*Note.* Modality (MOD: pictures (pics), electrical stimulation (zaps)), and valence (VAL: negative (neg), neutral (neu)). *M* = Mean, *SD* = standard deviation, *df* = degrees of freedom, and *t*-test statistic. Significance level: *** = $p < .001$, ** = $p < .01$, and * = $p < .05$.

**Table 7.70**

*Repeated Measures ANOVAs for Task-evoked Anxiety Rating with Factors Valence, and Predictability within Stimulus Modality*

| MOD | Effect | df | F | p | $\eta^2$ |
|---|---|---|---|---|---|
| Pics | VAL | 1,34 | 74.677 | <0.000 | .687 |
| | PRED | 1,34 | 18.047 | <0.000 | .347 |
| | VAL*PRED | 1,34 | 1.365 | <0.251 | .039 |
| Zaps | VAL | 1,34 | 62.806 | <0.000 | .649 |
| | PRED | 1,34 | 30.048 | <0.000 | .469 |
| | VAL*PRED | 1,34 | 11.156 | <0.002 | .247 |

*Note.* Modality (MOD: pictures (pics), electrical stimulation(zaps)), valence (VAL: negative, neutral), and predictability (PRED: predictable (pred), unpredictable(unpr)). *Df* = degrees of freedom, *F* = F-statistic, *p* = *p*-value, and *η²* = partial eta squared

**Table 7.71**

*Significant Post-hoc Comparisons of Repeated Measures ANOVAs for RT with Factors Valence, and Predictability Within Picture Trials*

| Effect | Condition | M | SD | df | t-test |
|---|---|---|---|---|---|
| VAL | neg | 3.97 | 1.69 | 34 | 8.642*** |
| | neu | 1.87 | 1.00 | | |
| PRED | pred | 2.74 | 1.15 | 34 | -4.248*** |
| | unpr | 3.10 | 1.28 | | |

*Note.* Valence (VAL: negative (neg), neutral (neu)) ), and predictability (PRED: predictable (pred), unpredictable(unpr)). *M* = Mean, *SD* = standard deviation *df* = degrees of freedom, and *t*-test statistic. Significance level: **\*\*\*** = *p* < .001, **\*\*** = *p* < .01, and **\*** = *p* < .05.

**Table 7.72**

*Significant Post-hoc Comparisons of Repeated Measures ANOVAs for RT with Factors Valence, and Predictability Within Electrical Stimulation Trials*

| Effect | Condition | *M* | *SD* | *df* | *t-test* |
|---|---|---|---|---|---|
| VAL | neg | 4.50 | 1.95 | 34 | 7.925*** |
| | neu | 2.47 | 1.26 | | |
| PRED | pred | 3.23 | 1.37 | 34 | -5.482*** |
| | unpr | 3.74 | 1.59 | | |
| VAL*PRED | neg pred | 4.17 | 1.86 | 34 | 7.573*** |
| | neu pred | 2.30 | 1.18 | | |
| | neg unpr | 4.82 | 2.10 | 34 | 8.032*** |
| | neu unpr | 2.65 | 1.39 | | |
| | neg pred | 4.17 | 1.86 | 34 | 5.944*** |
| | neu unpr | 2.65 | 1.39 | | |
| | neu pred | 2.30 | 1.12 | 34 | -8.812*** |
| | neg unpr | 4.82 | 2.10 | | |
| | neg pred | 4.17 | 1.86 | 34 | -5.876*** |
| | neg unpr | 4.82 | 2.10 | | |
| | neu pred | 2.30 | 1.18 | 34 | -3.841*** |
| | neu unpr | 2.65 | 1.39 | | |

*Note.* Valence (VAL: negative (neg), neutral (neu)). *M* = Mean, *SD* = standard deviation, *df* = degrees of freedom, and *t*-test statistic. Significance level: **\*\*\*** = *p* < .001.

**Table 7.73**

*Correlations Between Questionnaires and Task-evoked Anxiety Rating across Picture and Electrical Stimulation Trials*

| Variable | | ASI | IUS | PANAS-PA | PANAS-NA | STAI-S-Pre | STAI-S-Post | NegPred | NegUnpr | NeuPred | NeuUnpr |
|---|---|---|---|---|---|---|---|---|---|---|---|
| | | **Pearson Correlations** | | | | | | | | | |
| ASI | r | 1 | | | | | | | | | |
| | p | | | | | | | | | | |
| | N | | | | | | | | | | |
| IUS | r | .590** | 1 | | | | | | | | |
| | p | 0.000 | | | | | | | | | |
| | N | 35 | 35 | | | | | | | | |
| PANAS-PA | r | -0.020 | -0.017 | 1 | | | | | | | |
| | p | 0.907 | 0.925 | | | | | | | | |
| | N | 35 | 35 | 35 | | | | | | | |
| PANAS-NA | r | .519** | 0.251 | -0.045 | 1 | | | | | | |
| | p | 0.001 | 0.145 | 0.797 | | | | | | | |
| | N | 35 | 35 | 35 | 35 | | | | | | |
| STAI-S-Pre | r | .370* | 0.222 | -0.251 | .717** | 1 | | | | | |
| | p | 0.028 | 0.200 | 0.146 | 0.000 | | | | | | |
| | N | 35 | 35 | 35 | 35 | 35 | | | | | |
| STAI-S-Post | r | .424* | .406* | 0.167 | 0.323 | 0.164 | 1 | | | | |
| | p | 0.011 | 0.016 | 0.336 | 0.059 | 0.348 | | | | | |
| | N | 35 | 35 | 35 | 35 | 35 | 35 | | | | |
| NegPred | r | 0.262 | 0.179 | -0.155 | 0.221 | 0.010 | .411* | 1 | | | |
| | p | 0.129 | 0.305 | 0.375 | 0.203 | 0.953 | 0.014 | | | | |
| | N | 35 | 35 | 35 | 35 | 35 | 35 | 35 | | | |
| NegUnpr | r | **.341*** | 0.139 | 0.134 | **.480**** | 0.275 | **.446**** | .557** | 1 | | |
| | p | 0.045 | 0.425 | 0.442 | 0.004 | 0.110 | 0.007 | 0.001 | | | |
| | N | 35 | 35 | 35 | 35 | 35 | 35 | 35 | 35 | | |
| NeuPred | r | 0.208 | 0.205 | -0.164 | 0.158 | -0.038 | 0.301 | .926** | .403* | 1 | |
| | p | 0.231 | 0.237 | 0.348 | 0.365 | 0.830 | 0.079 | 0.000 | 0.016 | | |
| | N | 35 | 35 | 35 | 35 | 35 | 35 | 35 | 35 | 35 | |
| NeuUnpr | r | **.352*** | 0.043 | 0.118 | **.497**** | 0.195 | **.396*** | .590** | .882** | .500** | 1 |
| | p | 0.038 | 0.805 | 0.499 | 0.002 | 0.263 | 0.018 | 0.000 | 0.000 | 0.002 | |
| | N | 35 | 35 | 35 | 35 | 35 | 35 | 35 | 35 | 35 | 35 |

*Note.* Questionnaires (ASI: Anxiety Sensitivity Index, IUS: Intolerance to Uncertainty Scale, PANAS-PA: Positive Affect Schedule, PANAS-NA: Negative Affect Schedule, and STAI-S: State Anxiety Inventory (pre and post). Valence (negative (neg), neutral (neu)), and predictability (predictable (pred), unpredictable(unpr)). *R* = correlation coefficient (Pearson), *p* = *p*-value, and *N* = number of subjects. Significance level: *** = $p < .001$, ** = $p < .01$, and * = $p < .05$.

**Table 7.74**

*Correlations Between Questionnaires and Task-evoked Anxiety Rating in Picture Trials*

| Variable | | ASI | IUS | PANAS-PA | PANAS-NA | STAI-S-Pre | STAI-S-Post | PicsNegPred | PicsNegUnpr | PicsNeuPred | PicsNeuUnpr |
|---|---|---|---|---|---|---|---|---|---|---|---|
| | | | | | **Pearson Correlations** | | | | | | |
| ASI | r | 1 | | | | | | | | | |
| | p | | | | | | | | | | |
| | N | 35 | | | | | | | | | |
| IUS | r | .590** | 1 | | | | | | | | |
| | p | 0.000 | | | | | | | | | |
| | N | 35 | 35 | | | | | | | | |
| PANAS-PA | r | -0.020 | -0.017 | 1 | | | | | | | |
| | p | 0.907 | 0.925 | | | | | | | | |
| | N | 35 | 35 | 35 | | | | | | | |
| PANAS-NA | r | .519** | 0.251 | -0.045 | 1 | | | | | | |
| | p | 0.001 | 0.145 | 0.797 | | | | | | | |
| | N | 35 | 35 | 35 | 35 | | | | | | |
| STAI-S-Pre | r | .370* | 0.222 | -0.251 | .717** | 1 | | | | | |
| | p | 0.028 | 0.200 | 0.146 | 0.000 | | | | | | |
| | N | 35 | 35 | 35 | 35 | 35 | | | | | |
| STAI-S-Post | r | .424* | .406* | 0.167 | 0.323 | 0.164 | 1 | | | | |
| | p | 0.011 | 0.016 | 0.336 | 0.059 | 0.348 | | | | | |
| | N | 35 | 35 | 35 | 35 | 35 | 35 | | | | |
| PicsNegPred | r | 0.262 | 0.179 | -0.155 | 0.221 | 0.010 | .411* | 1 | | | |
| | p | 0.129 | 0.305 | 0.375 | 0.203 | 0.953 | 0.014 | | | | |
| | N | 35 | 35 | 35 | 35 | 35 | 35 | 35 | | | |
| PicsNegUnpr | r | 0.208 | 0.205 | -0.164 | 0.158 | -0.038 | 0.301 | .926** | 1 | | |
| | p | 0.231 | 0.237 | 0.348 | 0.365 | 0.830 | 0.079 | 0.000 | | | |
| | N | 35 | 35 | 35 | 35 | 35 | 35 | 35 | 35 | | |
| PicsNeuPred | r | **.341*** | 0.139 | 0.134 | **.480**** | 0.275 | **.446**** | .557** | .403* | 1 | |
| | p | 0.045 | 0.425 | 0.442 | 0.004 | 0.110 | 0.007 | 0.001 | 0.016 | | |
| | N | 35 | 35 | 35 | 35 | 35 | 35 | 35 | 35 | 35 | |
| PicsNeuUnpr | r | **.352*** | 0.043 | 0.118 | **.497**** | 0.195 | **.396*** | .590** | .500** | .882** | 1 |
| | p | 0.038 | 0.805 | 0.499 | 0.002 | 0.263 | 0.018 | 0.000 | 0.002 | 0.000 | |
| | N | 35 | 35 | 35 | 35 | 35 | 35 | 35 | 35 | 35 | 35 |

*Note.* Questionnaires (ASI: Anxiety Sensitivity Index, IUS: Intolerance to Uncertainty Scale, PANAS-PA: Positive Affect Schedule, PANAS-NA: Negative Affect Schedule, and STAI-S: State Anxiety Inventory (pre and post). Picture modality (pics), Valence (negative (neg), neutral (neu)), and predictability (predictable (pred), unpredictable(unpr)). *R* = correlation coefficient (Pearson), *p* = *p*-value, and *N* = number of subjects. Significance level: *** = *p* < .001, ** = *p* < .01, and * = *p* < .05.

**Table 7.75**

*Correlations Between Questionnaires and Task-evoked Anxiety Rating in Electrical Stimulation Trials*

| Variable | | ASI | IUS | PANAS-PA | PANAS-NA | STAI-S-Pre | STAI-S-Post | ZapsNegPred | ZapsNegUnpr | ZapsNeuPred | ZapsNeuUnpr |
|---|---|---|---|---|---|---|---|---|---|---|---|
| | | | | | | **Pearson Correlations** | | | | | |
| ASI | r | 1 | | | | | | | | | |
| | p | | | | | | | | | | |
| | N | 35 | | | | | | | | | |
| IUS | r | .590** | 1 | | | | | | | | |
| | p | 0.000 | | | | | | | | | |
| | N | 35 | 35 | | | | | | | | |
| PANAS-PA | r | -0.020 | -0.017 | 1 | | | | | | | |
| | p | 0.907 | 0.925 | | | | | | | | |
| | N | 35 | 35 | 35 | | | | | | | |
| PANAS-NA | r | .519** | 0.251 | -0.045 | 1 | | | | | | |
| | p | 0.001 | 0.145 | 0.797 | | | | | | | |
| | N | 35 | 35 | 35 | 35 | | | | | | |
| STAI-S-Pre | r | .370* | 0.222 | -0.251 | .717** | 1 | | | | | |
| | p | 0.028 | 0.200 | 0.146 | 0.000 | | | | | | |
| | N | 35 | 35 | 35 | 35 | 35 | | | | | |
| STAI-S-Post | r | .424* | .406* | 0.167 | 0.323 | 0.164 | 1 | | | | |
| | p | 0.011 | 0.016 | 0.336 | 0.059 | 0.348 | | | | | |
| | N | 35 | 35 | 35 | 35 | 35 | 35 | | | | |
| ZapsNegPred | r | 0.235 | 0.146 | 0.116 | 0.078 | -0.125 | .446** | 1 | | | |
| | p | 0.175 | 0.404 | 0.507 | 0.655 | 0.473 | 0.007 | | | | |
| | N | 35 | 35 | 35 | 35 | 35 | 35 | 35 | | | |
| ZapsNegUnpr | r | 0.219 | 0.163 | 0.102 | 0.104 | -0.154 | .422* | .955** | 1 | | |
| | p | 0.206 | 0.348 | 0.560 | 0.550 | 0.377 | 0.012 | 0.000 | | | |
| | N | 35 | 35 | 35 | 35 | 35 | 35 | 35 | 35 | | |
| ZapsNeuPred | r | 0.129 | -0.043 | 0.024 | 0.283 | 0.100 | 0.182 | .594** | .569** | 1 | |
| | p | 0.460 | 0.808 | 0.892 | 0.099 | 0.569 | 0.297 | 0.000 | 0.000 | | |
| | N | 35 | 35 | 35 | 35 | 35 | 35 | 35 | 35 | 35 | |
| ZapsNeuUnpr | r | 0.080 | -0.086 | 0.023 | 0.234 | -0.062 | 0.134 | .583** | .620** | .932** | 1 |
| | p | 0.647 | 0.623 | 0.894 | 0.175 | 0.722 | 0.444 | 0.000 | 0.000 | 0.000 | |
| | N | 35 | 35 | 35 | 35 | 35 | 35 | 35 | 35 | 35 | 35 |

*Note.* Questionnaires (ASI: Anxiety Sensitivity Index, IUS: Intolerance to Uncertainty Scale, PANAS-PA: Positive Affect Schedule, PANAS-NA: Negative Affect Schedule, and STAI-S: State Anxiety Inventory (pre and post). Electrical stimulation (zaps), Valence (negative (neg), neutral (neu)), and predictability (predictable (pred), unpredictable(unpr)). *R* = correlation coefficient (Pearson), *p* = *p*-value, and *N* = number of subjects. Significance level: *** = *p* < .001, ** = *p* < .01, and * = *p* < .05.

# 8 REFERENCES

Aboraya, A., Rankin, E., France, C., El-Missiry, A., & John, C. (2006). The Reliability of Psychiatric Diagnosis Revisited: The Clinician's Guide to Improve the Reliability of Psychiatric Diagnosis. *Psychiatry (Edgmont), 3*(1), 41–50.

Acevedo, E. O., & Ekkekakis, P. (2006). *Psychobiology of physical activity.* Champaign, Ill.: Human Kinetics.

Adolphs, R., Tranel, D., & Damasio, A. R. (1998). The human amygdala in social judgment. *Nature, 393*(6684), 470–474, from https://www.nature.com/articles/30982.

Adolphs, R., Tranel, D., Hamann, S., Young, A.W., Calder, A.J., Phelps, E.A., et al. (1999). Recognition of facial emotion in nine individuals with bilateral amygdala damage. *Neuropsychologia, 37*(10), 1111–1117.

Adolphs, R. (2013). The biology of fear. *Current biology : CB, 23*(2), R79-93.

Allan, N. P., Raines, A. M., Capron, D. W., Norr, A. M., Zvolensky, M. J., & Schmidt, N. B. (2014). Identification of anxiety sensitivity classes and clinical cut-scores in a sample of adult smokers: results from a factor mixture model. *Journal of anxiety disorders, 28*(7), 696–703.

American Psychiatric Association (Ed.) (2013). *Diagnostic and statistical manual of mental disorders* (5th ed.). Arlington: American Psychiatric Publishing.

Bahn, S., Schwarz, E., Harris, L. W., Martins-de-Souza, D., Rahmoune, H., & Guest, P. C. (2013). Testes sanguíneos de biomarcadores para diagnóstico e tratamento de desordens mentais: foco em esquizofrenia. *Archives of Clinical Psychiatry (São Paulo), 40*(1), 2–9.

Balderston, N. L., Liu, J., Roberson-Nay, R., Ernst, M., & Grillon, C. (2017). The relationship between dlPFC activity during unpredictable threat and CO2-induced panic symptoms. *Translational Psychiatry, 7*(12), 1266.

Bandelow, B., & Michaelis, S. (2015). Epidemiology of anxiety disorders in the 21st century. *Dialogues in Clinical Neuroscience, 17*(3), 327–335.

Bandelow, B., Seidler-Brandler, U., Becker, A., Wedekind, D., & Rüther, E. (2007). Meta-analysis of randomized controlled comparisons of psychopharmacological and psychological treatments for anxiety disorders. *The world journal of biological psychiatry : the official journal of the World Federation of Societies of Biological Psychiatry, 8*(3), 175–187.

Bandelow, B., Sher, L., Bunevicius, R., Hollander, E., Kasper, S., Zohar, J., & Möller, H.-J. (2012). Guidelines for the pharmacological treatment of anxiety disorders, obsessive-compulsive disorder and posttraumatic stress disorder in primary care. *International journal of psychiatry in clinical practice, 16*(2), 77–84.

Barrett, L. F., Bliss-Moreau, E., Duncan, S. L., Rauch, S. L., & Wright, C. I. (2007). The amygdala and the experience of affect. *Social cognitive and affective neuroscience, 2*(2), 73–83.

Baune, B. (2020). *Personalized psychiatry.* London, San Diego, CA: Academic Press, an imprint of Elsevier.

Bernik, M., Sampaio, T. P. A., & Gandarela, L. (2013). Fibromyalgia comorbid with anxiety disorders and depression: combined medical and psychological treatment. *Current Pain and Headache Reports, 17*(9), 358, from https://link.springer.com/article/10.1007%2Fs11916-013-0358-3.

Biomarkers and surrogate endpoints (2001). Biomarkers and surrogate endpoints: preferred definitions and conceptual framework. *Clinical pharmacology and therapeutics, 69*(3), 89–95.

Biomarkers for Mental Disorders (2017). Biologically-Inspired Biomarkers for Mental Disorders. *EBioMedicine, 17*, 1–2.

Birrell, J., Meares, K., Wilkinson, A., & Freeston, M. (2011). Toward a definition of intolerance of uncertainty: a review of factor analytical studies of the Intolerance of Uncertainty Scale. *Clinical psychology review, 31*(7), 1198–1208.

Bishop, S. J., Jenkins, R., & Lawrence, A. D. (2007). Neural processing of fearful faces: effects of anxiety are gated by perceptual capacity limitations. *Cerebral Cortex, 17*(7), 1595–1603, from https://academic.oup.com/cercor/article/17/7/1595/406020.

Boksa, P. (2013). A way forward for research on biomarkers for psychiatric disorders. *Journal of Psychiatry & Neuroscience : JPN, 38*(2), 75–77.

Brainard, D. H. (1997). The Psychophysics Toolbox. *Spatial Vision, 10*(4), 433–436.

Carleton, R. N., Norton, M. A. P. J., & Asmundson, G. J. G. (2007). Fearing the unknown: a short version of the Intolerance of Uncertainty Scale. *Journal of anxiety disorders, 21*(1), 105–117, from http://www.sciencedirect.com/science/article/pii/S088761850600051X.

Carlsson, A. M. (1983). Assessment of chronic pain. I. Aspects of the reliability and validity of the visual analogue scale. *Pain, 16*(1), 87–101.

Cohen, J. R., & D'Esposito, M. (2016). The Segregation and Integration of Distinct Brain Networks and Their Relationship to Cognition. *Journal of Neuroscience, 36*(48), 12083–12094.

Cohen, J. N., Taylor Dryman, M., Morrison, A. S., Gilbert, K. E., Heimberg, R. G., & Gruber, J. (2017). Positive and Negative Affect as Links Between Social Anxiety and Depression: Predicting Concurrent and Prospective Mood Symptoms in Unipolar and Bipolar Mood Disorders. *Behavior Therapy, 48*(6), 820–833.

Collins, P. Y., Patel, V., Joestl, S. S., March, D., Insel, T. R., Daar, A. S., et al. (2011). Grand challenges in global mental health. *Nature, 475*(7354), 27–30, from https://www.nature.com/articles/475027a.

Crawford, J. R., & Henry, J. D. (2004). The positive and negative affect schedule (PANAS): construct validity, measurement properties and normative data in a large non-clinical sample. *The British journal of clinical psychology, 43*(Pt 3), 245–265.

Cuijpers, P., Sijbrandij, M., Koole, S. L., Andersson, G., Beekman, A. T., & Reynolds, C. F. (2013). The efficacy of psychotherapy and pharmacotherapy in treating depressive and anxiety disorders: a meta-analysis of direct comparisons. *World psychiatry : official journal of the World Psychiatric Association (WPA), 12*(2), 137–148.

Davis, M. (1992). The role of the amygdala in fear and anxiety. *Annual review of neuroscience, 15*, 353–375.

Davis, M. (1998). Are different parts of the extended amygdala involved in fear versus anxiety? *Biological Psychiatry, 44*(12), 1239–1247.

Davis, M., Walker, D. L., Miles, L., & Grillon, C. (2010). Phasic vs sustained fear in rats and humans: role of the extended amygdala in fear vs anxiety. *Neuropsychopharmacology : official publication of the American College of Neuropsychopharmacology, 35*(1), 105–135.

Davis, T., & Poldrack, R. A. (2013). Measuring neural representations with fMRI: practices and pitfalls. *Annals of the New York Academy of Sciences, 1296*, 108–134.

Desikan, R. S., Ségonne, F., Fischl, B., Quinn, B. T., Dickerson, B. C., Blacker, D., et al. (2006). An automated labeling system for subdividing the human cerebral cortex on MRI scans into gyral based regions of interest. *NeuroImage, 31*(3), 968–980, from http://www.sciencedirect.com/science/article/pii/S1053811906000437.

Di Marino, V., Etienne, Y., & Niddam, M. (2016). *The Amygdaloid Nuclear Complex: Anatomic Study of the Human Amygdala* (1st ed. 2016). Cham, s.l.: Springer International Publishing.

Díaz-García, A., González-Robles, A., Mor, S., Mira, A., Quero, S., García-Palacios, A., et al. (2020). Positive and Negative Affect Schedule (PANAS): psychometric properties of the online Spanish version in a clinical sample with emotional disorders. *BMC Psychiatry, 20*(1), 56.

Dugas, M. J., Hedayati, M., Karavidas, A., Buhr, K., Francis, K., & Phillips, N. A. (2005). Intolerance of Uncertainty and Information Processing: Evidence of Biased Recall and Interpretations. *Cognitive Therapy and Research, 29*(1), 57–70.

Ekman, P. (1992). An argument for basic emotions. *Cognition and Emotion, 6*(3-4), 169–200.

Ekman, P., & Cordaro, D. (2011). What is Meant by Calling Emotions Basic. *Emotion Review, 3*(4), 364–370.

The Ekmans' Atlas of Emotion (2020). *The Ekmans' Atlas of Emotion.* Retrieved June 09, 2020, from http://atlasofemotions.org/#states/fear.

Elman, I., & Borsook, D. (2018). Threat Response System: Parallel Brain Processes in Pain vis-à-vis Fear and Anxiety. *Frontiers in psychiatry, 9*, 29.

Endler, N. S. (1983). Interactionism: a personality model, but not yet a theory. *Nebraska Symposium on Motivation. Nebraska Symposium on Motivation*, 155–200.

Esteve, M. R., & Camacho, L. (2008). Anxiety sensitivity, body vigilance and fear of pain. *Behaviour Research and Therapy, 46*(6), 715–727, from http://www.sciencedirect.com/science/article/pii/S0005796708000533.

Etkin, A., Büchel, C., & Gross, J. J. (2015). The neural bases of emotion regulation. *Nature Reviews Neuroscience, 16*(11), 693–700, from https://www.nature.com/articles/nrn4044.

Fanselow, M. S., & Pennington, Z. T. (2017). The Danger of LeDoux and Pine's Two-System Framework for Fear. *The American journal of psychiatry, 174*(11), 1120–1121.

Farach, F. J., Pruitt, L. D., Jun, J. J., Jerud, A. B., Zoellner, L. A., & Roy-Byrne, P. P. (2012). Pharmacological treatment of anxiety disorders: current treatments and future directions. *Journal of anxiety disorders, 26*(8), 833–843.

Fernandes, B. S., Williams, L. M., Steiner, J., Leboyer, M., Carvalho, A. F., & Berk, M. (2017a). The new field of 'precision psychiatry'. *BMC medicine, 15*(1), 80.

Fernandes, O., Portugal, L. C. L., Alves, Rita de Cássia S., Arruda-Sanchez, T., Rao, A., Volchan, E., et al. (2017b). Decoding negative affect personality trait from patterns of brain activation to threat stimuli. *NeuroImage, 145*(Pt B), 337–345, from http://www.sciencedirect.com/science/article/pii/S1053811915011635.

Ferreira-Garcia, R., Mochcovitch, M., Costa do Cabo, M., Nardi, A. E., & Christophe Freire, R. (2017). Predictors of Pharmacotherapy Response in Generalized Anxiety Disorder: A Systematic Review. *Harvard review of psychiatry, 25*(2), 65–79.

Ferry, R. A., & Nelson, B. D. (2020). Differential impact of threat type on defensive motivation and attention during the NPU-threat task. *Motivation and Emotion*, 1–16, from https://link.springer.com/article/10.1007/s11031-020-09835-5.

Finan, P. H., & Garland, E. L. (2015). The role of positive affect in pain and its treatment. *The Clinical Journal of Pain, 31*(2), 177–187, from https://pubmed.ncbi.nlm.nih.gov/24751543/.

Frazier, J. A., Chiu, S., Breeze, J. L., Makris, N., Lange, N., Kennedy, D. N., et al. (2005). Structural brain magnetic resonance imaging of limbic and thalamic volumes in pediatric bipolar disorder. *The American journal of psychiatry, 162*(7), 1256–1265.

Friston, K. (2010). The free-energy principle: a unified brain theory? *Nature Reviews Neuroscience, 11*(2), 127–138.

*fsl_anat - FslWiki* (2020). Retrieved July 09, 2020, from https://fsl.fmrib.ox.ac.uk/fsl/fslwiki/fsl_anat.

Fullana, M. A., Harrison, B. J., Soriano-Mas, C., Vervliet, B., Cardoner, N., Àvila-Parcet, A., & Radua, J. (2016). Neural signatures of human fear conditioning: an updated and extended meta-analysis of fMRI studies. *Molecular Psychiatry, 21*(4), 500–508, from https://www.nature.com/articles/mp201588.

Gazzaniga, M. S., Grafton, S. T., Bizzi, E., Heatherton, T. F., Caramazza, A., & Chalupa, L. M. (2009). *The cognitive neurosciences* (4. ed.). *A Bradford book.* Cambridge, Mass.: MIT Press.

George, S. Z., & Hirsh, A. T. (2009). Psychologic influence on experimental pain sensitivity and clinical pain intensity for patients with shoulder pain. *The journal of pain : official journal of the American Pain Society, 10*(3), 293–299.

Gerlach, A. L., Andor, T., & Patzelt, J. (2008). Die Bedeutung von Unsicherheitsintoleranz für die Generalisierte Angststörung Modellüberlegungen und Entwicklung einer deutschen Version der Unsicherheitsintoleranz-Skala. *Zeitschrift für Klinische Psychologie und Psychotherapie, 37*(3), 190–199.

Glenn, C. R., Lieberman, L., & Hajcak, G. (2012). Comparing electric shock and a fearful screaming face as unconditioned stimuli for fear learning. *International journal of psychophysiology : official journal of the International Organization of Psychophysiology, 86*(3), 214–219.

Global Burden of Disease Collaborative Network. Global Burden of Disease Study 2017 (GBD 2017) Burden by Risk 1990-2017. Seattle, United States: Institute for Health Metrics and Evaluation (IHME), 2018.

Goldstein, J. M., Seidman, L. J., Makris, N., Ahern, T., O'Brien, L. M., Caviness, V. S., et al. (2007). Hypothalamic abnormalities in schizophrenia: sex effects and genetic vulnerability. *Biological Psychiatry, 61*(8), 935–945, from https://pubmed.ncbi.nlm.nih.gov/17046727/.

# REFERENCES

Grillon, C., Baas, J. P., Lissek, S., Smith, K., & Milstein, J. (2004). Anxious responses to predictable and unpredictable aversive events. *Behavioral neuroscience, 118*(5), 916–924.

Grupe, D. W., & Nitschke, J. B. (2013). Uncertainty and anticipation in anxiety: an integrated neurobiological and psychological perspective. *Nature reviews. Neuroscience, 14*(7), 488–501.

Gustafson, L. W., Gabel, P., Hammer, A., Lauridsen, H. H., Petersen, L. K., Andersen, B., et al. (2020). Validity and reliability of State-Trait Anxiety Inventory in Danish women aged 45 years and older with abnormal cervical screening results. *BMC Medical Research Methodology, 20*(1), 89.

Gustavsson, A., Svensson, M., Jacobi, F., Allgulander, C., Alonso, J., Beghi, E., et al. (2011). Cost of disorders of the brain in Europe 2010. *European neuropsychopharmacology : the journal of the European College of Neuropsychopharmacology, 21*(10), 718–779, from http://www.sciencedirect.com/science/article/pii/S0924977X1100215X.

Hahn, T., Nierenberg, A. A., & Whitfield-Gabrieli, S. (2017). Predictive analytics in mental health: applications, guidelines, challenges and perspectives. *Molecular Psychiatry, 22*(1), 37–43, from https://www.nature.com/articles/mp2016201.

Haxby, J. V., Connolly, A. C., & Guntupalli, J. S. (2014). Decoding neural representational spaces using multivariate pattern analysis. *Annual review of neuroscience, 37*, 435–456.

Hay, J. L., Okkerse, P., van Amerongen, G., & Groeneveld, G. J. (2016). Determining Pain Detection and Tolerance Thresholds Using an Integrated, Multi-Modal Pain Task Battery. *Journal of Visualized Experiments : JoVE*. (110).

Hayes, N. (2000). *Foundations of psychology* (3. ed.). Australia: Thomson Learning.

Henderson, C., Evans-Lacko, S., & Thornicroft, G. (2013). Mental illness stigma, help seeking, and public health programs. *American journal of public health, 103*(5), 777–780.

Holaway, R. M., Heimberg, R. G., & Coles, M. E. (2006). A comparison of intolerance of uncertainty in analogue obsessive-compulsive disorder and generalized anxiety disorder. *Journal of anxiety disorders, 20*(2), 158–174.

Hood, L., & Friend, S. H. (2011). Predictive, personalized, preventive, participatory (P4) cancer medicine. *Nature reviews. Clinical oncology, 8*(3), 184–187.

Hovenkamp-Hermelink, J. H. M., van der Veen, D. C., Oude Voshaar, R. C., Batelaan, N. M., Penninx, B. W. J. H., Jeronimus, B. F., et al. (2019). Anxiety sensitivity, its stability and longitudinal association with severity of anxiety symptoms. *Scientific Reports, 9*(1), 4314, from https://www.nature.com/articles/s41598-019-39931-7.

Hudson, M., Seppälä, K., Putkinen, V., Sun, L., Glerean, E., Karjalainen, T., et al. (2020). Dissociable neural systems for unconditioned acute and sustained fear. *NeuroImage, 216*, 116522.

Hunt, C., Keogh, E., & French, C. C. (2007). Anxiety sensitivity, conscious awareness and selective attentional biases in children. *Behaviour Research and Therapy, 45*(3), 497–509.

IBM Corp. Released 2019. IBM SPSS Statistics for Windows, Version 25.0. Armonk, NY: IBM Corp.

REFERENCES

Insel, T., Cuthbert, B., Garvey, M., Heinssen, R., Pine, D. S., Quinn, K., et al. (2010). Research domain criteria (RDoC): toward a new classification framework for research on mental disorders. *The American journal of psychiatry, 167*(7), 748–751.

Janak, P. H., & Tye, K. M. (2015). From circuits to behaviour in the amygdala. *Nature, 517*(7534), 284–292.

Jenkinson, M. (2002). Improved Optimization for the Robust and Accurate Linear Registration and Motion Correction of Brain Images. *NeuroImage, 17*(2), 825–841.

Jenkinson, M., & Chappell, M. (2018). *Introduction to neuroimaging analysis* (1st edition). *Oxford neuroimaging primers.* Oxford, New York, NY: Oxford University Press.

Jenkinson, M., & Smith, S. (2001). A global optimisation method for robust affine registration of brain images. *Medical Image Analysis, 5*(2), 143–156.

Jordan, K. D., & Okifuji, A. (2011). Anxiety disorders: differential diagnosis and their relationship to chronic pain. *Journal of pain & palliative care pharmacotherapy, 25*(3), 231–245.

Kasper, S. (2006). Anxiety disorders: under-diagnosed and insufficiently treated. *International journal of psychiatry in clinical practice, 10 Suppl 1*, 3–9.

Kastner, S., Pinsk, M. A., Weerd, P. de, Desimone, R., & Ungerleider, L. G. (1999). Increased Activity in Human Visual Cortex during Directed Attention in the Absence of Visual Stimulation. *Neuron, 22*(4), 751–761.

Kensinger, E. A., & Schacter, D. L. (2006). Processing emotional pictures and words: effects of valence and arousal. *Cognitive, affective & behavioral neuroscience, 6*(2), 110–126.

King, J.-R., & Dehaene, S. (2014). Characterizing the dynamics of mental representations: the temporal generalization method. *Trends in Cognitive Sciences, 18*(4), 203–210, from https://pubmed.ncbi.nlm.nih.gov/24593982/.

Kirwilliam, S. S., & Derbyshire, S. W. G. (2008). Increased bias to report heat or pain following emotional priming of pain-related fear. *Pain, 137*(1), 60–65, from https://pubmed.ncbi.nlm.nih.gov/17881129/.

Koerner, N., & Dugas, M. J. (2008). An investigation of appraisals in individuals vulnerable to excessive worry: the role of intolerance of uncertainty. *Cognitive Therapy and Research, 32*(5), 619–638, from https://link.springer.com/article/10.1007/s10608-007-9125-2.

Kohn, R., Saxena, S., Levav, I., & Saraceno, B. (2004). The treatment gap in mental health care. *Bulletin of the World Health Organization, 82*(11), 858–866.

Koo, T. K., & Li, M. Y. (2016). A Guideline of Selecting and Reporting Intraclass Correlation Coefficients for Reliability Research. *Journal of Chiropractic Medicine, 15*(2), 155–163.

Kriegeskorte, N., & Kievit, R. A. (2013). Representational geometry: integrating cognition, computation, and the brain. *Trends in Cognitive Sciences, 17*(8), 401–412.

Krohne, H. W. (1993). Vigilance and cognitive avoidance as concepts in coping research. *UR - https://www.semanticscholar.org/paper/Vigilance-and-cognitive-avoidance-as-concepts-in-Krohne/fc2a1ad212e6ab581e75aeccc5c2be6de0cd717d.*

# REFERENCES

Kuhn, T. S., & Hacking, I. (2012). *The structure of scientific revolutions* (Fourth edition). Chicago, London: The University of Chicago Press.

LaBerge, D. (1997). Attention, awareness, and the triangular circuit. *Consciousness and cognition, 6*(2-3), 149–181.

Lai, C.-H. (2019). Fear Network Model in Panic Disorder: The Past and the Future. *Psychiatry Investigation, 16*(1), 16–26.

Lang, P. (2005). *International affective picture system (IAPS): affective ratings of pictures and instruction manual.* Gainesville Fla: NIMH Center for the Study of Emotion & Attention.

Lawrence MA (2015) Package 'ez'. http://cran.r-project.org/web/packages/ez/ez.pdf.

LeDoux, J. E. (2000). Emotion circuits in the brain. *Annual review of neuroscience, 23*, 155–184.

LeDoux, J. (1996). Chapter 26 Emotional networks and motor control: a fearful view. In C. B. Saper, G. Holstege, & R. Bandler (Eds.), *Progress in Brain Research: v.107. The emotional motor system* (pp. 437–446). Amsterdam, New York: Elsevier Science.

LeDoux, J. (1998). Fear and the brain: where have we been, and where are we going? *Biological Psychiatry, 44*(12), 1229–1238.

LeDoux, J. E. (2014). Coming to terms with fear. *Proceedings of the National Academy of Sciences of the United States of America, 111*(8), 2871–2878.

LeDoux, J. E., & Pine, D. S. (2016). Using Neuroscience to Help Understand Fear and Anxiety: A Two-System Framework. *The American journal of psychiatry, 173*(11), 1083–1093.

Letzen, J. E., Sevel, L. S., Gay, C. W., O'Shea, A. M., Craggs, J. G., Price, D. D., & Robinson, M. E. (2014). Test-retest reliability of pain-related brain activity in healthy controls undergoing experimental thermal pain. *The journal of pain : official journal of the American Pain Society, 15*(10), 1008–1014.

Levine, S. M., Kumpf, M., Rupprecht, R., & Schwarzbach, J. V. (2020). *Supracategorical fear information revealed by aversively conditioning multiple categories.*

Levine, S. M., Pfaller, M., Reichenberger, J., Shiban, Y., Mühlberger, A., Rupprecht, R., & Schwarzbach, J. V. (2018a). Relating experimentally-induced fear to pre-existing phobic fear in the human brain. *Social cognitive and affective neuroscience, 13*(2), 164–172.

Levine, S. M., Wackerle, A., Rupprecht, R., & Schwarzbach, J. V. (2018b). The neural representation of an individualized relational affective space. *Neuropsychologia, 120*, 35–42, from https://pubmed.ncbi.nlm.nih.gov/30321612/.

Liddell, B. J., Brown, K. J., Kemp, A. H., Barton, M. J., Das, P., Peduto, A., et al. (2005). A direct brainstem-amygdala-cortical 'alarm' system for subliminal signals of fear. *NeuroImage, 24*(1), 235–243.

Loewenstein, G. F., Weber, E. U., Hsee, C. K., & Welch, N. (2001). Risk as feelings. *Psychological Bulletin, 127*(2), 267–286.

Loftus, G. R., & Masson, M. E. (1994). Using confidence intervals in within-subject designs. *Psychonomic bulletin & review, 1*(4), 476–490.

Lonsdorf, T. B., Menz, M. M., Andreatta, M., Fullana, M. A., Golkar, A., Haaker, J., et al. (2017). Don't fear 'fear conditioning': Methodological considerations for the

design and analysis of studies on human fear acquisition, extinction, and return of fear. *Neuroscience and biobehavioral reviews, 77*, 247–285.

Makris, N., Goldstein, J. M., Kennedy, D., Hodge, S. M., Caviness, V. S., Faraone, S. V., et al. (2006). Decreased volume of left and total anterior insular lobule in schizophrenia. *Schizophrenia research, 83*(2-3), 155–171.

Manchia, M., Pisanu, C., Squassina, A., & Carpiniello, B. (2020). Challenges and Future Prospects of Precision Medicine in Psychiatry. *Pharmacogenomics and personalized medicine, 13*, 127–140.

Marchewka, A., Zurawski, Ł., Jednoróg, K., & Grabowska, A. (2014). The Nencki Affective Picture System (NAPS): introduction to a novel, standardized, wide-range, high-quality, realistic picture database. *Behavior Research Methods, 46*(2), 596–610.

Margoles, M., & Weiner, R. S. (1999). *Chronic pain: Assessment, diagnosis, and management.* Boca Raton: CRC Press.

MATLAB (2019). version 9.6.0 (R2019a). Natick, Massachusetts: The MathWorks Inc.

Mauss, I. B., & Robinson, M. D. (2009). Measures of emotion: A review. *Cognition and Emotion, 23*(2), 209–237.

McDonald, C. (2015). Brain Structural Effects of Psychopharmacological Treatment in Bipolar Disorder. *Current neuropharmacology, 13*(4), 445–457.

McFarquhar, M., McKie, S., Emsley, R., Suckling, J., Elliott, R., & Williams, S. (2016). Multivariate and repeated measures (MRM): A new toolbox for dependent and multimodal group-level neuroimaging data. *NeuroImage, 132*, 373–389.

McGraw, K. O., & Wong, S. P. (1996). Forming inferences about some intraclass correlation coefficients. *Psychological Methods, 1*(1), 30–46.

McNeil, D. W., & Rainwater, A. J. (1998). Development of the Fear of Pain Questionnaire--III. *Journal of behavioral medicine, 21*(4), 389–410.

Michel Dugas, Mark Freeston, & Robert Ladouceur (1997). Intolerance of Uncertainty and Problem Orientation in Worry1. *Cognitive Therapy & Research, 21*(6), 593–606, from https://insights.ovid.com/cotr/199721060/00001076-199721060-00001.

Mikels, J. A., Fredrickson, B. L., Larkin, G. R., Lindberg, C. M., Maglio, S. J., & Reuter-Lorenz, P. A. (2005). Emotional category data on images from the International Affective Picture System. *Behavior research methods, 37*(4), 626–630, from https://link.springer.com/article/10.3758/BF03192732.

Miłkowska, P., Popko, K., Demkow, U., & Wolańczyk, T. (2017). Pro-inflammatory Cytokines in Psychiatric Disorders in Children and Adolescents: A Review. In M. Pokorski (Ed.), *Neuroscience and Respiration. Pulmonary Care and Clinical Medicine* (pp. 73–80). Cham: Springer International Publishing AG z.Hd. Alexander Grossmann.

Miller, D. N. (2011). Positive Affect. In S. Goldstein & J. A. Naglieri (Eds.), *Encyclopedia of child behavior and development* (pp. 1121–1122). Boston, MA: Springer Science+Business Media LLC.

Mineka, S., & Öhman, A. (2002). Phobias and preparedness: the selective, automatic, and encapsulated nature of fear. *Biological Psychiatry, 52*(10), 927–937.

Mobbs, D., Adolphs, R., Fanselow, M. S., Barrett, L. F., LeDoux, J. E., Ressler, K., & Tye, K. M. (2019). Viewpoints: Approaches to defining and investigating fear. *Nature Neuroscience, 22*(8), 1205–1216.

Morris, J. S., Friston, K. J., Büchel, C., Frith, C. D., Young, A. W., Calder, A. J., & Dolan, R. J. (1998). A neuromodulatory role for the human amygdala in processing emotional facial expressions. *Brain : a journal of neurology, 121 ( Pt 1)*, 47–57.

Morriss, J., Christakou, A., & van Reekum, C. M. (2016). Nothing is safe: Intolerance of uncertainty is associated with compromised fear extinction learning. *Biological Psychology, 121*(Pt B), 187–193.

Mugler, J. P., & Brookeman, J. R. (1990). Three-dimensional magnetization-prepared rapid gradient-echo imaging (3D MP RAGE). *Magnetic resonance in medicine, 15*(1), 152–157.

Murray, C. J. L., Barber, R. M., Foreman, K. J., Ozgoren, A. A., Abd-Allah, F., Abera, S. F., et al. (2015). Global, regional, and national disability-adjusted life years (DALYs) for 306 diseases and injuries and healthy life expectancy (HALE) for 188 countries, 1990–2013: quantifying the epidemiological transition. *Lancet (London, England), 386*(10009), 2145–2191.

Naaz, F., Knight, L. K., & Depue, B. E. (2019). Explicit and Ambiguous Threat Processing: Functionally Dissociable Roles of the Amygdala and Bed Nucleus of the Stria Terminalis. *Journal of cognitive neuroscience, 31*(4), 543–559.

National Research Council (2011). *Toward precision medicine: Building a knowledge network for biomedical research and a new taxonomy of disease:* National Academies Press.

Nelson, B. D., Hodges, A., Hajcak, G., & Shankman, S. A. (2015). Anxiety sensitivity and the anticipation of predictable and unpredictable threat: Evidence from the startle response and event-related potentials. *Journal of anxiety disorders, 33*, 62–71.

Neugebauer, V. (2015). Amygdala pain mechanisms. *Handbook of experimental pharmacology, 227*, 261–284.

Ohman, A., & Mineka, S. (2001). Fears, phobias, and preparedness: toward an evolved module of fear and fear learning. *Psychological Review, 108*(3), 483–522.

Onat, S., & Büchel, C. (2015). The neuronal basis of fear generalization in humans. *Nature Neuroscience, 18*(12), 1811–1818, from https://www.nature.com/articles/nn.4166.

Panksepp, J., Fuchs, T., & Iacobucci, P. (2011). The basic neuroscience of emotional experiences in mammals: The case of subcortical FEAR circuitry and implications for clinical anxiety. *Applied Animal Behaviour Science, 129*(1), 1–17.

Panksepp, J., Knutson, B., & Pruitt, D. L. (2013). Toward a Neuroscience of Emotion. In M. F. Mascolo & S. Griffin (Eds.), *Emotions, Personality, and Psychotherapy Ser. What Develops in Emotional Development?* (pp. 53–84). New York, NY: Springer.

Pātil, W., Chisholm, D., Dua, T., Laxminarayan, R., & Medina Mora, M. E. (Eds.) (2015). *Disease control priorities: volume 4. Mental, neurological, and substance use disorders* (Third edition). Washington, DC, USA: World Bank Group.

Pedersen, W. S., Muftuler, L. T., & Larson, C. L. (2019). A high-resolution fMRI investigation of BNST and centromedial amygdala activity as a function of affective stimulus predictability, anticipation, and duration. *Social cognitive and affective neuroscience, 14*(11), 1167–1177.

Perusini, J. N., & Fanselow, M. S. (2015). Neurobehavioral perspectives on the distinction between fear and anxiety. *Learning & Memory, 22*(9), 417–425.

Peterson, R. A., & Heilbronner, R. L. (1987). The anxiety sensitivity index. *Journal of anxiety disorders, 1*(2), 117–121.

Phan, N. Q., Blome, C., Fritz, F., Gerss, J., Reich, A., Ebata, T., et al. (2012). Assessment of pruritus intensity: prospective study on validity and reliability of the visual analogue scale, numerical rating scale and verbal rating scale in 471 patients with chronic pruritus. *Acta dermato-venereologica, 92*(5), 502–507.

Pinto, A. C. S., Luna, I. T., Sivla, A. d. A., Pinheiro, P. N. d. C., Braga, V. A. B., & Souza, A. M. A. E. (2014). Fatores de risco associados a problemas de saúde mental em adolescentes: revisão integrativa [Risk factors associated with mental health issues in adolescents: a integrative review]. *Revista da Escola de Enfermagem da U S P, 48*(3), 555–564.

Plamper, J., & Lazier, B. (2012). *Fear: Across the disciplines. EBSCO ebook academic collection.* Pittsburgh, Pa: University of Pittsburgh Press.

Popov, V., Ostarek, M., & Tenison, C. (2018). Practices and pitfalls in inferring neural representations. *NeuroImage, 174*, 340–351.

Porta-Casteràs, D., Fullana, M. A., Tinoco, D., Martínez-Zalacaín, I., Pujol, J., Palao, D. J., et al. (2020). Prefrontal-amygdala connectivity in trait anxiety and generalized anxiety disorder: Testing the boundaries between healthy and pathological worries. *Journal of affective disorders, 267*, 211–219.

Quiñones-Camacho, L. E., Wu, R., & Davis, E. L. (2018). Motivated attention to fear-related stimuli: Evidence for the enhanced processing of fear in the late positive potential. *Motivation and Emotion, 42*(2), 299–308, from https://link.springer.com/article/10.1007/s11031-018-9670-x.

Recla, J. M. (2010). New and emerging therapeutic agents for the treatment of fibromyalgia: an update. *Journal of pain research, 3*, 89–103.

Reiss, S. (1987). Theoretical perspectives on the fear of anxiety. *Clinical psychology review, 7*(6), 585–596.

Reiss, S., Peterson, R. A., Gursky, D. M., & McNally, R. J. (1986). Anxiety sensitivity, anxiety frequency and the prediction of fearfulness. *Behaviour Research and Therapy, 24*(1), 1–8.

Rhudy, J. L., Williams, A. E., McCabe, K. M., Nguyen, M. A. T. V., & Rambo, P. (2005). Affective modulation of nociception at spinal and supraspinal levels. *Psychophysiology, 42*(5), 579–587.

Rhudy, J. L., Williams, A. E., McCabe, K. M., Rambo, P. L., & Russell, J. L. (2006). Emotional modulation of spinal nociception and pain: the impact of predictable noxious stimulation. *Pain, 126*(1-3), 221–233.

Riegel, M., Żurawski, Ł., Wierzba, M., Moslehi, A., Klocek, Ł., Horvat, M., et al. (2016). Erratum to: Characterization of the Nencki Affective Picture System by discrete emotional categories (NAPS BE). *Behavior Research Methods, 48*(2), 613.

Robinson, M. E., Staud, R., & Price, D. D. (2013). Pain measurement and brain activity: will neuroimages replace pain ratings? *The journal of pain : official journal of the American Pain Society, 14*(4), 323–327.

Rodriguez, B. F., Bruce, S. E., Pagano, M. E., Spencer, M. A., & Keller, M. B. (2004). Factor structure and stability of the Anxiety Sensitivity Index in a longitudinal study of anxiety disorder patients. *Behaviour Research and Therapy, 42*(1), 79–91.

Roelofs, J., Peters, M. L., Deutz, J., Spijker, C., & Vlaeyen, J. W. S. (2005). The Fear of Pain Questionnaire (FPQ): further psychometric examination in a non-clinical sample. *Pain, 116*(3), 339–346, from http://www.sciencedirect.com/science/article/pii/S0304395905002150.

Rosier, E. M., Iadarola, M. J., & Coghill, R. C. (2002). Reproducibility of pain measurement and pain perception. *Pain, 98*(1), 205–216, from https://pubmed.ncbi.nlm.nih.gov/12098633/.

Rossi, V., & Pourtois, G. (2012). Transient state-dependent fluctuations in anxiety measured using STAI, POMS, PANAS or VAS: a comparative review. *Anxiety, stress, and coping, 25*(6), 603–645.

Rudert, T., & Lohmann, G. (2008). Conjunction analysis and propositional logic in fMRI data analysis using Bayesian statistics. *Journal of magnetic resonance imaging : JMRI, 28*(6), 1533–1539.

Sanchez, T. A., Mocaiber, I., Erthal, F. S., Joffily, M., Volchan, E., Pereira, M. G., et al. (2015). Amygdala responses to unpleasant pictures are influenced by task demands and positive affect trait. *Frontiers in Human Neuroscience, 9*, 107.

Sansone, R. A., & Sansone, L. A. (2008). Pain, pain, go away: antidepressants and pain management. *Psychiatry (Edgmont), 5*(12), 16–19.

Schacht, A., & Sommer, W. (2009). Emotions in word and face processing: early and late cortical responses. *Brain and cognition, 69*(3), 538–550.

Schienle, A., Köchel, A., Ebner, F., Reishofer, G., & Schäfer, A. (2010). Neural correlates of intolerance of uncertainty. *Neuroscience letters, 479*(3), 272–276.

Schmitz, A., & Grillon, C. (2012). Assessing fear and anxiety in humans using the threat of predictable and unpredictable aversive events (the NPU-threat test). *Nature protocols, 7*(3), 527–532.

Schroijen, M., Fantoni, S., Rivera, C., Vervliet, B., Schruers, K., van den Bergh, O., & van Diest, I. (2016). Defensive activation to (un)predictable interoceptive threat: The NPU respiratory threat test (NPUr). *Psychophysiology, 53*(6), 905–913, from https://onlinelibrary.wiley.com/doi/full/10.1111/psyp.12621?casa_token=mAJ9wLP ozZcAAAAA%3ApZ2sY2F6f84KAtzdCAr8lPxmYUgzbqZIa- aWmqx06wkZbjCZ3XDeZ8DMAIrnbp30JSpRMRVfoDxJ.

Schwarzbach, J. (2011). A simple framework (ASF) for behavioral and neuroimaging experiments based on the psychophysics toolbox for MATLAB. *Behavior Research Methods, 43*(4), 1194–1201, from https://link.springer.com/article/10.3758/s13428- 011-0106-8.

Scult, M. A., Fresco, D. M., Gunning, F. M., Liston, C., Seeley, S. H., García, E., & Mennin, D. S. (2019). Changes in Functional Connectivity Following Treatment With Emotion Regulation Therapy. *Frontiers in behavioral neuroscience, 13*, 10.

Sehlmeyer, C., Schöning, S., Zwitserlood, P., Pfleiderer, B., Kircher, T., Arolt, V., & Konrad, C. (2009). Human fear conditioning and extinction in neuroimaging: a systematic review. *PloS one, 4*(6), e5865.

Seidel, P., Levine, S. M., Tahedl, M., & Schwarzbach, J. V. (2020). Temporal Signal- to-Noise Changes in Combined Multislice- and In-Plane-Accelerated Echo-Planar Imaging with a 20- and 64-Channel Coil. *Scientific Reports, 10*(1), 5536, from https://www.nature.com/articles/s41598-020-62590-y.

Seligman, M. E. (1970). On the generality of the laws of learning. *Psychological Review, 77*(5), 406–418.

Setsompop, K., Gagoski, B. A., Polimeni, J. R., Witzel, T., van Wedeen, J., & Wald, L. L. (2012). Blipped-controlled aliasing in parallel imaging for simultaneous multislice echo planar imaging with reduced g-factor penalty. *Magnetic resonance in medicine, 67*(5), 1210–1224, from https://pubmed.ncbi.nlm.nih.gov/21858868/.

Shackman, A. J., & Fox, A. S. (2016). Contributions of the Central Extended Amygdala to Fear and Anxiety. *The Journal of Neuroscience, 36*(31), 8050–8063.

Shy, M. E., Frohman, E. M., So, Y. T., Arezzo, J. C., Cornblath, D. R., Giuliani, M. J., et al. (2003). Quantitative sensory testing: report of the Therapeutics and Technology Assessment Subcommittee of the American Academy of Neurology. *Neurology, 60*(6), 898–904, from https://n.neurology.org/content/60/6/898.

Sibille, K. T., Kindler, L. L., Glover, T. L., Staud, R., Riley, J. L., & Fillingim, R. B. (2012). Affect balance style, experimental pain sensitivity, and pain-related responses. *The Clinical Journal of Pain, 28*(5), 410–417.

Smith, S. M., Jenkinson, M., Woolrich, M. W., Beckmann, C. F., Behrens, T. E. J., Johansen-Berg, H., et al. (2004). Advances in functional and structural MR image analysis and implementation as FSL. *NeuroImage, 23 Suppl 1*, S208-19, from http://www.sciencedirect.com/science/article/pii/S1053811904003933.

Sobkow, A., Traczyk, J., & Zaleskiewicz, T. (2016). The Affective Bases of Risk Perception: Negative Feelings and Stress Mediate the Relationship between Mental Imagery and Risk Perception. *Frontiers in Psychology, 7*, 932.

Somerville, L. H., Wagner, D. D., Wig, G. S., Moran, J. M., Whalen, P. J., & Kelley, W. M. (2013). Interactions between transient and sustained neural signals support the generation and regulation of anxious emotion. *Cerebral Cortex (New York, NY), 23*(1), 49–60.

Somerville, L. H., Whalen, P. J., & Kelley, W. M. (2010). Human bed nucleus of the stria terminalis indexes hypervigilant threat monitoring. *Biological Psychiatry, 68*(5), 416–424.

Spielberger, C. (1966). *Anxiety and behavior.* New York: Academic Press.

Spielberger, C. D. (1983). *State-Trait Anxiety Inventory for Adults:* American Psychological Association (APA).

Sprooten, E., Rasgon, A., Goodman, M., Carlin, A., Leibu, E., Lee, W. H., & Frangou, S. (2017). Addressing reverse inference in psychiatric neuroimaging: Meta-analyses of task-related brain activation in common mental disorders. *Human brain mapping, 38*(4), 1846–1864.

Stegmann, Y., Reicherts, P., Andreatta, M., Pauli, P., & Wieser, M. J. (2019). The effect of trait anxiety on attentional mechanisms in combined context and cue conditioning and extinction learning. *Scientific Reports, 9*(1), 8855, from https://www.nature.com/articles/s41598-019-45239-3.

Steimer, T. (2002). The biology of fear- and anxiety-related behaviors. *Dialogues in Clinical Neuroscience, 4*(3), 231–249.

Stein, B. E., & Meredith, M. A. (1994). *The merging of the senses* (2. print). *A Bradford book.* Cambridge, Mass.: MIT Press.

Stringer, D. M. (2013). Negative Affect. In *Encyclopedia of Behavioral Medicine* (pp. 1303–1304). Springer, New York, NY.

Suhr, J., & Spickard, B. (2012). Pain-related fear is associated with cognitive task avoidance: exploration of the cogniphobia construct in a recurrent headache sample. *The Clinical neuropsychologist, 26*(7), 1128–1141, from https://pubmed.ncbi.nlm.nih.gov/22928643/.

Sylvers, P., Lilienfeld, S. O., & LaPrairie, J. L. (2011). Differences between trait fear and trait anxiety: implications for psychopathology. *Clinical psychology review, 31*(1), 122–137.

Tabbert, K., Stark, R., Kirsch, P., & Vaitl, D. (2005). Hemodynamic responses of the amygdala, the orbitofrontal cortex and the visual cortex during a fear conditioning paradigm. *International journal of psychophysiology : official journal of the International Organization of Psychophysiology, 57*(1), 15–23.

Teixeira, A. L., Salem, H., Frey, B. N., Barbosa, I. G., & Machado-Vieira, R. (2016). Update on bipolar disorder biomarker candidates. *Expert review of molecular diagnostics, 16*(11), 1209–1220.

Tovote, P., Fadok, J. P., & Lüthi, A. (2015). Neuronal circuits for fear and anxiety. *Nature Reviews Neuroscience, 16*(6), 317–331, from https://www.nature.com/articles/nrn3945?draft=collection.

Tyrer, P. (2014). A comparison of DSM and ICD classifications of mental disorder. *Advances in Psychiatric Treatment, 20*(4), 280–285.

Vambheim, S. M., Lyby, P. S., Aslaksen, P. M., Flaten, M. A., Åsli, O., & Martinussen, L. M. (2017). The Fear of Pain Questionnaire-III and the Fear of Pain Questionnaire-Short Form: a confirmatory factor analysis. *Journal of pain research, 10*, 1871–1878.

van den Heuvel, M. P., & Hulshoff Pol, H. E. (2010). Exploring the brain network: a review on resting-state fMRI functional connectivity. *European neuropsychopharmacology : the journal of the European College of Neuropsychopharmacology, 20*(8), 519–534.

Vujanovic, A. A., Arrindell, W. A., Bernstein, A., Norton, P. J., & Zvolensky, M. J. (2007). Sixteen-item Anxiety Sensitivity Index: confirmatory factor analytic evidence, internal consistency, and construct validity in a young adult sample from the Netherlands. *Assessment, 14*(2), 129–143.

Wager, T. D., Atlas, L. Y., Lindquist, M. A., Roy, M., Woo, C.-W., & Kross, E. (2013). An fMRI-based neurologic signature of physical pain. *The New England journal of medicine, 368*(15), 1388–1397.

Wang, P. S., Lane, M., Olfson, M., Pincus, H. A., Wells, K. B., & Kessler, R. C. (2005). Twelve-month use of mental health services in the United States: results from the National Comorbidity Survey Replication. *Archives of General Psychiatry, 62*(6), 629–640.

Watson, A. B., & Pelli, D. G. (1983). QUEST: a Bayesian adaptive psychometric method. *Perception & psychophysics, 33*(2), 113–120.

Watson, D., Clark, L. A., & Tellegen, A. (1988). Development and validation of brief measures of positive and negative affect: The PANAS scales. *Journal of Personality and Social Psychology, 54*(6), 1063–1070.

Wittchen, H. U., Jacobi, F., Rehm, J., Gustavsson, A., Svensson, M., Jönsson, B., et al. (2011). The size and burden of mental disorders and other disorders of the brain in Europe 2010. *European neuropsychopharmacology : the journal of the European College of Neuropsychopharmacology, 21*(9), 655–679.

# REFERENCES

Wium-Andersen, I. K., Vinberg, M., Kessing, L. V., & McIntyre, R. S. (2017). Personalized medicine in psychiatry. *Nordic journal of psychiatry, 71*(1), 12–19.

Woolrich, M. W., Ripley, B. D., Brady, M., & Smith, S. M. (2001). Temporal autocorrelation in univariate linear modeling of FMRI data. *NeuroImage, 14*(6), 1370–1386.

Woolrich, M. W., Behrens, T. E. J., Beckmann, C. F., Jenkinson, M., & Smith, S. M. (2004). Multilevel linear modelling for FMRI group analysis using Bayesian inference. *NeuroImage, 21*(4), 1732–1747.

World Health Organization (1993). *The ICD-10 classification of mental and behavioural disorders: Diagnostic criteria for research. Drugs used in Skin Diseases.* Geneva: World Health Organization.

World Medical Association Declaration of Helsinki: ethical principles for medical research involving human subjects (2013). *JAMA, 310*(20), 2191–2194.

World Medical Association Declaration of Helsinki: ethical principles for medical research involving human subjects (2014). *The Journal of the American College of Dentists, 81*(3), 14–18, from https://pubmed.ncbi.nlm.nih.gov/25951678/.

Xia, W., Mørch, C. D., & Andersen, O. K. (2016). Test-Retest Reliability of 10 Hz Conditioning Electrical Stimulation Inducing Long-Term Potentiation (LTP)-Like Pain Amplification in Humans. *PloS one, 11*(8), e0161117.

Yang, Y., Lueken, U., Wittmann, A., Holtz, K., Kleint, N. I., Herrmann, M. J., et al. (2016). Neural correlates of individual differences in anxiety sensitivity: an fMRI study using semantic priming. *Social cognitive and affective neuroscience, 11*(8), 1245–1254.

Yori, G. (2013). Trait Anxiety. In *Encyclopedia of Behavioral Medicine* (p. 1989). Springer, New York, NY.

Zheng, W., Woo, C.-W., Yao, Z., Goldstein, P., Atlas, L. Y., Roy, M., et al. (2020). Pain-Evoked Reorganization in Functional Brain Networks. *Cerebral Cortex (New York, NY), 30*(5), 2804–2822.

Zoicas, I., Slattery, D. A., & Neumann, I. D. (2014). Brain oxytocin in social fear conditioning and its extinction: involvement of the lateral septum. *Neuropsychopharmacology, 39*(13), 3027–3035.

# ACKNOWLEDGEMENTS

# SELBSTÄNDIGKEITSERKLÄRUNG

Ich, Viola Wagner geboren am 20.07.1988 in Frankfurt am Main erkläre hiermit, dass ich die vorliegende Arbeit ohne unzulässige Hilfe Dritter und ohne Benutzung anderer als der angegebenen Hilfsmittel angefertigt habe. Die aus anderen Quellen direkt oder indirekt übernommenen Daten und Konzepte sind unter Angabe der Quelle gekennzeichnet. Insbesondere habe ich nicht die entgeltliche Hilfe von Vermittlungs- bzw. Beratungsdiensten (Promotionsberater oder andere Personen) in Anspruch genommen. Die Arbeit wurde bisher weder im In- noch im Ausland in gleicher oder ähnlicher Form einer anderen Prüfungsbehörde vorgelegt.

_____

Ort, Datum eigenhändige Unterschrift des Promovenden